



UNIVERSITY *of the*
WESTERN CAPE

Evaluation of selected polycyclic compounds as resistance modulators in *Mycobacterium tuberculosis*

Erika Kapp

Thesis submitted in fulfilment of the requirements for the degree
Doctor of Philosophy in Pharmaceutical Chemistry at the School of
Pharmacy of the University of the Western Cape

Supervisor: Prof. S.F. Malan
Co-supervisors: Prof. J. Joubert
Prof S. Sampson

University of the Western Cape 2022

Dedicated to my late father, Brink Grobler and brother, Gerrit Grobler who encouraged me to pursue my dreams and to my mother Hanli Grobler, husband Frans Kapp and daughter Hanli-Mari Kapp whose love and support brightens my path.



Acknowledgements

I would like to express my sincere appreciation to my supervisor, Prof Sarel Malan and co-supervisors, Prof Jacques Joubert and Samantha Sampson, for their support and guidance towards the completion of this thesis:

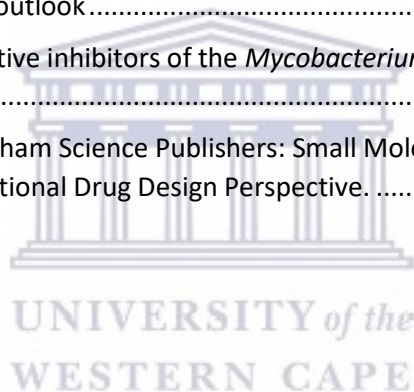
I would like to thank my collaborators at Stellenbosch University, University of Cape Town, the South African National Institute of Bioinformatics and the School of Pharmacy at the University of the Western Cape for their input in the research presented in this thesis. I would also like to thank all my colleagues within the School of Pharmacy at the University of the Western Cape for their support throughout the completion of this project.

Finally, I would like to extend a special thank you to my family for their understanding and unconditional support.



Table of Contents

Abstract	1
Author contributions	3
Chapter 1: Introduction and Rationale.....	4
Chapter 2: Small Molecule Efflux Pump Inhibitors in <i>Mycobacterium tuberculosis</i> : A Rational Drug Design Perspective.	14
Chapter 3: Molecular modelling and simulation studies of <i>Mycobacterium tuberculosis</i> multidrug efflux pump protein Rv1258c.....	42
Chapter 4: Discovery and biological evaluation of an adamantyl-amide derivative with likely MmpL3 inhibitory activity. (Concept article).....	58
Chapter 5: Versatility of 7-Substituted Coumarin Molecules as Antimycobacterial Agents, Neuronal Enzyme Inhibitors and Neuroprotective agents.....	81
Chapter 6: Antimycobacterial activity, Synergism and Mechanism of Action Evaluation of Novel Polycyclic Amines against <i>Mycobacterium tuberculosis</i>	107
Chapter 7: Conclusion and future outlook.....	122
Annexure 1: Identification of putative inhibitors of the <i>Mycobacterium tuberculosis</i> Rv1258c efflux pump utilizing <i>in silico</i> methods.....	129
Annexure 2: Copyright Policy Bentham Science Publishers: Small Molecule Efflux Pump Inhibitors in <i>Mycobacterium tuberculosis</i> : a Rational Drug Design Perspective.	136



Abstract

Progressive development of resistance to various chemotherapeutic agents used in the management of infectious diseases presents a serious problem in global public health. Increasing levels of antimicrobial resistance in *Mycobacterium tuberculosis* (Mtb) is particularly concerning in resource poor countries with a high incidence of tuberculosis (TB), as it is particularly difficult and very costly to treat. The Global Tuberculosis report released by the World Health Organization (WHO) in 2022 (based on data from 2021) reports that South Africa is one of only 5 countries in the world with more than 500 cases per 100 000 people. It also falls in the WHO's top 7 countries with the highest multidrug resistant (MDR) TB incidence.¹ The same report released in 2021 states that global TB reporting rates dropped dramatically in 2020, and that TB death rates saw the first year-on-year increase since 2005.² This is likely a direct consequence of COVID-19 and although improvements in reporting was seen in 2021, the trend has not yet been reversed.¹ The pandemic had a negative impact on the progress made in the fight against TB and a renewed effort is needed to achieve the goals previously set out in the WHO End TB Strategy.

Mtb is naturally resistant to a number of antibiotics due to the unique composition of the cell wall and natural abundance of efflux pumps that limit accumulation of active substances within the cell.³⁻⁵ The resulting sub-optimal intracellular accumulation of antibiotics is central to intrinsic resistance but also plays a large role in the development of acquired resistance mutations.³⁻⁷ Drug resistance in Mtb necessitates novel approaches in the design of new antimycobacterials as well as the utilization of available treatment options. Any strategy that increases the accumulation of active substrates within the target cell has the potential to increase the efficacy of antimycobacterials and reduce the selection of genetically-encoded resistance brought on by sub-inhibitory chemotherapeutic exposure.

It was noted that the unique polycyclic amine-containing compounds in the Drug Design group compound library in the School of Pharmacy at the University of the Western Cape have the potential to address drug resistance through several of the strategies mentioned above. These compounds contain bulky lipophilic carriers which could support compound accumulation within the mycobacterial cell, chemical properties that may promote interaction with efflux pumps as well as moieties with possible inherent antimycobacterial activity. As a starting point, the unique database of compounds in our in-house library was assessed for antimycobacterial activity and a series of compounds were selected to be evaluated for resistance reversal ability. In conjunction with this, the possibility of rational drug design of efflux pump inhibitors (EPIs) was explored and further *in silico* studies were done to visualize protein-ligand interactions and identify novel compounds that may interact with proteins of interest.

A comprehensive literature review was done to assess the possibility of rational drug design of efflux pump inhibitors as described in article 1 in chapter 2. A theme that emerged from the review is that the lack of crystal structures of efflux pumps in Mtb complicates rational drug design of small molecule EPI's. The well-known efflux pump, Rv1258c, has been implicated in resistance to a variety of antimycobacterial drugs including isoniazid, rifampicin, aminoglycoside antibiotics and spectinomycin.⁵ A homology model of Rv1258c in Mtb was therefore developed in collaboration with

the South African National Bioinformatics Institute and is described in article 2 in chapter 3. The developed homology model was then utilized to perform *in silico* evaluation for the purpose of identifying molecules that may interact with the Rv1258c efflux pump. This is described in Addendum 1. The compounds identified were purchased and are currently being evaluated for synergism with spectinomycin in Mtb.

Antimycobacterial activity of the compound library was evaluated through a collaboration with the DSI/NRF Centre of Excellence for Biomedical Tuberculosis Research at the Faculty of Medicine and Health Sciences, University of Stellenbosch. A series of compounds with antimycobacterial activity was identified. The most promising compound, an adamantane amide derivative was further evaluated to determine a possible mechanism of action. The likely target of the compound was identified as MmpL3, a mycobacterial membrane protein essential for the survival of the bacteria. *In silico* evaluations utilizing the recently elucidated MmpL3 protein as well as a mutant protein generated as part of this study was done to gain insight on the binding of the compound in the MmpL3 protein. This is described in article 3 included as chapter 4.

The majority of the top compounds that were identified as part of the evaluation of the compound library, comprised of a series of coumarin derivatives originally designed as neuronal enzyme inhibitors. Coumarins are privileged molecules with highly versatile binding properties. As such, improving the selectivity for compounds containing a coumarin scaffold is of utmost importance. Further investigations on the structure activity relationships for antimycobacterial activity of the multifunctional coumarins are described in article 4 in chapter 5. The albumin binding properties of the compounds, which were explored to better explain the variances in activity observed in different growth media types, are also described in this chapter.

Concurrently, a smaller series of compounds from the compound library were identified to evaluate resistance reversal activity. The possession of potential ion channel inhibitory properties, which may directly or indirectly inhibit efflux pump efficacy, was an important consideration in compound selection. The selected compounds were evaluated through a collaboration with the SAMRC/NHLS/UCT Molecular Mycobacteriology Research Unit and the DSI/NRF Centre of Excellence for Biomedical Tuberculosis Research. The antimycobacterial activity, mechanism of action and efflux pump inhibitory activity for this smaller series are described in article 5 in chapter 6.

The possibility of addressing drug resistance in Mtb was thus explored through the development of a homology model to facilitate identification and design of novel compounds, the evaluation of novel polycyclic compounds for antimycobacterial activity and the evaluation of specifically selected polycyclic amine containing compounds for efflux pump inhibitory activity and antimycobacterial synergism.

Author contributions:

1. Small molecule efflux pump inhibitors in *Mycobacterium tuberculosis*: A rational drug design perspective.

Erika Kapp performed the literature review and wrote the manuscript. Sarel Malan, Jacques Joubert and Samantha Sampson reviewed the final draft.

2. Molecular Modelling and Simulation Studies of the *Mycobacterium Tuberculosis* Multidrug Efflux Pump Protein Rv1258c.

Erika Kapp conceptualised the study. Erika Kapp, Sarel Malan and Jacques Joubert gave input on the functionality, current knowledge and specific considerations to facilitate the development of the homology model for the Rv1258c efflux pump. Ruben Cloete constructed the homology model and wrote the first draft of the manuscript. Erika Kapp contributed to the review and editing of the first draft and Sarel Malan, Jacques Joubert and Alan Christoffels contributed to the final draft of the manuscript.

3. Discovery and biological evaluation of an adamantly-amide derivative with likely MmpL3 inhibitory activity. (Concept article)

Erika Kapp wrote the manuscript with the support of Hanri Calitz and Samantha Sampson. Erika Kapp and Samuel Egieyeh performed the *in silico* analysis. Hanri Calitz and Audrey Jordaan performed the biological assays with support from Elizabeth Streicher, Anzaan Dippenaar and Digby Warner. Jacques Joubert and Sarel Malan, Samuel Egieyeh, Elizabeth Streicher, Anzaan Dippenaar and Digby Warner contributed to the final draft.

4. Versatility of 7-Substituted Coumarin Molecules as Antimycobacterial Agents, Neuronal Enzyme Inhibitors and Neuroprotective agents.

Erika Kapp wrote the manuscript and Erika Kapp and Hanri Calitz (née Visser) performed the MIC assays with support from Samantha Sampson and Elizabeth Streicher and Digby Warner. Erika Kapp and Jacques Joubert performed, analysed and validated the albumin binding assay. Erika Kapp co-developed and validated the MAO and ChE assays and Frank Zindo, Sylvester I. Omoruyi, Adaze B. Enogieru, and Okobi E. Ekpo contributed to- and performed the ChE, MAO, neuroprotection and cytotoxicity assays. Germaine Foka and Jacques Joubert synthesized the compounds. Sarel Malan, Jacques Joubert and Samantha Sampson and Hanri Calitz (née Visser) contributed to the final draft.

5. Antimycobacterial Activity, Synergism and Mechanism of Action Evaluation of Novel Polycyclic Amines against *Mycobacterium tuberculosis*.

Erika Kapp conceptualised the study and drafted the manuscript. Digby Warner, Ronnett Seldon, Audrey Jordaan and Margaretha de Vos were involved in the MIC, mechanism of action and synergism assays. Erika Kapp was involved in the analysis and interpretation of raw data. Jacques Joubert and Rajan Sharma synthesized the compounds. Sarel Malan, Jacques Joubert, Samantha Sampson and Digby Warner contributed to the final draft.

Chapter 1: Introduction and Rationale

Expanding drug resistance to agents used in the management of infectious diseases, is fast becoming a global health emergency. The World Health Organization (WHO) defines antimicrobial drug resistance (AMR), as resistance to medication that occurs when microorganisms like bacteria, viruses, fungi and parasites change in ways which render medications ineffective. A recent report by the WHO confirms that levels of AMR are increasing with proportionally higher increases in drug resistance observed in low- and middle-income countries.⁸ AMR reduces our ability to treat common infections, and negatively affects morbidity and mortality from previously treatable conditions. A concerted, cross-sectional effort within the public and private sectors, research institutions, funders, regulatory authorities and society as a whole is required to manage and mitigate the serious risk that drug resistance holds.⁹

Tuberculosis (TB), and particularly drug-resistant TB, is one of the most concerning communicable diseases of our time. TB is currently one of the top 10 causes of death worldwide with approximately 1.6 million TB deaths in 2021.¹ Due to the COVID-19 pandemic reporting rates of TB dropped dramatically,² but of the estimated 10 million people diagnosed with TB in 2019, approximately half a million people had drug-resistant TB. TB affects primarily poor communities where living conditions and health and nutrition are not optimal. TB cases relative to population size varies from 10 in 100 000 people in most high-income countries, to 150–400 in 100 000 people in most of the 30 high TB burden countries. The WHO Global Tuberculosis Report of 2022 reports that Lesotho and South Africa are 2 out of only 5 countries in the world that see more than 500 TB cases per 100 000 population.¹ Treatment of TB is hampered by the development of multidrug-resistant (MDR) and extensively drug-resistant (XDR) TB as well as co-morbidities including HIV. South Africa is one of only 11 countries worldwide that feature in the top 20 of all three WHO high burden country lists (i.e. high TB incidence, high TB/HIV co-infection and high MDR TB incidence) with 23 out of 615 TB cases per 100 000 population noted as MDR TB.¹

Drug resistance in *Mycobacterium tuberculosis* (Mtb) can be intrinsic or acquired. The unusual structure of the mycobacterial cell wall, as well as the presence of efflux pumps, which limit intracellular accumulation of various antibiotics, are major contributors to intrinsic resistance.^{5,10} Intrinsic resistance limits the number of classes of antibiotics that are available for the treatment of a mycobacterial infection. A large range of antibiotics including tetracyclines, certain fluoroquinolones, macrolides and β -lactam antibiotics are affected by intrinsic resistance.^{11,12} Strategies that address intrinsic resistance mechanisms could allow the use of a wider range of antibiotics in the treatment of TB.

Acquired resistance in mycobacteria can usually be attributed to mutations in chromosomal genes. These mutations occur spontaneously, rather than through horizontal transfer of genetic elements as is the case in many other species of bacteria.⁴ Resistant mutants are selected for by sub-optimal therapeutic pressure. Chromosomal alterations or deletions in these mutants can affect the drug target, bacterial enzymes that activate/inactivate the drug and influx and efflux of drugs into/from the intracellular environment.^{6,12,13} It has been established that mutations responsible for the resistance to various drugs are not linked and that multidrug resistance is not due to a single genetic mutation, but rather a result of a combination of multiple different mutations.⁶ It is however possible that a

complex association exists between mutations associated with one drug and the development of further resistance mutations.⁴

Reduced absorption of active molecules through the unique mycobacterial cell wall, as well as the abundance of efflux pumps available for extrusion, play a role in both intrinsic resistance as well as the promotion of resistance mutations. Apart from being a key contributor to antimycobacterial drug resistance, the ability of Mtb to limit accumulation of active moieties within the cell is also a hindrance to successful antimycobacterial drug design. The effective permeability barrier and active efflux mechanisms in mycobacteria reduce the usefulness of accepted parameters for drug-like molecules. It also means that compounds identified through target-based screenings are often not active in whole cell assays.¹⁴ Strategies that may increase permeability of the cell wall, facilitate passive transport of drugs across the cell wall, and limit active efflux of antimycobacterial compounds would therefore address antimycobacterial resistance on various levels. Compounds with antimycobacterial properties that can overcome or address reduced entry or active efflux not only have the potential to be excellent antimycobacterial agents, but may also improve the activity of existing compounds affected by limited accumulation.

1.1 Drug design considerations to overcome the low permeability of the mycobacterial cell wall.

The mycobacterial cell wall is uniquely complex and incorporates characteristics from both gram-positive and gram-negative bacteria. The cell wall is an essential part of the bacterial physiology and virulence and is composed of 3 main sections.¹⁴⁻¹⁶ The innermost layer is a peptidoglycan layer which is a standard component of the cell wall of most bacterial species. The peptidoglycan layer is followed by a liposaccharide layer which contains amongst others, arabinogalactan. The outermost layer of the mycobacterial cell wall, also referred to as a mycomembrane, contains primarily mycolic acids and is distinctive to mycobacteria.^{16,17}

The unique lipid rich mycobacterial cell wall provides an effective permeability barrier to numerous standard antibiotics, but also creates an opportunity for selective targeting of mycobacteria specifically. It is not surprising that this characteristic mycobacterial feature is the target of numerous antimycobacterial agents. Apart from β -lactam antibiotics and other antibiotics that target the peptidoglycan component of the cell wall, mycobacterial cell wall inhibitors include, amongst others, isoniazid, ethionamide, ethambutol, the nitroimidazole derivatives, delamanid and pretomanid, SQ109 which is currently in phase 2 clinical trials, the lipophilic adamantyl urea AU1235 and a few other candidates in various phases of development.^{14,18,19}

SQ109 and AU1235 contain an adamantane scaffold similar to a number of compounds evaluated in this study. SQ109, was originally designed as an ethambutol derivative but, unlike ethambutol, it does not target the arabinogalactan component of the cell wall. It does however target mycolic acid synthesis through inhibition of MmpL3 which is a validated Mtb target. AU1235 also targets MmpL3 and, although both SQ109 and AU1235 have an adamantane scaffold, these 2 compounds have vastly different side chains. The adamantane moiety may therefore play an important part in the distribution and mechanism of action of these MmpL3 inhibitors. In addition to adamantane containing moieties, a number of structurally diverse prospective antimycobacterial compounds have also been classified as likely MmpL3 inhibitors.²⁰⁻²⁴

MmpL3 is an attractive target as it plays a crucial role in the survival and virulence of mycobacteria. MmpL3 is also highly conserved in mycobacteria which points to the possibility of using MmpL3 inhibitors to combat other strains of mycobacteria where treatment options are very limited.²⁵⁻²⁷

Inhibition of the mycobacterial cell wall can be bactericidal, particularly in actively replicating bacteria. Importantly, disrupting of the cell wall integrity can increase the entry of other antimycobacterial agents.^{28,29} Various cell wall inhibitors have been shown to act synergistically with a range of unrelated antimycobacterial drugs. An example of synergism caused by increased intracellular accumulation is rifampicin where increased accumulation was demonstrated in the presence of a series of cell wall inhibitors including ethambutol, isoniazid, SQ109 and AU1235. AU1235 was able to increase rifampicin accumulation at sub-inhibitory concentrations.²⁹

An alternative to decreasing cell wall integrity is to increase passive diffusion of the active antimycobacterial across the highly lipophilic cell wall. It has been noted that increased lipophilicity seems to improve antimycobacterial activity in replicating as well as dormant Mtb.³⁰⁻³² In fact, a number of current antimycobacterial drugs well exceed the generally accepted LogP of 5,^{33,34} often used as an exclusion filter in the drug design process. A possible drug design strategy may therefore be to increase the upper limit for lipophilicity in the identification of druggable candidates in compound library screenings. In addition to this, rational drug design could consider including lipophilic auxophoric functional groups or lipophilic carrier molecules to increase the intracellular accumulation of active moieties.

1.1.1 Polycyclic scaffolds as carrier moieties for active antimycobacterial compounds

In certain molecules, enhanced passive diffusion can be achieved by increasing the lipophilicity of the compound. This can be done through modification of functional groups or conjugation to lipophilic scaffolds. Research suggests that more lipophilic derivatives within a class of antibiotics are likely to demonstrate higher antimycobacterial activity than their hydrophilic counterparts.^{12,30-32} The addition of hydrocarbon moieties to drugs has been shown to improve movement across cell membranes and increase the binding of drugs to lipophilic regions of target receptors.

The conjugation of lipophilic, bulky moieties to compounds can be utilized to change the pharmacokinetic as well as pharmacodynamic properties of compounds. It is likely that polycyclic cage derivatives could interact with- or cross the mycobacterial cell membrane in sufficient quantities to exert an effect. Conjugation to a bulky lipophilic cage moiety could improve the cell membrane permeability of various antimycobacterials, antibiotics or other active molecules. The cage moiety could also change how the antimycobacterial binds to the target protein or possibly reduce the sensitivity of conjugates to deactivating bacterial enzymes by means of steric hindrance.

1.2 Drug design considerations to address efflux pump-based resistance.

Bacterial efflux pumps are grouped into 6 families based on the structure and energy source used to facilitate active transport. Primary active transporters utilize ATP hydrolysis as energy source and include efflux pumps from the ATP-binding cassette (ABC) superfamily. The major facilitator superfamily (MFS), the small multidrug resistance family (SMR), the resistance-nodulation-cell division superfamily (RND) and the multi antimicrobial extrusion protein family (MATE) are all classified as

secondary active transporters and employ an electrochemical potential difference or proton-motive force (PMF) to drive active efflux.^{7,35} Proteobacterial antimicrobial compound efflux pumps (PACE) were recently described.³⁶ The genome of Mtb includes genes coding for efflux pumps from the first 5 bacterial efflux pump families³⁷ and various ABC, MFS, SMR and RND efflux pumps have been characterised as antibiotic transporters.¹²

Efflux pumps contribute to mycobacterial resistance through natural abundance, their highly inducible expression and mutations that enhance efflux activity.^{12,38} Overexpression of efflux pumps is a well-recognized contributor of drug resistance to various chemotherapeutic agents employed in the management of Mtb.^{5,12,39,40} Efflux pumps actively transport substrate compounds out of the cell and can be substrate specific or, in the case of multidrug resistance pumps, facilitate efflux of a range of chemically unrelated compounds.^{5,41}

Efflux pumps reduce the intracellular concentration of substrate compounds to sub-therapeutic levels, thereby directly conferring resistance to the given substrate and likely facilitating the development of additional resistance mutations brought on by sub-inhibitory chemotherapeutic exposure.^{38,40,42} Phenotypic drug resistance is likely a combination between increased drug efflux and genetic mutations that affect the efficacy of the drug in question.⁴³ Inhibition of efflux is expected to increase the efficacy of a wide range of antimycobacterial compounds and prevent the formation and selection of additional resistant mutants.⁵

Rv1258c is a MSF type mycobacterial efflux pump that has been implicated in drug resistance to a wide variety of antimycobacterial compounds.^{20,44-47} It has been demonstrated that Rv1258c is also important for bacterial survival.⁴⁸ Inhibition of Rv1258c with chlorpromazine restored activity of spectinomycin which reaffirms the utility of Rv1258c efflux pump inhibitors in synergistic combinations with existing antimycobacterials affected by efflux through this pump.⁴⁴ Clinical use of efflux pump inhibitors e.g. chlorpromazine has thus far been obstructed by toxicity concerns due to the promiscuous inhibition of prokaryotic and eukaryotic efflux pumps.^{5,41,49} The search for efflux pump inhibitors selectively targeting prokaryotic efflux pumps is ongoing.

1.2.1 Polycyclic cage compounds as efflux pump inhibitors

The synthesis, pharmacology and medicinal application of the polycyclic cage compounds have been the focus of various research groups since the discovery of the antiviral properties of amantadine.⁵⁰ Initial interest in the polycyclic amantadine and pentacycloundecane derivatives evaluated in this study centred on their role in cardiovascular disease and neuroprotection. A review on the polycyclic cage derivatives discuss the L-type calcium channel inhibitory properties of these compounds, their *N*-methyl-D-Aspartate (NMDA) and sigma receptor antagonistic properties, their role in monoamine oxidase B inhibition and the ability of these derivatives to inhibit nitric oxide synthase. The review also discusses the importance of the polycyclic cage moiety as a lipophilic scaffold to improve the blood brain barrier permeability of selected structures.⁵¹

Of particular interest to efflux inhibitory activity is the ability of these compounds to block L-type calcium channels or modulate intracellular calcium levels. The L-type calcium channel inhibitor verapamil is a known inhibitor of various classes of efflux pumps implicated in drug resistance in protozoa, bacteria and mammalian cancer cell lines. Although not used clinically due to systemic side

effects, verapamil is widely used in biological evaluation of efflux activity across a range of cell lines. The L-type calcium channel inhibitory activity as well as structure activity relationships for calcium channel inhibition in the polycyclic cage derivatives have been well described. Various studies have demonstrated neuronal cell calcium channel inhibitory activity for a range of polycyclic cage derivatives.⁵²⁻⁵⁴ These compounds are also believed to be p-glycoprotein inhibitors and a study on a range of chloroquine-based cage compound derivatives demonstrated chloroquine resistance reversal in chloroquine resistant *Plasmodium falciparum*. NGP1-01, a pentacycloundecane derivative with L-type calcium channel and NMDA receptor inhibitory activity, reduced the IC₅₀ value of chloroquine in chloroquine resistant *Plasmodium* by approximately 50 % at a 10 µM concentration.^{55,56} It is therefore possible that selected polycyclic cage derivatives would inhibit efflux pump activity with a similar mechanism of action to verapamil or other calcium channel inhibitors.

1.3 The use of *in silico* drug design methods to identify and better understand molecular interactions of antimycobacterial compounds.

Computer aided or *in silico* drug design has become a fundamental part of the drug design and discovery process. Computer aided drug design (CADD) is more cost effective than conventional drug design strategies and has numerous advantages including visualization of molecular interactions of compounds with a target, fast screening of compound libraries, prediction of pharmacokinetic properties of compounds of interest and a reduction in the use of animal models. The crystal structure of the target protein is central to many of the *in silico* methodologies including screening of compound libraries for activity and prediction of binding of molecules within the target receptor. When the crystal structure of the protein of interest is not available, as is the case with mycobacterial efflux pumps, it is possible to predict the three-dimensional structure of the protein through homology modelling.

Homology modelling is a computational method of building a target protein based on the three-dimensional structure of a template protein with a high sequence similarity. Sequence alignment of the target protein with the template protein is performed after which a backbone is constructed and additional side chains are added. Once the model is constructed, it is further refined using various computational techniques based on existing knowledge of protein structures and the structure is validated. The identification of a suitable template to use as a starting point for the homology model is of great importance. Homology modelling of membrane bound proteins, as is the case with efflux pumps, requires further consideration of the constraints of the environment on the structure and fold of the protein.⁵⁷ If done correctly a homology model of a protein can be a valuable tool to use in molecular modelling studies.

It is also possible to predict the effects of single nucleotide polymorphisms and other mutations in proteins with a known crystal structure to model the effects of the observed mutations on the binding of compounds to the target protein. The prediction of the effect of mutations on the structure and function of proteins forms a part of what is referred to as computer aided mutagenesis studies and can be used to predict the effects of mutations on the function and structure of the protein of interest and can contribute to the understanding of experimental observation.⁵⁸

1.4 Conclusion

In conclusion, all of the considerations mentioned in this discussion are ultimately aimed at increasing the accumulation of active compounds within the mycobacterial cell, either through increased entry, reduced active efflux or diminished integrity of the mycobacterial cell wall. Active moieties linked to polycyclic carriers may successfully enter the mycobacterial cell and synergise with other antimycobacterial agents by nature of decreased cell wall integrity and efflux inhibition. Computer aided drug design can be used to identify efflux pump inhibitors and further investigate study observations through molecular modelling and mutagenesis studies. The aims for this study were therefore:

1. Evaluate a series of polycyclic compounds from the Drug Design Group compound library for antimycobacterial activity.
2. Investigate the mechanism of antimycobacterial activity for active molecules and further explore compounds which may promote resistance reversal.
3. Explore possible efflux pump inhibition of selected compounds utilizing synergism assays with known mycobacterial efflux pump substrates.
4. Utilize *in silico* methods to promote the rational drug design and discovery of mycobacterial efflux pump inhibitors and further explore compound-protein interactions to determine the role of protein mutations on drug resistance.

A number of research activities were performed to achieve the objectives as set out above. The results of the research activities were published in 5 peer reviewed articles included in chapters 2 to 6. The order of inclusion of the research articles are based on the flow of research activities, rather than the date of publication. Initial research activities included a literature review on rational drug design of efflux pump inhibitors, which was followed by the development of a homology model of the well-known mycobacterial efflux pump, Rv1258c. Publications stemming from these research activities are presented in chapters 2 and 3. In parallel, an evaluation of the antimycobacterial activity for the full series of in-house polycyclic compounds were performed. The results of the evaluations were published and are included in chapters 4 and 5. Chapter 6 contains the publication on the evaluation of efflux pump inhibitory activity of a smaller series of specifically selected compounds.

References:

1. Global tuberculosis report 2022. <https://www.who.int/publications/i/item/9789240061729>. Accessed November 16, 2022.
2. World Health Organisation. Global tuberculosis report 2021. <https://www.who.int/publications/i/item/9789240037021>. Published 2021. Accessed September 9, 2022.
3. Viveiros M, Martins M, Rodrigues L, et al. Inhibitors of mycobacterial efflux pumps as potential boosters for anti-tubercular drugs. *Expert Rev Anti Infect Ther*. 2012;10(9):983-998. doi:10.1586/eri.12.89
4. da Silva PE, Groll A Von, Martin A, Palomino JC. Efflux as a mechanism for drug resistance in *Mycobacterium tuberculosis*. *FEMS Immunol Med Microbiol*. 2011;63(1):1-9. doi:10.1111/j.1574-695X.2011.00831.x
5. Rodrigues L, Cravo P, Viveiros M. Efflux pump inhibitors as a promising adjunct therapy

- against drug resistant tuberculosis: a new strategy to revisit mycobacterial targets and repurpose old drugs. *Expert Rev Anti Infect Ther.* 2020;18(8):741-757. doi:10.1080/14787210.2020.1760845
6. Bottger EC. Drug resistance in Mycobacterium tuberculosis: Molecular mechanisms and susceptibility testing. In: Donald PR, Van Helden PD, eds. 1st ed. Antituberculosis Chemotherapy. Basel: Karger Medicinal and Scientific Publishers; 2011:128.
 7. Hernando-Amado S, Blanco P, Alcalde-Rico M, et al. Multidrug efflux pumps as main players in intrinsic and acquired resistance to antimicrobials. *Drug Resist Updat.* 2016;28:13-27. doi:10.1016/J.DRUP.2016.06.007
 8. World Health Organization. GLASS | Global antimicrobial resistance and use surveillance system (GLASS) report. Global antimicrobial resistance and use surveillance system report 2020. <https://www.who.int/glass/resources/publications/early-implementation-report-2020/en/>. Accessed May 19, 2021.
 9. World Health Organization. Antimicrobial resistance: global report on surveillance. 2014;2016(06/24). <http://www.who.int/drugresistance/documents/surveillancereport/en/>.
 10. Rodrigues L, Parish T, Balganesch M, Ainsa JA. Antituberculosis drugs: reducing efflux = increasing activity. *Drug Discov Today.* 2017;22(3). doi:10.1016/j.drudis.2017.01.002
 11. Da Silva PEA, Palomino JC. Molecular basis and mechanisms of drug resistance in Mycobacterium tuberculosis: classical and new drugs. *J Antimicrob Chemother.* 2011;66(7):1417-1430. doi:10.1093/jac/dkr173
 12. Sarathy JP, Dartois V, Lee EJD. The Role of Transport Mechanisms in Mycobacterium Tuberculosis Drug Resistance and Tolerance. *Pharmaceuticals.* 2012;5(11):1210-1235. doi:10.3390/ph5111210
 13. Peterson E, Kaur P. Antibiotic resistance mechanisms in bacteria: Relationships between resistance determinants of antibiotic producers, environmental bacteria, and clinical pathogens. *Front Microbiol.* 2018;9(NOV):2928. doi:10.3389/fmicb.2018.02928
 14. Vilchèze C. Mycobacterial Cell Wall: A Source of Successful Targets for Old and New Drugs. *Appl Sci 2020, Vol 10, Page 2278.* 2020;10(7):2278. doi:10.3390/APP10072278
 15. Abrahams KA, Besra GS. Mycobacterial cell wall biosynthesis: a multifaceted antibiotic target. *Parasitology.* 2018;145(2):116-133. doi:10.1017/S0031182016002377
 16. Chiaradia L, Lefebvre C, Parra J, et al. Dissecting the mycobacterial cell envelope and defining the composition of the native mycomembrane. *Sci Reports 2017 71.* 2017;7(1):1-12. doi:10.1038/s41598-017-12718-4
 17. Vincent AT, Nyongesa S, Morneau I, Reed MB, Tocheva EI, Veyrier FJ. The mycobacterial cell envelope: A relict from the past or the result of recent evolution? *Front Microbiol.* 2018;9(OCT):2341. doi:10.3389/FMICB.2018.02341/BIBTEX
 18. Butler MS, Paterson DL. Antibiotics in the clinical pipeline in October 2019. *J Antibiot 2020* 736. 2020;73(6):329-364. doi:10.1038/s41429-020-0291-8
 19. Degiacomi G, Belardinelli JM, Pasca MR, Rossi E De, Riccardi G, Chiarelli LR. Promiscuous Targets for Antitubercular Drug Discovery: The Paradigm of DprE1 and MmpL3. *Appl Sci 2020, Vol 10, Page 623.* 2020;10(2):623. doi:10.3390/APP10020623
 20. Liu J, Shi W, Zhang S, et al. Mutations in efflux pump Rv1258c (Tap) cause resistance to pyrazinamide, isoniazid, and streptomycin in M. tuberculosis. *Front Microbiol.* 2019;10(FEB). doi:10.3389/fmicb.2019.00216
 21. Shao M, McNeil M, Cook GM, Lu X. MmpL3 inhibitors as antituberculosis drugs. *Eur J Med*

- Chem.* 2020;200. doi:10.1016/J.EJMECH.2020.112390
22. Umare MD, Khedekar PB, Chikhale R V. Mycobacterial Membrane Protein Large 3 (MmpL3) Inhibitors: A Promising Approach to Combat Tuberculosis. *ChemMedChem.* 2021;16(20):3136-3148. doi:10.1002/CMDC.202100359
 23. Williams JT, Haiderer ER, Coulson GB, et al. Identification of New MmpL3 Inhibitors by Untargeted and Targeted Mutant Screens Defines MmpL3 Domains with Differential Resistance. *Antimicrob Agents Chemother.* 2019;63(10). doi:10.1128/AAC.00547-19
 24. Li M, Phua ZY, Xi Y, et al. Potency Increase of Spiroketal Analogs of Membrane Inserting Indolyl Mannich Base Antimycobacterials Is Due to Acquisition of MmpL3 Inhibition. *ACS Infect Dis.* 2020;6(7):1882. doi:10.1021/ACSINFECDIS.0C00121
 25. Zhang B, Li J, Yang X, et al. Crystal Structures of Membrane Transporter MmpL3, an Anti-TB Drug Target. *Cell.* 2019;176(3):636-648.e13. doi:10.1016/J.CELL.2019.01.003
 26. Viljoen A, Dubois V, Girard-Misguich F, Blaise M, Herrmann JL, Kremer L. The diverse family of MmpL transporters in mycobacteria: from regulation to antimicrobial developments. *Mol Microbiol.* 2017;104(6):889-904. doi:10.1111/MMI.13675
 27. Bolla JR. Targeting MmpL3 for anti-tuberculosis drug development. *Biochem Soc Trans.* 2020;48(4):1463-1472. doi:10.1042/BST20190950
 28. Chen P, Gearhart J, Protopopova M, Einck L, Nacy CA. Synergistic interactions of SQ109, a new ethylene diamine, with front-line antitubercular drugs in vitro. *J Antimicrob Chemother.* 2006;58(2):332-337. doi:10.1093/jac/dkl227
 29. McNeil MB, Chettiar S, Awasthi D, Parish T. Cell wall inhibitors increase the accumulation of rifampicin in Mycobacterium tuberculosis. *Access Microbiol.* 2019;1(1):e000006. doi:10.1099/ACMI.0.000006
 30. Dashti Y, Grkovic T, Quinn RJ. Predicting natural product value, an exploration of anti-TB drug space. *Nat Prod Rep.* 2014;31(8):990-998. doi:10.1039/C4NP00021H
 31. Makarov V, Lechartier B, Zhang M, et al. Towards a new combination therapy for tuberculosis with next generation benzothiazinones. *EMBO Mol Med.* 2014;6(3):372. doi:10.1002/EMMM.201303575
 32. Piccaro G, Poce G, Biava M, Giannoni F, Fattorini L. Activity of lipophilic and hydrophilic drugs against dormant and replicating Mycobacterium tuberculosis. *J Antibiot (Tokyo).* 2015;68(11):711-714. doi:10.1038/ja.2015.52
 33. Benet LZ, Hosey CM, Ursu O, Oprea TI. BDDCS, the Rule of 5 and Drugability. *Adv Drug Deliv Rev.* 2016;101:89. doi:10.1016/J.ADDR.2016.05.007
 34. Lipinski CA. Drug-like properties and the causes of poor solubility and poor permeability. *J Pharmacol Toxicol Methods.* 2000;44(1):235-249. doi:10.1016/S1056-8719(00)00107-6
 35. Putman M, van Veen HW, Konings WN. Molecular properties of bacterial multidrug transporters. *Microbiol Mol Biol Rev.* 2000;64(4):672-693.
 36. Hassan KA, Liu Q, Henderson PJF, Paulsen IT. Homologs of the Acinetobacter baumannii aceI transporter represent a new family of bacterial multidrug efflux systems. *MBio.* 2015;6(1). doi:10.1128/MBIO.01982-14
 37. Rossi E De, Aínsa JA, Riccardi G. Role of mycobacterial efflux transporters in drug resistance: an unresolved question. *FEMS Microbiol Rev.* 2006;30(1):36-52. doi:10.1111/J.1574-6976.2005.00002.X
 38. Alcalde-Rico M, Hernando-Amado S, Blanco P, Martínez JL. Multidrug efflux pumps at the crossroad between antibiotic resistance and bacterial virulence. *Front Microbiol.*

- 2016;7(SEP):1483. doi:10.3389/FMICB.2016.01483
39. Ghajavand H, Kargarpour Kamakoli M, Khanipour S, et al. Scrutinizing the drug resistance mechanism of multi- and extensively-drug resistant Mycobacterium tuberculosis: Mutations versus efflux pumps. *Antimicrob Resist Infect Control*. 2019;8(1):1-8. doi:10.1186/S13756-019-0516-4
 40. Ismail N, Ismail NA, Omar S V., Peters RPH. In Vitro Study of Stepwise Acquisition of rv0678 and atpE Mutations Conferring Bedaquiline Resistance. *Antimicrob Agents Chemother*. 2019;63(8). doi:10.1128/AAC.00292-19
 41. Kapp E, Malan SF, Joubert J, Sampson SL. Small Molecule Efflux Pump Inhibitors in Mycobacterium tuberculosis: A Rational Drug Design Perspective. *Mini-Reviews Med Chem*. 2017;18(1). doi:10.2174/1389557517666170510105506
 42. Schmalstieg AM, Srivastava S, Belkaya S, et al. The antibiotic resistance arrow of time: efflux pump induction is a general first step in the evolution of mycobacterial drug resistance. *Antimicrob Agents Chemother*. 2012;56(9):4806-4815. doi:10.1128/AAC.05546-11
 43. Machado D, Coelho TS, Perdigão J, et al. Interplay between Mutations and Efflux in Drug Resistant Clinical Isolates of Mycobacterium tuberculosis. *Front Microbiol*. 2017;0(APR):711. doi:10.3389/FMICB.2017.00711
 44. Omollo C, Singh V, Kigonda E, et al. Developing Synergistic Drug Combinations To Restore Antibiotic Sensitivity in Drug-Resistant Mycobacterium tuberculosis. *Antimicrob Agents Chemother*. 2021;65(5). doi:10.1128/aac.02554-20
 45. Balganes M, Dinesh N, Sharma S, Kuruppath S, Nair A V., Sharma U. Efflux Pumps of Mycobacterium tuberculosis Play a Significant Role in Antituberculosis Activity of Potential Drug Candidates. *Antimicrob Agents Chemother*. 2012;56(5):2643-2651. doi:10.1128/AAC.06003-11
 46. Lee RE, Hurdle JG, Liu J, et al. Spectinamides: a new class of semisynthetic antituberculosis agents that overcome native drug efflux. *Nat Med*. 2014;20(2):152-158. doi:10.1038/nm.3458
 47. Rodrigues L, Machado D, Couto I, Amaral L, Viveiros M. Contribution of efflux activity to isoniazid resistance in the Mycobacterium tuberculosis complex. *Infect Genet Evol*. 2012;12(4):695-700. doi://dx.doi.org/10.1016/j.meegid.2011.08.009
 48. Jia H, Chu H, Dai G, Cao T, Sun Z. Rv1258c acts as a drug efflux pump and growth controlling factor in Mycobacterium tuberculosis. *Tuberculosis*. 2022;133:102172. doi:10.1016/j.tube.2022.102172
 49. Opperman TJ, Nguyen ST. Recent advances toward a molecular mechanism of efflux pump inhibition. *Front Microbiol*. 2015;6:421. doi:10.3389/fmicb.2015.00421
 50. Davies WL, Grunert RR, Haff RF, et al. Antiviral Activity of 1-Adamantanamine (Amantadine). *Science*. 1964;144(3620):862-863.
 51. Joubert J, Geldenhuys WJ, VanderSchyf CJ, et al. Polycyclic Cage Structures as Lipophilic Scaffolds for Neuroactive Drugs. *ChemMedChem*. 2012;7(3):375-384. doi:10.1002/cmdc.201100559
 52. Grobler E, Grobler A, Van der Schyf CJ, Malan SF. Effect of polycyclic cage amines on the transmembrane potential of neuronal cells. *Bioorg Med Chem*. 2006;14(4):1176-1181. doi:10.1016/j.bmc.2005.09.042
 53. J.R. Lemmer H, Joubert J, van Dyk S, H. van der Westhuizen F, F. Malan S. S-Nitrosylation and Attenuation of Excessive Calcium Flux by Pentacycloundecane Derivatives. *Med Chem (Los Angeles)*. 2012;8(3):361-371. doi:10.2174/1573406411208030361

54. Zindo FT, Barber QR, Joubert J, Bergh JJ, Petzer JP, Malan SF. Polycyclic propargylamine and acetylene derivatives as multifunctional neuroprotective agents. *Eur J Med Chem*. 2014;80:122-134. doi:10.1016/j.ejmech.2014.04.039
55. Joubert J, Kapp E, Taylor D, Smith PJ, Malan SF. Polycyclic amines as chloroquine resistance modulating agents in Plasmodium falciparum. *Bioorg Med Chem Lett*. 2016;26(4):1151-1155. doi:10.1016/j.bmcl.2016.01.052
56. Yvette OM, Malan SF, Taylor D, Kapp E, Joubert J. Adamantane amine-linked chloroquinoline derivatives as chloroquine resistance modulating agents in Plasmodium falciparum. *Bioorganic Med Chem Lett*. 2018;28(8):1287-1291. doi:10.1016/j.bmcl.2018.03.026
57. Nikolaev DM, Shtyrov AA, Panov MS, et al. A Comparative Study of Modern Homology Modeling Algorithms for Rhodopsin Structure Prediction. *ACS Omega*. 2018;3(7):7555-7566. doi:10.1021/acsomega.8b00721
58. Verma R, Schwaneberg U, Roccatano D. Computer-Aided Protein Directed Evolution: A Review of Web Servers, Databases and Other Computational Tools For Protein Engineering. *Comput Struct Biotechnol J*. 2012;2(3):e201209008. doi:10.5936/CSBJ.201209008
59. Stanley SA, Kawate T, Iwase N, et al. Diarylcoumarins inhibit mycolic acid biosynthesis and kill Mycobacterium tuberculosis by targeting FadD32. *Proc Natl Acad Sci U S A*. 2013;110(28):11565-11570. doi:10.1073/pnas.1302114110



Chapter 2: Small Molecule Efflux Pump Inhibitors in *Mycobacterium tuberculosis*: A Rational Drug Design Perspective.

Kapp E, Malan SF, Joubert J, Sampson SL. Small Molecule Efflux Pump Inhibitors in *Mycobacterium tuberculosis*: A Rational Drug Design Perspective. Mini Rev Med Chem. 2018;18(1):72-86. doi: [10.2174/1389557517666170510105506](https://doi.org/10.2174/1389557517666170510105506)

Copyright statement: See Appendix 2.



Small Molecule Efflux Pump Inhibitors in *Mycobacterium tuberculosis*: a Rational Drug Design Perspective.

Erika Kapp^a, Sarel F. Malan^{*a}, Jacques Joubert^a, Samantha L. Sampson^b

*Address correspondence to this author at the School of Pharmacy, Faculty of Natural Sciences, University of the Western Cape, Private Bag X17, Bellville 7535, Republic of South Africa; Tel/Fax +27 21 959 2193, +27 21 959 1588; E-mail: sfmalan@uwc.ac.za.

Abstract: Drug resistance in *Mycobacterium tuberculosis* (*M. tuberculosis*) complicates management of tuberculosis. Efflux pumps contribute to low level resistance and acquisition of additional high-level resistance mutations through sub-therapeutic concentrations of intracellular antimycobacterials. Various efflux pump inhibitors (EPIs) have been described for *M. tuberculosis* but little is known regarding the mechanism of efflux inhibition. As knowledge relating to the mechanism of action and drug target is central to the rational drug design of safe and sufficiently selective EPIs, this review aims to examine recent developments in the study of EPIs in *M. tuberculosis* from a rational drug development perspective and to provide an overview to facilitate systematic development of therapeutically effective EPIs. Review of literature points to a reduction in cellular energy or direct binding to the efflux pump as likely mechanisms for most EPIs described for *M. tuberculosis*. This review demonstrates that, where a direct interaction with efflux pumps is expected, both molecular structure and general physicochemical properties should be considered to accurately predict efflux pump substrates and inhibitors. Non-competitive EPIs do not necessarily demonstrate the same requirements as competitive inhibitors and it is therefore essential to differentiate between competitive and non-competitive inhibition to accurately determine structure activity relationships for efflux pump inhibition. It is also evident that there are various similarities between inhibitors of prokaryotic and eukaryotic efflux pumps but, depending on the specific chemical scaffolds under investigation, it may be possible to design EPIs that are less prone to inhibition of human P-glycoprotein, thereby reducing side effects and drug-drug interactions.

Keywords:

Efflux pump inhibitor

Mycobacterium tuberculosis

Rational drug design

Drug resistance

Active efflux

Antimicrobial active transport systems

1. Introduction

Microbial drug resistance is fast becoming a significant risk to global public health. With the emergence of the human immunodeficiency virus (HIV) epidemic, tuberculosis (TB) was re-established as one of the most dangerous communicable diseases of our time. Treatment of TB is hampered by the development of multidrug-resistant (MDR) and extensively drug-resistant (XDR) TB. Drug resistance in *M. tuberculosis* can be intrinsic or acquired. Intrinsic resistance is attributed to the unusual structure of the mycobacterial cell wall as well as the natural abundance of efflux pumps (EPs) limiting the

intracellular accumulation of various classes of antibiotics [1 - 3]. Acquired resistance can usually be attributed to mutations in chromosomal genes. It has been established that mutations responsible for the resistance to various drugs are often not linked and that multidrug resistance is not due to a single genetic mutation but rather a result of a combination of multiple different mutations [4]. It is however possible that a complex association exists between mutations associated with one drug and the development of further resistance mutations [1]. Chromosomal alterations or deletions can affect the drug target, bacterial enzymes that activate/inactivate the drug and influx or efflux of drugs into/from the intracellular environment [2, 4, 5].

EPs contribute towards intrinsic and acquired mycobacterial resistance through their natural abundance, inducible expression and development of mutations that enhance efflux activity [2, 3]. Active efflux reduces the intracellular concentration of substrate compounds to sub-therapeutic levels thereby directly conferring resistance to the given substrate and likely facilitating the selection of genetically-encoded resistance brought on by sub-inhibitory chemotherapeutic exposure. Although overexpression of EPs is a well-recognized contributor to drug resistance to various chemotherapeutic agents employed in the management of mycobacterial disease, surprisingly little is known about the mechanism of efflux inhibition [2, 3, 6 - 8].

Five families of well-characterized antimicrobial active transport systems are described in literature. EPs are grouped into these families based on their structure and energy source used to facilitate active transport. Primary active transporters utilize ATP hydrolysis as energy source and include efflux pumps from the ATP-binding cassette (ABC) superfamily. The major facilitator superfamily (MFS), the small multidrug resistance family (SMR), the resistance-nodulation-cell division superfamily (RND) and the multi antimicrobial extrusion protein family (MATE) are all classified as secondary active transporters and employ an electrochemical potential difference or proton-motive force (PMF) to drive active efflux [9]. EPs can be substrate specific or, in the case of multidrug resistant pumps, facilitate efflux of a range of structurally unrelated compounds [5, 6]. The genome of *M. tuberculosis* encodes for efflux pumps from all 5 bacterial efflux pump families [7] and various ABC, MFS, SMR and RND efflux pumps have been characterised as antibiotic transporters [2]. It has however been suggested that PMF-driven efflux pumps play a larger role than ABC-type EPs in *M. tuberculosis* due to its strict aerobic nature [2].

Any strategy that increases the accumulation of active substrates within the target cell has the potential to mediate efflux pump-based resistance. These strategies could include interventions to increase the permeability of the cell wall, mechanisms to facilitate passive transport of drugs into the cell, adapting structures of molecules to reduce their tendency to act as substrates for EPs as well as inhibition of active efflux of antimycobacterials through efflux pumps. These approaches may address acquired resistance but can also be employed to overcome intrinsic resistance thereby allowing the use of a wider range of previously ineffective antibiotics in the treatment of *M. tuberculosis* [10 - 12]. Improved entry of the anti-mycobacterial compounds into the cell can be attained by disrupting the cell wall or by adapting the structure of the molecule to improve passive diffusion. Research suggests that more lipophilic derivatives within a class of antibiotics are likely to demonstrate higher antimycobacterial activity than their hydrophilic counterparts [2]. Enhanced passive diffusion can be achieved for certain molecules by increasing the lipophilicity of the compound through modification of functional groups or conjugation to lipophilic scaffolds. Increased entry into the mycobacterial cell may result in intracellular antimycobacterial concentrations beyond the extrusion capacity of EPs.

It is generally accepted that efflux pumps also recognize potential substrates based on the physicochemical properties of the compounds rather than just specific functional groups or chemical structure. It has also been suggested that efflux pumps preferentially transport amphiphilic compounds with distinct hydrophilic and lipophilic regions [10, 11, 14]. As various antimycobacterials

fall into this category, they are easily recognized and extruded by efflux pumps. Reducing the polarity of potential substrates may reduce the susceptibility of compounds to active efflux [15]. The rational development of spectinamides is an example of where structural modification of a lead compound resulted in derivatives that were able to circumvent efflux-based resistance [15, 16].

Active efflux may be modulated through alteration of the expression or functional assembly of efflux pumps (biological inhibition), through collapse or depletion of the efflux pump energy source or through direct interaction with the efflux pump (competitive and non-competitive inhibition of efflux) [10, 17 - 19]. The term efflux pump inhibitor (EPI) is widely used in literature to describe compounds that modulate efflux activity via any of these mechanisms, and does not necessarily refer to a direct interaction of the inhibitor with the efflux pump. Direct inhibition of prokaryotic efflux pumps through binding of the inhibitor to the efflux pump is rarely demonstrated [20].

Pharmaceutical inhibition of active efflux presents an attractive target for drug development as co-administration of EPIs with existing chemotherapeutic agents has the potential to restore activity and increase potency of a range of chemotherapeutic agents. In addition to increasing intracellular levels of co-administered compounds, inhibition of efflux pumps may also affect natural biological functions and energy metabolism of target cells, thereby directly interfering with the cell viability [21, 22]. EPIs in *M. tuberculosis* could circumvent innate resistance to antibiotics, minimize the development of resistance mutations, act synergistically with, or restore activity of standard antimycobacterials in resistant strains, decrease bacterial survival and reduce the duration of tuberculosis treatment [3, 23].

The ideal therapeutic efflux pump inhibitor should demonstrate limited toxicity to healthy host cells at the dosages required to obtain a sufficient synergistic chemotherapeutic effect against the cells or pathogens being targeted. This selective toxicity may be attained through specific inhibition of EPs that do not occur (or occur in lower numbers) in mammalian cells or through increased affinity for EP in target cell *versus* similar transporter proteins in mammalian cells. Increased sensitivity of target cells to modulation of efflux may also augment selective toxicity. It is important to remember that EPIs which also influence eukaryotic transporter activity, will likely affect the absorption, distribution and excretion of a range of compounds resulting in unpredictable plasma levels of co-administered medication. The possibility of these drug-drug interactions may limit the therapeutic safety of certain EPIs [10, 21, 24] and clinical development of several potential bacterial EPIs had to be halted due to toxicity problems [25].

2. A rational drug design perspective

Medicinal chemistry aims to link the chemical properties of molecules to bioactivity, and use this knowledge to aid drug discovery or improve the therapeutic index, pharmacokinetic profile and physicochemical properties of currently available therapeutic agents. Structure activity relationships (SAR) for bioactivity is easier to determine where a mechanism of action or specific drug target has been elucidated, or where activity is limited to entities with similar structural and chemical properties. A number of studies successfully suggested SAR or employed computer-based drug design of EPIs in bacteria where crystal structures for EPs are available [14]. The limited availability of crystal structures for EPs (particularly in *M. tuberculosis*), large structural diversity of putative EPIs, indiscriminate inhibition of a range of EPs by similar EPIs and limited knowledge relating to the specific interactions with EPs or even EPI mechanism of action, complicates rational drug design of EPIs [12, 13]. Thus far, authors have employed ligand-based drug design approaches or homology modelling of efflux pumps to suggest preliminary SARs for EPI activity in *M. tuberculosis* [23, 26, 27].

Efflux-mediated resistance and the development of EPIs is an ongoing research interest of various research groups and original research and review articles are regularly published in this field. In prokaryotic cells, and *Mycobacteria* in particular, there however seems to be a gap in investigations and reviews into the mechanism of action of efflux pump inhibition [3, 17, 29, 28]. One could argue that whole cell phenotypic screenings of compound libraries have been, and remain, effective identifiers of antimycobacterials [23] and EPIs, and that information relating to specific mechanisms of action or inhibition of efflux is not essential for this method of drug discovery. Rational drug development, as an alternative (or contributor to the aforementioned approach), could produce therapeutically active compounds that demonstrate suitable host pharmacokinetic properties, acceptable safety profiles and possibly exhibit reduced tendencies for development of resistance. As knowledge relating to the mechanism of action and drug target is central to the rational drug design approach, this review aims to examine recent developments in the study of EPIs in *M. tuberculosis* from a rational drug development perspective and provide an overview/platform to facilitate systematic development of safe and therapeutically effective EPIs.

3. Efflux pump inhibitors in *Mycobacterium tuberculosis*.

Various confirmed and putative EPI have been evaluated in *M. tuberculosis* over the past 2 decades. A paper by Kourtesi and colleagues describe a number of assays employed in the screening of EPI activity in bacteria [12]. A popular phenotypic assay for possible efflux inhibition in *Mycobacteria* is administration of the putative EPI with known antimycobacterials and assessment of the reduction in MIC or fold potentiation of the antimycobacterial. Some studies build on this MIC assessment by characterizing EPs that are overexpressed in the specific strains under evaluation and more recently performing fractional inhibitory concentration indices (FICI) assays that predict possible synergism between the putative EPI and the substrate in question. Researchers also utilize ethidium bromide (EB) and other fluorescent efflux pump substrates or dyes in functional assays of EP activity in mycobacteria. It is however pertinent to note that (1) reduction of the MIC or synergism observed with antimycobacterials may be obtained by mechanisms other than EP inhibition; (2) characterization of overexpressed EPIs does not confirm that the compound under evaluation interacts with all/any of the pumps identified; (3) EB assays measure accumulation of EB which reflects the balance between cell wall permeability and efflux activity and it may therefore be difficult to distinguish by which mechanism the compound under evaluation influences the accumulation of EB. However, when viewed together, these assays give a good indication of the likelihood of EP inhibitory activity and may indicate possible EP targets of the compound under evaluation. It is also important to note that extensive variation exists in the expression of EPs in different strains of *M. tuberculosis* and that experimental conditions, the substrate being evaluated and the concentration [30] of the EPI being used, to a large extent influences the activation of EPs and inhibition of efflux. That being said, table 1 provides a general classification of the more prominent putative EPIs that have been used in- or evaluated for activity in EPI assays in *M. tuberculosis*.

Table 1: Putative efflux pump inhibitors for *Mycobacterium tuberculosis*.

Efflux pump inhibitor class	Classification	References
Verapamil & analogues	Ion channel inhibitor	[18] [27 - 30] [33] [34] [37 -42]
Phenothiazine derivatives	Antipsychotic; Ion channel inhibitor	[23] [29] [30] [35] [45 - 49] [51] [54] [55] [59]
PaβN	RND-type efflux pump inhibitor	[25] [89 - 92]
Timcodar	P-gp inhibitor	[86 - 88]
Reserpine	Antihypertensive and antipsychotic, inhibitor of transport pumps and ion channels	[78 - 84]
Piperine	Activates TRPV ion channels; enzyme inhibitor; P-gp inhibitor.	[26] [27] [30] [63 - 70]
Berberine	Efflux pump substrate; potentiates effects of antibiotics and antifungals	[12] [71] [72 - 76] [81]
Tetrandrine	L-type calcium channel antagonist; P-gp inhibitor	[77] [84]

4. Mechanisms by which efflux is mediated.

Various mechanisms have been suggested for EP inhibition in prokaryotic cells. Interference with energy required for active efflux of substrates feature prominently but a direct interaction with efflux pumps, likely competitive inhibition, has also been suggested.

Energy for many cell processes including the activity of active transport systems is dependent on the ability of the cell to maintain transmembrane potential and generate and use ATP [31, 32]. Any compound that targets the electron transport chain and interferes with energy production of a cell directly affects cell viability but may also interfere with the ability of the cell to actively extrude compounds from the intracellular environment, thereby increasing the intracellular concentration of co-administered compounds [8, 22]. Proton motive force is the direct energy source for all secondary active transport pumps but also plays an important part in the production of ATP as utilized by the ABC super family to drive active efflux. The ability of a cell to maintain membrane potential is vital to generating sufficient PMF and energy for cellular processes. As transmembrane electrochemical potential is a function of the electrostatic or charge difference (electrical gradient) as well as the concentration difference of specific ions (chemical gradient) across the cell membrane, the action of ionophores, but also ion channel blockers, influence cellular energy levels. [22, 31, 33]. Compounds

that inhibit metabolic enzymes that yield hydronium ions required for the maintenance of PMF may also affect efflux in a similar fashion [20].

Various current and prospective antimycobacterials target the generation of proton motive force and ATP [8] and a number of putative EPIs have also been shown to deplete cellular energy [8, 34, 35]. As there are many similarities in the mechanisms of generation of cellular energy across cell types, selective toxicity to the cells that are targeted is a significant concern in the use and future development of therapeutic agents that utilize this mechanism of action. Even though protonophores are used as EPIs in some *in vitro* assays, their indiscriminate mechanism of action and/or host toxicity at doses required to inhibit efflux complicates (but does not exclude) development of these and similar compounds into viable therapeutic options [36]. Ion channel blockers instead, interact with specific channels to alter physiological movement of ions across membranes. Although blockage of ion channels may influence membrane potential and generation of cellular energy [22] as do protonophores, the mechanism by which this is achieved is more specific and eases systematic development of compounds with selective toxicity in cellular energy depletion. Depending on their potency and the role of the pumps being influenced, ion channel inhibitors could have direct antimicrobial activity and/or act synergistically with antimycobacterials as part of combination therapy [35].

Alternatively, a direct interaction with efflux pumps has also been suggested as a mechanism of action for efflux pump inhibition. This type of inhibition could be competitive or non-competitive in nature. Non-competitive inhibition could block access to substrate binding cavity or interfere with efflux pump conformation through interaction with an alternative binding site. In the case of competitive inhibition, the inhibitor would likely occupy the same binding cavity as the substrate. It could therefore be postulated that molecular and physicochemical properties for these competitive inhibitors may overlap with substrates for the specific efflux pump.

The molecular mechanism of action for substrate recognition and subsequent efflux depends on the efflux pump type, likely with additional variation between various pumps in that category, and within different species of bacteria. Fundamentally, the substrate would migrate or gain access to the efflux pump binding pocket and interact with various amino acids within this binding site, thereby initiating a change in conformation of the protein domain(s) with resulting extrusion of the substrate from the cytoplasm. The rate and extent of efflux would amongst others depend on the availability of energy (PMF or ATP) to drive active efflux. In certain efflux pump types, protonation or deprotonation of a number of ionisable amino acid residues within the various pump domains likely play a role in the extrusion process [9]. The suggested good recognition of amphiphilic compounds as substrates of efflux pumps may point to the need for both lipophilic interactions between the substrate and the binding cavity residues with hydrophobic side chains as well as interactions with residues with polar or charged side chains. The latter may influence the extent of ionization of various amino acids and thereby directly link to changes in the efflux pump conformation. Depending on the importance of ionic or polar interactions in efflux function as well as substrate and inhibitor recognition, the pKa of the compound and pH of the immediate environment may affect efflux to a greater or lesser extent. The non-specific nature of substrate recognition by a number of efflux pumps may result from the involvement of different residues within the binding pocket in the binding of diverse substrates [9, 14, 25]. Although there may be overlap between species and efflux pump types, the exact nature of substrate-efflux pump interactions and proceeding conformational changes are specific to an efflux pump and the particular substrate (or inhibitor) involved. These interactions are often investigated *in silico* where crystal structures of the efflux pump proteins are available [14]. It should also be possible to successfully predict interactions with the use of carefully constructed homology models. The lack of

crystal structures and homology models for efflux pumps in *M. tuberculosis* thus largely contribute to limited knowledge pertaining to the molecular mechanism of action of EPIs in *M. tuberculosis*.

Competitive inhibition has been demonstrated for various P-glycoprotein inhibitors in mammalian cells as well as for inhibitors of a number of efflux family types in bacterial cells. In *M. tuberculosis* a direct interaction with efflux pumps has been suggested as a mechanism of efflux inhibition for verapamil [27] and piperine [26]. Both publications suggest that the altered efflux activity of mycobacterial cells observed in the respective assays is due to an interaction of the evaluated derivatives with the MFS-type efflux pump Rv1258c. In *M. tuberculosis* Rv1258c has been extensively implicated in drug resistance to various antimycobacterials [27, 37].

5. Verapamil analogues

Verapamil is an inhibitor of L-type voltage dependent calcium channels and is used clinically to manage hypertension, cardiac arrhythmias, angina pectoris and cluster headaches [33, 38]. It is a phenylalkylamine derivative with one chiral carbon yielding the two stereoisomers, *R*- and *S*-verapamil (Figure 1). Clinically, verapamil is administered as a racemate even though different therapeutic properties and potencies have been described for the respective enantiomers [39, 40].

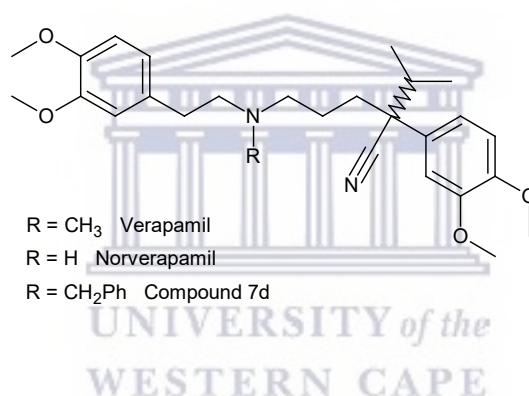


Figure 1: Chemical structures of verapamil and derivatives.

The ability of verapamil to block efflux pumps across cell types has been well described in literature. Numerous studies have demonstrated that verapamil blocks efflux pumps in *M. tuberculosis* and is able to decrease resistance to- and reduce the minimum inhibitory concentration of various antimycobacterials [27, 29, 30, 41, 42]. Verapamil inhibits efflux of several structurally unrelated compounds, seemingly extruded by both ATP-dependent and a range of proton motive force driven efflux pumps.

The mechanism of prokaryotic efflux pump inhibition of verapamil has not been fully elucidated. Some studies suggest a direct interaction with efflux pumps [27] while others propose a depletion of energy required for active efflux by ion channel inhibitors in general [18, 28, 29, 34]. Verapamil is an amphipathic molecule with a tertiary amine which is protonated at physiological pH (pKa 9.68 Chemaxon). As is the case with local anaesthetics with similar physicochemical properties, accumulation of verapamil within the lipid membrane may increase membrane permeability and interfere with the function of membrane proteins [43]. It has been suggested that the natural substrate pool for SMR and MFS efflux pumps comprise largely out of amphipathic cations [21] which may point to a certain extent of competitive antagonism of efflux. It is thus possible that the mechanism of efflux

inhibition may be a combination of the methods suggested above and that the experimental conditions, cell type, the substrate as well as specific EPs expressed and activated may to a large extent determine the mechanism through which efflux is inhibited.

5.1. Cellular energy: An article recently published by Machado and colleagues confirmed EPI activity of a range of therapeutic ion channel blockers (verapamil, chlorpromazine, thioridazine, flupenthixol and haloperidol) in an EB efflux assay in *M. tuberculosis* [35]. Of the compounds evaluated, verapamil showed the most potent inhibition of efflux. The same study demonstrated that these compounds resulted in a rapid reduction in intracellular ATP levels in *M. tuberculosis*. This depletion in energy could result from interference with membrane potential and generation of ATP. It might be worth noting that, in addition to interference with membrane potential, compounds that interfere with calcium movement and transport (e.g. verapamil and phenothiazines) may interfere with calcium dependent generation of energy from hydrolysis of ATP and thereby activity of efflux pumps [28, 34].

5.2. Direct interaction with efflux pumps: The use of verapamil as a chemosensitizer in multidrug resistant cancer cell lines has been extensively studied. The suggested mechanism of action in eukaryotic cells is *via* competitive antagonism of efflux through irreversible binding to the p-glycoprotein transporter. Studies suggest that efflux pump inhibition is likely independent of calcium channel blocking activity [44]. In *M. tuberculosis*, Adams and colleagues demonstrated that, despite their reduced cardiac activity, *R*-verapamil and norverapamil (pKa 10.29 Chemaxon) were as effective as verapamil in reducing macrophage-induced drug tolerance in an infected macrophage model. This would suggest that the mechanism of reversal of drug tolerance is not directly linked to the mammalian calcium channel activity of verapamil analogues [30].

Although many studies were able to characterize specific EPs that were overexpressed in *M. tuberculosis* strains where verapamil was able to reduce the MIC of- or reverse resistance to antimycobacterial agents (see table 1), few studies have demonstrated a direct interaction with any of the overexpressed EPs. One of these studies by Singh and colleagues evaluated the effect of verapamil and analogues on the MIC of rifampicin in *M. tuberculosis*. The authors suggested preliminary structure activity relationships for the interaction of verapamil with the efflux protein Rv1258c [27] that encodes for a secondary-active transporter from the major facilitator superfamily. Singh and colleagues synthesized a series of verapamil analogues and calculated fractional inhibitory concentration indices (FICI) to evaluate possible synergistic activity of these compounds with rifampicin against the laboratory strain H37Rv. Docking studies, using a validated homology model of Rv1258c, were performed with the derivatives demonstrating the best synergistic activity (7d, Figure 1, FICI = 0.3 *versus* verapamil FICI 0.5) and the binding affinity and residue interactions of 7d was compared to that of piperine, reserpine and verapamil. The authors were able to demonstrate favourable interactions with Rv1258c binding sites and multiple interactions with a combination of residues that also featured in the binding of verapamil, reserpine and piperine respectively. Compound 7d was shown to interact amongst others with the same arginine and glycine functions as piperine whereas verapamil formed hydrogen bonds with the same arginine amino acid as well as an additional tryptophan function [27]. Sharma and colleagues used a similar method to prepare an Rv1258c model for docking of piperine analogues as discussed in more detail later in the review [26].

Although not yet used clinically due to uncertainties relating to systemic side effects and drug-drug interactions with commonly used antimycobacterials, various authors have identified verapamil and verapamil analogues as good lead compounds for development of therapeutically useable EPIs.

6. Phenothiazine analogues

The phenothiazine class of compounds exhibit a wide range of therapeutic effects including antipsychotic, antiemetic, antihistaminergic and anticholinergic activities. Apart from these well-known effects, phenothiazines have also been evaluated for their anti-proliferative effect on various cell types as well as their ability to act synergistically with various chemotherapeutic agents [45].

The chemical structures of chlorpromazine and thioridazine, as examples of the general phenothiazine structure, are given in Figure 2.

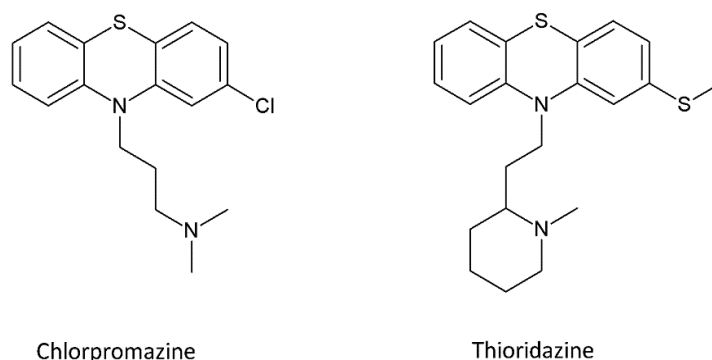


Figure 2: Phenothiazine chemical structures.

The polycyclic ring structure, which is important for the neurological action of the class, contributes to the lipophilicity of the compound and can be substituted with various groups on C-2 as well as the thiazine nitrogen to yield derivatives with varying therapeutic, and side effect profiles. A number of side effects including dyskinesia and extrapyramidal effects are commonly associated with these compounds but, when the intended therapeutic effect is antibacterial or chemotherapeutic synergism, any effect on eukaryotic cells may become an unwanted effect. The structure activity relationships for antipsychotic, calmodulin inhibitory, anti-proliferative and P-glycoprotein inhibitory activity of the phenothiazines were reviewed by Jaszczyszyn and colleagues [45]. Phenothiazine-type compounds are often designated as piperazine, piperidine or aliphatic phenothiazines based on the nature of the thiazine nitrogen substitution. Piperazine phenothiazines exhibit the strongest neuroleptic action with electronegative substitutions on C-2 further increasing the antipsychotic activity. The length of the carbon linker between the phenothiazine ring and the terminal nitrogen moiety influences the affinity of these compounds for the dopamine receptor but has also been linked to the calmodulin inhibitory activity of the phenothiazines. Calmodulin inhibition may play a role in the anti-proliferative and P-glycoprotein (P-gp) inhibitory activity of this class [46]. The C-2 substitution on the phenothiazine core, the presence of the lipophilic aromatic ring and the terminal amine function also seems to play an important role in calmodulin inhibition. Phenothiazine derivatives are weak bases which are mostly protonated at physiological pH. The amphiphilic nature of these compounds is important for their calmodulin inhibitory activity but may also play a role in their interaction with efflux pumps. The lipophilic cationic nature of the molecule also determines the degree of interaction with lipid membranes and thus influences the distribution patterns of the class [45 - 48].

Many authors are currently advocating for the inclusion of phenothiazines, more specifically thioridazine, in the treatment regimen for drug resistant tuberculosis (TB). Thioridazine has proven

effective as an adjunct therapy in non-responsive MDR patients, and with careful management of its side effects, may become a valuable drug in the management of drug resistant TB [49 - 51]. Various therapeutically employed phenothiazines have been evaluated for antimycobacterial activity. Thioridazine and chlorpromazine demonstrate comparatively effective *in vitro* activity [52] but, as thioridazine presents a better side effect profile, most research efforts have focused on thioridazine and derivatives thereof [51]. It has been suggested that phenothiazines exert their activity through (1) enhancement of intracellular killing by macrophages, (2) direct antimycobacterial activity *via* various mechanisms as well as (3) modulation of the pathogen efflux activity thereby potentiating activity of co-administered antimycobacterials.

The mechanism of antimicrobial activity of the phenothiazines has been investigated by a number of researchers. Thioridazine may modulate mycobacterial cell envelope integrity as well as interact with enzymes and proteins involved in the electron transport chain and aerobic respiration of bacterial cells, thereby altering the energy metabolism of *M. tuberculosis* [53 - 55]. Antimicrobial activity may be due to one, or a combination of these actions and even though concentrations necessary for *in vitro* antimycobacterial activity is therapeutically unattainable, accumulation of phenothiazines in macrophages afford these compounds *in vivo* activity [47, 51, 56].

Basic lipophilic drugs are known to accumulate extensively in tissues. This tissue accumulation is attributed to binding to phospholipids and accumulation in acidic compartments like lysosomes. The physicochemical properties of molecules as well as the phospholipid pattern and lysosome distribution of tissues determine which of the abovementioned methods are mainly responsible for the tissue accumulation [47]. Phospholipid binding results from an interaction of the basic functional groups of the molecules with the outward facing acidic moieties of the phospholipid layer [57] whereas lysosomal trapping is a function of the pH difference between the cytosol and lysosome. Amine containing neutral or weakly basic molecules in their unionised form diffuse across lysosomal membranes and become ionised in the acidic lysosomal environment. Protonation of these compounds limits passive diffusion across the lysosomal membrane and accordingly results in accumulation of the compound within the lysosome [47, 48]. The lipophilicity and acid dissociation constant of the various functional groups of drugs prone to lysosomal trapping will influence the amount and rate of accumulation within the lysosome. Chlorpromazine (Log P = 4.54, and pK_a = 9.2 Chemaxon) and thioridazine (Log P = 5.47, and pK_a = 8.93 Chemaxon) are prone to lysosomal accumulation and accordingly concentrate in macrophages which are rich in lysosomes [47,56]. Small changes in physicochemical properties or intracellular conditions may result in significant changes in the degree of lysosomal accumulation. It may also be worth noting that lysosomal accumulation is energy dependent (proton gradient between cytosol and lysosome is maintained by ATP-dependent proton pumps) and the extent of the trapping will likely be influenced by drug-drug interactions at a cellular distribution level [47, 48]. As the build-up of these compounds in macrophages plays an important part in achieving sufficient concentrations for *in vivo* antimycobacterial activity, functional and physicochemical properties that allow for this accumulation must be considered when phenothiazines are derivatized for the purpose of improving antimycobacterial activity.

Various reviews on the activity of phenothiazines in *Mycobacteria* mention that, apart from their direct antimicrobial action, phenothiazines promote intracellular killing of *M. tuberculosis* in macrophages [3, 34, 51, 58 - 61]. Potentiation of intracellular killing is attributed to the ability of these compounds to modulate potassium and calcium transport to- and from the lysosome resulting in acidification of the lysosomal environment and subsequent killing of the bacteria [28, 34, 58]. Martins and colleagues demonstrated that various compounds that inhibit K^+ and Ca^{2+} movement across membranes (e.g. verapamil and reserpine) have the ability to promote intracellular killing of MDR tuberculosis by non-

killing macrophages. The authors subsequently suggest that this approach could be explored as an alternative method of managing mycobacterial infections [28, 58]. Targeting eukaryotic K^+ and Ca^{2+} transport may result in host toxicity but accumulation of phenothiazines in macrophages affords these compounds a certain degree of selective toxicity as systemic concentrations could be maintained at concentrations below that which would result in unacceptable host side effects. The phenothiazine group may therefore be good lead compounds for drugs that promote intracellular killing of bacteria [58]. As noted above, properties that result in the accumulation of these compounds in macrophages should be maintained in the rational design of compounds that target this pathway.

In addition to the 2 antimycobacterial mechanisms described above, a number of studies report phenothiazine-mediated intracellular EB accumulation and antimycobacterial potentiation. These effects were attributed to possible efflux pump inhibitory activity by this group of compounds [28, 61, 62]. As mentioned previously, EB accumulation and potentiation of the activity or synergy observed with co-administered antimycobacterials may be due to effects other than efflux pump inhibition. A study by De Keijzer and colleagues quantitatively studied the proteome of *M. tuberculosis* and evaluated the accumulation of fluorescent dyes in cells of mycobacteria treated with thioridazine [55]. The authors suggest that increased cell wall permeability induced by thioridazine treatment may be the basis for the synergistic effect observed between thioridazine and various antimycobacterials. The study however also mentions that thioridazine may indirectly inhibit the activity of efflux pumps through reduction of energy available for active efflux as well as membrane mediated inhibition of efflux pumps resulting from the effect of thioridazine on mycobacterial cells. These mechanisms for efflux pump inhibition were also suggested by other authors [59, 61]. There have thus far not been any reports of a direct interaction of the phenothiazine-type compounds with mycobacterial efflux pumps and where these compounds inhibit efflux, it is likely through indirect modulation of efflux pump activity.

A recent study by Pieroni and colleagues used a ligand-based approach to design and synthesize thioridazine derivatives for the purpose of obtaining a compound with improved efficacy as an antimycobacterial adjuvant while limiting the side effects observed with thioridazine [23]. The nature of the heterocyclic ring was adapted to minimize neurological side effects while the *N*-methylpiperidine moiety was maintained, likely in consideration of efflux pump substrate affinity as well as basic amine related protonation in acidic lysosomes. The four derivatives that were selected for screening on *M. tuberculosis* all demonstrated reduced direct antimycobacterial activity, reduced toxicity towards human macrophages, good synergistic activity with various first and second line antimycobacterials *in vitro*, and potentiated the effect of rifampicin and isoniazid *ex vivo* at concentrations that were shown to be nontoxic to macrophages. The study also measured the effect of the synthesized compounds on EB accumulation and ultimately suggests efflux pump inhibitory activity as a mechanism for observed potentiation of antimycobacterials. This study is unique as it is the first report of rational design efforts aimed at the improvement of thioridazine for the purpose of enhancing its potential specifically as adjuvant antimycobacterial therapy. Positive results from this study show that with careful consideration of molecular properties required for activity and cellular distribution, it may be possible to use a ligand-based approach for the rational development of adjuvants for TB therapy, even in the absence of sufficient information relating to target or mechanism of action of the compounds.

7. Piperine

Piperine is the primary alkaloid responsible for the pungency of black pepper. The experienced pungency results from activation of highly calcium selective, vanilloid-type transient receptor potential cation channels (TRPV) [63]. Piperine is a piperidine derivative linked to a benzodioxole moiety *via* a 5-carbon linker. The ketone adjacent to the basic nitrogen of the piperidine moiety influences the protonation of the tertiary piperidine nitrogen at physiological pH. It has a predicted logP of 2.78 (Chemaxon) and is poorly soluble above 100 µg/ml, complicating its evaluation on the growth of microbes above this concentration [30].

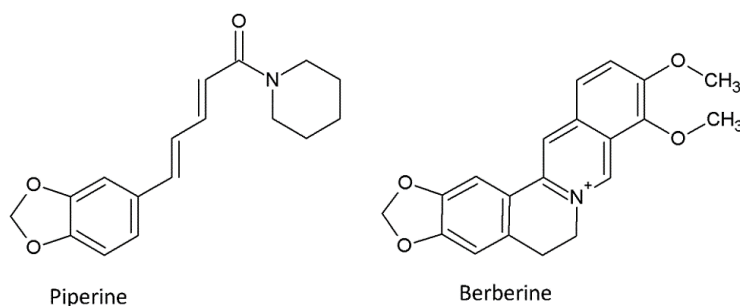


Figure 3: Piperine and berberine.

A plethora of therapeutic activities have been described for piperine and its derivatives [64, 65]. Amongst others, piperine non-competitively inhibits P-glycoprotein activity and is able to reduce the MIC of rifampicin and inhibit intracellular growth of *M. tuberculosis* [26, 30]. Piperine is reported to enhance the bioavailability of several unrelated pharmaceuticals and supplements through interference with drug absorption and metabolism [66]. The structure activity relationships for a number of these activities were recently reviewed [67]. Of particular interest to this review are the SAR for potentiation of ciprofloxacin activity (attributed to inhibition of the NorA efflux pump inhibitory activity) [26, 68, 69] and SAR for modulation of CYP450 enzyme activity. The NorA efflux pump is a MFS-type efflux pump in *Staphylococcus aureus* and as piperine has been shown to modulate both NorA and Rv1258c efflux activity [26], it may be worth considering SAR for NorA EPI when designing piperidine derivatives aimed at EP inhibition in *Mycobacteria*. SAR evaluations for NorA inhibitory activity have shown that the amide carbonyl is important for EP inhibition. The piperidine ring can however be replaced by various moieties on the amide nitrogen to enhance EPI activity. Substitutions containing electron withdrawing groups in this position also potentiate efflux inhibition. An unsaturated aliphatic chain seems to be important for EP inhibitory activity and the addition of alkyl chains, particularly ethyl and *n*-propyl, on C-4 further increases potency. The benzodioxole moiety was found to contribute to the NorA EP inhibition of these compounds [67].

Docking studies performed by Sharma and colleagues used a predicted 3D model of Rv1258c to model the interaction of piperine with this MSF-type *Mycobacterial* efflux pump [26]. Docking predictions indicated that the ketone function in piperine may form a hydrogen bond with an arginine moiety within the suggested active site of the Rv1258c model. Several other interactions were also observed with various residues within this binding pocket. The authors suggest that the abovementioned hydrogen bond may contribute to the efflux pump inhibitory activity of piperine. As discussed

previously, Singh and colleagues also used a model of Rv1258c to perform docking studies of reserpine, piperine, verapamil and verapamil analogues [27]. Apart from the verapamil binding interactions observed, their docking predictions also indicated possible hydrogen bond formation of the oxygen functions of the benzodioxole moiety of piperine with an arginine and glycine moiety in the putative binding site of Rv1258c. The authors suggest that hydrogen bonds may stabilize these protein-inhibitor complexes.

Unfortunately, the ability of piperine to interact with P-glycoprotein [66] and CYP450 enzymes will likely result in indiscriminate drug-drug interactions with co-administered medication and is certain to complicate the use of piperine-type compounds as boosters of antimycobacterial activity. SAR evaluations for enzyme inhibitory activity have shown that the specific combination of the methylenedioxyphenyl ring, alkyl linker and basic piperine moiety plays an important role in enzyme inhibition. Altering one or a combination of these moieties influences enzyme inhibitory activity but can also alter selectivity towards either inducible or constitutive enzymes specifically. A detailed overview of SAR for rat hepatic microsomal constitutive and inducible cytochrome P450 enzyme activity is described in a paper by Koul and colleagues [70] and these activities could be considered to potentially minimize enzyme inhibition.

Thus, taking the above into consideration, rational drug design endeavours targeting selective prokaryotic efflux pump inhibitory activity of piperine derivatives may consider maintaining the hydrophobic portion of the molecule but also including various hydrogen bond acceptors in order to allow stabilization of the interaction of the molecule with the efflux pump. Excluding structural features that potentiate enzyme interactions but which are not essential for EPI activity may reduce the side effect profile and drug-drug interaction of derivatives.

8. Other structures of interest

Although limited data exists around the *M. tuberculosis* EPI activity and mechanism of potentiation of other antimycobacterials for the compounds discussed below, the potential for development of these structures into future EPIs and/or structural and bioactivity similarities with well described *M. tuberculosis* EPIs warrant a brief mention in this review.

8.1. Berberine.

Berberine (Figure 3) shares a number of structural features with piperine and is an amphipathic, naturally occurring isoquinoline-type alkaloid with antimicrobial properties. It is a well-recognized efflux pump substrate and it has been demonstrated that the intracellular concentration of berberine is increased, and antimicrobial effect potentiated, when it is co-administered with efflux pump inhibitors [71, 72]. Berberine however similarly, potentiates the effect of several classes of co-administered antibiotics [73, 74]. Potentiation of antibiotic effect may result from competitive inhibition of efflux. Direct antimycobacterial activity has also been reported for berberine and derivatives [75] thereby adding to the overall value of including these compounds as part of an antimycobacterial regimen. Oral bioavailability of berberine may however be problematic and the reported low plasma levels after oral administration is attributed to, amongst others, poor absorption from the GIT, extensive first pass metabolism in the intestine and P-glycoprotein mediated efflux [76].

8.2. Tetrandrine.

The natural bis-benzylisoquinoline alkaloid, L-type calcium channel and P-glycoprotein inhibitor, tetrandrine (Figure 4) was able to reduce the MIC of isoniazid and ethambutol in clinical *M. tuberculosis* strains [77]. Similar to verapamil, tetrandrine contains hydrophobic planar aromatic rings as well as

tertiary nitrogens of which at least one will likely be protonated at physiological pH. These moieties have been identified as important structural features of P-gp mediated MDR reversing agents [77]. Tetrandrine may therefore modulate *Mycobacterial* efflux pump activity *via* a similar mechanism as verapamil.

8.3. Reserpine.

Reserpine is classified as an indole-type alkaloid with antipsychotic and antihypertensive properties. It is however rarely used therapeutically due to its extensive side effect profile. Reserpine binds irreversibly to the vesicular monoamine transporter membrane protein to block the transport of monoamine neurotransmitters [78]. Calcium channel antagonism has also been described for this compound [79]. Reserpine is able to inhibit efflux mediated by a variety of classes of efflux pumps and various studies have demonstrated that reserpine is able to reduce the MIC of- or increase mycobacterial susceptibility to a number of antimycobacterials [80 - 84]. It has been reported that reserpine mediates efflux *via* an interaction with glycine residues within the MFS-type, *Bacillus subtilis* efflux pump (Bmr) [85].

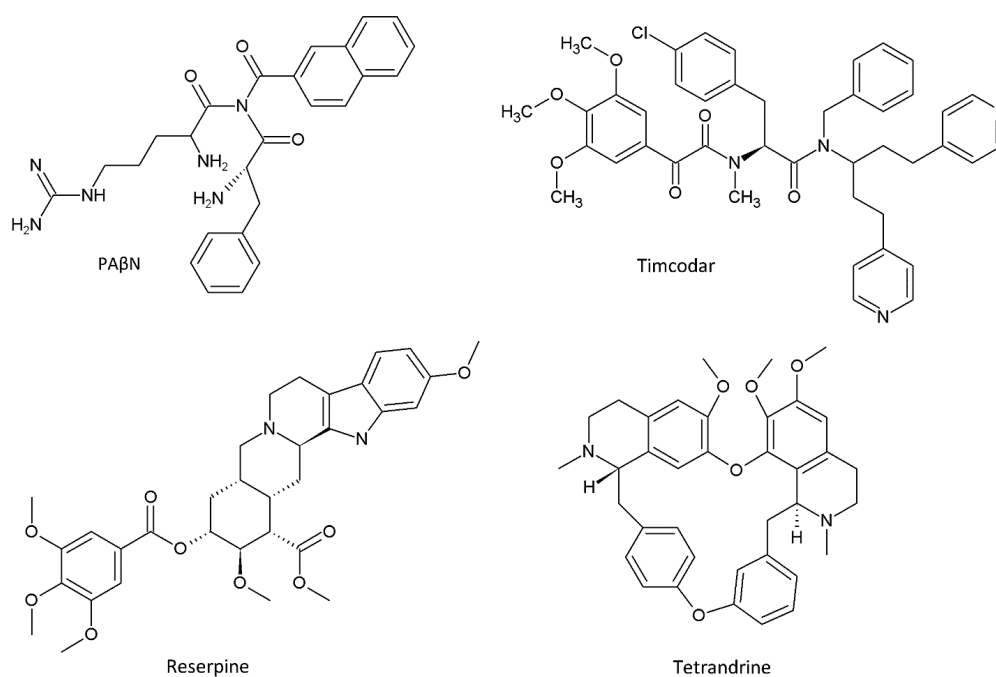


Figure 4: Structures of interest for EPI activity

8.4. Timcodar.

It was recently demonstrated that timcodar is able to increase the potency of rifampicin, bedaquiline and clofazimine *in vitro*, *ex vivo* and *in vitro*. The authors suggest that this potentiation likely results from a combination of bacterial and host-targeted mechanisms [86]. Timcodar and biricodar are 3rd generation modulators of P-gp and multidrug resistance proteins (MRPs) evaluated as enhancers of cancer therapy [87, 88]. Timcodar is highly lipophilic (log P = 6.87 chemaxon) with none of the tertiary nitrogens likely to be protonated at physiological pH. Despite biricodar entering phase II clinical trials

in 1998, neither of these compounds has received FDA approval as adjunctive therapy in cancer chemotherapy.

8.5. PA β N.

Phenylalanyl arginyl β -naphthylamide (PA β N) is a peptidomimetic EPI primarily reviewed for its activity on RND-type efflux pumps. The compound contains a guanidine moiety which will likely be protonated, as well as a number of primary amines which may be protonated to some extent at physiological pH. The development of PA β N and derivatives into therapeutic agents has been complicated by pharmacokinetic and toxicity problems experienced with this class. PA β N was identified as a lead compound from a large-scale screening of small molecules and a number of subsequent derivatives were made with the goal of improving activity, serum stability and toxicity profiles of the group [25, 89]. Compared to verapamil and thioridazine, PA β N has not been as extensively evaluated for mycobacterial EPI activity. Balganes and colleagues constructed *M. tuberculosis* knockout (KO) mutants of a number of efflux pumps from various efflux pump families and demonstrated that, when incubated with PA β N over the course of a few days, it was able to reduce the MIC of a pyrazolone-type compounds in the wild type but also to a lesser extent the KO mutants [90]. Their results indicate that the MIC reduction brought on by PA β N is likely due to inhibition of efflux activity. The ability of PA β N to still influence the MIC in the various KO mutants may however point to indiscriminate inhibition of a number of efflux pumps and/or contribution of an additional potentiation mechanism. After recent reports of outer membrane permeabilizing activity by PA β N [91], a study by Misra and colleagues employed real-time efflux assays to distinguish between efflux inhibition and membrane activity. The study concluded that the main mechanism of action of PA β N is inhibition of efflux activity followed by a delayed and weaker membrane destabilizing action likely observed after prolonged incubation of cells with PA β N. The authors do however mention that the cell wall permeabilizing activity of PA β N may be amplified in cells not sufficiently expressing efflux pumps [92]. These results may shed some light on the activity of PA β N as observed on knockout mutants of efflux pumps from various EP families as observed by Balganes [90]. PA β N and derivatives are believed to competitively inhibit efflux of several substrates of RND-type efflux pumps to varying degrees depending on their exact binding pocket in the transporter protein. A comprehensive review on the mechanism of efflux inhibition of RND-type efflux pumps describes efforts to maximize activity and reduce toxicity of this class of compounds in gram negative bacteria [25]. The basic moieties on the structure that were shown to be important for efflux inhibitory activity of this class also afford unfavourable pharmacokinetic properties and increased toxicity to these compounds and PA β N is therefore primarily used in efflux assays with little prospect of being developed into a therapeutic agent [25, 89].

8.6. Spectinomides.

Spectinomycin (Figure 5) is an antibiotic with structural similarities to the aminoglycoside antibiotics. The 1,3-diaminoinositol pharmacophore is uniquely linked to a sugar moiety to form tricyclic-type structure. It demonstrates strong bacterial ribosomal affinity with resulting inhibition of bacterial protein synthesis. It binds selectively to the bacterial ribosomal subunit and therefore does not share the toxicity profile of the standard aminoglycoside antibiotics. The unexpectedly low antimycobacterial effect of spectinomycin is attributed to extensive efflux by the Rv1258c efflux pump [16]. Lee and colleagues were able to design spectinomycin analogues that are able to circumvent active efflux by substituting the ketone function on the sugar with various amide carbonyl-linked functional groups. Pyrrole and piperidine rings, particularly halogen substituted piperidine analogues seem to demonstrate the most promising antimycobacterial and efflux pump circumventory activity [16]. These spectinomide derivatives demonstrate good affinity and selectivity for the bacterial ribosome with significantly improved antimycobacterial activity compared to the original spectinomycin molecule.

Subsequent research by this group established that the lead spectinamide derivative 1599 (Figure 5) is able to reduce the MIC of various co-administered antimycobacterials [93]. The researchers observed that co-administration of 1599 did not potentiate the activity of spectinomycin. This would suggest that the ability of 1599 to circumvent EP-mediated resistance is not due to inhibition of Rv1258c efflux as EP inhibition would have resulted in improved activity of spectinomycin when co-administered with 1599.

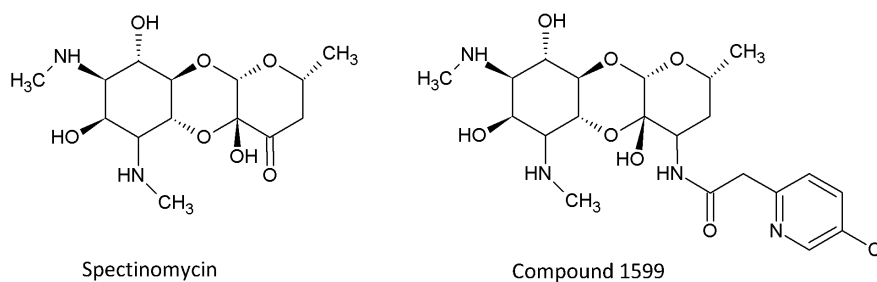


Figure 5: Spectinomycin and spectinamide derivatives

9. P-glycoprotein transport inhibitors

P-gps are well characterized transmembrane ATP-type transporter pumps that modulate transport of a large variety of substrates in the intestine, liver, kidneys and across the blood brain barrier amongst others [94]. P-gp transporter pumps influence the distribution and toxicity profiles of a broad range of compounds and their overexpression in certain cancer cells made modulation of these, and other similar pumps attractive targets to improve the efficacy of chemotherapy. Various P-gp inhibitors, of which verapamil was one of the first, were characterised and developed in an attempt to modulate the effect of efflux through these transporter pumps. The wide distribution and large range of physiological functions of P-gp pumps as well as the nonspecific substrate recognition observed with these efflux proteins, however resulted in unpredictable effects and numerous drug-drug interactions. To better predict the likelihood of inhibition of P-gp pumps and aid rational drug development of more specific P-gp inhibitors, various structure activity relationship studies were undertaken, and numerous models developed to predict substrates and inhibitors of this efflux pump type.

In silico prediction of substrates and inhibitors of P-gp activity is complicated by the promiscuous substrate recognition as well as a multifaceted molecule-transporter pump interaction profile which could include competitive as well as non-competitive inhibition or modulation [95]. A recent article by Montenari and colleagues reviewed current advances in prediction of ABC-transporter substrate and inhibitor interactions [96]. The authors report that structure activity relationships for P-gp interaction have been described for a range of diverse molecular scaffolds and suggest that this may point to local effects or binding sites unique to the type of scaffold within the P-gp pump. The suggested structure activity relationships often relate to general physicochemical properties of the molecule which may include lipophilicity, the presence of aromatic rings, functional groups that may become charged and the ability of the molecule to form hydrogen bonds. The authors also state that a clear set of rules for the molecular basis for molecule-pump interaction is yet to be established and that there is currently no definitive guide to aid the rational development of P-gp inhibitors or modulators [96].

Research published by Broccatelli and colleagues in 2011 [97] demonstrated the importance of considering both specific (related to the pharmacophore) and non-specific (general physicochemical / ADME) descriptors when predicting P-gp inhibition. The authors also note that molecules which may non-competitively inhibit P-gp efflux for example flavonoid and steroid type molecules require special consideration when attempting to predict P-gp inhibition *in silico*. Through a combination of model types that consider specific as well as general properties, the authors were able to predict P-gp inhibition with a good degree of accuracy. For competitive inhibition, the size, shape and flexibility of the molecule, the presence of a large hydrophobic area and at least one hydrogen bond acceptor as well as Log P of the molecule, seem to be strong predictors of inhibitory activity. The authors noted that a log P of less than 2 was a strong indicator of a non-inhibitor. Similarly, the role of nitrogens able to accept or donate hydrogens depending on the environment, was also highlighted as an important consideration of P-gp activity. For non-competitive inhibition (e.g. flavonoid and steroid-type molecules), size and flexibility seem to play a lesser role in predicting activity [97].

P-gp activity would most likely be an undesirable trait for efflux pump inhibitors targeting bacterial efflux pumps and it would be pertinent to consider, and where possible minimise, molecular properties that increase the likelihood of P-gp modulation. Due to the large variety of substrate and inhibitor scaffolds as well as the variable binding sites within the P-gp pump, the guidelines for predicting P-gp interaction are relatively vague. Consideration of the specific chemical scaffold as well as whether competitive or non-competitive (e.g. piperine) inhibition would be more likely for the structure under investigation would allow the design of a molecule that might be less likely to interact with P-gp pumps.

10. Conclusion

Ever increasing levels of drug resistance in *M. tuberculosis* necessitates novel approaches in utilization of available treatment options as well as in the design of future antimycobacterials. Apart from effectively targeting the pathogen, approaches to drug therapy of *M. tuberculosis* should centre around 1) preventing development of resistance, 2) overcoming current resistance and 3) developing future antimycobacterials that are less prone to the development of resistance.

Efflux pump activity in *M. tuberculosis* contribute to low level antimycobacterial resistance as well as the development of high level resistance through reduction of intracellular antimycobacterial concentrations. Inhibition of efflux activity is therefore an attractive target to overcome and prevent development of resistance to antimycobacterials. Various *Mycobacterial* EPIs are described in literature. Therapeutic use of these EPIs are however hampered by their side effect profile and unpredictable drug-drug interactions resulting from inhibition of mammalian transporter pumps and ion channels, amongst others.

Rational drug design endeavours have the potential to yield safer therapeutic EPIs with improved pharmacokinetic and pharmacodynamic properties. Knowledge relating to the mechanism of action and molecular target of the inhibition of efflux is however central to the rational drug design approach. Surprisingly little is known about the target site or even mechanism of action of EPIs in *Mycobacteria*. The aim of this review was therefore to examine what is known about the molecular properties and mechanism of action of a range of compounds that have been identified as putative EPIs in *M. tuberculosis* and highlight key considerations for the design of compounds for the purpose of minimizing efflux of antimycobacterials.

From the literature it is evident that the term efflux pump inhibitor is not necessarily indicative of a compound that directly binds to an efflux pump in order to inhibit efflux. Most studies investigating efflux pump inhibitory activity measure one or a combination of factors that may result from efflux

pump inhibition by the compound under investigation. As a matter of fact, binding to efflux pumps is rarely demonstrated. The lack of crystal structures for efflux proteins in *M. tuberculosis* hampers in-depth investigation into possible binding of EPIs to efflux pumps and researchers have thus far resorted to homology modelling to predict binding interactions of a handful of putative EPIs.

Apart from biological inhibition of efflux pump expression, efflux can be inhibited by direct interaction with the efflux pump or through interference with the energy source required for active efflux. Depending on the efflux pump family, efflux pumps rely on PMF or ATP-based energy to effect active efflux. Any compound that interferes with the availability or effective utilization of cellular energy could thus potentially inhibit efflux pump activity. In fact, interference with energy availability is a popular theory for the mechanism of efflux inhibition for various classes of EPIs. Not only protonophores, but any compound that interferes with the electrical or chemical gradient across the bacterial cell wall has the potential to reduce energy available for cellular functions. Amongst these are any compounds that interfere with the movement of ions across cell membranes for example verapamil and other calcium channel blockers as well as phenothiazine-type compounds. There seems to be consensus amongst authors that the phenothiazine class effects efflux inhibition through mechanisms other than a direct interaction with efflux pumps. Limited information and varied opinions however exist regarding the mechanism of efflux inhibition for other EPIs. It is possible that certain EPIs could inhibit efflux *via* an energy dependent or direct binding mechanisms, or a combination thereof, depending on assay conditions. It is clear from this review that there is limited information available relating to the mechanism of action of any of the classes of putative EPIs in *Mycobacteria*. Rational drug design efforts will therefore have to draw on information available for a particular type of EPI in other cell types, explore ligand-based drug design routes and consider employing homology models of the target efflux pump to predict binding interactions and thereby molecular requirements to maximise ligand-protein interactions.

In addition to good efflux inhibition, selective toxicity of EPIs should be a key consideration in the rational design of therapeutically safe EPIs. Achieving sufficient selective toxicity with compounds that afford efflux inhibition *via* a reduction in cellular energy may be difficult due to similarities in energy generation and utilization across cell types. Lysosomal accumulation of the phenothiazine-type compounds allows for the use of this class despite host side effects as accumulation in macrophages allow for the use of much lower doses than would normally be required to affect antimycobacterial activity. Any compounds designed to target the availability of energy for active efflux should accordingly prioritize selectivity over activity if compounds are to be used therapeutically. Similarly, where a direct interaction with efflux pumps is targeted, this interaction should be selective towards prokaryotic efflux pumps. Interactions with the P-gp efflux pumps for example, will complicate use of EPIs as these interactions are likely to result in drug-drug interactions and unpredictable plasma levels of any co-administered medication. P-gp inhibitory activity is relatively common with putative bacterial EPIs and has been described for verapamil, piperine, timcodar, tetrandrine and reserpine amongst others. This is not surprising as there seems to be a good degree of overlap between molecular properties that increase recognition by bacterial as well as mammalian efflux pumps. These characteristics include a higher Log P, distinct hydrophobic and hydrophilic areas within the molecule, the presence of atoms like basic nitrogens which may become charged and the ability of the molecule to form hydrogen bonds. In addition to P-gp inhibitory activity, a tendency to modulate mammalian ion channel activity also seem to be a common trend across numerous classes of compounds for which prokaryotic EPI activity has been described. Verapamil, tetrandrine, reserpine and the phenothiazine class compounds, amongst others, all demonstrate ion channel inhibitory activity. The ability of these compounds to block efflux pumps may however not necessarily be linked to their ability to block ion channels as is observed with *R*-verapamil and norverapamil which are able to maintain their capacity

to reverse drug tolerance despite their reduced cardiac activity when compared to verapamil. In order to minimize side effects and reduce drug-drug interactions, molecular properties that potentiate interactions with host transporter pumps, ion channels and enzyme systems should be considered throughout the drug design process.

Efflux pumps likely recognise potential substrates based on their physicochemical properties in addition to their molecular structure. This likely contributes to the indiscriminate efflux of a range of structurally diverse compounds by a single efflux pump type. To afford a compound efflux antagonism *via* competitive interaction with an efflux pump, the potential antagonist would likely have to share similar features to efflux pump substrates in order to gain entry or get into close proximity to the substrate binding pocket within the efflux protein. Once access to the binding pocket is attained, binding interactions with residues within the pocket should be of a more permanent nature than the substrate if anything more than purely competitive inhibition is to be achieved. The presence of moieties which are able to form hydrogen bonds may increase binding affinity of the putative EPI. Research suggests that efflux pumps preferentially transport compounds with clear hydrophilic and lipophilic regions and in a similar fashion, many putative EPIs also share this amphiphilic nature. Verapamil with its tertiary amine which is protonated at physiological pH is an example of this. It may therefore be useful to examine the molecular properties of known efflux pump substrates when embarking on rational drug design of an efflux pump inhibitor targeting a particular efflux pump(s). This approach may however not apply to compounds which act as non-competitive inhibitors of efflux.

The strategies mentioned above describe the rational development of EPIs that would likely be used in combination with an antibiotic which is a substrate for efflux pump(s). An alternative approach to employing EPIs in a polypharmacy approach is to design new, or adapt current antimycobacterials to naturally circumvent efflux. This was achieved with the spectinomycin antibiotics through altering the physicochemical properties that increase the likelihood of compounds being recognized as efflux pump substrates. Alternatively, strategies that increase cell wall permeation of compounds also has the potential to increase the intracellular concentration of antimycobacterials to concentrations above the extrusion capacity of efflux pumps. The addition of bulky polycyclic moieties to current or new antimycobacterials may reduce the effect of active efflux by decreasing the substrate fit within the efflux pump as well as through increased penetration into the mycobacterial cell by means of the increased lipophilicity afforded by the addition of these lipophilic moieties. Hybrid compounds as an alternate to the polypharmacy approach may also have several, particularly pharmacokinetic, advantages over co-administration of EPIs with antimycobacterials.

Circumvention of efflux-based resistance remains an attractive strategy to improve the therapeutic management of *Mycobacterial* disease. Even though this field has been explored for quite some time, the side effect profiles and unpredictable drug-drug interactions observed with possible EPI candidates has thus far precluded the therapeutic use of these compounds. Rational drug design may offer a solution to this problem through consideration of molecular properties that may increase selectivity of drug candidates for bacterial efflux pumps or afford selective toxicity through various other mechanisms. With limited information available regarding the mechanism of action and/or binding site of EPIs, the medicinal chemist will have to draw information from various sources and employ a combination of strategies to enable rational drug design of therapeutic EPIs.

Conflict of interest

None declared.

Acknowledgements

We are grateful to the National Research Foundation of South Africa for financial support. SLS is funded by the South African Research Chairs Initiative of the Department of Science and Technology and National Research Foundation (NRF) of South Africa, award number UID 86539. The content is solely the responsibility of the authors and does not necessarily represent the official views of the NRF.

References

1. da Silva, P. E.; Von Groll, A.; Martin, A.; Palomino, J. C. Efflux as a mechanism for drug resistance in Mycobacterium tuberculosis. *FEMS Immunol. Med. Microbiol.* **2011**, *63*, 1-9.
2. Sarathy, J. P.; Dartois, V.; Lee, E. J. D. The Role of Transport Mechanisms in Mycobacterium Tuberculosis Drug Resistance and Tolerance. *Pharmaceuticals (Basel)* **2012**, *5*, 1210-1235.
3. Viveiros, M.; Martins, M.; Rodrigues, L.; Machado, D.; Couto, I.; Ainsa, J.; Amaral, L. Inhibitors of mycobacterial efflux pumps as potential boosters for anti-tubercular drugs. *Expert Rev. Anti Infect. Ther.* **2012**, *10*, 983-998.
4. Bottger, E. C. In *Drug resistance in Mycobacterium tuberculosis: Molecular mechanisms and susceptibility testing*; Donald, P. R., Van Helden, P. D., Eds.; Antituberculosis Chemotherapy; Karger Medicinal and Scientific Publishers: Basel, 2011; pp 128.
5. Marquez, B. Bacterial efflux systems and efflux pumps inhibitors. *Biochimie* **2005**, *87*, 1137-1147.
6. Louw, G. E.; Warren, R. M.; Gey van Pittius, N. C.; McEvoy, C. R.; Van Helden, P. D.; Victor, T. C. A balancing act: efflux/influx in mycobacterial drug resistance. *Antimicrob. Agents Chemother.* **2009**, *53*, 3181-3189.
7. De Rossi, E.; Ainsa, J. A.; Riccardi, G. Role of mycobacterial efflux transporters in drug resistance: an unresolved question. *FEMS Microbiol. Rev.* **2006**, *30*, 36-52.
8. Black, P. A.; Warren, R. M.; Louw, G. E.; van Helden, P. D.; Victor, T. C.; Kana, B. D. Energy Metabolism and Drug Efflux in Mycobacterium tuberculosis. *Antimicrobial Agents and Chemotherapy* **2014**, *58*, 2491-2503.
9. Putman, M.; van Veen, H. W.; Konings, W. N. Molecular properties of bacterial multidrug transporters. *Microbiol. Mol. Biol. Rev.* **2000**, *64*, 672-693.
10. Van Bambeke, F.; Pages, J. M.; Lee, V. J. Inhibitors of bacterial efflux pumps as adjuvants in antibiotic treatments and diagnostic tools for detection of resistance by efflux. *Recent. Pat. Antiinfect Drug Discov.* **2006**, *1*, 157-175.
11. Dinesh, N.; Sharma, S.; Balganes, M. Involvement of Efflux Pumps in the Resistance to Peptidoglycan Synthesis Inhibitors in Mycobacterium tuberculosis. *Antimicrobial Agents and Chemotherapy* **2013**, *57*, 1941-1943.
12. Kourtesi, C.; Ball, A. R.; Huang, Y. Y.; Jachak, S. M.; Vera, D. M.; Khondkar, P.; Gibbons, S.; Hamblin, M. R.; Tegos, G. P. Microbial efflux systems and inhibitors: approaches to drug discovery and the challenge of clinical implementation. *Open Microbiol. J.* **2013**, *7*, 34-52.
13. Van Bambeke, F.; Michot, J. M.; Tulkens, P. M. Antibiotic efflux pumps in eukaryotic cells: occurrence and impact on antibiotic cellular pharmacokinetics, pharmacodynamics and toxicodynamics. *J. Antimicrob. Chemother.* **2003**, *51*, 1067-1077.

14. Roy, K., Ed.; In *Quantitative structure-activity relationships in drug design, predictive toxicology, and risk assessment*; Medical Information Science: Hershey PA, USA, 2015.
15. Viveiros, M.; Pieroni, M. Spectinamides: a challenge, a proof, and a suggestion. *Trends Microbiol.* **2014**, *22*, 170-171.
16. Lee, R. E.; Hurdle, J. G.; Liu, J.; Bruhn, D. F.; Matt, T.; Scherman, M. S.; Vaddady, P. K.; Zheng, Z.; Qi, J.; Akbergenov, R.; Das, S.; Madhura, D. B.; Rathi, C.; Trivedi, A.; Villellas, C.; Lee, R. B.; Rakesh, ; Waidyarachchi, S. L.; Sun, D.; McNeil, M. R.; Ainsa, J. A.; Boshoff, H. I.; Gonzalez-Juarrero, M.; Meibohm, B.; Bottger, E. C.; Lenaerts, A. J. Spectinamides: a new class of semisynthetic antituberculosis agents that overcome native drug efflux. *Nat. Med.* **2014**, *20*, 152-158.
17. Pagès, J.; Amaral, L. Mechanisms of drug efflux and strategies to combat them: Challenging the efflux pump of Gram-negative bacteria. *Biochimica et Biophysica Acta (BBA) - Proteins and Proteomics* **2009**, *1794*, 826-833.
18. Zechini, B.; Versace, I. Inhibitors of multidrug resistant efflux systems in bacteria. *Recent. Pat. Antiinfect Drug Discov.* **2009**, *4*, 37-50.
19. Bhardwaj, A. K.; Mohanty, P. Bacterial efflux pumps involved in multidrug resistance and their inhibitors: rejuvenating the antimicrobial chemotherapy. *Recent. Pat. Antiinfect Drug Discov.* **2012**, *7*, 73-89.
20. Amaral, L.; Martins, A.; Spengler, G.; Molnar, J. Efflux pumps of Gram-negative bacteria: what they do, how they do it, with what and how to deal with them. *Frontiers in Pharmacology* **2013**, *4*, 168.
21. Tegos, G. P.; Haynes, M.; Strouse, J. J.; Khan, M. M.; Bologna, C. G.; Oprea, T. I.; Sklar, L. A. Microbial efflux pump inhibition: tactics and strategies. *Curr. Pharm. Des.* **2011**, *17*, 1291-1302.
22. Martins, A.; Machado, L.; Costa, S.; Cerca, P.; Spengler, G.; Viveiros, M.; Amaral, L. Role of calcium in the efflux system of *Escherichia coli*. *Int. J. Antimicrob. Agents* **2011**, *37*, 410-414.
23. Pieroni, M.; Machado, D.; Azzali, E.; Santos Costa, S.; Couto, I.; Costantino, G.; Viveiros, M. Rational Design and Synthesis of Thioridazine Analogues as Enhancers of the Antituberculosis Therapy. *J. Med. Chem.* **2015**, *58*, 5842-5853.
24. Te Brake, L. H.; Russel, F. G.; van den Heuvel, J. J.; de Knecht, G. J.; de Steenwinkel, J. E.; Burger, D. M.; Aarnoutse, R. E.; Koenderink, J. B. Inhibitory potential of tuberculosis drugs on ATP-binding cassette drug transporters. *Tuberculosis (Edinb)* **2016**, *96*, 150-157.
25. Opperman, T. J.; Nguyen, S. T. Recent advances toward a molecular mechanism of efflux pump inhibition. *Frontiers in Microbiology* **2015**, *6*, 421.
26. Sharma, S.; Kumar, M.; Sharma, S.; Nargotra, A.; Koul, S.; Khan, I. A. Piperine as an inhibitor of Rv1258c, a putative multidrug efflux pump of *Mycobacterium tuberculosis*. *Journal of Antimicrobial Chemotherapy* **2010**, *65*, 1694-1701.
27. Singh, K.; Kumar, M.; Pavadai, E.; Naran, K.; Warner, D. F.; Ruminski, P. G.; Chibale, K. Synthesis of new verapamil analogues and their evaluation in combination with rifampicin against *Mycobacterium tuberculosis* and molecular docking studies in the binding site of efflux protein Rv1258c. *Bioorg. Med. Chem. Lett.* **2014**, *24*, 2985-2990.
28. Martins, M.; Viveiros, M.; Amaral, L. Inhibitors of Ca²⁺ and K⁺ transport enhance intracellular killing of *M. tuberculosis* by non-killing macrophages. *In Vivo* **2008**, *22*, 69-75.

29. Rodrigues, L.; Machado, D.; Couto, I.; Amaral, L.; Viveiros, M. Contribution of efflux activity to isoniazid resistance in the Mycobacterium tuberculosis complex. *Infection, Genetics and Evolution* **2012**, *12*, 695-700.
30. Adams, K. N.; Szumowski, J. D.; Ramakrishnan, L. Verapamil, and Its Metabolite Norverapamil, Inhibit Macrophage-induced, Bacterial Efflux Pump-mediated Tolerance to Multiple Anti-tubercular Drugs. *Journal of Infectious Diseases* **2014**, *210*, 456-466.
31. Hille, B. *Ion Channels of Excitable Membranes*; Sinauer Associates inc: Sunderland, Massachusetts, **2001**.
32. Wright, S. H. Generation of resting membrane potential. *Adv. Physiol. Educ.* **2004**, *28*, 139-142.
33. Golan, D. E., Ed.; In *Principles of Pharmacology The Pathophysiologic Basis of Drug Therapy*; Lippincott Williams & Wilkins: Philadelphia, **2012**.
34. Amaral, L.; Martins, M.; Viveiros, M. Enhanced killing of intracellular multidrug-resistant Mycobacterium tuberculosis by compounds that affect the activity of efflux pumps. *Journal of Antimicrobial Chemotherapy* **2007**, *59*, 1237-1246.
35. Machado, D.; Pires, D.; Perdigo, J.; Couto, I.; Portugal, I.; Martins, M.; Amaral, L.; Anes, E.; Viveiros, M. Ion Channel Blockers as Antimicrobial Agents, Efflux Inhibitors, and Enhancers of Macrophage Killing Activity against Drug Resistant Mycobacterium tuberculosis. *PLoS One* **2016**, *11*, e0149326.
36. Farha, M.; Verschoor, C.; Bowdish, D.; Brown, E. Collapsing the Proton Motive Force to Identify Synergistic Combinations against Staphylococcus aureus. *Chem. Biol.* **2013**, *20*, 1168-1178.
37. Adams, K.; Takaki, K.; Connolly, L.; Wiedenhoft, H.; Winglee, K.; Humbert, O.; Edelstein, P.; Cosma, C.; Ramakrishnan, L. Drug Tolerance in Replicating Mycobacteria Mediated by a Macrophage-Induced Efflux Mechanism. *Cell* **2011**, *145*, 39-53.
38. Weaver-Agostoni, J. Cluster headache. *Am. Fam. Physician* **2013**, *88*, 122-128.
39. Hoon, T. J.; Bauman, J. L.; Rodvold, K. A.; Gallestegui, J.; Hariman, R. J. The pharmacodynamic and pharmacokinetic differences of the D- and L-isomers of verapamil: Implications in the treatment of paroxysmal supraventricular tachycardia. *Am. Heart J.* **1986**, *112*, 396-403.
40. Busse, D.; Templin, S.; Mikus, G.; Schwab, M.; Hofmann, U.; Eichelbaum, M.; Kivisto, K. T. Cardiovascular effects of (R)- and (S)-verapamil and racemic verapamil in humans: a placebo-controlled study. *Eur. J. Clin. Pharmacol.* **2006**, *62*, 613-619.
41. Gupta, S.; Cohen, K. A.; Winglee, K.; Maiga, M.; Diarra, B.; Bishai, W. R. Efflux Inhibition with Verapamil Potentiates Bedaquiline in Mycobacterium tuberculosis. *Antimicrobial Agents and Chemotherapy* **2014**, *58*, 574-576.
42. Gupta, S.; Tyagi, S.; Bishai, W. R. Verapamil Increases the Bactericidal Activity of Bedaquiline against Mycobacterium tuberculosis in a Mouse Model. *Antimicrobial Agents and Chemotherapy* **2015**, *59*, 673-676.
43. Andersen, C. L.; Holland, I. B.; Jacq, A. Verapamil, a Ca²⁺ channel inhibitor acts as a local anesthetic and induces the sigma E dependent extra-cytoplasmic stress response in E. coli. *Biochimica et Biophysica Acta (BBA) - Biomembranes* **2006**, *1758*, 1587-1595.
44. Hait, W. N., Ed.; In *Drug Resistance*; Kluwer Academic Publishers: Boston, **1996**.
45. Jaszczyszyn, A.; Gasiorowski, K.; Swiatek, P.; Malinka, W.; Cieslik-Boczula, K.; Petrus, J.; Czarnik-Matusiewicz, B. Chemical structure of phenothiazines and their biological activity. *Pharmacol. Rep.* **2012**, *64*, 16-23.

46. Weiss, B.; Prozialeck, W. C.; Wallace, T. L. Interaction of drugs with calmodulin. Biochemical, pharmacological and clinical implications. *Biochem. Pharmacol.* **1982**, *31*, 2217-2226.
47. Daniel, W. A. Mechanisms of cellular distribution of psychotropic drugs. Significance for drug action and interactions. *Prog. Neuropsychopharmacol. Biol. Psychiatry* **2003**, *27*, 65-73.
48. Kornhuber, J.; Henkel, A. W.; Groemer, T. W.; Stadtler, S.; Welzel, O.; Tripal, P.; Rotter, A.; Bleich, S.; Trapp, S. Lipophilic cationic drugs increase the permeability of lysosomal membranes in a cell culture system. *J. Cell. Physiol.* **2010**, *224*, 152-164.
49. Amaral, L.; Boeree, M. J.; Gillespie, S. H.; Udawadia, Z. F.; van Soolingen, D. Thioridazine cures extensively drug-resistant tuberculosis (XDR-TB) and the need for global trials is now! *Int. J. Antimicrob. Agents* **2010**, *35*, 524-526.
50. Abbate, E.; Vescovo, M.; Natiello, M.; Cufre, M.; Garcia, A.; Gonzalez Montaner, P.; Ambroggi, M.; Ritacco, V.; van Soolingen, D. Successful alternative treatment of extensively drug-resistant tuberculosis in Argentina with a combination of linezolid, moxifloxacin and thioridazine. *J. Antimicrob. Chemother.* **2012**, *67*, 473-477.
51. Amaral, L.; Viveiros, M. Why thioridazine in combination with antibiotics cures extensively drug-resistant Mycobacterium tuberculosis infections. *Int. J. Antimicrob. Agents* **2012**, *39*, 376-380.
52. Bettencourt, M. V.; Bosne-David, S.; Amaral, L. Comparative in vitro activity of phenothiazines against multidrug-resistant Mycobacterium tuberculosis. *Int. J. Antimicrob. Agents* **2000**, *16*, 69-71.
53. Dutta, N. K.; Mehra, S.; Kaushal, D. A Mycobacterium tuberculosis sigma factor network responds to cell-envelope damage by the promising anti-mycobacterial thioridazine. *PLoS One* **2010**, *5*, e10069.
54. Amaral, L.; Molnar, J. Mechanisms by which thioridazine in combination with antibiotics cures extensively drug-resistant infections of pulmonary tuberculosis. *In Vivo* **2014**, *28*, 267-271.
55. de Keijzer, J.; Mulder, A.; de Haas, P. E.; de Ru, A. H.; Heerkens, E. M.; Amaral, L.; van Soolingen, D.; van Veelen, P. A. Thioridazine Alters the Cell-Envelope Permeability of Mycobacterium tuberculosis. *J. Proteome Res.* **2016**, *15*, 1776-1786.
56. Crowle, A. J.; Douvas, G. S.; May, M. H. Chlorpromazine: a drug potentially useful for treating mycobacterial infections. *Chemotherapy* **1992**, *38*, 410-419.
57. Smith, D. A., Ed.; In *Metabolism, Pharmacokinetics and Toxicity of Functional groups. Impact of the building blocks of medicinal chemistry on ADMET*; Royal Society of Chemistry: Cambridge, **2010**.
58. Martins, M.; Viveiros, M.; Couto, I.; Amaral, L. Targeting human macrophages for enhanced killing of intracellular XDR-TB and MDR-TB. *Int. J. Tuberc. Lung Dis.* **2009**, *13*, 569-573.
59. Amaral, L.; Martins, A.; Molnar, J.; Kristiansen, J. E.; Martins, M.; Viveiros, M.; Rodrigues, L.; Spengler, G.; Couto, I.; Ramos, J.; Dastidar, S.; Fanning, S.; McCusker, M.; Pages, J. M. Phenothiazines, bacterial efflux pumps and targeting the macrophage for enhanced killing of intracellular XDRTB. *In Vivo* **2010**, *24*, 409-424.
60. Dutta, N. K.; Karakousis, P. C. Thioridazine for treatment of tuberculosis: promises and pitfalls. *Tuberculosis (Edinb)* **2014**, *94*, 708-711.
61. Rodrigues, L.; Ainsa, J. A.; Amaral, L.; Viveiros, M. Inhibition of drug efflux in mycobacteria with phenothiazines and other putative efflux inhibitors. *Recent. Pat. Antiinfect Drug Discov.* **2011**, *6*, 118-127.

62. Rodrigues, L.; Wagner, D.; Viveiros, M.; Sampaio, D.; Couto, I.; Vavra, M.; Kern, W. V.; Amaral, L. Thioridazine and chlorpromazine inhibition of ethidium bromide efflux in *Mycobacterium avium* and *Mycobacterium smegmatis*. *J. Antimicrob. Chemother.* **2008**, *61*, 1076-1082.
63. Okumura, Y.; Narukawa, M.; Iwasaki, Y.; Ishikawa, A.; Matsuda, H.; Yoshikawa, M.; Watanabe, T. Activation of TRPV1 and TRPA1 by black pepper components. *Biosci. Biotechnol. Biochem.* **2010**, *74*, 1068-1072.
64. Meghwal, M.; Goswami, T. K. Piper nigrum and piperine: an update. *Phytother. Res.* **2013**, *27*, 1121-1130.
65. Ahmad, N.; Fazal, H.; Abbasi, B. H.; Farooq, S.; Ali, M.; Khan, M. A. Biological role of Piper nigrum L. (Black pepper): A review. *Asian Pacific Journal of Tropical Biomedicine* **2012**, *2*, S1945-S1953.
66. Bhardwaj, R. K.; Glaeser, H.; Becquemont, L.; Klotz, U.; Gupta, S. K.; Fromm, M. F. Piperine, a major constituent of black pepper, inhibits human P-glycoprotein and CYP3A4. *J. Pharmacol. Exp. Ther.* **2002**, *302*, 645-650.
67. Singh, I. P.; Choudhary, A. Piperine and Derivatives: Trends in Structure-Activity Relationships. *Curr. Top. Med. Chem.* **2015**, *15*, 1722-1734.
68. Kumar, A.; Khan, I. A.; Koul, S.; Koul, J. L.; Taneja, S. C.; Ali, I.; Ali, F.; Sharma, S.; Mirza, Z. M.; Kumar, M.; Sangwan, P. L.; Gupta, P.; Thota, N.; Qazi, G. N. Novel structural analogues of piperine as inhibitors of the NorA efflux pump of *Staphylococcus aureus*. *J. Antimicrob. Chemother.* **2008**, *61*, 1270-1276.
69. Khan, I. A.; Mirza, Z. M.; Kumar, A.; Verma, V.; Qazi, G. N. Piperine, a Phytochemical Potentiator of Ciprofloxacin against *Staphylococcus aureus*. *Antimicrob. Agents Chemother.* **2005**, *50*, 810-812.
70. Koul, S.; Koul, J. L.; Taneja, S. C.; Dhar, K. L.; Jamwal, D. S.; Singh, K.; Reen, R. K.; Singh, J. Structure-activity relationship of piperine and its synthetic analogues for their inhibitory potentials of rat hepatic microsomal constitutive and inducible cytochrome P450 activities. *Bioorg. Med. Chem.* **2000**, *8*, 251-268.
71. Stermitz, F. R.; Lorenz, P.; Tawara, J. N.; Zenewicz, L. A.; Lewis, K. Synergy in a medicinal plant: antimicrobial action of berberine potentiated by 5'-methoxyhydrnocarpin, a multidrug pump inhibitor. *Proc. Natl. Acad. Sci. U. S. A.* **2000**, *97*, 1433-1437.
72. Tegos, G.; Stermitz, F. R.; Lomovskaya, O.; Lewis, K. Multidrug Pump Inhibitors Uncover Remarkable Activity of Plant Antimicrobials. *Antimicrobial Agents and Chemotherapy* **2002**, *46*, 3133-3141.
73. Wojtyczka, R. D.; Dziedzic, A.; Kepa, M.; Kubina, R.; Kabala-Dzik, A.; Mularz, T.; Idzik, D. Berberine enhances the antibacterial activity of selected antibiotics against coagulase-negative *Staphylococcus* strains in vitro. *Molecules* **2014**, *19*, 6583-6596.
74. Zhou, X.; Ye, X.; He, L.; Zhang, S.; Wang, R.; Zhou, J.; He, Z. In vitro characterization and inhibition of the interaction between ciprofloxacin and berberine against multidrug-resistant *Klebsiella pneumoniae*. *J. Antibiot* **2016**, *10*, 741-746.
75. Wang, Y.; Fu, H.; Li, Y.; Jiang, J.; Song, D. Synthesis and biological evaluation of 8-substituted berberine derivatives as novel anti-mycobacterial agents. *Acta Pharmaceutica Sinica B* **2012**, *2*, 581-587.
76. Liu, C.; Zheng, Y.; Zhang, Y.; Long, X. Research progress on berberine with a special focus on its oral bioavailability. *Fitoterapia* **2016**, *109*, 274-282.

77. Fu, L.; Liang, Y.; Deng, L.; Ding, Y.; Chen, L.; Ye, Y.; Yang, X.; Pan, Q. Characterization of tetrandrine, a potent inhibitor of P-glycoprotein-mediated multidrug resistance. *Cancer Chemother. Pharmacol.* **2004**, *53*, 349-356.
78. Henry, J. P.; Scherman, D. Radioligands of the vesicular monoamine transporter and their use as markers of monoamine storage vesicles. *Biochem. Pharmacol.* **1989**, *38*, 2395-2404.
79. Login, I. S.; Judd, A. M.; Cronin, M. J.; Yasumoto, T.; MacLeod, R. M. Reserpine is a calcium channel antagonist in normal and GH3 rat pituitary cells. *Am. J. Physiol.* **1985**, *248*, E15-9.
80. Louw, G. E.; Warren, R. M.; Gey, v. P.; Leon, R.; Jimenez, A.; Hernandez-Pando, R.; McEvoy, C. R. E.; Grobbelaar, M.; Murray, M.; van Helden, P. D.; Victor, T. C. Rifampicin Reduces Susceptibility to Ofloxacin in Rifampicin-resistant Mycobacterium tuberculosis through Efflux. *Am. J. Respir. Crit. Care Med.* **2011**, *184*, 269-276.
81. Pule, C. M.; Sampson, S. L.; Warren, R. M.; Black, P. A.; van Helden, P. D.; Victor, T. C.; Louw, G. E. Efflux pump inhibitors: targeting mycobacterial efflux systems to enhance TB therapy. *J. Antimicrob. Chemother.* **2016**, *71*, 17-26.
82. Pasca, M. R.; Gugliera, P.; De Rossi, E.; Zara, F.; Riccardi, G. mmpL7 Gene of Mycobacterium tuberculosis Is Responsible for Isoniazid Efflux in Mycobacterium smegmatis. *Antimicrobial Agents and Chemotherapy* **2005**, *49*, 4775-4777.
83. Viveiros, M.; Portugal, I.; Bettencourt, R.; Victor, T. C.; Jordaan, A. M.; Leandro, C.; Ordway, D.; Amaral, L. Isoniazid-Induced Transient High-Level Resistance in Mycobacterium tuberculosis. *Antimicrobial Agents and Chemotherapy* **2002**, *46*, 2804-2810.
84. Zhang, Y.; Permar, S.; Sun, Z. Conditions that may affect the results of susceptibility testing of Mycobacterium tuberculosis to pyrazinamide. *J. Med. Microbiol.* **2002**, *51*, 42-49.
85. Klyachko, K. A.; Schuldiner, S.; Neyfakh, A. A. Mutations affecting substrate specificity of the Bacillus subtilis multidrug transporter Bmr. *Journal of Bacteriology* **1997**, *179*, 2189-2193.
86. Grossman, T. H.; Shoen, C. M.; Jones, S. M.; Jones, P. L.; Cynamon, M. H.; Locher, C. P. The Efflux Pump Inhibitor Timcodar Improves the Potency of Antimycobacterial Agents. *Antimicrob. Agents Chemother.* **2014**, *59*, 1534-1541.
87. Mullin, S.; Mani, N.; Grossman, T. H. Inhibition of antibiotic efflux in bacteria by the novel multidrug resistance inhibitors biricodar (VX-710) and timcodar (VX-853). *Antimicrob. Agents Chemother.* **2004**, *48*, 4171-4176.
88. Abdallah, H. M.; Al-Abd, A.; El-Dine, R.; El-Halawany, A. P-glycoprotein inhibitors of natural origin as potential tumor chemo-sensitizers: A review. *Journal of Advanced Research* **2014**, *6*, 45-62.
89. Lomovskaya, O.; Bostian, K. A. Practical applications and feasibility of efflux pump inhibitors in the clinic--a vision for applied use. *Biochem. Pharmacol.* **2006**, *71*, 910-918.
90. Balganes, M.; Dinesh, N.; Sharma, S.; Kurupath, S.; Nair, A. V.; Sharma, U. Efflux Pumps of Mycobacterium tuberculosis Play a Significant Role in Antituberculosis Activity of Potential Drug Candidates. *Antimicrob. Agents Chemother.* **2012**, *56*, 2643-2651.
91. Lamers, R. P.; Cavallari, J. F.; Burrows, L. L. The efflux inhibitor phenylalanine-arginine beta-naphthylamide (PAbetaN) permeabilizes the outer membrane of gram-negative bacteria. *PLoS One* **2013**, *8*, e60666.
92. Misra, R.; Morrison, K. D.; Cho, H. J.; Khoo, T. Importance of Real-Time Assays To Distinguish Multidrug Efflux Pump-Inhibiting and Outer Membrane-Destabilizing Activities in Escherichia coli. *J. Bacteriol.* **2015**, *197*, 2479-2488.

93. Bruhn, D. F.; Scherman, M. S.; Liu, J.; Scherbakov, D.; Meibohm, B.; Bottger, E. C.; Lenaerts, A. J.; Lee, R. E. In vitro and in vivo Evaluation of Synergism between Anti-Tubercular Spectinamides and Non-Classical Tuberculosis Antibiotics. *Sci. Rep.* **2015**, *5*, 13985.
94. Thiebaut, F.; Tsuruo, T.; Hamada, H.; Gottesman, M. M.; Pastan, I.; Willingham, M. C. Cellular localization of the multidrug-resistance gene product P-glycoprotein in normal human tissues. *Proc. Natl. Acad. Sci. U. S. A.* **1987**, *84*, 7735-7738.
95. Subramanian, N.; Condic-Jurkic, K.; O'Mara, M. L. Structural and dynamic perspectives on the promiscuous transport activity of P-glycoprotein. *Neurochem. Int.* **2016**, *98*, 146-152.
96. Montanari, F.; Ecker, G. F. Prediction of drug-ABC-transporter interaction--Recent advances and future challenges. *Adv. Drug Deliv. Rev.* **2015**, *86*, 17-26.
97. Broccatelli, F.; Carosati, E.; Neri, A.; Frosini, M.; Goracci, L.; Oprea, T. I.; Cruciani, G. A novel approach for predicting P-glycoprotein (ABCB1) inhibition using molecular interaction fields. *J. Med. Chem.* **2011**, *54*, 1740-1751.



Chapter 3: Molecular modelling and simulation studies of *Mycobacterium tuberculosis* multidrug efflux pump protein Rv1258c

Cloete, R.; Kapp, E.; Joubert, J.; Christoffels, A.; Malan, S. F. Molecular Modelling and Simulation Studies of the *Mycobacterium Tuberculosis* Multidrug Efflux Pump Protein Rv1258c. *PLoS One*, **2018**, *13* (11). <https://doi.org/10.1371/journal.pone.0207605>.

Copyright statement: Open access publication. PLOS applies the Creative Commons Attribution (CC BY) license to articles and other works published. Under this Open Access license, the author agrees that anyone can reuse the article in whole or part for any purpose, for free, even for commercial purposes. These permitted uses include but are not limited to self-archiving by authors of submitted, accepted and published versions of their papers in institutional repositories. Anyone may copy, distribute, or reuse the content as lo



Molecular modelling and simulation studies of *Mycobacterium tuberculosis* multidrug efflux pump protein Rv1258c

Ruben Cloete¹, Erika Kapp², Jacques Joubert², Alan Christoffels¹, Sarel F. Malan^{2*}

1 South African Medical Research Council Bioinformatics Unit, South African National Bioinformatics Institute, University of the Western Cape, Bellville, South Africa, **2** School of Pharmacy, University of the Western Cape, Bellville, South Africa

* sfmalan@uwc.ac.za

Abstract

Mycobacterial efflux pumps play a major role in the emergence of antimycobacterial drug resistance. Of particular interest is the proteinaceous multidrug efflux pump protein Rv1258c that encodes a tetracycline/aminoglycoside resistance (TAP-2)-like efflux pump which is active in susceptible and drug resistant *Mycobacterium tuberculosis*. Rv1258c is implicated in drug resistance to numerous antimycobacterials including first line drugs rifampicin and isoniazid as well as fluoroquinolone and aminoglycoside antibiotic classes. To date, compounds like verapamil and piperine have been shown to inhibit Rv1258c but no direct evidence for binding or mode of action exist. Therefore in the present study we generated an accurate 3D model of Rv1258c using MODELLER and validated its structure using molecular dynamic simulation studies with GROMACS software. The 3D-structures of Rv1258c and the homologous template 1pw4 were simulated within a POPE/POPG lipid bilayer and found to behave similar. Another important finding was the identification of one local energy minima state of the apo protein, which speaks to the flexibility of the protein and will be investigated further. Extraction of one of the open channel conformations of Rv1258c and blind docking of various structurally diverse putative inhibitors and substrates, allowed for the identification of a probable binding site. Spectinamide was found to bind to a different location on the outside surface of the protein suggesting its ability to avoid the efflux channel. We further identified 246 putative compounds that showed higher binding affinity values to Rv1258c compared to piperine and verapamil. Interaction analysis of the top 20 purchasable compounds identified crucial hydrogen bond interactions with Ser26, Ser45 and Glu243 as well as a pi-pi stacking interaction with Trp32 that accounted for the strong affinity of these compounds for Rv1258c. Future studies will entail purchasing a number of compounds for *in vitro* activity testing against *Mycobacterium tuberculosis*.

Introduction

Mycobacterium tuberculosis is an obligate parasite and the causative agent of tuberculosis. It is an infectious disease that accounts for approximately 1.4 million deaths and 10.4 million new cases per year [1]. Currently, 6.3 million new cases of tuberculosis (TB) are diagnosed annually and today it still remains one of the most common causes of morbidity and mortality among human populations [1]. Despite the use of the Bacillus Calmette-Gue´rin (BCG) vaccine and effective antibiotics, the bacterium continues to thrive and has developed innate mechanisms to overcome drug treatment. The mechanisms by which *M. tuberculosis* develops resistance to tuberculosis drugs has been the focus of intensive research but it is recognised that efflux pumps play an important role in intrinsic as well as acquired genetic resistance [2–4].

Sequencing of numerous *M. tuberculosis* isolates has led to the identification of a number of open reading frames that encode putative efflux pumps. However, the exact mechanism of these pumps associated with intrinsic and acquired drug resistance has not been elucidated [5, 6]. One such efflux pump is Rv1258c, a proteinaceous active transporter localized in the cytoplasmic membrane of the cells that encodes a tetracycline/aminoglycoside resistance (TAP-2)- like efflux pump. [7, 8]. Previous studies have shown that deletion of Rv1258c from the *Mycobacterium bovis* BCG increases the susceptibility of the organism to isoniazid and rifampicin [9]. Additionally, Rv1258c plays an important role in multidrug-resistant (MDR) TB; and over-expression of Rv1258c, under rifampicin pressure, has been linked to increased transcription levels of this tap-like pump preventing cytosolic accumulation of drugs [8, 10]. This efflux pump has also been linked to resistance development to second line fluoroquinolone and aminoglycoside antibiotics [11].

Previous experimental studies showed that compounds like piperine, verapamil and chlorpromazine, inhibit the functioning of Rv1258c however no direct evidence have been provided for the binding and mode of action of these small molecules [3, 12, 13, 14]. Spectinomycin acts as a substrate while spectinamide avoids efflux through structural modification [15]. One study attempted the modelling of Rv1258c protein structure but did not use a template structure which is structurally similar (i.e. shares a similar fold) to protein Rv1258c [12].

In the present study, we remodelled the structure of Rv1258c using a homologous protein that shares a similar fold and performed molecular dynamic simulation studies of the protein in a POPE-POPG lipid bilayer. We also investigated the possible binding of piperine, verapamil, chlorpromazine, spectinamide and spectinomycin to Rv1258c and describe their interactions with the efflux pump. In addition to this we identified novel compounds that could be used to inhibit Rv1258c utilising *in silico* pharmacophore modelling.

Materials and methods

Homology modelling

The PSIPRED web server was used to search for distantly related template structures for Rv1258c [16]. The amino acid sequence of Rv1258c was used as input and the option Gen-THREADER was selected to search for templates [17]. The search yielded six templates that were categorized in the order of hit confidence based on highly significant p-value (less than 0.001) which suggest the correct secondary structure fold was assigned to the protein. We selected the top ranked template (PDBID: 1pw4) a crystal structure of the glycerol-3-phosphate transporter membrane protein family from *Escherichia Coli* based on an alignment confidence score of 331 ($p = 4 \times 10^{-8}$) which represents the most closely related structure to Rv1258c. The routinely used python scripts in MODELLER were used to perform an alignment prediction between the template (1pw4) and sequence Rv1258c using align2d.py [18, 19]. Thereafter, ten random 3D models were built for Rv1258c using the model-ligand.py script. The lowest discrete optimized protein energy (DOPE) score model (LDSM) was selected for further quality inspection as the lowest DOPE score model represents the more accurate protein model at its native conformation. The DOPE score profile for the model was plotted using Gnuplot and compared to the templates energy profile to identify regions of high energy [20]. The Ramachandran plot was used to interrogate the phi and psi dihedral angle distributions of C-alpha residues within the protein model using Procheck [21]. The Prosa-web server was used to calculate the normalised Z-score for the protein model and template to determine if the protein model predicted falls within range of high quality experimental structures with a similar size and shape [22]. The ERRAT overall quality factor and the 3D-1D compatibility score was calculated for the protein model and the template using the tools ERRAT and Verify3D located at (<http://services.mbi.ucla.edu/SAVES/>). Superimposing all atoms of the protein model onto the template provided an RMSD value, with lower values suggesting that there is very little deviation in main chain atoms and indicates that the correct fold was assigned to protein Rv1258c.

Molecular dynamic simulation studies

The CHARMM-GUI interface was used to prepare protein-membrane systems for Rv1258c and template 1pw4 [23]. Briefly, we prepared two systems each; consisting of Rv1258c and 1pw4 in apo form. Each system was build using the membrane builder bilayer option with the protein aligned along the Z-axis of the membrane with the protein in the centre of the membrane ($Z = 0$). The number of lipids for the top (head) and bottom (tail) used for each system consisted of 96 palmitoyl-oleoyl-phosphatidylethanolamine (POPE) and 32 palmitoyl-oleoyl-phosphatidylglycerol (POPG) with a water thickness of 17.5Å from the top and bottom of the lipid head group and a per lipid hydration number of 50. We selected POPE and POPG as these are the main lipid components of the inner bacterial membrane [24]. Each system was neutralized by adding counter ions to each of the systems. These were 86 positive sodium and 28 negative chloride ions to apo 1pw4 to a 0.15 M concentration, while for the Rv1258c apo structure we added 91 potassium and 32 chloride ions. Each of the two systems underwent 50000 steps of steepest descents energy minimization to remove close van der Waals force contacts. Afterwards, all the systems were subjected to a two-step equilibration phase namely; NVT (constant number of particles, Volume and Temperature) for 500 ps to stabilize the temperature of the system and a short position restraint NPT (constant number of particles, Pressure and Temperature) for 500 ps to stabilize the pressure of the system by relaxing the system and keeping the protein restrained. The V-rescale temperature-coupling method was used for the NVT ensemble, with

constant coupling of 0.1 ps at 300 K under a random sampling seed. For NPT, Parrinello-Rahman pressure coupling [25] was turned on with constant coupling of 0.1ps at 300K under conditions of position restraints (all-bonds). Electrostatic forces were calculated for both NVT and NPT using Particle Mesh Ewald method [26]. All systems were subjected to a full 200 ns simulation under conditions of no restraints.

The analysis of the trajectory files was done using GROMACS utilities. The root mean square deviation (RMSD) was calculated using `g_rmsd` and RMSD per-residue analysis using `g_rms`. The change in the solvent accessibility surface area (SASA) was calculated using `g_sas` to determine if the system reached convergence over the 200 ns simulation. Clustering analysis was performed using the GROMACS tool `g_cluster` to identify different conformational states of the protein. The Visual Molecular Dynamics package (VMD) was used to visually inspect motions along the trajectory [27]. Each 200 ns simulation was repeated at a random seed number to validate reproducibility of results.

Principal component analysis and free energy landscape

Principal component analysis (PCA) is a statistical technique that reduces the complexity of a data set in order to extract biologically relevant movements of protein domains from irrelevant localized motions of atoms. For PCA analysis the translational and rotational movements were removed from the system using `g_covar` from GROMACS to construct a covariance matrix. Next the eigenvectors and eigenvalues were calculated by diagonalising the matrix. The eigen- vectors that correspond to the largest eigenvalues are called "principal components", as they represent the largest-amplitude collective motions. We filtered the original trajectory and project out the part along the most important eigenvectors namely: vector 1 and 2 using `g_anaeig` from GROMACS utilities. Furthermore, we visualized the sampled conformations in the subspace along the first two eigenvectors using `g_anaeig` in a two-dimensional projection. Afterwards we oversimplified the calculation of the free energy landscape (FEL) using the GROMACS utility `g_sham` only along the first two eigenvectors. The FEL represents all the possible different conformations a protein can adopt during a simulation and are typically reported as Gibbs free energy. The molecules free energy was calculated with the formula $\Delta G(r) = -kBT \ln P(x,y)/P_{min}$, where P is the probability distribution of the two Cartesian coordinates namely eigenvector 1 and 2, P_{min} is the maximum probability density function, Kb is the Boltzmann constant and T is the temperature of the simulation. Conformations sampled during the simulation are projected on a two-dimensional plane and the number of points in each cell was counted. The clustering of points in a specific cell represented a possible metastable conformation. All the simulations were carried out using the GROMACS 4.6.5 package [28] along with the CHARMM36 all-atom force field [29].

Molecular docking

Putative inhibitors as well as likely substrates of the Rv1258c efflux pump were identified from literature and docked to Rv1258c using AutoDock Vina [30]. Blind docking was performed using Vina by setting the grid box over the whole protein to determine the binding site of verapamil, piperine, chlorpromazine, spectinomide, spectinomycin and BNG to Rv1258c as no experimental binding site are known. Briefly, the receptor was prepared using AutoDock tools [31], which adds polar hydrogen's, Gasteiger charges and saves the output file in `pdbqt` format, while the five small molecules were

prepared with automated bash and python scripts namely, `split_multi_mol2_file.py` and `prepare_ligand4.py`. This was done to correct for errors such as missing atoms, added H₂O, more than one molecule chain break and alternate locations. The various parameters for the docking process was stored in a configuration file named: `conf.txt` (S1 Text). The configuration file contained input parameters for the docking simulation such as: centre of mass coordinates, grid space and exhaustiveness of the search algorithm.

Virtual screening

Pharmacophore search (ZincPharmer). A pharmacophore is the chemical feature(s) essential for binding of a ligand to a receptor or enzyme, which accounts for its effect on the protein's activity [32]. The single protein drug complexes of Rv1258c_verapamil and Rv1258c_piperine were used to generate a pharmacophoric model based on the interactions made by the docked small molecules. There were two features critical for binding and these were hydrogen-bonds and hydrophobic interactions, which were included in the pharmacophore model. Subsequently, the generated pharmacophore model was screened against the ZINC database to identify novel potential lead compounds that share similar chemical features when aligned in 3D space. The Pharmer technology implemented in ZINCPharmer is a "high-performance search engine that employs novel search methods such as; geometric hashing, generalized Hough transforms and Bloom fingerprints to perform an exact pharmacophore match and accelerate the search algorithm" [33].

The search yielded 548 compounds for the Rv1258c docked complexes when screening the ZINC database for purchasable compounds. These were further validated using docking studies.

Compound docking and scoring. The 548 compounds identified for the Rv1258c docked complexes from the ZINC database were prepared with automated bash and python scripts namely, `split_multi_mol2_file.py` and `prepare_ligand4.py` as mentioned previously. The same input parameters from the previous docking were used and the output of the docking run was filtered based on the docking score measured as kcal/mol. Subsequently, the interactions of the top binders that showed higher binding affinity than the five putative inhibitors was analysed using Poseview [34]. Poseview calculates four types of interactions namely; I) hydrogen bonds, II) hydrophobic, III) metal interactions and IV) π interactions.

Results

Molecular modelling and quality assessment

The amino acid sequence of Rv1258c shared very low sequence identity of approximately 24% and an overall sequence coverage of 96% to that of the template 1pw4 (Fig 1). The overall arrangement of the secondary structure for the LDSM of Rv1258c is similar to that of template 1pw4 consisting of 17 helices, one beta sheet and 18 coil regions (S1 Fig). Although the sequence identity is low, the RMSD value after superimposition and aligning all atoms of the predicted model to the template 1pw4 was found to be 0.720 Å (Fig 2). This suggests very little deviation between carbon main chain atoms and indicates homology between the two structures. We also performed sequence and structural comparisons between the amino acid sequences of Rv1258c, Sharma (2010) template (2GFP) and 1pw4 and 3D structures of the three proteins using BLASTp pairwise alignment and Pymol. The

sequence identity was found to be 36% between Rv1258c and template sequence 2GFP and 24% with 1pw4. Comparing the sequence identity between template 1pw4 and 2GFP indicated a score of 26%, suggesting the two proteins are not homologs. Although, the sequence identity was low between the template 1pw4 and Rv1258c the fold was more similar to our predicted model for Rv1258c. The structural similarity between our predicted model and the template 2GFP was 7.16Å suggesting low similarity between the two 3D structures because the structural deviation was more than the threshold value of 2 Å (S2 Fig). Furthermore, aligning template 1pw4 used for our model to template (2GFP) showed an RMSD of 10.37 Å again suggesting large structural deviation between the two templates (S3 Fig). Additional inspection of the DOPE score energy profiles indicated no regions of extremely high energy, suggesting that the model is a reliable approximation of the protein's native fold (S4 Fig). The Prosa Z-score for the LDSM was equal to -4.57, comparable to the template Z-score of -5.29, suggesting that the model falls in the range of medium quality crystal structures of a similar size and shape. Ramachandran plot analysis indicated that more than 90% of residues for the LDSM of Rv1258c were found in favoured regions, meaning that 90% of residues in the protein structure satisfied phi and psi dihedral angle distributions. The ERRAT overall quality factor was calculated to be 72.66 and 73.71 for the LDSM and the template, respectively, which is above the expected accuracy threshold of 70% for medium resolution structures considering the template had a resolution value of 3.3 Å. Furthermore, using Verify3D we found that 63.25% of the model residues had an averaged 3D-1D score ≥ 0.2 while for the template 1pw4, 65.90% of the residues had an averaged 3D-1D score ≥ 0.2 , suggesting similarity between the two structures although both failing the 3D profile validation test. This is expected as the sequence identity is fairly low between the target and the template. Overall, the predicted model satisfied (RMSD, Prosa Z-score, ERRAT and Procheck) quality evaluation checks.

```

1pw4/19-438 19 ----- IDPTYRRLRWQIFLGIFFGYAAAYLVVRKNFALAMP 53
Rv1258c/1-419 1 ----- MRNSNRGGPAFLILFATLMAAAGDGVSVIVAFPWLV - 34

1pw4/19-438 54 YLVEQGFSRGDLGFALSGLISIAYGFSKFI MGSVSDR - SNPRVFLPAGLI 101
Rv1258c/1-419 35 -LQREG-SAGQASIVASATMLPLLFATLVAGTAVDYFGRRRVSMVADAL 81

1pw4/19-438 102 LAAAVMLFMGFVPWATS - - - SIAVMFVLLFLCGWFQGMGWP - - - - P 140
Rv1258c/1-419 82 SGAAGVAG-VPLMAWGYGGDAVNVVLAVALAALAAAFGPGAGMTARDSMLP 129

1pw4/19-438 141 CGRTMVHWSQKERGGIVSVWNCAHNVGGGIPPLFLFLGMAWFNDWHA 189
Rv1258c/1-419 130 EAAARAGWSLDRINGAYEALNLAFLVGPALIGGLMIATVGGITTMWITA 178

1pw4/19-438 190 LYMPAFCAILVALFAFAMMR-DTPQSCGLPPIIEEYKNDTAKQIFMQYVL 237
Rv1258c/1-419 179 T - - - AFGLSILAI AALQLEGAGKPHHTSR-P-QGLVSGIAEGLRFVWNL 222

1pw4/19-438 238 -PNKLLWYIAIANVFVYLLRYGILDWSPTYLKEVKHFALDKSSWAYFLY 285
Rv1258c/1-419 223 RVLRTLGMIDLTVTALYLPME SVL - - FPKYFTD - - HQQPVQLGWALMAI 267

1pw4/19-438 286 EYAGIPGTL LCGWMSDKVFRGNRGATGVFFMTLVTIATI VYWMNPAGNP 334
Rv1258c/1-419 268 AGGLLVGALGYAVLAIRVPRRVTMSTAVLTLGLASM - - VIALLP - - LP 312

1pw4/19-438 335 TVDMI CMI VIGFLIYGPVMLI GLHALEL - APKKAAGTAA GFTGLFGYLG 382
Rv1258c/1-419 313 VIMVLC - AMVG - LVYGP IQPIIYNYVIQTRAAQHLRGRVVGVMTSLAYAA 359

1pw4/19-438 383 GSVAASAIVGYTVDFFGWDGGFMVMIGGSI - LAVILLIVVMIGEKR RHE 430
Rv1258c/1-419 360 GPLGL - LLAGPLTD AAGLHATFLALALPIVCTGLVAIRLPALRELDLAP 407

1pw4/19-438 431 QL - LQELVP - - - 438
Rv1258c/1-419 408 QADIDRPMGSAQ 419

```

Fig 1. Sequence to structural alignment of Rv1258c to homologous template 1pw4. Blue highlighted boxes show conserved residues.

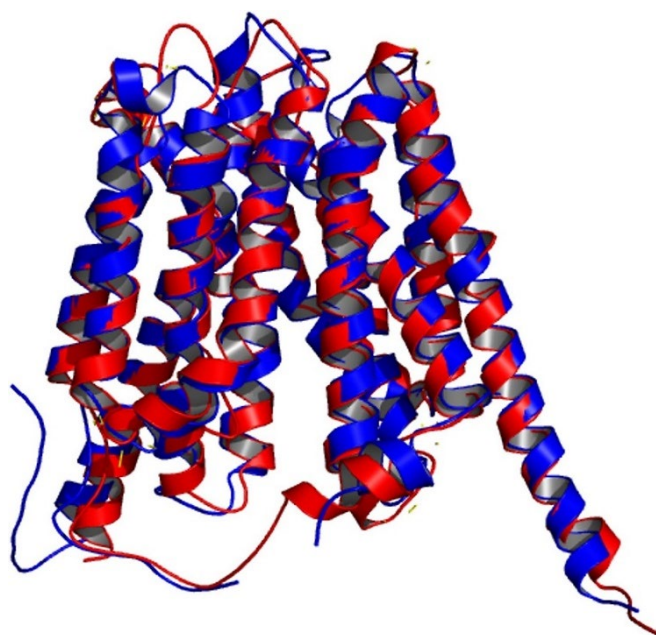


Fig 2. Superimposition of the LDSM Rv1258c (red) on the homologous template 1pw4 (blue).

Molecular dynamic simulation

The RMSD analysis of backbone atoms for the two systems confirmed similar behaviour whereby both Rv1258c and 1pw4 sampled both open and closed conformational states during the 200 ns simulation (Fig 3A), although the average mean for 1pw4 of $(0.29 \pm 0.06 \text{ nm})$ suggest it is more stable than Rv1258c $(0.55 \pm 0.09 \text{ nm})$. This is visually illustrated in the two simulation movies (S1 and S2 Movies). The RMSD per-residue analysis of the two systems indicated that 1pw4 had lower RMSD values of approximately $0.28 \pm 0.21 \text{ nm}$ compared to $0.48 \pm 0.36 \text{ nm}$ for Rv1258c, and with only one region encompassing residues (200–250) with extremely high fluctuation for 1pw4, but this corresponded to a C-terminal loop regions that contained a breakage in that region. Additionally, this region does not contain the known substrate binding site residues R45 and R269 (Fig 3B). Furthermore, the RMSD per-residue analysis indicated two regions (170–176, 200–230) with high RMSD fluctuation values that corresponded to flexible loop regions within the protein (Fig 3B). The total SASA values for the two proteins showed similar fluctuation patterns and reached equilibrium (Fig 3C).

Again the total SASA values were lower for 1pw4 ($227 \pm 4.57 \text{ nm}^2$) in comparison to Rv1258c ($248 \pm 4.71 \text{ nm}^2$). Principal component analysis of the first two eigenvectors for the two trajectories indicated smaller randomised movements for 1pw4 compared to Rv1258c after diagonalisation of the covariance matrix (a square matrix of numbers that describe the directionality of the eigenvector) with values 51.07 nm and 60.81 nm, respectively. Calculating the contribution of each PCA component for each system indicated for 1pw4 PCA component 1 and 2 each contributed 63 and 11% of the overall motion while for Rv1258c PCA components 1, 2, 3 and 4 each contributed 37, 20, 15 and 9%, respectively. Plotting the movement of the first two principal components throughout the free energy landscape indicated two metastable clusters for 1pw4, while Rv1258c showed only one conformational cluster (Fig 4A and 4B). Clustering analysis of the Rv1258c trajectory yielded 7 clusters at a 0.35 nm

average RMSD cut-off value. We selected one representative structure from the cluster that corresponded to time point ($t = 190700\text{ps}$) and that represented a metastable conformation as identified from the PCA analysis for docking studies.

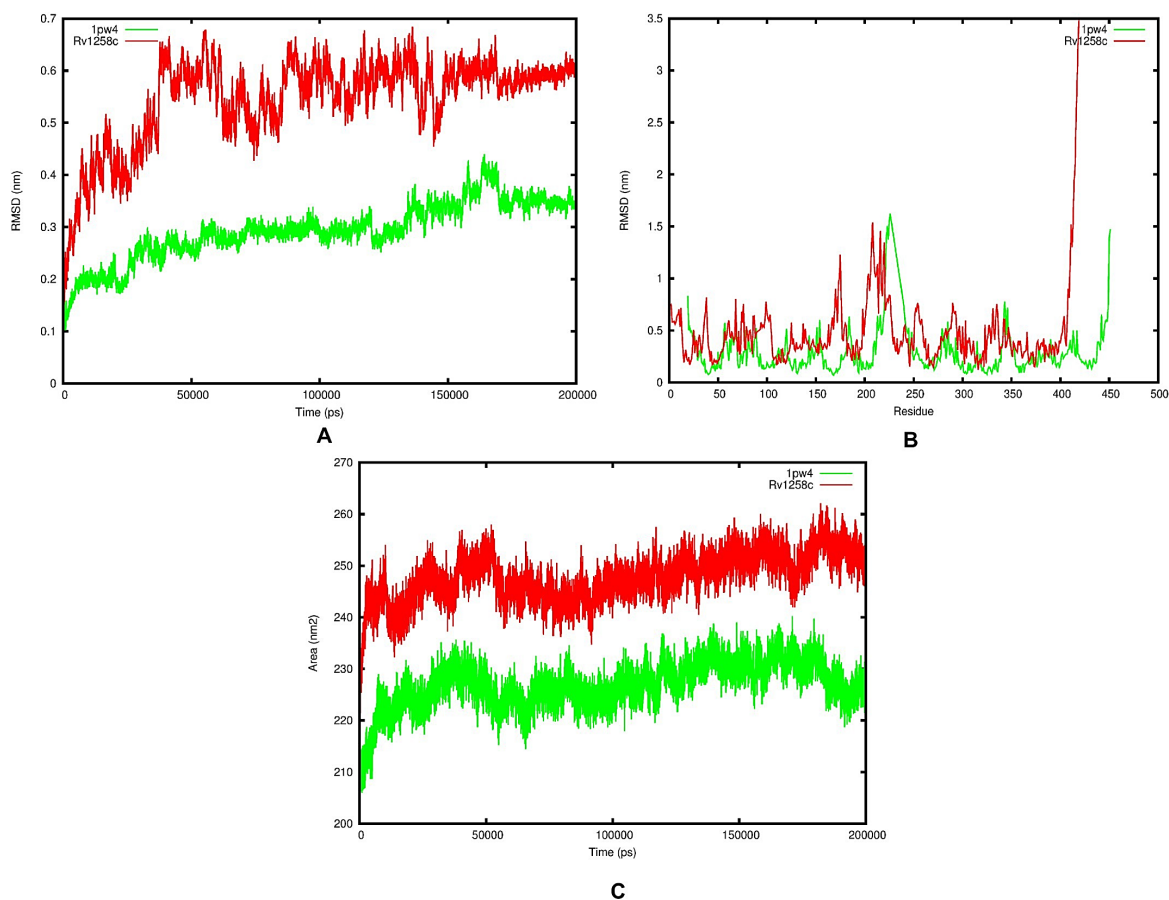


Fig 3. Trajectory analysis for Rv1258c (red) and 1pw4 (green) over the 200 ns simulation. (A) RMSD analysis of the backbone atoms, (B) RMSD per-residue analysis of the protein atoms and (C) The total SASA values of the protein atoms.

Docking and interaction analysis

Autodock VINA was first used to perform a convergence test that included blind docking of six small molecules to the open channel conformational cluster 7 of Rv1258c at exhaustive parameter values of 16, 32, 64 and 128. Afterwards, docking was performed at an exhaustive value of 50 to determine which of the six small molecules showed the highest affinity for the Rv1258c enzyme. The six small molecules were first inspected to determine if the docking results showed convergence based on the clustering of the top predicted modes using Pymol. Based on the visual inspection clustering of the top five modes occurred more frequently at higher exhaustiveness values 64 and 128. This is reported for piperine and Verapamil as they obtained the highest binding affinity scores (S5–S12 Figs). The top modes also exploited the same binding space indicating that the search space was extensively explored by the algorithm. The docked molecules (piperine, spectinomycin, spectinamide, chlorpromazine and verapamil) to the Rv1258c cluster indicated that piperine had the strongest binding affinity (-9.3 kcal/mol) followed by verapamil (-8.4 kcal/mol) and then by chlorpromazine (-7.7 kcal/mol), spectinomycin (-7.6 kcal/mol) and spectinamide (-7.4 kcal/mol). Interestingly, spectinamide showed a higher binding affinity than spectinomycin although binding to an allosteric site located on the outside

solvent accessible surface area of the protein. The sugar, BNG showed the lowest binding affinity for Rv1258c (-6.2 kcal/mol). To validate the binding affinity values we performed interaction analysis to identify the residues that contributed to the overall binding energy. Interaction analysis indicated that verapamil and piperine showed the highest number of hydrophobic interactions each having 5 non polar contacts followed by chlorpromazine, spectinomycin and BNG with each four hydrophobic contacts, while spectinamide showed no hydrophobic contacts (Table 1, S13–S18 Figs). Spectinamide showed the highest number of hydrogen bond interactions (3), compared to spectinomycin, BNG and chlorpromazine having 2, 2 and 1 polar contact with Rv1258c, respectively (Table 1, S13–S18 Figs).

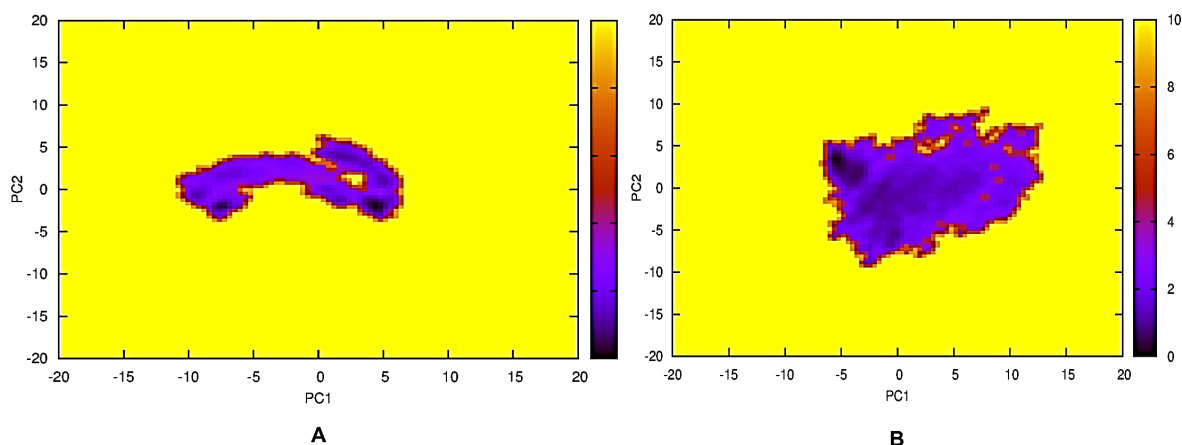


Fig 4. Free energy landscape of the protein backbone atoms for principal components 1 and 2 over 200 ns simulation. (A) For Rv1258c and (B) For 1pw4.

Pharmacophore search and docking

The Rv1258c-verapamil and -piperine complexes were selected as a pharmacophore to search for potential compounds that could inhibit Rv1258c as these compounds demonstrated the lowest binding energy of the 5 compounds evaluated in the initial blind docking. Both verapamil and piperine has previously been shown to inhibit Rv1258c experimentally although the mechanism by which inhibition occurs is still under debate [3, 12, 13, 14, 15, 35]. Both these compounds also docked to the same binding pocket site on the protein model of Rv1258c and showed two similar interacting residues Trp32 and Phe251. The interactions observed from the previous docking experiment were used to generate pharmacophore features for each complex. The Rv1258c-verapamil complex had five hydrophobic and we included one hydrogen bond feature and Rv1258c-piperine had three hydrophobic and three additional hydrogen bond features and only one additional aromatic feature. Including more features increases the likelihood of finding compounds with higher specificity for Rv1258c. Using these features, the ZINC database was searched using ZINCPharmer for potential compounds that shared similar features to the two small molecules aligned in three-dimensional space. For cluster 7 we identified in total 548 hits for Rv1258c-piperine and Rv1258c-verapamil. Each of the compounds identified were validated by docking them to cluster 7 (open channel cluster) using VINA to determine if they showed higher binding affinity compared to that of verapamil and piperine. Out of the total 548 compounds 246 showed higher affinity than verapamil and piperine.

Table 1. Docking scores and interaction residues for the five putative inhibitors and potential substrate BNG

Protein	Cluster	Compound	Docking score(kcal/mol)	H-bonds	Hydrophobic	Pi-PiStacking
Rv1258c	7	Piperine	-9.3	None	5 (Trp32, Glu243, Phe247, Phe251, Gly363)	None
		Verapamil	-8.4	None	5 (Trp32, Gly161, Ile165, Pro248, PHE251)	None
		Chlopromazine	-7.7	1 (Glu243)	4 (Val28, Pro248, Phe251, Leu264)	None
		Spectinomycin	-7.6	2 (Val25, Glu243)	None	None
		Spectinamide_1599	-7.4	2 (Asp125, Arg217, Asn221)	None	None
		BNG	-6.2	2 (Thr179, Leu183)	4 (Leu33, Met164, Ile165, Val168)	None

BNG, B-nonylglucoside; H-bonds, hydrogen bonds, Pi-Pi aromatic stacking interaction. The numbers in front of brackets indicate the total amount of interactions formed with the residues listed inside the brackets.

Table 2. Docking scores and interaction residues for the top 20 compounds bound to Rv1258c cluster 7.

Cluster	Docking score(kcal/mol)	ZINC_ID	Hydrogen-bond	Hydrophobic	Pi-Pi stacking
7	-11.2	ZINC36652490	Ser26	Ala29, Leu33, Val168	-None
	-11.0	ZINC16608089	Ser45	Val25, Val28	Trp32
	-11.0	ZINC35729457	Ser45, Glu243	Val25, Pro158	None
	-11.0	ZINC35729461	Ser45	Trp32, Leu33, Met164, Pro248	None
	-10.9	ZINC16608087	Ser45	Val25, Ile27, Val28, Ala29, Trp32, Leu264	Trp32
	-10.9	ZINC15947760	Glu243	Gly363	None
	-10.9	ZINC90733545	Ser45	Trp32, Leu33, Met164, Pro248	None
	-10.8	ZINC45943747	Ser45	Val28, Ala29, Trp32, Pro248,	None
	-10.8	ZINC08920371	Glu243	Val25, Trp32, Ala44, Ala48, Pro248,	None
	-10.8	ZINC72034391	Ser45	Leu240	None
	-10.7	ZINC45943751	Ser45	Val28, Ala29, Leu33, Met164, Pro248, Leu264	None
	-10.7	ZINC16608126	Ser45	Val25, Leu264	Trp32
	-10.7	ZINC08920366	Glu234	Val25, Trp32, Ala44, Pro248	None
	-10.7	ZINC06793104	None	Trp32, Ala41, Ala44, Pro158, Leu246, Pro248, Leu264	Trp32
	-10.7	ZINC45943745	Ser45	Val 29, Ala29, Trp32, Ile165, Pro248	None
	-10.6	ZINC09701714	Ser26	Leu33, Met164, Val168, Leu264	None
	-10.6	ZINC35933009	Ser45	Val25, Ala29, Trp32, Pro248, Leu264	None
	-10.6	ZINC78721136	Trp32	Val28, Ala29, Trp32, Leu33, Met164, Leu264	None
	-10.6	ZINC15947762	Glu243	Gly363	None
	-10.3	ZINC16608150	Ser26	Val28, Ala29, Trp32, Leu33, Pro248	Trp32

Subsequently, interaction analysis of the top 20 ranking compounds provided support for the higher binding affinity which was due to important hydrogen-bond interactions between the compounds and residues Ser26, Ser45, Glu243 and a pi-pi stacking interaction with Trp32 of Rv1258c (Table 2, S19–S38 Figs). We also observed a variety of hydrophobic interactions being formed between the top 20 compounds and Rv1258c non polar residues ranging from one to seven (Table 2, S19–S38 Figs).

Discussion

The mechanism of efflux pump inhibition of piperine and verapamil and other efflux pump inhibitors has been under debate for some time. The absence of a crystal structure for Rv1258c made it difficult to prove (or disprove) inhibition of efflux function through direct binding to the protein. Particularly in the case of verapamil, a number of studies propose conflicting mechanisms for observed augmented antimycobacterial efficacy in *Mycobacterium tuberculosis* and the possibility exists that this may be due to a multimodal mechanism of action [13, 14, 35, 36]. Verapamil is a calcium channel blocker and has been shown to have a significant inhibitory effect on mycobacterial efflux pump activity but has severe adverse effects at high concentrations and therefore, cannot be considered for tuberculosis treatment in humans [3, 13]. Piperine on the other hand is present in black pepper and is a drug potentiator that inhibits human P-glycoprotein. Piperine was shown to have synergistic properties with rifampicin and decreased the number of bacteria in the lung of mice [12, 37, 38]. However, piperine is not currently used in the treatment of tuberculosis infected patients due to its likely and unpredictable drug-drug interactions with other co-administered medication. This study therefore aimed to identify alternatives for Rv1258c efflux pump inhibition.

The 3D structure of Rv1258c was predicted through homology modelling and validated using molecular dynamic simulation studies in a lipid bilayer consisting of POPE/POPG lipids. Pharmacophore modelling of Rv1258c-drug complexes was performed to search for new putative compounds and these were then validated by performing blind docking studies to Rv1258c. The Lowest Dope score protein model predicted for Rv1258c showed good consensus with our homologous template protein based on the structural comparison and a very low root mean square deviation between atoms suggesting that a correct fold was assigned to Rv1258c. Furthermore, the predicted model of Rv1258c passed all the quality evaluation tests suggesting that a reliable model was predicted. Additional validation of the model using molecular dynamics simulation indicated similar trajectory behaviours based on RMSD, RMSD per-residue and SASA analysis between Rv1258c and its homologous template 1pw4, providing support for template selection. The homologous template however showed lower RMSD, RMSD per-residue and SASA suggesting that it is less flexible and more compact than the predicted 3D model of Rv1258c. The PCA analysis affirmed previous statistics that Rv1258c explored a larger area of the phase space suggesting that Rv1258c is more flexible and dynamic in comparison to the template 1pw4 as was seen by analysis of the variance data.

Interestingly, the first four PCA's contributed significantly to the mobility of Rv1258c. Another important finding of our study is the identification of one local energy minima state of the apo-protein Rv1258c, which suggests that the structure of Rv1258c is highly flexible and dynamic. However, a limitation of this study is the use of only two principal components (Cartesian coordinates) to estimate the correct rugged free energy landscape that may result in artifacts due to the mixing of internal coordinates and overall motion of the protein [39]. Also, using only two-dimensional representations to estimate the free energy landscape of biomolecules may result in missing numerous metastable conformations of the protein because of minima overlapping [40]. The resolution here is to use dihedral angle PCA analysis using internal coordinates such as bond lengths and dihedral angles for dimensional reduction and including more than two PCA components to enhance minima detection. Another option is to perform replica exchange dynamics for longer simulation durations where the temperature is increased systematically to overcome high energy barriers. We selected one of the

clusters which represented a potential metastable conformation for our docking studies. The result for the blind docking study of the five small molecules confirmed piperine and verapamil as the strongest binders to Rv1258c. They also bound to the same location within the binding cleft while spectinomide bound to a different location on the outside surface of the protein suggesting its ability to avoid the efflux channel. Contrary to the study of Sharma and colleagues, (2010), we identified a different active site (confirmed by metaPocket 2.0 analysis, S39 Fig) located deep within a binding cleft pocket which is in an open channel conformation. In our study no hydrogen bond interactions are found but rather non-polar contacts which are crucial for the binding of piperine and verapamil. This is foreseeable as we used a different homologous template (1pw4) and simulated the Rv1258c apo-protein structure in a lipid bilayer of POPE/POPG. Subsequently, we leveraged one of the open states in docking studies and then used the high binding complexes in a pharmacophore search against the ZINC database, identifying 548 possible compounds. Additional docking validation was performed to the Rv1258c cluster and 246 compounds showed higher binding affinities than the known inhibitors piperine and verapamil. In contrast to piperine and verapamil the top 20 compounds made important hydrogen bonds (Ser26, Ser45 and Glu243), pi-pi stacking (Trp32) and a number of hydrophobic interactions that accounted for the higher affinity for Rv1258c. The top compounds will now be analysed and a number selected, purchased and tested *in vitro* to determine their ability to restore sensitivity of H37rV to rifampicin by inhibiting the efflux pump Rv1258c. These compounds could serve as alternatives to piperine and verapamil in the combination treatment of multidrug resistant tuberculosis strains and could provide lead structures for further drug development.

Conclusions

This study predicted the 3D-structure of the multidrug efflux pump protein Rv1258c that is important to model protein-drug interactions. The 3D-structures of Rv1258c and the homologous template 1pw4 were also further utilized in molecular dynamic simulation studies within a POPE/POPG lipid bilayer and showed similar kinetic behaviour based on dynamics. Extraction of one cluster that represented a metastable conformation of Rv1258c allowed the identification of a putative binding site within a binding cleft when the protein channel has an open conformation. We identified 246 putative ligands using docking studies and also validated residues Ser26, Ser45, Glu243, and Trp32 as crucial interaction partners responsible for the higher affinity. A selection of the top compounds will be purchased to validate them *in vitro* as potential modulators of antimycobacterial treatment. The implications of this study will provide alternatives to piperine and verapamil for Tuberculosis treatment to improve the bacterium's susceptibility to various antimicrobials by inhibiting the efflux pump Rv1258

Funding

This work was supported by the South African Research Chairs initiative of the Department of Science and Technology and the National Research Foundation of South Africa (64751 to AC) and the South African Medical Research Council (MRC-RFA-UFSP-01-2013/COMBAT-TB to AC). The funders had no role in the study design, data collection and analysis, decision to publish or preparation of the manuscript.

Author Contributions

Conceptualization: Erika Kapp. **Formal analysis:** Ruben Cloete. **Methodology:** Erika Kapp, Jacques Joubert, Sarel Malan. **Writing – original draft:** Ruben Cloete. **Writing – review & editing:** Ruben Cloete, Erika Kapp, Jacques Joubert, Alan Christoffels, Sarel F. Malan.

Citation: Cloete R, Kapp E, Joubert J, Christoffels A, Malan SF (2018) Molecular modelling and simulation studies of the *Mycobacterium tuberculosis* multidrug efflux pump protein Rv1258c. PLoS ONE 13(11): e0207605. <https://doi.org/10.1371/journal.pone.0207605>

Editor: Claudio M. Soares, Universidade Nova de Lisboa Instituto de Tecnologia Quimica e Biologica, PORTUGAL

Received: June 14, 2018; **Accepted:** November 2, 2018; **Published:** November 26, 2018

Copyright: © 2018 Cloete et al. This is an open access article distributed under the terms of the Creative Commons Attribution License, which permits unrestricted use, distribution, and reproduction in any medium, provided the original author and source are credited.

Data availability statement: All relevant data are within the paper and its Supporting Information files.

Competing interests: The authors have declared that no competing interests exist.

References

1. World Health Organization Global tuberculosis report 2016.
2. Balganes M, Dinesh N, Sharma S, Kuruppath S, Nair AV, Sharma U. Efflux pumps of *Mycobacterium tuberculosis* play a significant role in antituberculosis activity of potential drug candidates. *Antimicrobial agents and chemotherapy*. 2012; 56: 2643–2651. <https://doi.org/10.1128/AAC.06003-11> PMID: 22314527
3. Pule CM, Sampson SL, Warren RM, Black PA, van Helden PD, Victor TC, et al. Efflux pump inhibitors: targeting mycobacterial efflux systems to enhance TB therapy. *Journal of Antimicrobial Chemotherapy*. 2015; 71: 17–26. <https://doi.org/10.1093/jac/dkv316> PMID: 26472768
4. te Brake LH, de Knecht GJ, de Steenwinkel JE, van Dam TJ, Burger DM, Russel FG, et al. The role of efflux pumps in tuberculosis treatment and their promise as a target in drug development: unraveling the black box. *Annual review of pharmacology and toxicology*. 2017.
5. St Cole, Brosch R, Parkhill J, Garnier T, Churcher C, Harris D, et al. Deciphering the biology of *Mycobacterium tuberculosis* from the complete genome sequence. *Nature*. 1998; 393: 537–544. <https://doi.org/10.1038/31159> PMID: 9634230
6. Amaral L, Martins M, Viveiros M. Enhanced killing of intracellular multidrug-resistant *Mycobacterium tuberculosis* by compounds that affect the activity of efflux pumps. *Journal of antimicrobial chemotherapy*. 2007; 59: 1237–1246. <https://doi.org/10.1093/jac/dkl500> PMID: 17218448
7. Aínsa JA, Blokpoel MC, Otal I, Young DB, De Smet KA, Martín C. Molecular cloning and characterization of Tap, a putative multidrug efflux pump present in *Mycobacterium fortuitum* and *Mycobacterium tuberculosis*. *Journal of bacteriology*. 1998; 180: 5836–5843. PMID: 9811639

8. Siddiqi N, Das R, Pathak N, Banerjee S, Ahmed N, Katoch VM, et al. Mycobacterium tuberculosis iso- late with a distinct genomic identity overexpresses a tap-like efflux pump. *Infection*. 2004; 32: 109–111. <https://doi.org/10.1007/s15010-004-3097-x> PMID: 15057575
9. Rossi ED, A´insa JA, Riccardi G. Role of mycobacterial efflux transporters in drug resistance: an unre- solved question. *FEMS microbiology reviews*. 2006; 30: 36–52. <https://doi.org/10.1111/j.1574-6976.2005.00002.x> PMID: 16438679
10. Jiang X, Zhang W, Zhang Y, Gao F, Lu C, Zhang X, et al. Assessment of efflux pump gene expression in a clinical isolate Mycobacterium tuberculosis by real-time reverse transcription PCR. *Microbial drug resistance*. 2008;14: 7–11. <https://doi.org/10.1089/mdr.2008.0772> PMID: 18321205
11. Malinga LA. Characterization of efflux pumps genes involved in second-line drug resistance of tubercu- losis. University of Pretoria. 2017.
12. Sharma S, Kumar M, Sharma S, Nargotra A, Koul S, Khan IA. Piperine as an inhibitor of Rv1258c, a putative multidrug efflux pump of Mycobacterium tuberculosis. *Journal of Antimicrobial Chemotherapy*. 2010; 65: 1694–1701. <https://doi.org/10.1093/jac/dkq186> PMID: 20525733
13. Adams KN, Szumowski JD, Ramakrishnan L. Verapamil, and its metabolite norverapamil, inhibit macro- phage-induced, bacterial efflux pump-mediated tolerance to multiple anti-tubercular drugs. *The Journal of infectious diseases*. 2014; 210: 456–466. <https://doi.org/10.1093/infdis/jiu095> PMID: 24532601
14. Kapp E, Malan SF, Joubert J, Sampson SL. Small molecule efflux pump inhibitors in Mycobacterium tuberculosis: a rational drug design perspective. *Mini reviews in medicinal chemistry*. 2018; 18: 72–86. <https://doi.org/10.2174/1389557517666170510105506> PMID: 28494730
15. Lee RE, Hurdle JG, Liu J, Bruhn DF, Matt T, Scherman MS, et al. Spectinamides: a new class of semi- synthetic antituberculosis agents that overcome native drug efflux. *Nature medicine*. 2014; 20: 152– 158. <https://doi.org/10.1038/nm.3458> PMID: 24464186
16. Buchan DW, Minneci F, Nugent TC, Bryson K, Jones DT. Scalable web services for the PSIPRED Pro- tein Analysis Workbench. *Nucleic acids research*. 2013; 41: W349–W357. <https://doi.org/10.1093/nar/ gkt381> PMID: 23748958
17. Lobley A, Sadowski MI, Jones DT. pGenTHREADER and pDomTHREADER: new methods for improved protein fold recognition and superfamily discrimination. *Bioinformatics*. 2009; 25: 1761–1767. <https://doi.org/10.1093/bioinformatics/btp302> PMID: 19429599
18. S`ali A, Blundell TL. Comparative protein modelling by satisfaction of spatial restraints. *Journal of molec- ular biology*. 1993; 234: 779–815. <https://doi.org/10.1006/jmbi.1993.1626> PMID: 8254673
19. Eswar N, Eramian D, Webb B, Shen M-Y, Sali A. Protein structure modeling with MODELLER. *Methods Mol Biol*. 2008;426.
20. Williams T, Kelley C, Bro`ker H-B, Campbell J, Cunningham R, Denholm D, et al. An Interactive Plotting Program. *Environment*. 1998; 4: 5.
21. Laskowski RA, MacArthur MW, Moss DS, Thornton JM. PROCHECK: a program to check the stereo- chemical quality of protein structures. *J Appl Crystallogr*. 1993;26.
22. Wiederstein M, Sippl MJ. ProSA-web: interactive web service for the recognition of errors in three- dimensional structures of proteins. *Nucleic Acids Res*. 2007;35. <https://doi.org/10.1093/nar/gkl987>
23. Lee J, Cheng X, Swails JM, Yeom MS, Eastman PK, Lemkul JA, et al. CHARMM-GUI input generator

- for NAMD, GROMACS, AMBER, OpenMM, and CHARMM/OpenMM simulations using the CHARMM36 additive force field. *Journal of chemical theory and computation*. 2015; 12: 405–413. <https://doi.org/10.1021/acs.jctc.5b00935> PMID: 26631602
24. Murzyn K, Róg T, Pasenkiewicz-Gierula M. Phosphatidylethanolamine-phosphatidylglycerol bilayer as a model of the inner bacterial membrane. *Biophysical journal*. 2005; 88: 1091–1103. <https://doi.org/10.1529/biophysj.104.048835> PMID: 15556990
 25. Parrinello M, Rahman A. Polymorphic transitions in single crystals: A new molecular dynamics method. *Journal of Applied physics*. 1981; 52: 7182–7190.
 26. Essmann U, Perera L, Berkowitz ML, Darden T, Lee H, Pedersen LG. A smooth particle mesh Ewald method. *Journal of Chemical Physics*. 1995; 103: 8577–8593.
 27. Humphrey W, Dalke A, Schulten K. VMD: visual molecular dynamics. *Journal of molecular graphics*. 1996; 14: 33–38. PMID: 8744570
 28. Van Der Spoel D, Lindahl E, Hess B, Groenhof G, Mark AE, Berendsen HJ. GROMACS: fast, flexible, and free. *Journal of computational chemistry*. 2005; 26: 1701–1718. <https://doi.org/10.1002/jcc.20291> PMID: 16211538
 29. Huang J, MacKerell AD. CHARMM36 all-atom additive protein force field: Validation based on comparison to NMR data. *Journal of computational chemistry*. 2013; 34: 2135–2145. <https://doi.org/10.1002/jcc.23354> PMID: 23832629
 30. Trott O, Olson AJ. AutoDock Vina: improving the speed and accuracy of docking with a new scoring function, efficient optimization, and multithreading. *J Comput Chem*. 2010; 31.
 31. Morris GM, Huey R, Lindstrom W, Sanner MF, Belew RK, Goodsell DS, et al. AutoDock4 and AutoDockTools4: Automated docking with selective receptor flexibility. *Journal of computational chemistry*. 2009; 30: 2785–2791. <https://doi.org/10.1002/jcc.21256> PMID: 19399780
 32. Gund P. Three-dimensional pharmacophoric pattern searching. *Progress in molecular and subcellular biology*. Springer; 1977. pp. 117–143.
 33. Koes DR, Camacho CJ. Pharmer: efficient and exact pharmacophore search. *Journal of chemical information and modelling*. 2011; 51: 1307–1314.
 34. Stierand K, Rarey M. PoseView—molecular interaction patterns at a glance. *J Cheminf*. 2010; 2.
 35. Chen C, Gardete S, Jansen RS, Shetty A, Dick T, Rhee KY, et al. Verapamil targets membrane energetics in *Mycobacterium tuberculosis*. *Antimicrobial agents and chemotherapy*. 2018; AAC. 02107–17.
 36. Martins M, Viveiros M, Amaral L. Inhibitors of Ca²⁺ and K⁺ transport enhance intracellular killing of *M. tuberculosis* by non-killing macrophages. *in vivo*. 2008; 22: 69–75. PMID: 18396785
 37. Atal CK, Dubey RK, Singh J. Biochemical basis of enhanced drug bioavailability by piperine: evidence that piperine is a potent inhibitor of drug metabolism. *Journal of Pharmacology and Experimental Therapeutics*. 1985; 232: 258–262. PMID: 3917507
 38. Bhardwaj RK, Glaeser H, Becquemont L, Klotz U, Gupta SK, Fromm MF. Piperine, a major constituent of black pepper, inhibits human P-glycoprotein and CYP3A4. *Journal of Pharmacology and Experimental Therapeutics*. 2002; 302: 645–650. <https://doi.org/10.1124/jpet.102.034728> PMID: 12130727
 39. Mu Y, Nguyen PH, Stock G. Energy landscape of a small peptide revealed by dihedral angle principal component analysis. *Proteins: Structure, Function, and Bioinformatics*. 2005; 58: 45–52.
 40. Krivov SV, Karplus M. Hidden complexity of free energy surfaces for peptide (protein) folding. *Proceedings of the National Academy of Sciences*. 2004; 101: 14766–14770.

Chapter 4: Discovery and biological evaluation of an adamantyl-amide derivative with likely MmpL3 inhibitory activity.

The manuscript was submitted to Tuberculosis on the 1st of November (TUBE-D-22-00289).

Copyright Statement: Should this article be published in an Elsevier journal, the author and co-authors maintain the right to share their works for scholarly purposes including, inclusion in a thesis or dissertation, provided it is not published commercially.

Author Contributions

Erika Kapp: *Conceptualization; Data curation; Formal analysis; Investigation; Methodology; Software; Validation; Visualization; Writing – Original draft, review and editing.*

Hanri Calitz (née Visser): *Data curation; Formal analysis; Investigation; Methodology; Validation; Visualization; Writing – original draft.*

Elizabeth M. Streicher: *Project administration; Resources; Supervision; Writing – review & editing.*

Anzaan Dippenaar: *Data curation; Formal analysis; Investigation; Methodology; Software; Writing – review & editing.*

Samuel Egieyeh: *Formal analysis; Investigation; Methodology; Validation; Visualization; Writing – review and editing.*

Audrey Jordaan: *Formal analysis; Investigation; Methodology.*

Digby F. Warner: *Resources; Validation; Writing – review & editing.*

Jacques Joubert: *Conceptualization; Resources; Supervision; Writing – review and editing.*

Sarel F. Malan: *Conceptualization; Supervision; Writing – review and editing.*

Samantha L. Sampson: *Conceptualization; Data curation; Funding acquisition;; Methodology; Project administration; Resources; Supervision; Visualization; Writing – planning, review & editing.*

Discovery and biological evaluation of an adamantyl-amide derivative with likely MmpL3 inhibitory activity

Erika Kapp¹, Hanri Calitz², Elizabeth M. Streicher², A. Dippenaar^{2, 3}, Samuel Egieyeh¹, Audrey Jordaan⁴, Digby F. Warner⁴, Jacques Joubert¹, Sarel F. Malan¹, Samantha L. Sampson^{2*}

*Corresponding author

ssampson@sun.ac.za

¹School of Pharmacy, Faculty of Natural Sciences, University of the Western Cape, Cape Town, South Africa. University of the Western Cape, Private Bag x17, Bellville 7535. ekapp@uwc.ac.za; segieyeh@uwc.ac.za; jjoubert@uwc.ac.za; sfmalan@uwc.ac.za

²DSI/NRF Centre of Excellence for Biomedical Tuberculosis Research/South African Medical Research Council Centre for Tuberculosis Research, Division of Molecular Biology and Human Genetics, Faculty of Medicine and Health Sciences, Stellenbosch University, Cape Town, South Africa. P.O. Box 241, Cape Town, South Africa, 8000. vhanri@gmail.com; lizma@sun.ac.za;

³Global Health Institute, Department of Family Medicine and Population Health, Faculty of Medicine and Health Sciences, University of Antwerp, Antwerp, Belgium. Anzaan.Dippenaar@uantwerpen.be

⁴Molecular Mycobacteriology Research Unit, DSI/NRF Centre of Excellence for Biomedical Tuberculosis Research, Department of Pathology and Institute of Infectious Disease and Molecular Medicine, Faculty of Health Sciences, University of Cape Town, Cape Town, South Africa. Private Bag X3, Rondebosch 7701, Cape Town, South Africa. Audrey.jordaan@uct.ac.za; Digby.warner@uct.ac.za

Abstract

A series of molecules containing bulky lipophilic scaffolds was screened for activity against *Mycobacterium tuberculosis* and a number of compounds with antimycobacterial activity were identified. The most active compound, (2E)-N-(adamantan-1-yl)-3-phenylprop-2-enamide (**C1**), has a low micromolar minimum inhibitory concentration, low cytotoxicity (therapeutic index = 32.26), low mutation frequency and is active against intracellular *Mycobacterium tuberculosis*. Whole genome sequencing of mutants resistant to **C1** showed a mutation in *mmpL3* which may point to the involvement of MmpL3 in the antimycobacterial activity of the compound. *In silico* mutagenesis and molecular modelling studies were performed to better understand the binding of **C1** within MmpL3 and the role that the specific mutation may play in the interaction at protein level. These analyses revealed that the mutation increases the energy required for binding of **C1** within the protein translocation channel of MmpL3. The mutation also decreases the solvation energy of the protein, suggesting that the mutant protein might be more solvent-accessible, thereby restricting its interaction with other molecules. The results reported here describe a new molecule that may interact with the MmpL3 protein, providing insights into the effect of mutations on protein-ligand interactions and enhancing our understanding of this essential protein as a priority drug target.

Key Words

Mycobacterium tuberculosis

MmpL3

Drug resistance

Mutation

Introduction

The World Health Organization (WHO) 2021 Global Tuberculosis (TB) report estimates that approximately 1.6 million individuals died from TB in 2021.¹ The first year-on-year increase in TB mortality rate in over a decade was reported in 2020 and is, in all probability, linked to the COVID-19 pandemic which has set the fight against TB back by a number of years.^{1,2} The lengthy duration of first-line treatment recommended by the WHO² often leads to poor adherence with the associated risk of the selection of drug-resistant mutants of the causative organism, *Mycobacterium tuberculosis*. It is estimated that almost 80% of identified cases of mycobacterial drug resistance are in fact multidrug-resistant TB (MDR-TB), resistant to both isoniazid (INH) and rifampicin (RIF).³ New antimycobacterial agents that effectively target drug-resistant *Mycobacterium tuberculosis* and achieve a shorter treatment duration are urgently needed. While some new and repurposed drugs have entered the clinical setting, resistance often follows rapidly,⁴⁻⁶ emphasising the need for a broad drug development pipeline.

A significant impediment to the search for effective new antimycobacterial drugs is the barrier posed by the mycobacterial cell wall, a complex, lipid-rich structure, with limited and selective permeability. Further, *M. tuberculosis* is an intracellular pathogen, which can subvert host killing mechanisms when taken up by macrophages, and go on to survive in complex granulomatous lesions.⁷ The development of new anti-TB drug candidates needs to take these different microenvironments into consideration, especially for their potential to decrease penetration to the infecting bacillus. One approach to enhancing uptake, and / or reducing the efflux of potentially active compounds, is to couple them to bulky lipophilic carrier molecules. Studies have shown that more lipophilic drugs are more likely to be active against *M. tuberculosis*^{8,9} and may be more active against both replicating and metabolically quiescent mycobacteria compared to their more hydrophilic counterparts.¹⁰

In this study, a number of derivatives with bulky polycyclic scaffolds including adamantane, coumarin, pentacycloundecane (PCU) and isatin were screened for antimycobacterial activity. The lipophilic polycyclic cage-like moieties were speculated to increase passive diffusion across the mycobacterial cell wall and, possibly, to limit extrusion *via* efflux pumps. Compounds with antimycobacterial activity were selected and further analysed for cytotoxicity and activity against intracellular *M. tuberculosis*. Whole genome sequencing of spontaneous resistant mutants generated *in vitro* provided insight into the likely mechanism of action and resistance.

Materials and Methods

This study was approved by the Stellenbosch University Health Research Ethics Committee (S15/06/135).

Mycobacterial Reporter Strain

The episomal plasmid, pCHERRY3, was a gift from Tanya Parish (Addgene plasmid # 24659).¹¹ pCHERRY3, which carries the red fluorescent reporter mCHERRY and contains a hygromycin B resistance cassette, was transformed into electrocompetent *Mycobacterium tuberculosis* H37Rv (ATCC 27294), according to standard protocols.¹² Following transformation, *M. tuberculosis* was plated onto 7H10 agar supplemented with 10% OADC, 0.5% glycerol and 50 µg/ml hygromycin, and incubated at 37°C for approximately 3 weeks. Colonies were picked and transferred into Middlebrook 7H9 broth (Becton, Dickinson and Co., USA) (enriched with 10% OADC, 0.05% Tween 80 and 0.2% glycerol (7H9 complete)) in 96-well microtiter plates, and the presence of the red fluorescent reporter was

confirmed using a BMG Labtech POLARstar Omega plate reader (Excitation: 587 nm, Emission: 610 nm). Growth curve comparisons showed no significant difference in growth between strains with and without the reporter plasmid (data not shown). Subsequently, all *M. tuberculosis* H37Rv::pCHERRY3 stock and starter cultures were grown with 50 µg/ml hygromycin B in 7H9 complete medium; hygromycin B was omitted for drug activity assays in microtiter plates.

Initial medium-throughput *in vitro* activity screen of compounds

The 101 compounds received from the University of the Western Cape Drug Design group were reconstituted to a concentration of 10 mM in dimethyl sulfoxide (DMSO) and stored in aliquots at -80°C. The antimycobacterial activities of the synthetic compounds were determined using a 96-well plate assay. *M. tuberculosis* H37Rv with and without the reporter was cultured in 7H9 complete at 37°C to an OD₆₀₀ of approximately 1.0. Following this, the culture was strained through a 40 µm cell strainer to minimize clumps, and the OD₆₀₀ reading adjusted to 1.0. Culture was added to white, flat bottom 96-well microtiter plates with a final volume of 200 µl in each well to give a final OD₆₀₀ of 0.02. The final compound concentrations were 100 µM, 50 µM or 1 µM, and controls included a gain, bacterial growth, DMSO, positive, negative and compound-only controls. *M. tuberculosis* H37Rv::pCHERRY3 diluted culture was added to each well except the gain, background and compound control wells. In the gain control wells, 100 µl of the undiluted *M. tuberculosis* H37Rv::pCHERRY3 culture was added and in the background control wells *M. tuberculosis* H37Rv without the fluorescent reporter was added.

The plates were sealed with breathable sealing film and incubated at 37°C for 6 days, taking readings on days 0, 2, 3, 4, and 5 using a BMG Labtech POLARstar Omega plate reader (Excitation: 587 nm, Emission: 610 nm). For fluorescence readings, the (opaque) breathable seal was replaced with an optically clear sealing film, which in turn was removed and replaced by a new breathable sealing film following the reading. The average of the background control was subtracted from the fluorescence readings whereafter the data was visualised using GraphPad Prism v7.01, by plotting the relative fluorescence units (as a measure of growth) over time. The percentage inhibition was also calculated on Day 5, by dividing the treated by the untreated values. Sixteen compounds that inhibited growth by more or equal to 50% at 50 µM were selected for further study (Table S1).

Following the initial screen, narrower concentration ranges were tested to more accurately ascertain the extent of the compound's antimycobacterial activity. This second round of screening was also performed using relative fluorescence as a proxy for growth, in a 96 well plate assay as above. Wells were prepared with the synthetic compounds diluted in 7H9 complete to the required concentrations, and plates included control wells as above. Plates were incubated and read as above and the resultant raw data was analysed similarly to the initial screen. Five compounds which showed the highest activity during the second screen were selected to undergo further analysis.

Minimum Inhibitory Concentration determination

Minimum inhibitory concentrations (MICs) were independently determined for the five compounds previously demonstrating highest activity, using two different methods.

The first MIC determination was performed at the Institute of Infectious Disease and Molecular Medicine, University of Cape Town (UCT). There, the standard broth microdilution method was performed using *M. tuberculosis* pMSP12::GFP, as reported previously (20). Briefly, a 10 ml culture was

grown in glycerol-alanine-salts with 0.05% Tween 80 and iron (0.05%; GAST-Fe), pH 6.6, to an OD₆₀₀ of 0.6 – 0.7. Thereafter, the culture was diluted 1:100 in GAST-Fe. In a 96-well microtiter plate, two-fold serial dilutions of each compound were prepared in GAST-Fe, whereafter 50 µl of the diluted culture was added to each serial dilution well resulting in an OD₆₀₀ of 0.004. Controls included a bacterial growth control (with 5% DMSO in GAST-Fe) and a positive control (0.15 µM RIF). The microtiter plate was incubated at 37°C with 5% CO₂ and humidity, and sealed within a secondary container. Using a plate reader (FLUOstar OPTIMA, BMG Labtech; Excitation: 485 nm; Emission: 520 nm) relative fluorescence was measured on day 7 and 14. The CDD Vault from Collaborative Drug Discovery was used to archive and analyse the fluorescence data. Analyses included normalisation to the bacterial growth and antimycobacterial growth control as the maximum and minimum growth representations respectively, generating a dose-response curve using the Levenberg-Marquardt damped least-squares method. This dose response curve was used to calculate the MIC₉₀ and MIC₉₉.

For the second method, dose response curves were performed by exposing *M. tuberculosis* H37Rv::pCHERRY3 to increasing concentrations of each compound in white flat bottom 96 well plates in complete 7H9 media. *M. tuberculosis* H37Rv with and without mCHERRY was prepared as described above. In a white, flat bottom 96 well microtiter plate, two-fold serial dilutions of the compounds were prepared with a 100 µl final volume and final bacterial OD₆₀₀ of 0.04. The controls included were a background control (*M. tuberculosis* H37Rv in 7H9 complete), a negative control (*M. tuberculosis* H37Rv::pCHERRY3 in 7H9 complete) and a positive control (*M. tuberculosis* H37Rv::pCHERRY3 with 2 µM RIF in 7H9 complete). Plates were incubated and read as described above. To analyse the relative fluorescence data, the average of the background control was subtracted from each well, and the subsequent data set was analysed in GraphPad Prism v.7.01. Data was first normalised using built in non-linear dose-response curve analysis. This gave an output of IC₅₀ as well as a Hill Slope which was used to determine the IC₉₀ and IC₉₉ of each compound. IC₉₀ and IC₉₉ were defined as the concentration where 90% and 99% of growth was inhibited, respectively.

Cytotoxicity determination

Cytotoxicities of the 5 selected compounds were determined using a colorimetric MTT assay.¹³ Chemosensitivity and cellular growth were measured through the reduction of tetrazolium salt (MTT) to formazan salt. 96-well plates were seeded with Chinese hamster ovary (CHO) cells at a density of 10⁵ cells/ml, in Dulbeccos Modified Eagle Medium (DMEM; Sigma, St Louis, MO, USA), enriched with 10% heat-inactivated foetal bovine serum (Gibco, Life Technologies, Carlsbad, CA, USA) (D10), and incubated for a period of 24 hours at 37°C. 20 mg/ml stock solutions of the compounds were prepared and added to the wells in a ten-fold dilution series between 100 µg/ml and 0.001 µg/ml to a final volume of 200 µl. Following 44 hours drug exposure, the plates were developed through the addition of MTT (Sigma, St Louis, MO, USA) solution. Plates were incubated at 37°C for an additional 4 hours whereafter the supernatant was removed. DMSO was added to dissolve the dye crystals and the plates were measured spectrophotometrically at 540 nm to determine the relative amount of formazan in each well. Wells containing untreated cells and growth media only was used as 100% and 0% survival respectively. The amount of formazan measured in each treated well was converted to a survival percentage relative to these two extremes. The experiment was performed once in triplicate. The concentration where 50% of cell growth was inhibited (CC₅₀) was used together with the IC₅₀ to determine the therapeutic index.

Antimycobacterial activity in mammalian cells

A macrophage infection model was used to determine if **C1** is able to enter the host cell and inhibit intracellular *M. tuberculosis*. Infections were performed in 96-well microtiter plates, with RAW264.7 murine macrophages (ATCC TIB-71) infected with *M. tuberculosis* H37Rv at an MOI of 10:1 in a 200 µl final volume of DMEM (Gibco, Life Technologies Ltd) supplemented with 10% Foetal calf serum (Gibco, Life Technologies Ltd) (D10). Following a 3-hour uptake period, wells were treated with 100 U/ml of penicillin/streptomycin (Lonza Group Ltd.) for 1 hour, to remove any extracellular *M. tuberculosis*. Monolayers were subsequently washed 3 times with D10, and either lysed by the addition of sterile distilled water, or incubated further with 200 µl D10 at 37°C with 5% CO₂ and humidity. **C1** and RIF were added to selected wells at 2.26 µM and 2 µM, respectively, and untreated control wells were included for each time point. Colony forming units (CFUs) were determined on day 0, 2 and 3 by serial dilution plating of macrophage lysates on Middlebrook 7H10 agar (Becton, Dickinson and Co., USA) (supplemented with 10% OADC and 0.5% glycerol (7H10+OADC)). CFUs were determined at the respective time points following three weeks incubation at 37°C.

The CFUs were determined at day 0 to confirm uptake, and at days 2 and 3 to ascertain the antimycobacterial effect within the host cell. Data analysis was carried out using GraphPad Prism v.7.01 built-in analysis tools. *In vivo* and *in vitro* CFUs determined on day 2 and 3 were plotted on separate histograms, each statistically analysed by comparing **C1** and RIF treated-wells to untreated wells. Statistical analysis included performing a one-way ANOVA followed by a Bonferroni multiple comparisons test.

C1 *in vitro* spontaneous mutant generation

M. tuberculosis H37Rv was cultured to an optical density (OD₆₀₀) of 0.5, in 10 ml 7H9 complete, whereafter it was centrifuged (3500 rpm; 5-10 min) to pellet the cells. The cells were resuspended in 500 µl 7H9+OADC and 100 µl of the cells were then plated in quadruplicate onto 7H10+OADC which contained 20 µM (~9× MIC) of **C1**. Serial dilutions of the culture were plated in triplicate on 7H10 supplemented with 10% OADC and 0.5% glycerol without compound as a no-compound control. Plates were incubated at 37°C for 30 days whereafter colonies were counted, picked from compound-containing plates and cultured in T25 tissue culture flasks (Sigma-Aldrich, USA) in 10 ml 7H9 complete without **C1**.

Resistance to **C1** was verified using a 96-well microtiter assay. To achieve this, possible mutants were cultured in 7H9 complete without the compound for 7 days, whereafter they were transferred to 96-well microtiter plate with black-sided wells and clear, flat bottoms, at an OD₆₀₀ of 0.02. Triplicate wells were exposed to 0, 10 µM (~4.5× MIC) or 20 µM (~9× MIC) **C1**, and growth kinetics were monitored over 6 days using OD₆₀₀ readings on a BMG Labtech POLARstar Omega plate reader (BMG, Germany). Following the verification of spontaneous mutants, the mutation frequency was calculated by comparing the number of spontaneous resistant mutants that developed in comparison to the colony forming units (CFUs) that were observed on the no compound control plates.

Whole Genome Sequencing

Genomic DNA was extracted from the progenitor, drug-susceptible *M. tuberculosis* H37Rv and 11 **C1** resistant isolates using a previously described method.¹⁴ Genomic DNA from these isolates was sequenced on an Illumina NextSeq 550 platform using a paired-end approach with ±600 base fragment

sizes. Analysis of the Illumina sequencing data was done using an in-house pipeline as previously described¹⁵. Pairwise comparisons of the variants identified in the *M. tuberculosis* H37Rv progenitor and the 11 C1 resistant isolates were done to identify genomic variants acquired by the resistant mutants. The WGS data were deposited to the European Nucleotide Archive under accession number: PRJEB56028.

Mutagenesis and molecular docking

The crystal structure of mycolic acid transporter MmpL3 from *M. smegmatis* complexed with the experimental MmpL3 inhibitor AU1235 (6AJH PDB DOI: [10.2210/pdb6AJH/pdb](https://doi.org/10.2210/pdb6AJH/pdb)) was used to perform the mutagenesis and docking studies. Although the cryo-EM structure of MmpL3 in *M. tuberculosis* is available (7NVH PDB DOI: [10.2210/pdb7NVH/pdb](https://doi.org/10.2210/pdb7NVH/pdb)), 6AJH which is commonly used as a reference protein in structure based research,^{16,17} because it has a slightly better resolution and is complexed with AU1235 which is structurally similar to **C1**. *M. tuberculosis* and *M. smegmatis* share 61% sequence identity and notable similarities in ligand interactions with *M. tuberculosis* MmpL3.¹⁸ Through sequence analysis it was determined that the Phe644 amino acid observed in the wildtype *M. tuberculosis* MmpL3 protein translates to Phe649 in 6AJH due to changes in the upstream residues in the *M. smegmatis* protein sequence that does not influence the binding site in question.

The *M. smegmatis* Phe649Leu mutant (Phe649Leu^s) was generated utilizing the CHARMM- GUI¹⁹ and PBEQ-Solver in CHARMM-GUI was used to calculate solvation free energy of the wild type and mutant proteins.¹⁹ The wildtype and mutant proteins were prepared for docking in Molecular Operating Environment software (MOE, 2020.09 Chemical Computing Group ULC, 1010 Sherbooke St. West, Suite #910, Montreal, QC, Canada, H3A 2R7, 2022). The well-known MmpL3 inhibitor, SQ109, and **C1** were washed, protonated and minimized with Amber10:EHT forcefield. SQ109 and **C1** were docked into the wild type and mutant proteins in MOE using the Triangle Matcher placement method and the initial top 30 poses were scored with London dG. The placement of the initial 30 poses was refined with the Induced Fit method and the top 6 poses were rescored with GBVI/WSA dG. The binding free energy of the top six poses of SQ109 and **C1** in the wild type and mutant proteins were extracted and plotted against the poses.

Results

Minimum inhibitory concentration determination.

Of the 101 compounds included in the initial medium throughput *in vitro* screen, 16 compounds inhibited growth by $\geq 50\%$ at 50 μM (Table S1). The 16 compounds identified were screened at narrower concentration ranges and 5 compounds (**C1**, **C2**, **C3**, **C4** and **C5**, Figure 1) which showed more than 85% growth inhibition at 50 μM during this second screen were selected for further evaluation.

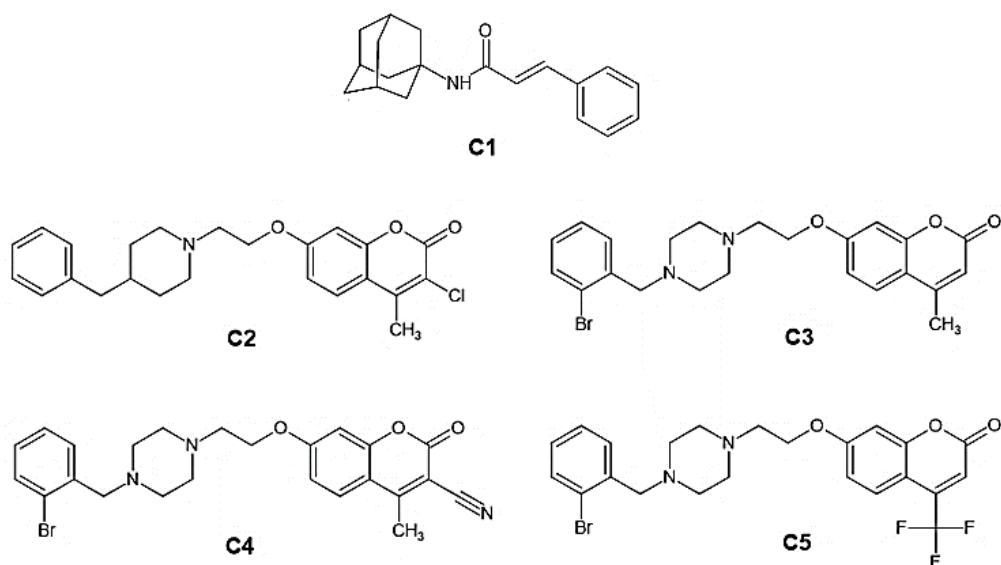


Figure 1: Structures of the 5 top compounds selected for further evaluation.

The MICs of these five compounds were assessed using two independent methods which utilized different *M. tuberculosis* fluorescence bioreporters and growth media. In both assays, the five compounds displayed promising antimycobacterial activities (Table 1). There was a consistent trend towards greater potency in GAST-Fe medium, potentially indicating protein binding in the albumin-containing 7H9 complete medium. Notably, however, both assays identified **C1** as most potent compound, with an MIC₉₀ of <0.244 and 2.26 μM using the GAST-Fe and 7H9 complete methods, respectively.

Table 1: Minimum inhibitory concentrations of the top 5 compounds.

Compound	GFP – GAST-Fe		mCHERRY – 7H9+OADC	
	MIC ₉₀ (μM)	MIC ₉₉ (μM)	MIC ₉₀ (μM)	MIC ₉₉ (μM)
C1	< 0.244	< 0.244	2.26	3.47
C2	19.6	25.2	40.55	44.15
C3	14	29.7	40.89	50.40
C4	16.7	28	45.22	54.46
C5	3.2	8.31	43.78	57.17

Cytotoxicity Analysis

The cytotoxicities of the five most promising candidates were determined using an MTT assay following exposure of Chinese Hamster Ovary (CHO) to the compounds (Table 2). **C1** displayed no cytotoxicity up to 50 μM , while **C2**, **C3**, **C4** and **C5** were cytotoxic at concentrations between 16.5 and 41.2 μM . This suggests that compounds **C2**, **C3**, **C4** and **C5** would be cytotoxic at effective treatment concentrations. In contrast, **C1** has a favourable therapeutic index, since it inhibits *in vitro* *M. tuberculosis* growth by 90% at 2.26 μM .

Table 2: Cytotoxicity and therapeutic index.

Compound	CC ₅₀ (μM)	Therapeutic Index*
C1	>50	32.26
C2	33	0.88
C3	16.5	0.48
C4	41.2	1.07
C5	26.3	0.75

* The therapeutic index was calculated by dividing CC₅₀ by IC₅₀ (obtained from dose response curves).

Antimycobacterial Activity in Mammalian Cells

The intracellular activity of **C1** was determined in a macrophage infection model. *M. tuberculosis*-infected RAW264.7 macrophages were treated with **C1** or RIF, and bacterial survival was compared to that in untreated control macrophages through colony forming unit determination. This revealed that, on day 2 and 3 following the onset of treatment, both **C1** and RIF caused significant reduction of *M. tuberculosis* CFU *in vitro* and *in vivo* (Figure 1). This confirms that **C1** is effective against intracellular *M. tuberculosis*.

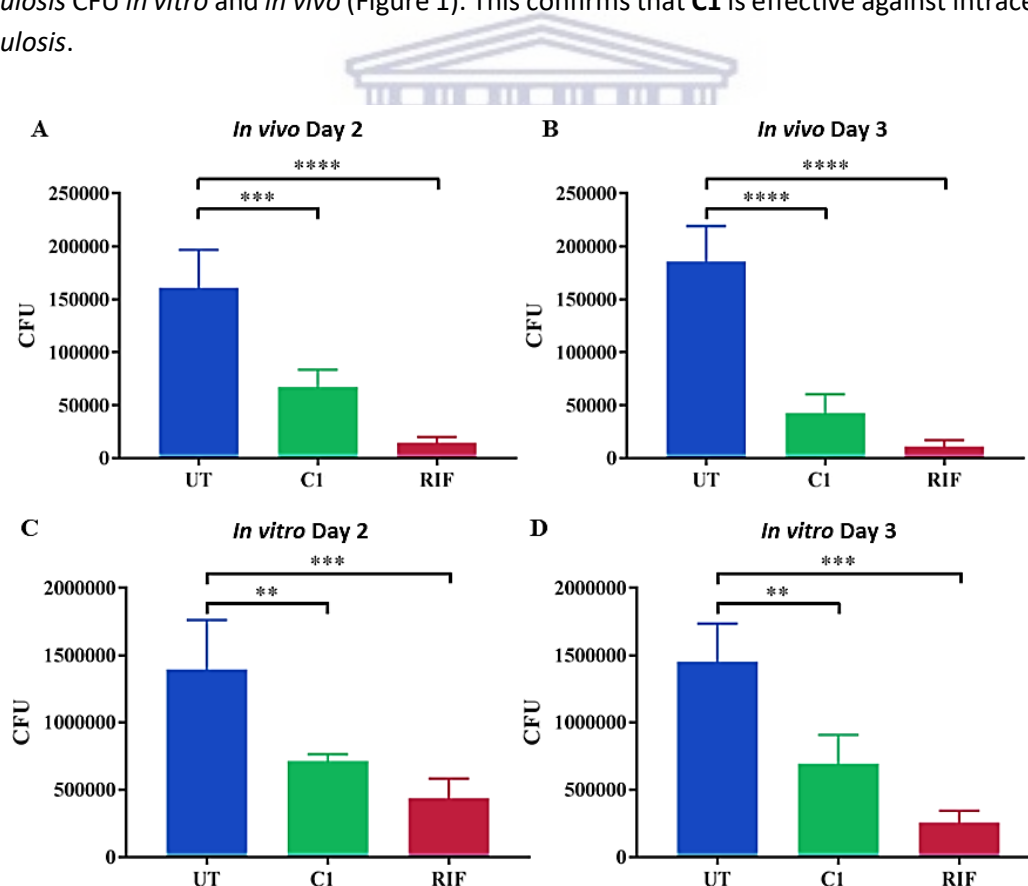


Figure 2: Antimycobacterial activity in mammalian cells.

Colony forming units (CFU) present in infected macrophages following **C1** and rifampicin (RIF) treatment. (A) and (B) represent *M. tuberculosis* H37Rv CFUs present intracellularly on day 2 and 3 respectively when left untreated or treated with either C1 or RIF. (C) and (D) represent *M. tuberculosis* H37Rv CFUs present in *in vitro* control on day 2 and 3 respectively following the same treatment as (A)

and (B). One representative biological repeat (with 4 technical replicates) is shown. Statistical analyses showed statistically significant inhibition of growth when comparing both C1 and RIF with UT *in vivo* and *in vitro*. (** $p \leq 0.01$, *** $p \leq 0.001$, **** $p < 0.0001$).

Mutation frequency and mechanism of resistance

To determine mutation frequency and identify a possible mechanism of resistance, the progenitor, drug-susceptible *M. tuberculosis* H37Rv, was cultured on solid agar plates containing 20 μM C1 ($\sim 9\times$ MIC). This resulted in the recovery of 66 putative mutants with a frequency of 1.65×10^{-12} . The reported mutation rate of *M. tuberculosis* H37Rv for first line antimycobacterial compounds are summarized in table 3. Subsequent sub-culturing and re-exposure to C1 in a microtiter assay confirmed that all of these isolates were resistant to 10 μM ($\sim 4\times$ MIC).

Table 3: Mutation frequency observed in antimycobacterial drugs in *M. tuberculosis*.

Antimycobacterial compound	Mutation frequencies
Isoniazid ²⁰	4.17×10^{-6}
Rifampicin ²⁰	6.86×10^{-8}
Bedaquiline ²¹	6×10^{-9}
Clofazimine ²¹	5×10^{-5}
Linezolid ²¹	1×10^{-8}

To identify possible resistance-causing mutations, DNA was extracted from 11 isolates resistant to C1 and subjected to whole-genome sequencing. Isolates had an average depth of coverage of 118x (median 90x) and $\geq 98\%$ of the reads mapped to the reference genome, reflecting that pure, contamination-free cultures were obtained. Subsequent bioinformatic analyses comparing the variants detected in the resistant mutants to the susceptible progenitor revealed no acquired insertion-deletion mutations and a total of five single nucleotide variants (SNVs) (Table 4). Three of the SNVs were only identified in one ($n=2$) or two ($n=1$) isolates, and were therefore deemed unlikely to explain the observed resistance. Specifically, a low frequency (approximately 25%) synonymous SNV was identified in a single isolate in *Rv1753* (encoding a PPE protein), and a low-frequency (approximately 17%) non-synonymous SNV was identified in one isolate in *Rv1574* (encoding a probable PhiRv1 phage-related protein); a fixed variant was identified in two isolates in *Rv2252* (encoding a diacylglycerol kinase). Two fixed SNVs were found in all 11 isolates, one of these was in *Rv3212* (a conserved alanine valine rich protein); however, since this was a synonymous SNV, this would be unlikely to explain the observed resistance. The only non-synonymous SNV which was present in all the isolates was identified in *mmpL3* (*Rv0206c*) and resulted in a phenylalanine to leucine amino acid change at codon 644 (Table 4).

Table 4: SNPs identified during whole genome sequencing analysis.

Gene	Protein	SNV	Effect on Protein	Number of isolates present
<i>Rv0206c</i>	MmpL3	C1932G	Phe644Leu	11
<i>Rv1574</i>	Probable PhiRv1 phage related protein	G143T	Arg48Leu	1
<i>Rv1753c</i>	PE/PPE	G1485A	None	1
<i>Rv2252</i>	Diacylglycerol Kinase	C609A	Asp203Glu	2
<i>Rv3212</i>	Conserved alanine valine rich protein	C987G	None	11

Mutagenesis and molecular docking

The crystal structure of *Mycobacterium smegmatis* MmpL3 complexed with the experimental inhibitor AU1235 (PDB 6AJH) was utilized to generate a Phe649Leu^s mutation which, based on sequence analysis, would represent a Phe644Leu mutation in *Mycobacterium tuberculosis* *mmpL3*. The predicted bilayer lipid membrane and orientation of the lipid transporter MmpL3 is shown in figure 3. The Phe649Leu^s mutation is located in the transmembrane region of the MmpL3 protein.

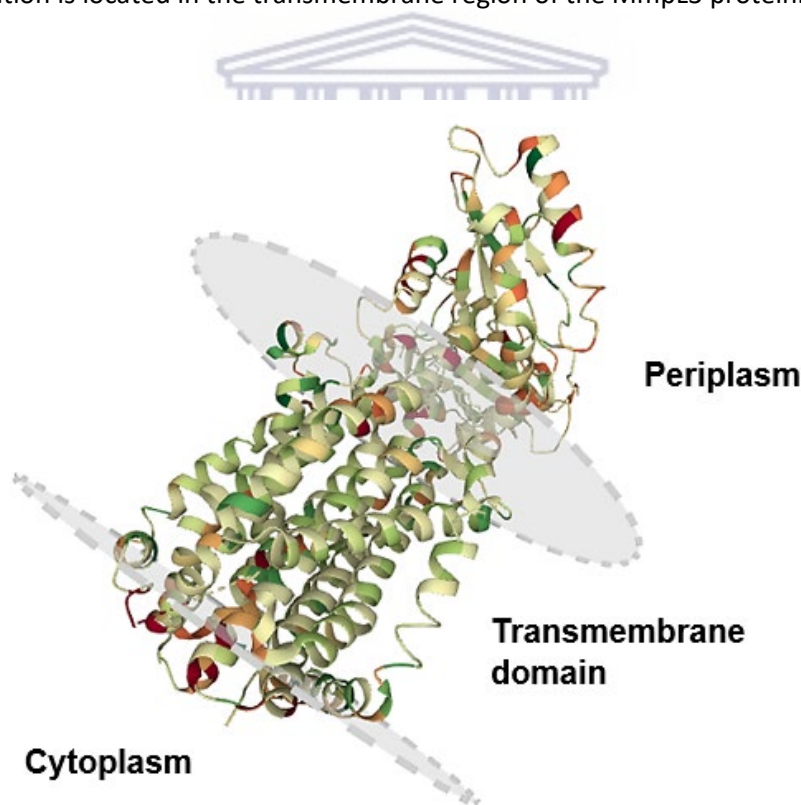


Figure 3: Predicted bilayer lipid membrane orientation of the MmpL3 protein.

Molecular docking of the known MmpL3 inhibitor, SQ109,²² and **C1** was performed utilizing the wildtype and mutant MmpL3 proteins in MOE. The binding free energy (presented as S score) was calculated to compare the binding of the respective compounds in the wild type and mutant proteins (Figure 4).

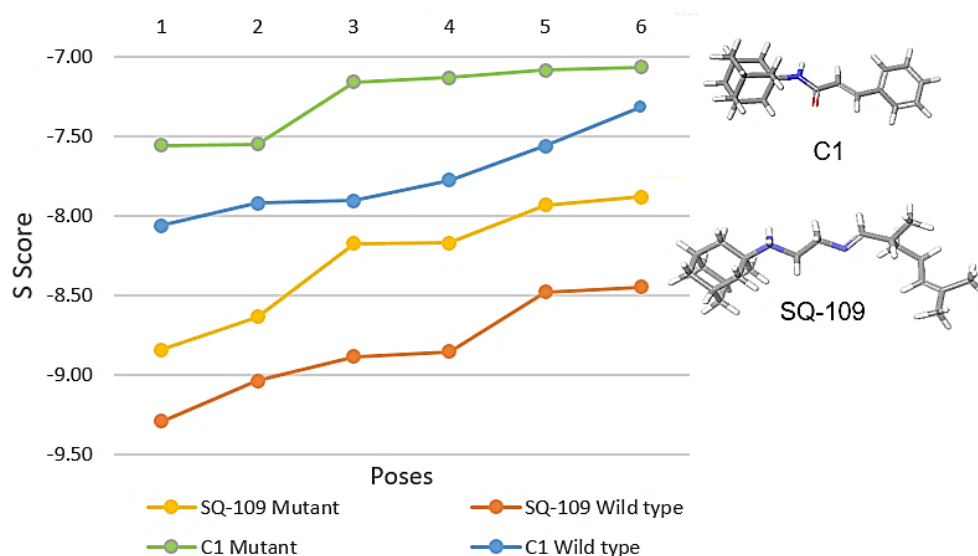


Figure 4: A comparison of the S Scores of **C1** and SQ109 in the wild type and Phe649Leu^s mutant proteins for the top 6 poses as predicted in MOE.

A higher binding free energy indicates a lower binding affinity between the protein and the ligand. As can be seen from the S Score which represents binding free energy, the energy required for binding to the mutant protein is higher for both SQ109 and **C1**. The highest binding energy was predicted for **C1** in the mutant MmpL3 protein which could explain the resistance observed for **C1** in the presence of a F644L mutation.

Residue interactions of the top poses of **C1** and SQ109 were further analysed. An additional hydrogen bond interaction was formed between the **C1** oxygen function and Tyr646 in the mutant protein which appears to impact the orientation of the molecule within the binding pocket (Figure 5). It was also observed that there is a reduced hydrophobic interaction between the adamantane moiety in **C1** and the mutant protein, which may contribute to the increased free binding energy observed.

The electrostatic potential distribution at the binding site of wildtype and mutant proteins was analysed (Figure 6). The mutant protein was predicted to have a lower solvation energy of -6871.32 kcal/mol compared to the -6847.145 kcal/mol observed for the wild type protein. The solvation affects the protein environment and determines how small molecules interact with such proteins.

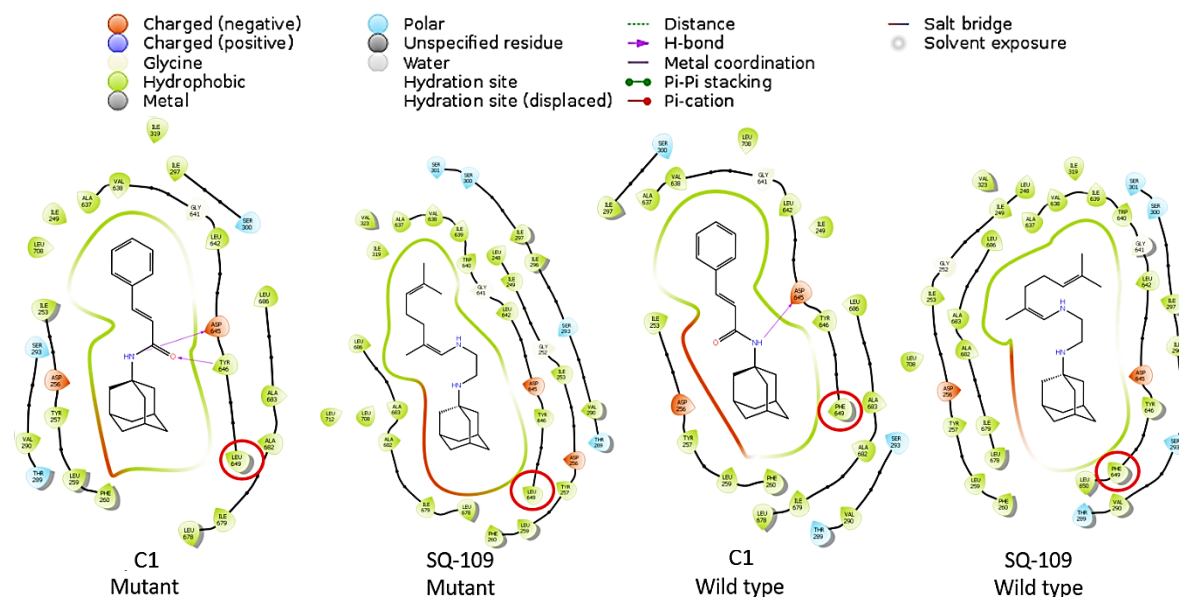


Figure 5: Residue interactions of the top poses of **C1** and **SQ109** in the wild type and mutant protein respectively. The Phe649Leu⁵ mutated residue is highlighted with a red circle. Darker colours indicate a stronger interaction, with the type of interaction described in the legend at the top of the figure.

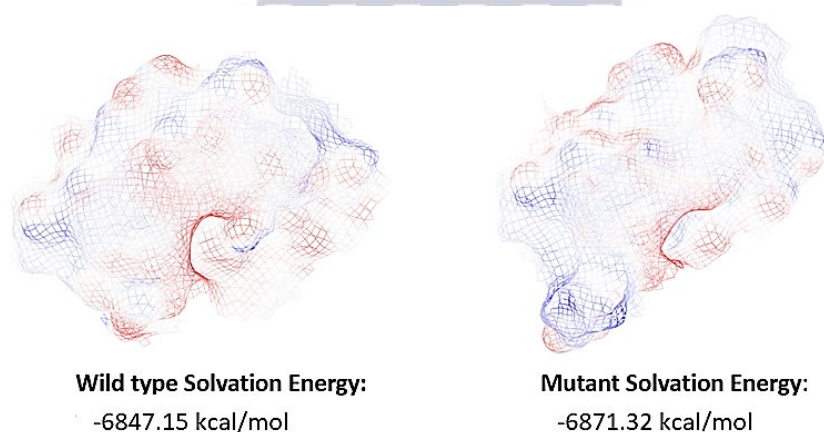


Figure 6: Electrostatic potential distribution at the binding site of the wild type and mutant MmpL3. (+2 kcal/(mol-e) in blue to -2 kcal/(mol-e) in red).

Discussion

As a step towards addressing the urgent need for feeding new candidates into the TB drug development pipeline, this study screened 101 synthetic compounds for activity against *M. tuberculosis*. This identified five compounds with promising inhibitory activity, which were further investigated.

The minimum inhibitory concentrations (MICs) of these five compounds were determined using two different approaches. The first method, utilizing a GFP bioreporter together with GAST-Fe media, yielded consistently lower MICs than the second in-house technique which employed the use of the

far-red mCHERRY reporter and 7H9 complete media. This difference could be due to the presence of albumin in 7H9 complete, the different reporter used,²³ or the difference in inoculum size, and the serial dilutions used during the method. However, even though the MICs differed between the two methods used, the observed trends were similar. In both assays **C1** was shown to be a promising hit displaying low MIC₉₀ for both the protein-containing and protein-free media, 2.26 μM (0.64 $\mu\text{g}/\text{ml}$) and <0.244 μM (<0.069 $\mu\text{g}/\text{ml}$) respectively. This falls within the range of activity of the first-line anti-tuberculosis drugs such as INH and ETH, with 3.63 μM and 4.84 μM respectively, in Middlebrook 7H9 media supplemented with glycerol and albumin-dextrose-catalase (ADC).¹³

An important step in the development of any new drug candidate is determining whether it would have any negative effects on host cells. As a first step towards assessing this, the potential cytotoxicity of the five compounds was assessed in a well-established Chinese hamster ovary assay. This revealed that compounds **C2**, **C3**, **C4** and **C5** are cytotoxic at MIC₉₀ which implies that these compounds would not be suitable for *M. tuberculosis* treatment. The CC₅₀ of **C1** was more than 50 μM and with an MIC₉₀ 2.26 μM and 3.47 μM that translates to a therapeutic index of ≥ 32.26 . **C1** therefore shows promise as an effective treatment for *M. tuberculosis* infection since it does not elicit a deleterious cytotoxic response within the host cell at effective *in vitro* treatment concentrations.

Since *M. tuberculosis* is an intracellular pathogen, with the host macrophage as a major survival niche, it is important that any new anti-TB candidates are effective against *M. tuberculosis* residing within this compartment. We therefore assessed activity of **C1** against *M. tuberculosis* within infected macrophages. This demonstrated that **C1** was able to kill intracellular *M. tuberculosis*, indicating that this compound is able to access *M. tuberculosis* within the host cell.

Oral bioavailability is also an important consideration for hit compounds. **C1** adheres to Lipinski's rule,²⁴ with a molecular weight of 281.92 g/mol, less than 5 and 10 hydrogen bond donors and acceptors respectively and a partition constant Log P value of 3.64 (predicted Marvin suite, Chemaxon, <https://www.chemaxon.com>). A drug that falls within the parameters of Lipinski's rule of 5 is more likely to be absorbed from the gastrointestinal tract. Once absorbed, first pass metabolism and distribution to the correct tissue are also important considerations. Although SQ109, the 1,2-ethylene diamine adamantane derivative, distributes well into tissue it only achieves between a 4 – 12 % oral bioavailability in mice.^{25,26} One of the factors that may result in this low oral bioavailability is metabolism by cytochrome P450 enzymes. Research has shown that SQ109 is rapidly metabolised by human microsomes and specifically the CYP2D6 and CYP2C19 cytochrome P450 enzymes. The 2' amine in particular is a metabolic soft spot where oxidation, N-demethylation as well as N-nitrosylation occurs.²⁶ The amide linker in **C1** may therefore promote the stability of the compound.

In light of ongoing emergence and transmission of drug-resistant *M. tuberculosis* strains, it is important to understand the likelihood of emergence of resistance to any new TB drug candidates. In this study, we showed that spontaneous *in vitro* mutants were generated with a frequency of 1.65×10^{-12} , which is very low compared to mutation frequencies observed for other classes of putative MmpL3 inhibitors²⁷ and published mutation frequencies for other first-line drugs. A mutation frequency of 2.18×10^{-9} was previously reported for SQ109.²⁸

To identify possible mechanisms of resistance to **C1**, we performed whole genome sequencing analysis of 11 resistant isolates. This identified five genes containing SNVs in the 11 isolates. Two of the genes, *Rv1753c* and *Rv3212*, contained synonymous SNVs, would most likely not play a role in **C1** resistance.

The other 3 genes, *mmpL3*, *Rv1574* and *Rv2252*, contained non-synonymous mutations. Of these, SNVs in *Rv1574* and *Rv2252* were found in only 1 or 2 isolates, respectively. The SNV identified in *mmpL3*, which caused a Phe644Leu amino acid change, was the only non-synonymous mutation found in all 11 sequenced isolates, suggesting that this could be the possible mechanism of resistance.

The *mmpL3* gene encodes MmpL3, which forms part of the mycobacterial membrane protein large (MmpL) family which shares structure homology with the Gram-negative drug resistance associated resistance-nodulation-cell division (RND) protein super family.^{29,30} Of the multiple MmpL proteins found in *M. tuberculosis*, MmpL3 is the only one found to be essential for growth both *in vitro* and *in vivo*.³¹ The MmpL3 protein has a highly conserved gene sequence across mycobacteria.^{32,33} Transformation of a *Mycobacterium tuberculosis mmpL3* gene into a *M. smegmatis mmpL3* knock-out mutant was able to restore the viability of the cells which demonstrates that the two proteins can act as substitutes for one another.³⁴ MmpL3 is suspected to play a role in trehalose monomycolate (TMM) transport across the plasma membrane using proton motive force (PMF).^{22,34,35} It was recently reported that the transport of TMM occurs via a linked movement of the transmembrane helices and periplasmic domain which moves the TMM across the plasma membrane.¹⁶ Following transport across the plasma membrane, TMM acts as a precursor for trehalose dimycolate (TDM), whereafter both these important mycolic acids are incorporated into the mycobacterial outer membrane of the cell wall together with other mycolic acids.³⁶ It is this mycobacterial cell wall that is unique to mycobacteria making the biosynthesis thereof an attractive target for new TB drug candidates.

MmpL3 consists of 12 transmembrane domains (TMs) and two porter domains (PN & PC) in the periplasm and a C-terminus in the cytoplasm.^{30,32} Numerous classes of compounds as well as an ever expanding list of new and unique scaffolds have been identified as MmpL3 inhibitors.^{17,27,32,37-39} As far as can be determined all current MmpL3 inhibitors bind within the proton translocation channel in the TM domain¹⁸ of the protein which leads to the concern that certain mutations within this common area may result in cross resistance to a number of identified MmpL3 inhibitors.

In recent years, mutations in *mmpL3* have been linked to resistance to a number of antimycobacterial compounds, the most notable being the ethambutol analogue SQ109 which has recently completed phase ii clinical trials.^{40,41} WGS of mutants found to be SQ109 resistant, showed non-synonymous SNVs in *mmpL3* in the periplasmic pore domain (PN) but primarily in the transmembrane domain (TM). Mutations at positions Gln40Arg (PN), Ser288Thr (TM5), Leu567Pro (TM8), and Ala700Thr (TM12) have been reported to cause resistance to SQ109.^{22,32} Resistance conferring mutations in *mmpL3* have also been reported for a number of the other structurally diverse inhibitors.^{27,42-45} The majority of the observed resistance mutations are located in the transmembrane domain of MmpL3 and although there is overlap in the patterns of resistance mutations observed between the different classes of compounds, there is a clear variation in the pattern of mutations selected by the various classes of compounds.^{18,27,46,47}

The adamantyl urea (e.g. AU1235) and the pyrrole and pyrazole (e.g., rimonabant and BM212) classes share a number of mutations with SQ109.³² The Phe644Leu resistance mutation observed for **C1** is shared with the tetrahydropyrazolopyrimidinecarboxamides (THPPs), AU125, a unique tetrahydropyran-amide derivative HC2091 and a class of recently published 4-phenyl piperidine derivatives.^{27,32,46} Although the THPP derivatives were originally thought to be MmpL3 inhibitors it was later shown that these compounds inhibit mycolic acid synthesis by acting as a competitive inhibitor

of the enoyl-CoA hydratase-like protein, EchA6.⁴⁸ The observed mutations impaired the uptake of the THPP derivatives into the mycobacterial cell.⁴⁶ Although this may point to the possibility of alternative targets for other compounds which have been classified as MmpL3 inhibitors, McNeil *et al.* demonstrated that MmpL3 is indeed the likely target of AU1235 as well as the spiral amide class evaluated in their study.⁴⁶

The molecular modelling and mutagenesis studies performed show that both SQ109 and **C1** would require higher energy for binding in the Phe649Leu^s *M. smegmatis* mutant protein than the wild type protein. As previously mentioned, the Phe649Leu^s mutation would translate to a Phe644Leu mutation in *M. tuberculosis*. This may explain the resistance observed for **C1** in this study and suggest that SQ109 would also be less effective in a strain with this particular mutation. Zheng *et al.* reported that *M. tuberculosis* harbouring the Phe644Leu mutation does indeed show low level resistance to SQ109.⁴⁹ It must be noted that, where a drug is reported to inhibit bacterial growth through a number of distinct mechanisms, as is the case for SQ109^{22,35} which is also active against organisms that do not contain mycolic acids,^{50,51} the level of phenotypic resistance will likely not correlate directly to the level of activity at one particular protein. The reason for the lower levels of resistance observed for SQ109 when compared to **C1** in a Phe644Leu mutant strain, could therefore be linked to multiple mechanisms of antimycobacterial activity, or the lower overall binding energy required for SQ109 binding in the wild type as well as the mutant proteins.

Solvation also plays a key role in a variety of biological mechanisms including ligand-protein association and has a strong impact on comparisons of binding energies for docked molecules. In substrate binding, but also in structure-based drug design, the thermodynamic properties of water molecules surrounding a given protein are of high interest. It is important to consider explicitly the water molecules, which are competing for interaction with the surface of the protein. The lower solvation energy of the mutant protein predicted in this study suggests that the protein might be more readily accessible to solvent thus requiring more energy for desolvation and limiting its interaction with other molecules.

The mutation identified in *mmpL3* point to a mechanism of resistance which may be related to a mechanism of action. Although further research would be required to identify the mechanism of action of **C1**, the current study lays a foundation for further anti-TB drug development. Specifically, these results provide a better understanding of the essential protein MmpL3 as a possible target.

Acknowledgements

SLS is funded by the South African Research Chairs Initiative of the Department of Science and Technology and National Research Foundation (NRF) of South Africa, award number UID 86539. The authors acknowledge the SAMRC Centre for TB Research and DST/NRF Centre of Excellence for Biomedical Tuberculosis Research for financial support for this work. UWC is grateful to the National Research Foundation of South Africa, grant number 117887 for financial support. This project was also supported through the Strategic Health Innovation Partnerships (SHIP) Unit of the South African Medical Research Council with funds received from the South African Department of Science Innovation (to DFW). The content is solely the responsibility of the authors and does not necessarily represent the official views of the SA MRC or the NRF. The authors would like to thank Dr. James Posey and the Centres for Disease Control and Prevention, Atlanta, GA, United States for sequencing the

isolates analysed in this study. AD acknowledges support from the Tuberculosis Omics Research Consortium, headed by Prof Annelies Van Rie, funded by the Research Foundation Flanders (FWO), under grant no. G0F8316N (FWO Odysseus).

Declaration of interest

The authors declare no conflict of interest.

References

1. World Health Organisation. Global tuberculosis report 2021. <https://www.who.int/publications/i/item/9789240037021>. Published 2021. Accessed September 9, 2022.
2. World Health Organization. Treatment of drug-susceptible tuberculosis: rapid communication. 2021. <https://www.cdc.gov/tb/topic/research/tbtc/default.htm>. Accessed February 18, 2022.
3. World Health Organization. Global tuberculosis report 2020. <https://www.who.int/publications/i/item/9789240013131>. Accessed May 19, 2021.
4. Liu Y, Gao M, Du J, et al. Reduced Susceptibility of Mycobacterium tuberculosis to Bedaquiline during Antituberculosis Treatment and Its Correlation with Clinical Outcomes in China. *Clin Infect Dis*. 2021;73(9):E3391-E3397. doi:10.1093/cid/ciaa1002
5. Wu SH, Chan HH, Hsiao HC, Jou R. Primary Bedaquiline Resistance Among Cases of Drug-Resistant Tuberculosis in Taiwan. *Front Microbiol*. 2021;12. doi:10.3389/FMICB.2021.754249
6. Sonnenkalb L, Carter J, Spitaleri A, et al. Deciphering Bedaquiline and Clofazimine Resistance in Tuberculosis: An Evolutionary Medicine Approach. *bioRxiv*. March 2021:2021.03.19.436148. doi:10.1101/2021.03.19.436148
7. Allué-Guardia A, García JI, Torrelles JB. Evolution of Drug-Resistant Mycobacterium tuberculosis Strains and Their Adaptation to the Human Lung Environment. *Front Microbiol*. 2021;12:137. doi:10.3389/FMICB.2021.612675/BIBTEX
8. Dashti Y, Grkovic T, Quinn RJ. Predicting natural product value, an exploration of anti-TB drug space. *Nat Prod Rep*. 2014;31(8):990-998. doi:10.1039/C4NP00021H
9. Makarov V, Lechartier B, Zhang M, et al. Towards a new combination therapy for tuberculosis with next generation benzothiazinones. *EMBO Mol Med*. 2014;6(3):372. doi:10.1002/EMMM.201303575
10. Piccaro G, Poce G, Biava M, Giannoni F, Fattorini L. Activity of lipophilic and hydrophilic drugs against dormant and replicating Mycobacterium tuberculosis. *J Antibiot (Tokyo)*. 2015;68(11):711-714. doi:10.1038/ja.2015.52
11. Carroll P, Schreuder LJ, Muwanguzi-Karugaba J, et al. Sensitive detection of gene expression in mycobacteria under replicating and non-replicating conditions using optimized far-red reporters. *PLoS One*. 2010;5(3):e9823. doi:10.1371/journal.pone.0009823 [doi]
12. Snapper SB, Melton RE, Mustafa S, Kieser T, Jacobs WR. Isolation and characterization of efficient plasmid transformation mutants of Mycobacterium smegmatis. *Mol Microbiol*. 1990;4(11):1911-1919. doi:10.1111/J.1365-2958.1990.TB02040.X
13. Mosmann T. Rapid colorimetric assay for cellular growth and survival: application to proliferation and cytotoxicity assays. *J Immunol Methods*. 1983;65(1-2):55-63. doi:0022-1759(83)90303-4
14. Warren R, De Kock M, Engelke E, et al. Safe Mycobacterium tuberculosis DNA extraction

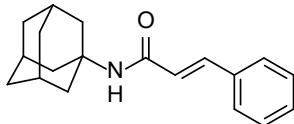
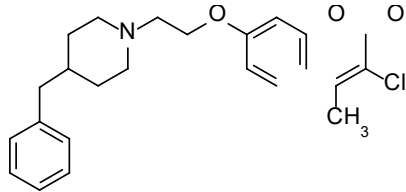
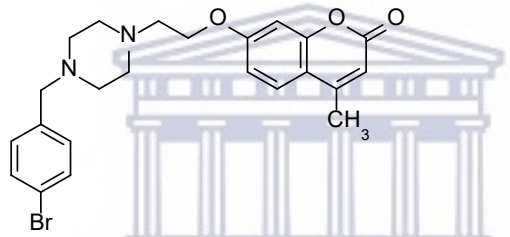
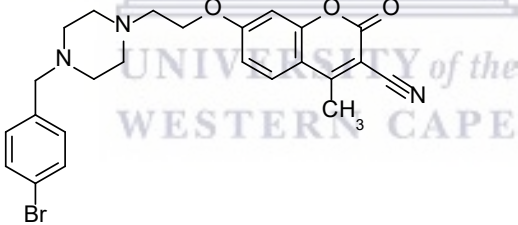
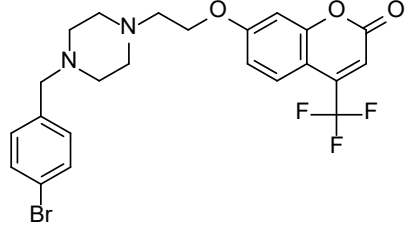
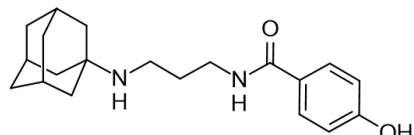
- method that does not compromise integrity. *J Clin Microbiol.* 2006;44(1):254-256. doi:10.1128/JCM.44.1.254-256.2006
15. Dippenaar A, De Vos M, Marx FM, et al. Whole genome sequencing provides additional insights into recurrent tuberculosis classified as endogenous reactivation by IS6110 DNA fingerprinting. *Infect Genet Evol.* 2019;75. doi:10.1016/J.MEEGID.2019.103948
 16. Su CC, Klenotic PA, Cui M, Lyu M, Morgan CE, Yu EW. Structures of the mycobacterial membrane protein MmpL3 reveal its mechanism of lipid transport. *PLoS Biol.* 2021;19(8). doi:10.1371/JOURNAL.PBIO.3001370
 17. Williams JT, Haiderer ER, Coulson GB, et al. Identification of New MmpL3 Inhibitors by Untargeted and Targeted Mutant Screens Defines MmpL3 Domains with Differential Resistance. *Antimicrob Agents Chemother.* 2019;63(10). doi:10.1128/AAC.00547-19
 18. Adams O, Deme JC, Parker JL, Fowler PW, Lea SM, Newstead S. Cryo-EM structure and resistance landscape of *M. tuberculosis* MmpL3: An emergent therapeutic target. *Structure.* 2021;29(10):1182-1191.e4. doi:10.1016/J.STR.2021.06.013
 19. Jo S, Kim T, Iyer VG, Im W. CHARMM-GUI: A web-based graphical user interface for CHARMM. *J Comput Chem.* 2008;29(11):1859-1865. doi:10.1002/JCC.20945
 20. Bergval IL, Schuitema ARJ, Klatser PR, Anthony RM. Resistant mutants of *Mycobacterium tuberculosis* selected in vitro do not reflect the in vivo mechanism of isoniazid resistance. *J Antimicrob Chemother.* 2009;64(3):515. doi:10.1093/JAC/DKP237
 21. Ismail N, Omar S V., Ismail NA, Peters RPH. In vitro approaches for generation of *Mycobacterium tuberculosis* mutants resistant to bedaquiline, clofazimine or linezolid and identification of associated genetic variants. *J Microbiol Methods.* 2018;153:1-9. doi:10.1016/J.MIMET.2018.08.011
 22. Tahlan K, Wilson R, Kastrinsky DB, et al. SQ109 Targets MmpL3, a Membrane Transporter of Trehalose Monomycolate Involved in Mycolic Acid Donation to the Cell Wall Core of *Mycobacterium tuberculosis*. *Antimicrob Agents Chemother.* 2012;56(4):1797-1809. doi:10.1128/AAC.05708-11
 23. Kapp E, Visser H, Sampson SL, et al. Versatility of 7-substituted coumarin molecules as antimycobacterial agents, neuronal enzyme inhibitors and neuroprotective agents. *Molecules.* 2017;22(10). doi:10.3390/molecules22101644
 24. Lipinski CA. Drug-like properties and the causes of poor solubility and poor permeability. *J Pharmacol Toxicol Methods.* 2000;44(1):235-249. doi:10.1016/S1056-8719(00)00107-6
 25. Jia L, Tomaszewski JE, Hanrahan C, et al. Pharmacodynamics and pharmacokinetics of SQ109, a new diamine-based antitubercular drug. *Br J Pharmacol.* 2005;144(1):80. doi:10.1038/SJ.BJP.0705984
 26. Jia L, Noker PE, Coward L, Gorman GS, Protopopova M, Tomaszewski JE. Interspecies pharmacokinetics and in vitro metabolism of SQ109. *Br J Pharmacol.* 2006;147(5):476. doi:10.1038/SJ.BJP.0706650
 27. Kumar A, Chettiar S, Brown BS, et al. Novel chemical entities inhibiting *Mycobacterium tuberculosis* growth identified by phenotypic high-throughput screening. *Sci Reports* 2022 121. 2022;12(1):1-27. doi:10.1038/s41598-022-19192-7
 28. O'Brien RJ, Spigelman M. New Drugs for Tuberculosis: Current Status and Future Prospects. *Clin Chest Med.* 2005;26(2):327-340. doi:10.1016/J.CCM.2005.02.013
 29. Poole K. Efflux pumps as antimicrobial resistance mechanisms. *Ann Med.* 2007;39(3):162-176. doi:10.1080/07853890701195262

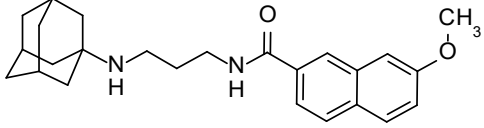
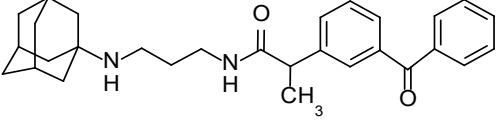
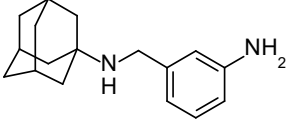
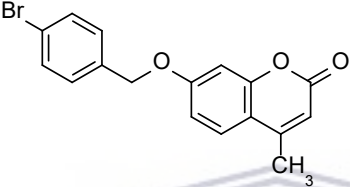
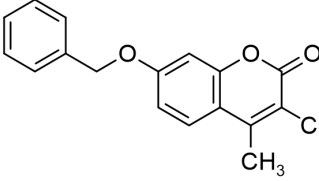
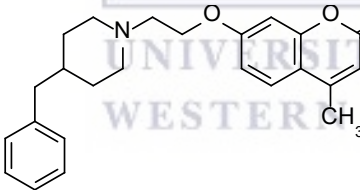
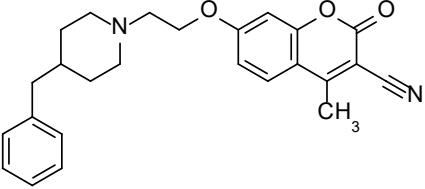
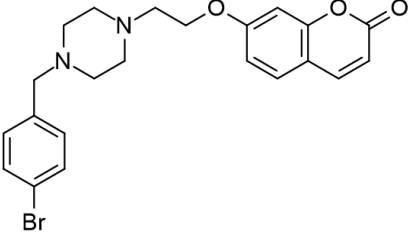
30. Belardinelli JM, Yazidi A, Yang L, et al. Structure-Function Profile of MmpL3, the Essential Mycolic Acid Transporter from Mycobacterium tuberculosis. *ACS Infect Dis*. 2016;2(10):702-713. doi:10.1021/ACSINFECDIS.6B00095
31. Li W, Obregón-Henao A, Wallach JB, et al. Therapeutic Potential of the Mycobacterium tuberculosis Mycolic Acid Transporter, MmpL3. *Antimicrob Agents Chemother*. 2016;60(9):5198. doi:10.1128/AAC.00826-16
32. Zhang B, Li J, Yang X, et al. Crystal Structures of Membrane Transporter MmpL3, an Anti-TB Drug Target. *Cell*. 2019;176(3):636-648.e13. doi:10.1016/J.CELL.2019.01.003
33. Viljoen A, Dubois V, Girard-Misguich F, Blaise M, Herrmann JL, Kremer L. The diverse family of MmpL transporters in mycobacteria: from regulation to antimicrobial developments. *Mol Microbiol*. 2017;104(6):889-904. doi:10.1111/MMI.13675
34. Grzegorzewicz AE, Pham H, Gundi VAKB, et al. Inhibition of mycolic acid transport across the Mycobacterium tuberculosis plasma membrane. *Nat Chem Biol*. 2012;8(4):334-341. doi:10.1038/NCHEMBIO.794
35. Li W, Upadhyay A, Fontes FL, et al. Novel insights into the mechanism of inhibition of MmpL3, a target of multiple pharmacophores in Mycobacterium tuberculosis. *Antimicrob Agents Chemother*. 2014;58(11):6413-6423. doi:10.1128/AAC.03229-14
36. Jackson M. The mycobacterial cell envelope-lipids. *Cold Spring Harb Perspect Med*. 2014;4(10). doi:10.1101/CSHPERSPECT.A021105
37. Shao M, McNeil M, Cook GM, Lu X. MmpL3 inhibitors as antituberculosis drugs. *Eur J Med Chem*. 2020;200. doi:10.1016/J.EJMECH.2020.112390
38. Umare MD, Khedekar PB, Chikhale R V. Mycobacterial Membrane Protein Large 3 (MmpL3) Inhibitors: A Promising Approach to Combat Tuberculosis. *ChemMedChem*. 2021;16(20):3136-3148. doi:10.1002/CMDC.202100359
39. Li M, Phua ZY, Xi Y, et al. Potency Increase of Spiroketal Analogs of Membrane Inserting Indolyl Mannich Base Antimycobacterials Is Due to Acquisition of MmpL3 Inhibition. *ACS Infect Dis*. 2020;6(7):1882. doi:10.1021/ACSINFECDIS.0C00121
40. Butler MS, Paterson DL. Antibiotics in the clinical pipeline in October 2019. *J Antibiot* 2020 736. 2020;73(6):329-364. doi:10.1038/s41429-020-0291-8
41. Degiacomi G, Belardinelli JM, Pasca MR, Rossi E De, Riccardi G, Chiarelli LR. Promiscuous Targets for Antitubercular Drug Discovery: The Paradigm of DprE1 and MmpL3. *Appl Sci* 2020, Vol 10, Page 623. 2020;10(2):623. doi:10.3390/APP10020623
42. Li W, Stevens CM, Pandya AN, et al. Direct Inhibition of MmpL3 by Novel Antitubercular Compounds. *ACS Infect Dis*. 2019;5(6):1001-1012. doi:10.1021/ACSINFECDIS.9B00048
43. La Rosa V, Poce G, Canseco JO, et al. MmpL3 Is the Cellular Target of the Antitubercular Pyrrole Derivative BM212. *Antimicrob Agents Chemother*. 2012;56(1):324. doi:10.1128/AAC.05270-11
44. Ray PC, Huggett M, Turner PA, et al. Spirocyclic MmpL3 Inhibitors with Improved hERG and Cytotoxicity Profiles as Inhibitors of Mycobacterium tuberculosis Growth. *ACS Omega*. 2021;6(3):2284-2311. doi:10.1021/ACSOMEGA.0C05589
45. Stanley SA, Grant SS, Kawate T, et al. Identification of novel inhibitors of M. tuberculosis growth using whole cell based high-throughput screening. *ACS Chem Biol*. 2012;7(8):1377. doi:10.1021/CB300151M
46. McNeil MB, O'Malley T, Dennison D, Shelton CD, Sunde B, Parish T. Multiple Mutations in Mycobacterium tuberculosis MmpL3 Increase Resistance to MmpL3 Inhibitors. *mSphere*.

- 2020;5(5). doi:10.1128/MSPHERE.00985-20
47. Bolla JR. Targeting MmpL3 for anti-tuberculosis drug development. *Biochem Soc Trans.* 2020;48(4):1463-1472. doi:10.1042/BST20190950
 48. Cox JAG, Abrahams KA, Alemparte C, et al. THPP target assignment reveals EchA6 as an essential fatty acid shuttle in mycobacteria. *Nat Microbiol* 2016 12. 2016;1(2):1-10. doi:10.1038/nmicrobiol.2015.6
 49. Zheng H, Williams JT, Coulson GB, Haiderer ER, Abramovitch RB. HC2091 kills mycobacterium tuberculosis by targeting the MmpL3 mycolic acid transporter. *Antimicrob Agents Chemother.* 2018;62(7). doi:10.1128/AAC.02459-17
 50. Gil Z, Martinez-Sotillo N, Pinto-Martinez A, et al. SQ109 inhibits proliferation of *Leishmania donovani* by disruption of intracellular Ca²⁺ homeostasis, collapsing the mitochondrial electrochemical potential ($\Delta\Psi_m$) and affecting acidocalcisomes. *Parasitol Res* 2020 1192. 2020;119(2):649-657. doi:10.1007/S00436-019-06560-Y
 51. Veiga-Santos P, Li K, Lameira L, et al. SQ109, a new drug lead for Chagas disease. *Antimicrob Agents Chemother.* 2015;59(4):1950-1961. doi:10.1128/aac.03972-14

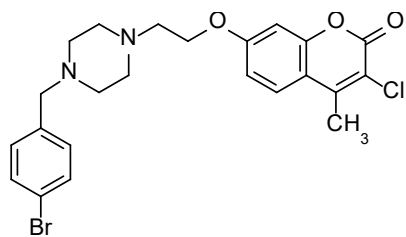


Table S1: Compounds showing a $\leq 50\%$ bacterial survival at $50 \mu\text{M}$ during the initial screen.

Compound	% Bacterial survival		
	100 μM	50 μM	
C1*		11.75	11.71
C2*		4.62	5.69
C3*		3.93	4.35
C4*		4.44	4.40
C5*		4.88	6.68
16		18.34	45.03

18		7.87	31.51
19		6.35	22.12
52		8.90	50.01
CP2		33.16	40.86
CP4		33.52	44.60
CP7		8.18	29.50
CP9		6.19	7.75
CP11		4.46	7.05

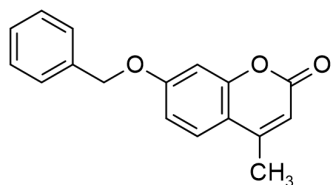
CP13



32.06

42.47

CP17



19.81

28.65

* Compounds selected for further analysis.



Chapter 5: Versatility of 7-Substituted Coumarin Molecules as Antimycobacterial Agents, Neuronal Enzyme Inhibitors and Neuroprotective agents.

Kapp E, Visser H, Sampson SL, *et al.* Versatility of 7-substituted coumarin molecules as antimycobacterial agents, neuronal enzyme inhibitors and neuroprotective agents. *Molecules*. 2017;22(10):10.3390/molecules22101644. <https://www.mdpi.com/1420-3049/22/10/1644#>

Copyright statement: For all articles published in MDPI journals, copyright is retained by the authors. Articles are licensed under an open access Creative Commons CC BY 4.0 license, meaning that anyone may download and read the paper for free. In addition, the article may be reused and quoted provided that the original published version is cited. These conditions allow for maximum use and exposure of the work, while ensuring that the authors receive proper credit.



Versatility of 7-Substituted Coumarin Molecules as Antimycobacterial Agents, Neuronal Enzyme Inhibitors and Neuroprotective Agents

Erika Kapp¹, Hanri Visser², Samantha L. Sampson², Sarel F. Malan¹, Elizabeth M. Streicher², Germaine B. Foka¹, Digby F. Warner³, Sylvester I. Omoruyi⁴, Adaze B. Enogieru⁴, Okobi E. Ekpo⁴, Frank T. Zindo¹ and Jacques Joubert^{1,*}

¹ School of Pharmacy, Faculty of Natural Sciences, University of the Western Cape, Cape Town, Bellville 7550, South Africa; ekapp@uwc.ac.za (E.K.); sfmalan@uwc.ac.za (S.F.M.); 3002811@myuwc.ac.za (G.B.F.); frankzindo@gmail.com (F.T.Z.)

² DST/NRF Centre of Excellence in Biomedical Tuberculosis Research, SA MRC Centre for Tuberculosis Research, Division of Molecular Biology and Human Genetics, Faculty of Medicine and Health Sciences, University of Stellenbosch, Cape Town, Tygerberg 7505, South Africa; hvisser@sun.ac.za (H.V.); ssampson@sun.ac.za (S.L.S.); lizma@sun.ac.za (E.M.S.)

³ Medical Research Council/National Health Laboratory Service/University of Cape Town Molecular Mycobacteriology Research Unit, Department of Science and Technology/National Research Foundation Centre of Excellence for Biomedical Tuberculosis Research, Institute of Infectious Disease and Molecular Medicine and Department of Clinical Laboratory Sciences, University of Cape Town, Cape Town, Rondebosch 7700, South Africa; digby.warner@uct.ac.za

⁴ Department of Medical Biosciences, University of the Western Cape, Cape Town, Bellville 7550, South Africa; 3405455@myuwc.ac.za (S.I.O.); 3581698@myuwc.ac.za (A.B.E.); oecko@uwc.ac.za (O.E.E.)

* Correspondence: jjoubert@uwc.ac.za; Tel.: +27-21-959-2195

Received: 15 September 2017; Accepted: 27 September 2017; Published: 30 September 2017

Abstract: A medium-throughput screen using *Mycobacterium tuberculosis* H37Rv was employed to screen an in-house library of structurally diverse compounds for antimycobacterial activity. In this initial screen, eleven 7-substituted coumarin derivatives with confirmed monoamine oxidase-B and cholinesterase inhibitory activities, demonstrated growth inhibition of more than 50% at 50 μ M. This prompted further exploration of all the 7-substituted coumarins in our library. Four compounds showed promising MIC₉₉ values of 8.31–29.70 μ M and 44.15–57.17 μ M on *M. tuberculosis* H37Rv in independent assays using GAST-Fe and 7H9+OADC media, respectively. These compounds were found to bind to albumin, which may explain the variations in MIC between the two assays. Preliminary data showed that they were able to maintain their activity in fluoroquinolone resistant mycobacteria. Structure-activity relationships indicated that structural modification on position 4 and/or 7 of the coumarin scaffold could direct the selectivity towards either the inhibition of neuronal enzymes or the antimycobacterial effect. Moderate cytotoxicities were observed for these compounds and slight selectivity towards mycobacteria was indicated. Further neuroprotective assays showed significant neuroprotection for selected compounds irrespective of their neuronal enzyme inhibitory properties. These coumarin molecules are thus interesting lead compounds that may provide insight into the design of new antimycobacterial and neuroprotective agents.

Keywords: coumarin; *Mycobacterium tuberculosis*; cholinesterase inhibitor; monoamine oxidase B inhibitor; structure-activity relationship; albumin binding; neuroprotection

1. Introduction

Progressive development of resistance to various chemotherapeutic agents used in the management of infectious diseases presents a very serious problem in global public health. Natural products have yielded various classes of effective antimicrobials over the last few decades and continue to play a large role in the identification of novel lead molecules for this purpose [1].

A large variety of coumarin derivatives have been isolated from natural products and an array of pharmacological activities have been described for these compounds, as well as related synthetic coumarins [2,3]. The ability of the coumarin moiety to form several possible interactions with a particular binding site (including hydrogen bonds, electrostatic, π - π and hydrophobic interactions) likely stabilize target binding and contribute to the versatile pharmacological profile of coumarin derivatives. Both the type and placement of functional groups on the coumarin scaffold determine the specific activity of a given derivative [2-4].

Antibacterial and more specifically, antimycobacterial activity are amongst the pharmacological effects that have been described for a range of structurally diverse coumarin derivatives. One prominent example of a coumarin-based antibacterial is novobiocin. Novobiocin, the structurally related chlorobiocin as well as coumermycin A₁ are 3-amino-4,7-dihydroxycoumarin derivatives, alternatively referred to as the classical aminocoumarin antibiotics. Classical aminocoumarins act as competitive inhibitors of bacterial topoisomerase, more precisely DNA gyrase [5,6]. Competitive inhibition of DNA gyrase by the classical aminocoumarin antibiotics results from an overlap in binding sites between the sugar moiety of the aminocoumarins (Figure 1, numbered in blue) and the adenine ring of adenosine triphosphate (ATP) which is required for the gyrase activity [7]. The non-classical aminocoumarin, simocyclinone D8 (Figure 1), lacks the 7-aminosugar moiety and inhibits bacterial DNA gyrase through simultaneous binding to two alternate binding pockets via interactions with the coumarin moiety and a terminal angucyclinone group. Simocyclinone D8 thus has a unique mechanism of action, despite structural similarities to the standard aminocoumarins [8-10]. Similarly, differences in the binding sites between the fluoroquinolone antibiotics (e.g., moxifloxacin which primarily inhibits topoisomerase IV but also interacts with gyrase) allow fluoroquinolone antibiotics to maintain potency in aminocoumarin resistant bacteria and vice versa [5,6,11]. Mycobacterial gyrase, which is a validated drug target in *Mycobacterium tuberculosis*, is also the likely target for the fluoroquinolone class antibiotics as *M. tuberculosis* does not express the topoisomerase IV enzyme [12].

Apart from an interaction with gyrase, bacterial DNA helicase is another suggested target of selected coumarin derivatives [13-15]. Like other non-classical coumarin antibiotics, the 7-position on these coumarin derivatives does not contain an amino sugar, but rather a moiety able to undergo hydrophobic interactions with the target site [13-15]. Compound **22** (Figure 1), a 4,8-dimethyl-3-propionic acid coumarin derivative with a 2-(4-chloro[1,1-biphenyl]4-yl)ethyl substitution on the 7-position was the most active helicase inhibitor in this series of 7-substituted biphenyl coumarin derivatives [14]. In this series, the methyl substitution in position 4 of the coumarin structure drastically increased the anti-helicase activity of the compounds.

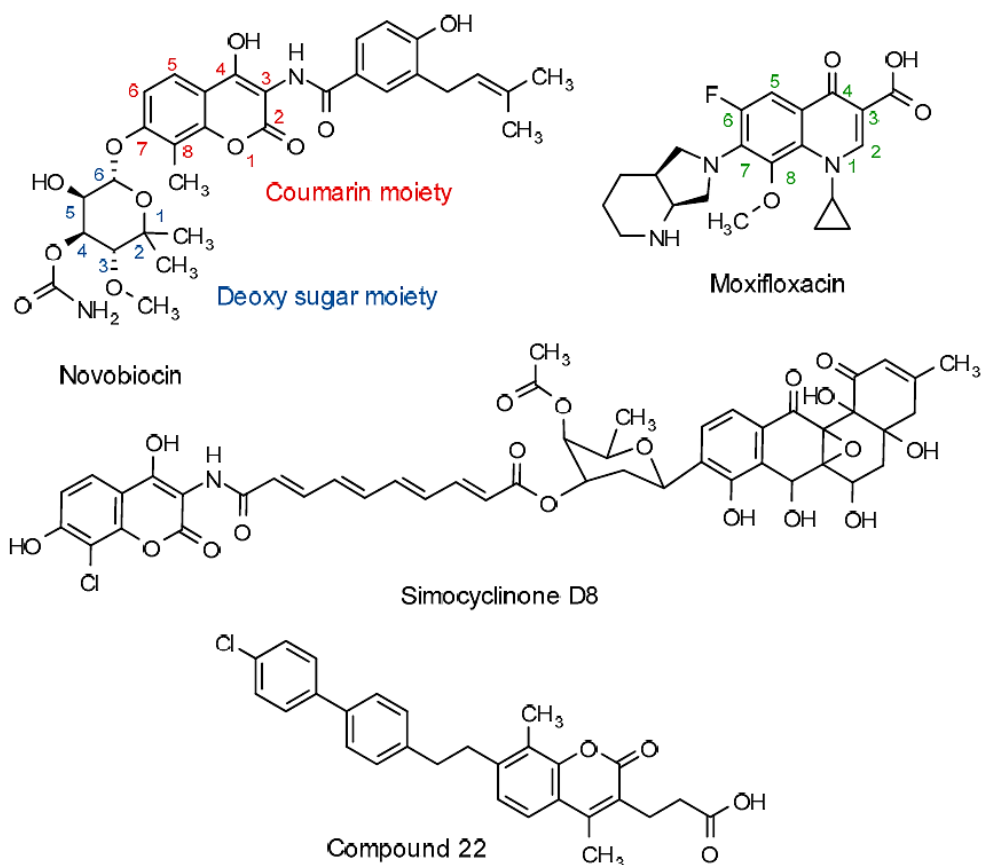


Figure 1. Molecular structure of novobiocin, moxifloxacin, simocyclinone D8 and compound **22** as examples of antimicrobial coumarin derivatives.

Various reports have been published on coumarin derivatives with antimycobacterial activity. Although most studies adequately describe and quantify the activity for respective series of coumarin derivatives, differences in assay methods prevent a direct comparison of antimycobacterial activity of these molecules. Novobiocin as discussed above, demonstrated a minimum inhibitory H37 concentration (MIC) of approximately 6.5 μM in the standard laboratory strain of *M. tuberculosis*, H37Rv [16]. Figure 2 depicts some of the most active compounds in their particular series as evaluated in *M. tuberculosis*. Compound **3** [17] was identified as a likely mycobacterial gyrase inhibitor whereas inhibition of FadD32, an enzyme involved in mycolic acid biosynthesis, was confirmed as target for compound **6** [4]. Mechanisms of action were not suggested for compounds **1** [18], **2** [19], **4** [20] and **5** [21].

As can be expected for compounds which do not necessarily attain their antimycobacterial effect through interaction with the same target sites, structural features important for activity differ between the respective series of compounds. Ultimately, various types and combinations of substitutions on all but positions 1 and 2 of the coumarin scaffold yielded generally effective antimycobacterials, though possibly through different mechanisms of action. This versatile nature of the coumarin scaffold may promote interaction with unique, or possibly multiple targets within the mycobacterial bacilli.

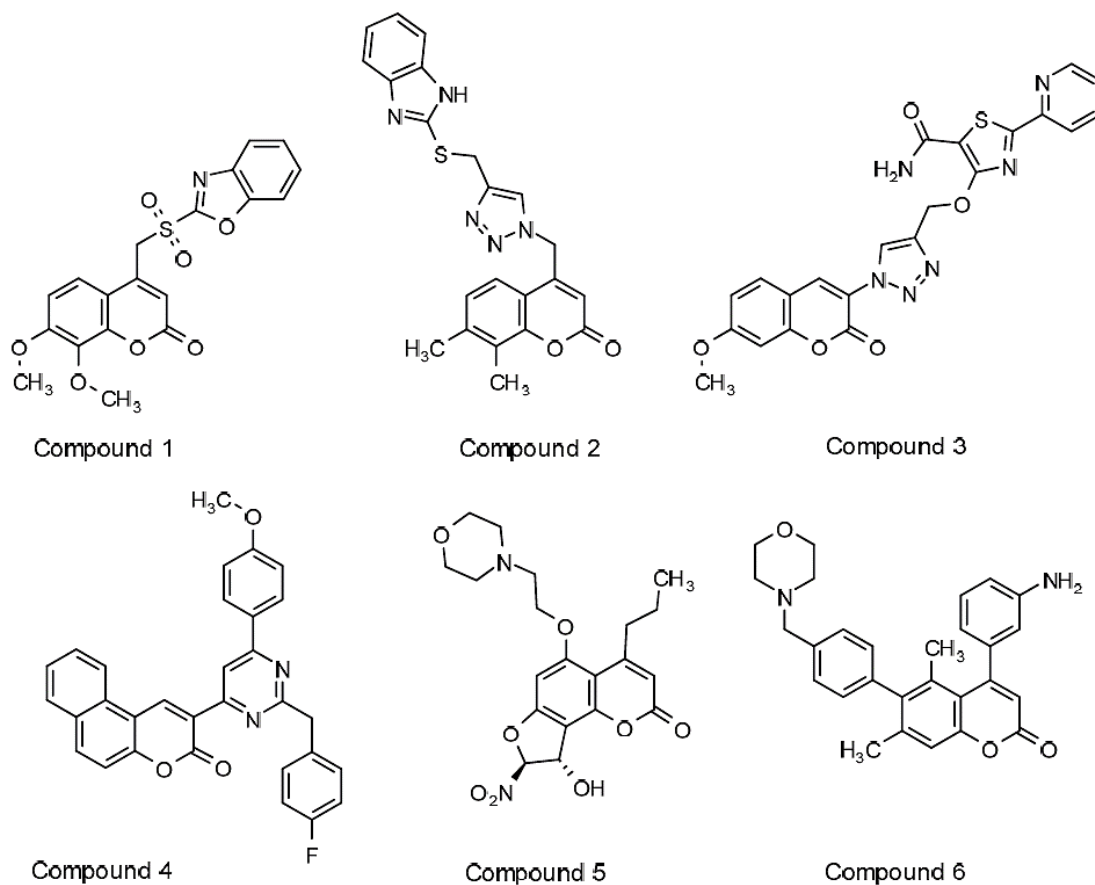


Figure 2. Selected coumarin derivatives demonstrating promising *Mycobacterium tuberculosis* activity across various assays.

Unfortunately, structure-activity relationships for the activity of various classes of coumarin derivatives (e.g., central nervous system acting, anticoagulant, and anti-cancer agents) often overlap with that for potent antimicrobial activity [3,22]. A number of review papers describe the importance of coumarin compounds in the field of neurodegenerative disorders where they have shown inhibitory properties towards monoamine oxidases, cholinesterases, β - and γ -secretase, and other targets involved in the progression of neurodegenerative disorders [23–25]. Similarly, coumarin derivatives described in this article also demonstrated neuronal enzyme inhibitory properties [26]. Therefore, the effective utilization of the coumarin scaffold may essentially be hampered by its versatility unless sufficient selectivity can be ensured. Early identification and structure-activity relationship evaluation of alternative pharmacological effects, over-and-above standard cytotoxicity assays, may increase the viability of coumarin-based antimycobacterial and/or neuroprotective agents.

As part of a collaborative project, a number of 7-substituted coumarin derivatives initially designed and synthesized as multifunctional neuronal enzyme inhibitors [26] were found to exhibit promising antimycobacterial activity (see Table 1) The compounds, originally designed to incorporate coumarin structures known to show monoamine oxidase B (MAO-B) inhibition [27] and selected structural elements of donepezil, a selective acetylcholinesterase (AChE) inhibitor [28], were able to selectively

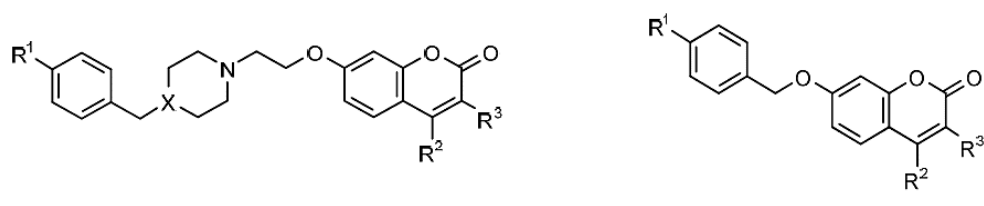
inhibit human MAO-B as well as electric eel AChE and equine butyrylcholinesterase (BuChE) [26]. Further evaluation of the structure-activity relationships for selectivity and specific characteristics of these compounds were therefore required in order to assess the viability of the compounds as neuronal enzyme inhibitors and/or antimycobacterial clinical agents. This article describes the antimycobacterial activity, plasma protein binding properties, cytotoxicity and neuroprotection data for the series of neuronal enzyme inhibitors. Preliminary evaluations on antimycobacterial activity in drug resistant *M. tuberculosis* are described and structure-activity relationships for neuronal enzyme inhibition versus antimycobacterial activity as well as a paired analysis of the neuroprotective properties of selected derivatives are discussed.

2. Results and Discussion

2.1. Medium Throughput Screen

A medium throughput screen (MTS) of various compounds from the University of the Western Cape School of Pharmacy drug-design compound library was done to identify novel antimycobacterial agents. A large proportion of the compounds which demonstrated potential antimycobacterial activity in the initial MTS, were coumarin derivatives. A total of 11 coumarin derivatives inhibited more than 50% mycobacterial growth at 50 μ M. Table 1 provides the structures and activity of two series of coumarin derivatives **CM1–CM19** identified in the MTS, as classified based on the substitution on the 7-position of the coumarin scaffold. The compound numbering from our library was maintained and the derivatives sorted in order of potency within their respective series. Antimycobacterial activity is indicated as the percentage mycobacterial growth on day 5 at 100 μ M, 50 μ M and 1 μ M of the respective derivatives.

Based on this screen, series 1 seems to contain more potent inhibitors of *M. tuberculosis* with the *p*-bromo-*N*-benzylpiperazine derivatives demonstrating higher activity than the benzyl substituted piperidine derivatives. The exception to this is **CM13** with a chloro substitution on the R³ position which reduces the antimycobacterial activity of the compound in this whole cell assay. Interestingly the chloro substitution on R³ improves the activity in the piperidine type compound, though it should be noted that the simultaneous removal of the bromine substitution may have contributed to the change in activity. The small activity differences between the 6 most active compounds in series 1 do not allow for prediction of structure-activity relationships within this range. It would however seem that the *p*-bromo-*N*-benzylpiperazine derivatives can tolerate various large and small substitutions in position 4 of the coumarin scaffold relatively well. No significant differences in activity were observed between the trifluoromethyl, methyl or unsubstituted 4-substituted coumarin derivatives for this series. This is not the case with series 2, where the trifluoromethyl group in position 4 of the coumarin scaffold seems to decrease the activity when compared to a methyl substitution in this position. The most active compound in series 2 is the R²-methyl substituted benzyl-ether (**CM17**) followed by a similar bromobenzyl-ether (**CM2**). Replacement of the hydrogen in position 3 of the coumarin scaffold with a nitrile moiety does not seem to influence activity, but a chloro-substitution in this position decreases activity similar to what was observed for the *p*-bromo-*N*-benzylpiperazine derivatives in series 1. The combination of halogens in R¹ and R³ with a methyl substitution on R² seems to decrease activity in both series 1 and 2.

Table 1. Molecular structure and activity of coumarin derivatives series 1 and 2.


	X	R ¹	R ²	R ³	100 μM	50 μM	1 μM
Series 1							
CM12 **	N	Br	CH ₃	H	3.93	4.35	95.23
CM14 **	N	Br	CH ₃	CN	4.44	4.40	99.53
CM8 **	CH	H	CH ₃	Cl	4.62	5.69	93.59
CM15 **	N	Br	CF ₃	H	4.88	6.68	106.71
CM11 *	N	Br	H	H	4.46	7.05	95.18
CM9 *	CH	H	CH ₃	CN	6.19	7.75	92.82
CM7 *	CH	H	CH ₃	H	8.18	29.50	95.10
CM6	CH	H	H	H	15.43	52.71	98.19
CM13 *	N	Br	CH ₃	Cl	32.06	42.47	97.03
Series 2							
CM17 *		H	CH ₃	H	19.81	28.65	97.59
CM2 *		Br	CH ₃	H	33.16	40.86	89.98
CM4 *		Br	CH ₃	CN	33.52	44.60	95.27
CM5		Br	CF ₃	H	56.09	65.04	106.87
CM19		H	CH ₃	CN	55.44	66.92	98.28
CM16		H	H	H	50.66	72.70	97.53
CM1		Br	H	H	63.63	79.77	96.28
CM18		H	CH ₃	Cl	75.52	87.91	97.30
CM3		Br	CH ₃	Cl	92.86	96.11	97.82

* Compounds that underwent further analysis; ** Compounds selected for MIC determination.

Comparison of the compounds evaluated in this study with other antimycobacterial coumarin derivatives described in literature (see Figure 2, Section 1) highlighted minor similarities and trends. Many of the more active derivatives described in literature only have small groups substituted at positions 5, 6, 7 and 8 of the coumarin scaffold whereas the compounds evaluated in this study carry the larger substitution at 7 position. Bi-substitution on these positions seems to increase activity. Compound 1 [18], a 4-substituted sulfonyl-benzoxazole derivative was more active when substituted with methoxy groups in both the 7 and 8 positions of the coumarin, than single- or unsubstituted derivatives. Compound 2 [19], a 4-substituted, triazole-linked benzimidazole coumarin with methyl

groups at the 5, 7 or 7, 8 positions on the coumarin scaffold similarly demonstrated the highest activity in its series. A common trend for most of these derivatives seems to be a large functional group on position 3 or 4 of the coumarin moiety. Compound **3** [17], bearing a triazole ring on the 3 position of the coumarin scaffold, was able to achieve an MIC value of 6.5 μM . Compound **4** [20], also with a large group on position 3, was the most active in a series of 3-substituted benzocoumarin-pyrimidine hybrid molecules. Series 1 derivatives evaluated in this study likewise seem to tolerate large substitutions on position 3 with no significant differences in activity between substituted or unsubstituted derivatives. In addition to substitutions on position 4, compounds **5** and **6** are substituted with larger morpholine-containing moieties in positions 5 and 6 respectively. Compound **6** [4], bearing a comparatively larger *N*-benzylmorpholine substitution on the 6-position of the coumarin scaffold, was previously shown to inhibit mycobacteria through inhibition of FadD32, a newly validated and promising mycobacterial drug target involved in mycolic acid biosynthesis [29]. Methyl substitutions on positions 5 and 7 were again crucial for activity. The importance of the methyl moieties may be their influence on the geometrical conformation of the adjoining aryl groups, indicating conformation-specific target binding [4]. Similar to the piperidine and piperazine derivatives in series 1 evaluated in this study, compounds **5** and **6** with the larger substitutions on the benzene ring of the coumarin scaffold were substituted with functional groups able to form hydrogen bonds with the target site.

The neuronal enzyme structure-activity relationships of the coumarin derivatives in Table 1 were discussed in detail in our recently published paper [26]. Briefly, the coumarin derivatives substituted at the 7-position with an *N*-benzylpiperidine or *p*-bromo-*N*-benzylpiperazine (series 1) showed better multifunctional neuronal inhibitory activities compared to their 7-benzyl only substituted counterparts (series 2). In addition, the substitution of a nitrile group at position 3 of the coumarin scaffold (**CM9** and **CM14**) improved the multifunctional neuronal inhibitory activities of the compounds in series 1 and the MAO-B activity (**CM4** and **CM19**) in series 2. In both series 1 and 2 substitution at position 4 with a large trifluoromethyl group drastically decreased their neuronal enzymatic activities. It was also noted that, in general, the *N*-benzylpiperidine substituted coumarin derivatives showed significantly improved activities over their *p*-bromo-*N*-benzylpiperazine substituted counterparts. From these studies compound **CM9** was identified as the most promising multifunctional neuronal enzyme inhibitor. It may therefore be possible to increase the selectivity of coumarin derivatives towards either neuronal enzyme inhibitory activity or antimycobacterial property through selective substitution in positions 4 and 7 of the coumarin scaffold.

All derivatives in series 1 and 2 that demonstrated more than 50% mycobacterial growth inhibition at 50 μM were further analysed at narrower concentration ranges using a similar method to the original MTS. Figure 3 depicts the mycobacterial growth inhibition for compounds **CM12** and **CM17**, which were the most active in their respective series in the initial screen. Relative fluorescence of the far-red fluorescent reporter mCHERRY was used as the indicator of growth during this screen which was performed once to validate the activity found during the initial screen. These graphs show the inhibitory effect of the compounds compared to the untreated as well as a known antimycobacterial rifampicin (RIF) at 6 μM . From this activity validation screen **CM8**, **CM12**, **CM14** and **CM15** (all in series 1) were identified as the most potent compounds and evaluated in further studies to gain insight into their antimycobacterial properties.

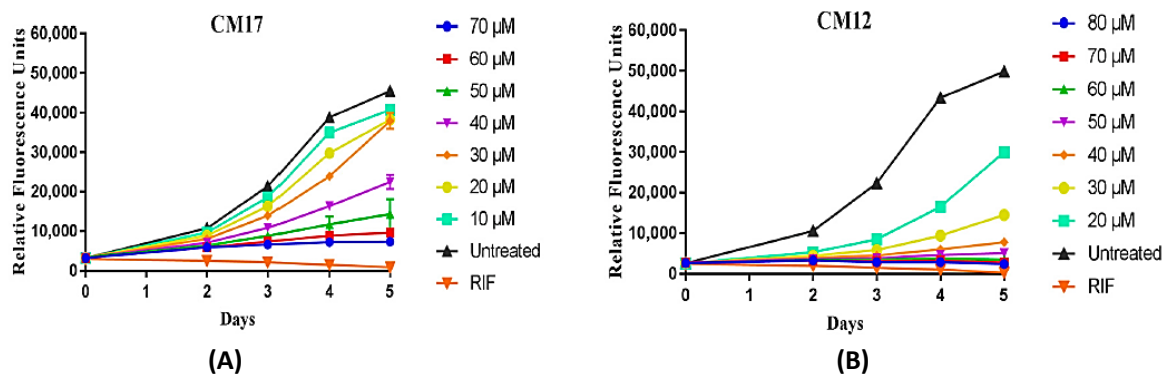


Figure 3. Mycobacterial growth inhibition by compounds **CM12** (A) and **CM17** (B) at narrower concentration intervals. *M. tuberculosis* H37Rv:pCHERRY3 was cultured in 96 well plates as described, with compounds at the concentrations as shown. Experiments were repeated in biological triplicates; each plot shown here shows a representative biological replicate with the mean and standard deviation of 3 technical replicates for each data point.

2.2. Evaluation of Compound Activity in Quinolone Resistant *Mycobacterium tuberculosis*

Various coumarin-based antimicrobials have been shown to target bacterial DNA gyrase, which is also the suggested target of the fluoroquinolone antibiotics in mycobacteria [5,6,11,12]. It was therefore decided to evaluate whether the coumarin derivatives evaluated in this study would be able to maintain potency in fluoroquinolone resistant mycobacteria.

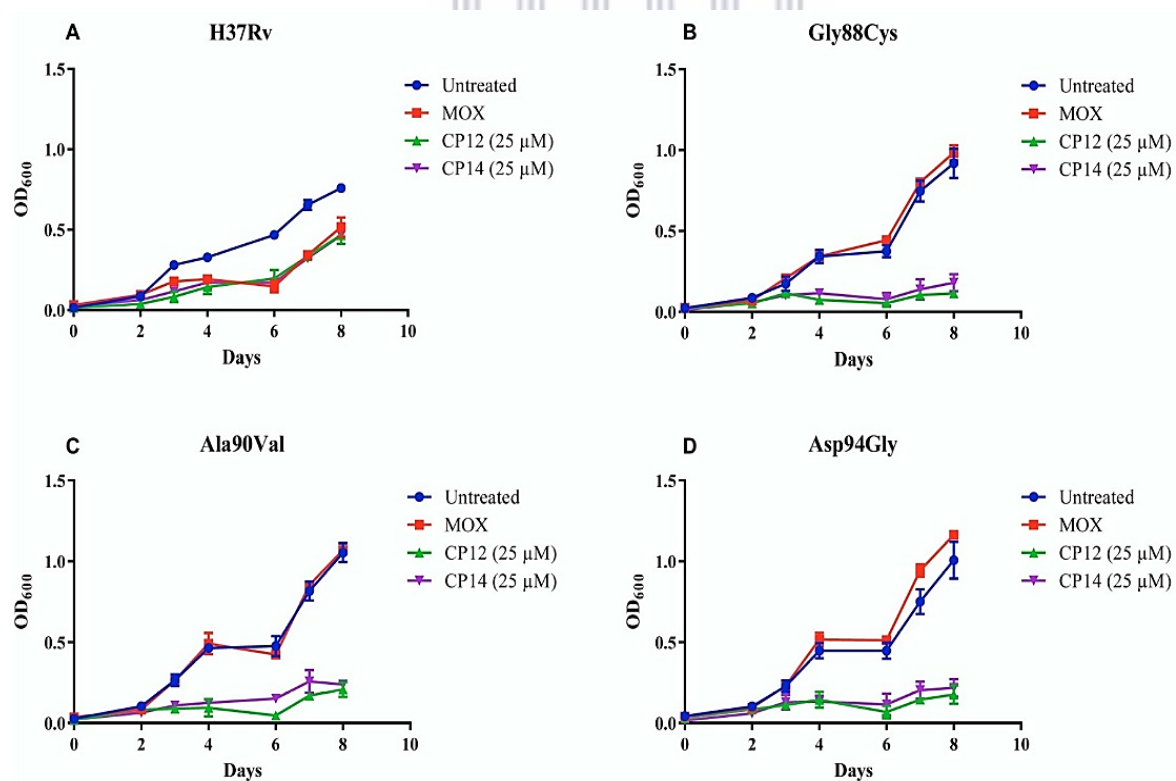


Figure 4. Preliminary evidence of maintained activity of **CM12** and **CM14** in fluoroquinolone sensitive (A: H37Rv) and resistant *M. tuberculosis* (B, C, and D: Gly88Cys, Ala90Val, and Asp94Gly, respectively). Moxifloxacin (MOX) was used at a concentration of 1.2 μM. OD₆₀₀: optical density measured at 600 nm.

2.3. Minimum Inhibitory Concentration Determination

MICs of the most active compounds from the initial evaluations (**CM8**, **CM12**, **CM14**, and **CM15**) were determined independently at the University of Stellenbosch (US, South Africa) and University of Cape Town (UCT, South Africa) utilizing different assay methods described in detail in the methodology section. Briefly, the US assay (similar to the assay used for the MTS), utilized a H37Rv strain transformed with a plasmid encoding a red fluorescent reporter (pCHERRY3 [31]), a gift from Tanya Parish (Addgene plasmid # 24659), in albumin-containing media (Middlebrook 7H9 broth, Becton, Dickinson and Co., Franklin Lakes, NJ, USA, enriched with 10% oleic albumin dextrose catalase (OADC), 0.2% glycerol and 0.05% Tween 80; 7H9+OADC). The UCT method utilized a standard broth microdilution method with *M. tuberculosis* H37RvMA pMSP12:GFP (green fluorescent protein) in glycerol-alanine-salts with 0.05% Tween 80 and iron (GAST-Fe) [32]. Consistently lower MICs were observed in the GFP GAST-Fe assay. **CM8**, **CM12**, and **CM14** all showed approximately 2- to 3-fold lower MIC₉₀ values in the UCT laboratory assay with **CM15** showing the largest discrepancy with a 14-fold difference between the two methods (Table 2). For the purposes of comparison with standard antimycobacterials under similar conditions, **CM12** and **CM14** at 25 µM were able to achieve growth inhibition in similar ranges to moxifloxacin at 1.2 µM whereas RIF at 6 µM resulted in 100% inhibition of bacterial growth in the pCHERRY3 assay. RIF has a MIC of 0.0274 µM in the GFP assay.

Table 2. Minimum inhibitory concentrations determined using two methods.

Compound	GFP GAST-Fe		mCHERRY—7H9+OADC	
	MIC ₉₀ (µM)	MIC ₉₉ (µM)	MIC ₉₀ (µM)	MIC ₉₉ (µM)
CM8	19.6	25.2	40.55	44.15
CM12	14	29.7	40.89	50.40
CM14	16.7	28	45.22	54.46
CM15	3.2	8.31	43.78	57.17

Abbreviations: St. Dev., standard deviation; MIC₉₀, minimum inhibitory concentration required to inhibit 90% of the organism; MIC₉₉, minimum inhibitory concentration required to inhibit 99% of the organism; GFP, green fluorescent protein; GAST-Fe, glycerol-alanine-salts with 0.05% Tween 80 and iron; 7H9+OADC, Middlebrook 7H9 broth, enriched with 10% oleic albumin dextrose catalase (OADC), 0.2% glycerol and 0.05% Tween 80.

Although it is relatively common to see differences in MIC between different media types, the drastic differences, in particularly for compound **CM15**, warranted further investigation. In the assay methods used in this study, differences in the observed MIC could be due to the lack and presence of albumin in GAST-Fe and 7H9+OADC media respectively, the unique reporters used in the two assays, the difference in inoculum size or alternatively, result directly from the mechanism of action of the compounds. The size of the inoculum has been shown to influence the MIC of antimycobacterials. A 10-fold increase in inoculum size resulted in an approximately 4-fold increase in MIC of bedaquiline [33]. The optical density measured at 600 nm (OD₆₀₀) of 0.004 and 0.04 for the GAST-Fe and 7H9+OADC methods respectively, could therefore contribute to the higher MIC observed using the second method.

Another likely contributor to the observed differences in MIC for the coumarin-based derivatives may be binding to albumin. Various coumarin derivatives (e.g., warfarin) are known to bind extensively to blood-soluble proteins. Serum albumins, which are the major soluble protein constituents of the circulatory system (4% w/v), have the ability to reversibly bind a large variety of exogenous compounds including fatty acids, amino acids, drugs and pharmaceuticals [34–36]. Plasma protein binding forms an integral part of distribution and bioavailability for numerous medications currently on the market but might also become problematic where binding is extensive [37,38]. In vitro, binding to albumin would reduce the amount of compound available to exert an effect on the mycobacterial cell and in theory reduce the observed MIC of the derivative. The impact of the albumin binding on in vivo MIC of compounds would however depend on the extent and nature of the binding to albumin within the host.

2.4. Albumin Binding Assay

To better understand the observed differences in MIC between the two assays, we investigated possible albumin binding for the two coumarin derivatives **CM14** and **CM15** with the largest differences in MIC between the GAST-Fe and 7H9+OADC media based assays. Albumin-enriched media contain approximately 0.5% w/v bovine serum albumin (BSA). Results of previous studies indicate that human serum albumin (HSA) and BSA are similar proteins in space structure and chemical composition [39–41]. BSA was therefore selected as a protein model to investigate fluorescence quenching as an indicator of the extent of interaction between coumarin derivatives **CM14** and **CM15** and albumin, using fluorescence spectroscopy. Fluorescence quenching is the decrease of the quantum yield of fluorescence from a fluorophore induced by a variety of molecular interactions with the quencher molecule. Fluorescence quenching can be dynamic, resulting from collisional encounters between the fluorophore and quencher, or static, resulting from the formation of a ground state complex between the fluorophore and quencher [42–44]. The effects of compounds **CM14** and **CM15** on the fluorescence quenching of BSA, excited at 295 nm are presented in Figure 5.

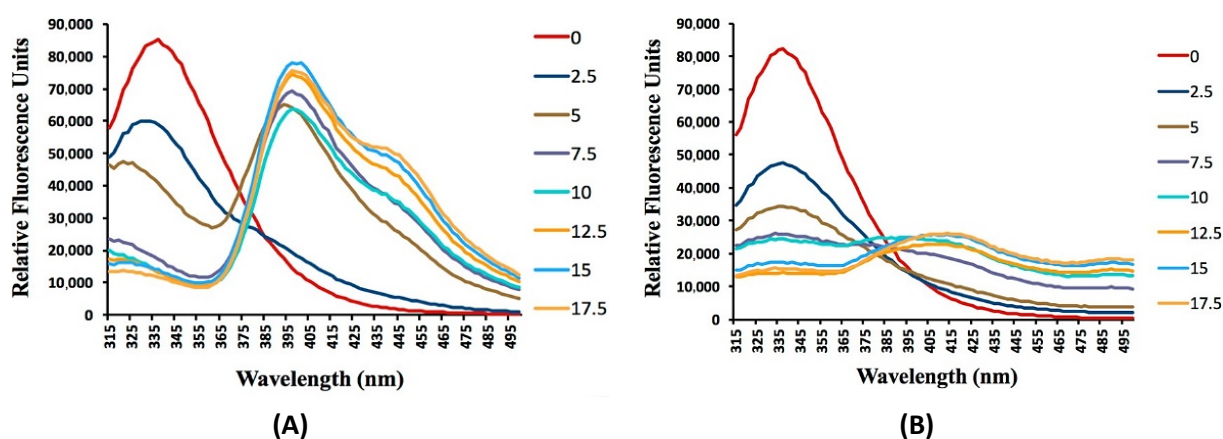


Figure 5. The effects of **CM14** (A) and **CM15** (B) on the fluorescence spectra of BSA at 22 °C. $\lambda_{ex} = 295 \text{ nm}$; $c(\text{BSA}) = 1.00 \times 10^{-5} \text{ mol L}^{-1}$; $c(\text{Q})/(\times 10^{-6} \text{ mol L}^{-1})$. Final concentrations of **CM14** and **CM15** = $0 \times 10^{-6} \text{ mol L}^{-1}$, $2.5 \times 10^{-6} \text{ mol L}^{-1}$, $5.0 \times 10^{-6} \text{ mol L}^{-1}$, $7.5 \times 10^{-6} \text{ mol L}^{-1}$, $10 \times 10^{-6} \text{ mol L}^{-1}$, $12.5 \times 10^{-6} \text{ mol L}^{-1}$, $15.0 \times 10^{-6} \text{ mol L}^{-1}$, and $17.5 \times 10^{-6} \text{ mol L}^{-1}$.

The emission spectrum of **CM14** showed two maxima, the first one at 335 nm (which is characteristic for tryptophan in BSA [45]) and the second peak at 400 nm (which is assigned to fluorescence of compound **CM14** at concentrations of $5 \times 10^{-6} \text{ mol L}^{-1}$ and upwards). The emission spectrum of **CM15** only showed a maximum at 335 nm for BSA and a weak emission peak of **CM15** at 415 nm at higher concentrations of the compound. The excitation and emission maxima of **CM14** and **CM15** are shown in Table 3.

The mechanism of the fluorescent quenching of **CM14** and **CM15** to BSA is described using the Stern-Volmer equation: $F_0/F = 1 + k_{sv}[Q] = 1 + k_q \tau_0 [Q]$, where F_0 and F are the fluorescence intensities before and after the addition of the quencher, respectively; k_{sv} is the dynamic quenching constant; k_q is the quenching rate constant; $[Q]$ is the concentration of quencher; τ_0 is the average lifetime of the molecule without quencher and its value is considered to be 10^{-8} s [46,47]. The Stern-Volmer plot of the **CM14** and **CM15** is presented in Figure 6. The plots show a good linear relationship within the investigated concentrations of **CM14** and **CM15**.

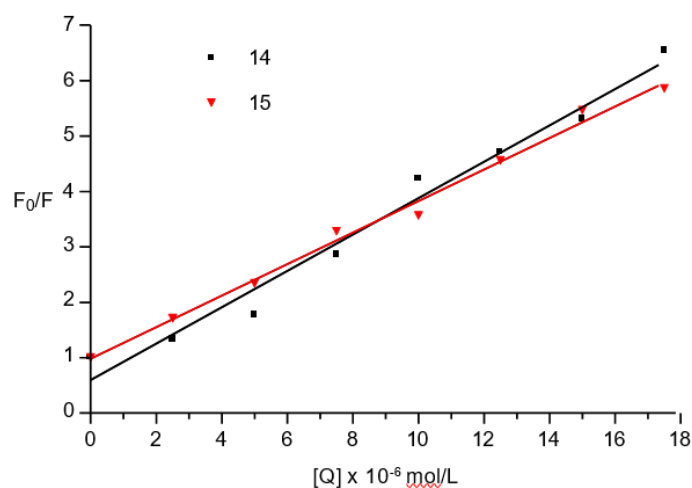


Figure 6: Stern-Volmer plots of BSA ($1.00 \times 10^{-5} \text{ mol L}^{-1}$) quenched by **CM14** and **CM15** at 22 °C.

The results in Table 3 show that k_q values were much greater than the limiting diffusion rate constant of the biomolecule ($2.0 \times 10^{10} \text{ mol L}^{-1} \text{ s}^{-1}$), which indicated that the probable quenching mechanism of BSA-**CM14** and BSA-**CM15** interactions was initiated by complex formation rather than by dynamic collision [48].

It is evident from the results that the fluorescence intensity of BSA decreases with increasing concentrations of compounds **CM14** and **CM15**. It can also be concluded that the fluorescence quenching of tryptophan in BSA as observed for compounds **CM14** and **CM15** results from complex formation between the two compounds and BSA. The more extensive decrease in fluorescence observed at lower concentrations of compound **CM15** likely indicate a higher binding affinity between compound **CM15** and albumin. These results indicate that albumin binding likely plays a large role in the observed differences in activity between the GAST-Fe and 7H9+OADC assays used in this study. The higher albumin binding affinity of **CM15** is likely the reason for the larger MIC variation perceived for this compound.

Table 3. Excitation and emission maxima of **CM14** and **CM15**, and the quenching constant of BSA by **CM14** and **CM15**.

Compound	T (°C)	λ_{Ex} (nm)	λ_{Em} (nm)	k_{sv} (mol L ⁻¹)	k_q (mol L ⁻¹ S ⁻¹)	R ²
CM14	22	350 ^a	395 ^a	3.80×10^5	2.63×10^{14}	0.9780
		350 ^b	400 ^b			
CM15	22	335 ^a	415 ^a	4.88×10^5	2.00×10^{14}	0.9927
		335 ^b	415 ^b			

^a Measured in Tris-HCl buffer at 1×10^{-6} mol L⁻¹. ^b Measured in BSA (1×10^{-5} mol L⁻¹) at 1×10^{-6} mol L⁻¹.

Abbreviations: λ_{Ex} : excitation; λ_{Em} : emission; k_{sv} : dynamic quenching constant; k_q : quenching rate constant; R²: coefficient of determination.

In addition to providing more clarity about the observed MICs, albumin binding properties may also provide some insight into the possible pharmacokinetic behaviour of these drugs. Binding and dissociation of compounds from plasma proteins is a dynamic process with only the unbound fraction of the drug available to exert an effect. In a clinical setting, the dosage of a drug is calculated to ensure that, at any point in time, sufficient free drug is available to have the required pharmacological effect. The same principle would apply to side effects or toxicity and thus, plasma protein binding becomes an important consideration, particularly in highly bound drugs. In light of the divergent albumin binding affinities observed in the evaluated compounds, it would likely be more pertinent to utilize the MIC values obtained in the albumin free GFP-GAST-Fe media for the purposes of determining structure-activity relationships for antimycobacterial activity. **CM15**, which seems to be at least 3-fold more active than the other top compounds in the GFP assay, has a large CF₃ substitution on the 4 position of the coumarin scaffold, and a *p*-bromo-*N*-benzylpiperazine substitution on C7. Activity differences between **CM8**, **CM12** and **CM14** are not pronounced enough to draw structure-activity relationship conclusions.

2.5. Cell Viability Assays

Cytotoxicity assays for the compounds showing the lowest MIC₉₉ (**CM8**, **CM12**, **CM14**, and **CM15**) were done on Chinese hamster ovary (CHO) epithelial cells using a standard MTT assay method (Table 4) [49]. Data was supplemented with further cytotoxicity analysis of **CM14** and **CM15** as well as **CM9** in a similar assay using the neuronal type SH-SY5Y neuroblastoma cells. The SH-SY5Y cytotoxicity assay results were used to determine the concentration at which the compounds do not affect the viability of the SH-SY5Y cells in order to determine their neuroprotective effect using the 1-methyl-4-phenyl pyridinium (MPP⁺) induced neurotoxicity method [50,51].

CM9 was included in the neuronal cell viability and MPP⁺ induced neurotoxicity assays because it was identified previously as the best multifunctional neuronal enzyme inhibitor (50% inhibitory concentration (IC₅₀): MAO-B = 0.30 μ M; AChE = 9.10 μ M; BuChE = 5.90 μ M) within the series of coumarin derivatives (Table 4) [23]. **CM9** did not show any significant antimycobacterial activity and was therefore not included in the CHO cytotoxicity assay. **CM14** was included to draw a comparison between the neurotoxicity and potential neuroprotective effect of the 3-nitro-4-methylcoumarin derivatives substituted at the 7-position with either an *N*-benzylpiperidine (**CM9**) or *p*-bromo-*N*-piperazine moiety (**CM14**). **CM15**, with a large trifluoromethyl substituent on position 4, showed the most promising antimycobacterial activity with minimal multifunctional neuronal enzyme inhibitory

activity. It was included in the neurotoxicity assays to study the effect of the neuronal enzyme inhibitory activities, or lack thereof, on the neuroprotective ability of these compounds or if other mechanisms of action are involved. **CM8** and **CM12** were not included in the neurotoxicity assays as their multifunctional neuronal enzyme inhibitory properties were not as pronounced as **CM9** and **CM14**.

Table 4. 50% cell viability (CC₅₀) and selectivity indices on Chinese hamster ovary (CHO) cells, cell viability on SH-SY5Y cells and 50% enzyme inhibition (IC₅₀) of selected test compounds.

CM	CC ₅₀ μM CHO	SI GFP ^a	SI mCHERRY ^b	CC 50% SH-SY5Y ^c	MAO-A IC ₅₀ μM ^d	MAO-B IC ₅₀ μM ^d	AChE IC ₅₀ μM ^d	BuChE IC ₅₀ μM ^d
CM8	33.0	1.31	0.75	ND	n.a.	0.29	31.30	1.27
CM9	ND	ND	ND	10–50	n.a.	0.30	9.10	5.90
CM12	15.5	0.52	0.31	ND	n.a.	3.60	12.8	9.70
CM14	41.2	1.47	0.76	50–100	n.a.	1.41	38.5	13.3
CM15	26.3	3.16	0.46	10–50	n.a.	5.64	>100	>100
Emetine	0.06	ND	ND	ND	ND	ND	ND	ND

^a Selectivity index (SI) = CC₅₀ CHO/MIC₉₉ GFP-GAST-Fe. ^b Selectivity index (SI) = CC₅₀ CHO/MIC₉₉ mCHERRY-7H9+OADC. ^c Inhibition range (μM) where 50% cell toxicity will be observed. ^d Data taken from Joubert et al., 2017 [23]. ND = not determined. n.a. = no activity.

Cytotoxicity (CC₅₀, 50% cytotoxic concentration) observed for **CM8**, **CM12**, **CM14** and **CM15** on CHO cells was moderate (CC₅₀: 15.5–41.2 μM) indicating low toxicity compared to the cytotoxic agent emetine (CC₅₀ = 0.06 μM). These compounds however showed low selectivity indices when both the GFP and mCHERRY MIC₉₉ assay results are compared to the CC₅₀ results (Table 4). The compounds, in general, were slightly more selective towards the mycobacterial strain when using the GFP assay results, with **CM15** showing the best selectivity (selectivity index (SI) = 3.16). The slight selectivity was however not retained when the results from the mCHERRY assay were used in the SI calculations. These poor selectivity indices may limit the further development of these coumarin derivatives. However, the structure-activity relationships identified in this paper may enable the design of coumarin structures with improved antimycobacterial activities and subsequently more favourable selectivity indices.

The viability of SHSY-5Y human neuroblastoma cells was assessed at different concentrations of compounds **CM9**, **CM14** or **CM15** (Figure 7A). Treatment with the compounds at 10 μM did not significantly affect the viability of the SH-SY5Y cells ($p > 0.05$). However, at higher concentrations (50 μM and 100 μM) the viability of the cells were significantly ($p < 0.001$) affected by the test compounds, although to a lesser extent by **CM14**. These results also correlate to the CC₅₀ CHO values obtained for **CM14** and **CM15** (Table 4).

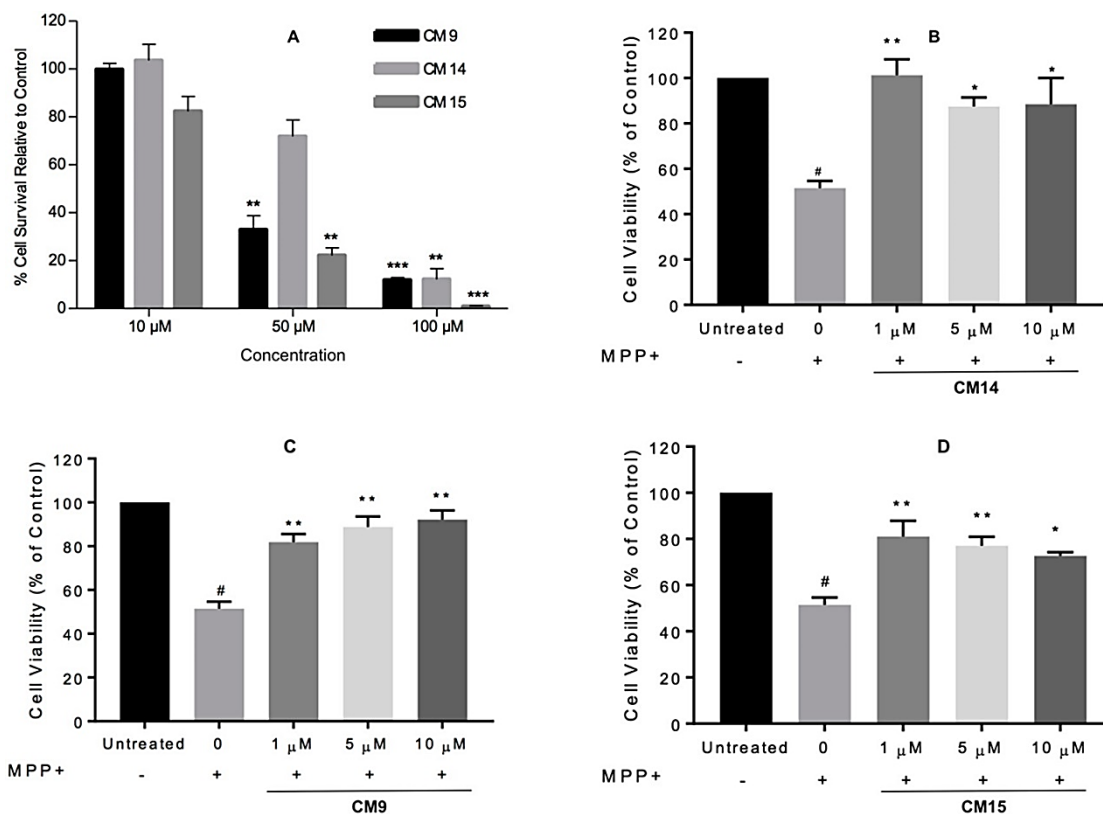


Figure 7. (A) Cellular viability of SH-SY5Y cells treated with compounds **CM9**, **CM14** or **CM15** at 10 μM , 50 μM and 100 μM for 48 h. Data is presented as mean \pm standard error of mean (SEM). Significance is set at a level of * $p < 0.05$ compared to vehicle treated control cells (taken as 100% cell viability). (B–D) The effects of compounds **CM9**, **CM14** or **CM15** on MPP⁺-induced (1000 μM) cytotoxicity in SH-SY5Y cells. The viability of the untreated control was defined as 100%. MPP⁺ without test compound showed a significant decrease in cell viability relative to the control (# $p < 0.05$). The level of significance for the test compounds is set at * $p < 0.05$ compared to the MPP⁺ only treated control (0). Statistical analysis (Turkey post hoc test) was performed on all raw data, with asterisks signifying significant inhibitory effect. * $p < 0.05$; ** $p < 0.001$; *** $p < 0.0001$.

Based on the SH-SY5Y cytotoxicity analysis it was decided that the MPP⁺ neuroprotection studies would be done at compound concentrations between 1 μM and 10 μM in order maintain the viability of the cells. MPP⁺ is highly toxic to neurons and has been widely used to induce neurodegeneration in various in vitro and in vivo models [50,51]. Several signalling pathways have been suggested to be responsible for MPP⁺-mediated neurotoxicity in SH-SY5Y cells, for instance, trigger of oxidative stress [52], induction of apoptosis [53], and inactivation of pro-survival phosphoinositide 3-kinase (PI3-K)/Akt cascade [54–56]. This assay was deemed appropriate to test for initial neuroprotective ability of **CM9**, **CM14** and **CM15** because of the multitude of pathways involved in MPP⁺ mediated neurotoxicity and the multifunctional enzyme inhibitory abilities of the test compounds, especially **CM9**.

SH-SY5Y cells were exposed to the neurotoxin MPP⁺ with or without test compound, and cell viability was evaluated using the MTT mitochondrial function assay [43]. As illustrated in Figure 7B–D, after the exposure to 1000 μM MPP⁺ for 48 h, the cell viability declined significantly to $51.42 \pm 3.18\%$. However,

its cytotoxic effects were ameliorated in the presence of **CM9**, **CM14** and **CM15** at 1 μM , 5 μM and 10 μM concentrations. The compounds, at a 1 μM concentration, restored cell survival to $81.86 \pm 3.72\%$, $101.2 \pm 6.00\%$ and $81.05 \pm 6.83\%$, respectively. **CM9** showed activity in a dose dependent manner exerting maximal cytoprotection of $92.2 \pm 4.18\%$ at 10 μM . At 5 μM and 10 μM a slight decrease in cytoprotection was observed for **CM14** and **CM15**. This may indicate that in the neurotoxin challenged state the SH-SY5Y cells may be more sensitive to the cytotoxic effect of the test compounds. Therefore, **CM14** and **CM15** might have enhanced the toxicity of the neurotoxin which resulted in lower neuroprotection values observed at higher concentrations. Thus, in general and especially at a 1 μM concentration, these compounds, and particularly **CM14**, exerted highly significant cytoprotection towards MPP^+ insults to the SH-SY5Y neural cells.

The results of the MPP^+ neuroprotection study did not provide any information on structure-activity relationships of these compounds as **CM9**, **CM14** and **CM15** showed similar levels of cytoprotection. It was however noted that the neuronal enzyme inhibitory activity of these compounds is not the only factor that play a role in cytoprotection and that other mechanisms of action are involved. For instance, **CM15** showed poor neuronal enzyme inhibitory activities but was still able to significantly protect the cells from MPP^+ induced injury. **CM9** with the best multifunctional enzyme inhibitory profile showed cytoprotection at the same level as **CM15**. As described in the literature coumarin derivatives may possess anti-inflammatory, anti-apoptotic and antioxidant effect [2,3]. These effects combined with the multifunctional neuronal enzyme inhibitory abilities of the compounds may explain the excellent neuroprotection observed. Therefore, further neuroprotection studies are necessary to elucidate the mechanism(s) of action of these compounds.

3. Materials and Methods

3.1. Compound Synthesis

Synthesis methods of the compounds described in this article are described in detail in previous publications by the drug design group at University of the Western Cape (UWC, South Africa) [26].

3.2. Initial Medium Throughput In Vitro Activity Screen

This study was approved by the Stellenbosch University Health Research Ethics Committee (S15/06/135). The *M. tuberculosis* H37Rv strain used during this study was obtained from the American Type Culture Collection (ATCC) (ATCC 27294) and whole genome sequencing [57] and virulence confirmation in a murine infection model [58] was used to verify the strain. The episomal plasmid pCHERRY3, a gift from Tanya Parish (Addgene plasmid #24659) [31], which expresses the far-red fluorescent reporter mCHERRY and contains a hygromycin B resistance cassette, was transformed into this electrocompetent *M. tuberculosis* H37Rv. Growth curve analysis of both *M. tuberculosis* H37Rv and *M. tuberculosis* H37Rv:pCHERRY was performed twice to ensure that the plasmid did not have any deleterious effects on growth.

The antimycobacterial activity of the synthetic compounds was determined using a medium throughput 96-well plate assay. *M. tuberculosis* H37Rv with and without the reporter was cultured in 7H9+OADC, without and with 50 $\mu\text{g}/\text{mL}$ hygromycin B respectively, whereafter the culture was strained (40 μm ; Becton, Dickinson, and Co.), and the OD_{600} was adjusted to 1.0. Culture was added to

each well, resulting in a final OD₆₀₀ of 0.02. White, flat bottom 96-well microtiter plates were prepared, with a final volume of 200 µL, final bacterial OD₆₀₀ of 0.02, and final compound concentration of 100 µM, 50 µM or 1 µM.

Controls included dimethyl sulfoxide (DMSO), positive, negative, and compound control. The background control, which contains *M. tuberculosis* H37Rv without the fluorescent reporter is subtracted from the fluorescence measurements since it displays the inherent fluorescence of *M. tuberculosis* H37Rv. Negative control is included as an untreated fluorescence control where the DMSO control is included to ensure that the maximum amount of DMSO present in the compound dilutions does not interfere with growth. The positive control wells contained 6 µM RIF and the compound controls contained 100 µM compound which was used to confirm that the compound does not autofluoresce in the absence of *M. tuberculosis*.

One-hundred microliters of the *M. tuberculosis* H37Rv:pCHERRY3 diluted culture was added to each well except the gain, background and compound control wells. In the gain control wells, 100 µL of the undiluted *M. tuberculosis* H37Rv:pCHERRY3 culture was added and in the background control wells *M. tuberculosis* H37Rv without the fluorescent reporter was added. The plates were sealed with breathable sealing film and incubated at 37 °C for 6 days, taking readings on days 0, 2, 3, 4, 5, and 6 using a BMG Labtech POLARstar Omega plate reader (BMG Labtech, Offenburg, Germany, excitation: 587 nm, emission: 610 nm). During the readings the breathable seal was removed and an optical sealing film was adhered, whereafter it was removed and replaced by a new breathable sealing film. The average of the background control was subtracted from the fluorescence readings whereafter the data were visualised using GraphPad Prism v7.01 (GraphPad software, La Jolla, CA, USA), by plotting the relative fluorescence units (as a measure of growth) over time. The percentage inhibition was also calculated on day 5, by dividing the treated by the untreated values. Compounds that inhibited more than 50% growth at 50 µM were selected for further study and screened at narrower concentration ranges to more accurately ascertain the extent of the compound's antimycobacterial activity. The second round of screening was also performed using relative fluorescence as a proxy for growth. The growth curves were set up similarly to the initial screen. Five compounds which showed the highest activity during the second screen were selected to undergo further analysis. Of these five compounds, four were coumarin derivatives.

3.3. Activity in Moxifloxacin Resistant *M. tuberculosis*

Three *M. tuberculosis* moxifloxacin resistant mutants, carrying G88C, A90V, or D94G amino acid changes in gyrase A, were tested for CM12 and CM14 cross-resistance. Moxifloxacin stock solutions were prepared at a concentration of 25 µM in DMSO and stored at -80 °C. The resistant mutants and an *M. tuberculosis* H37Rv susceptible strain were prepared as described in Section 3.2 and subsequently exposed to 1.2 µM moxifloxacin, 25 µM CM12 and 25 µM CM14 in technical triplicates in a black, flat, clear-bottom 96 well plate. Each well containing the respective strain was inoculated to an OD₆₀₀ of 0.02 in a final volume of 200 µL. Readings were taken as described in Section 3.2 over 8 days and OD₆₀₀ was plotted over time using GraphPad Prism v7.01.

3.4. Minimum Inhibitory Concentration Determination

MICs were determined for the four most active coumarin derivatives identified in the MTS.

CM8, **CM12**, **CM14**, and **CM15** were screened using two independent methods as described below.

M. tuberculosis pMSP12:GFP in GAST-Fe Media

The first MIC determination was performed at the Institute of Infectious Disease and Molecular Medicine, University of Cape Town (UCT) at a screening facility jointly managed by the MRC/NHLS/UCT Molecular Mycobacteriology Research Unit (A/Prof Digby Warner) and the H3D Drug Discovery and Development Unit (Prof Kelly Chibale). Here, the standard broth microdilution method was performed using *M. tuberculosis* H37RvMA pMSP12:GFP [32]. A 10 mL culture was grown in glycerol–alanine–salts with 0.05% Tween 80 and iron (0.05%; GAST-Fe) pH 6.6, to an OD₆₀₀ of 0.6–0.7. Thereafter the culture was diluted 1:100 in GSAT-Fe. In a 96-well microtiter plate, two-fold serial dilutions of each compound were prepared in GAST-Fe whereafter 50 µL of the diluted culture was added to each serial dilution well resulting in an OD₆₀₀ of 0.004. The plate layout used was modified from a previously described method [59]. Controls included a bacterial growth control (5% DMSO in GAST-Fe) and a positive control (0.15 µM RIF). The microtiter plate was incubated at 37 °C with 5% CO₂ and humidity, sealed within a secondary container. Using a plate reader (FLUOstar OPTIMA, BMG Labtech GmbH, Ortenberg, Germany; excitation: 485 nm; emission: 520 nm) relative fluorescence was measured on days 7 and 14. The CCD Vault from Collaborative Drug Discovery (Burlingame, CA, USA, www.collaboratedrug.com) was used to archive and analyse the fluorescence data. Analyses included normalisation to the bacterial growth and antimycobacterial growth control as the maximum and minimum growth representations respectively generating a dose-response curve using the Levenberg–Marquardt damped least-squares method. This dose response curve was used to calculate the MIC₉₀ and MIC₉₉ which is described as the lowest concentration at which the compound inhibits growth by more than 90% and 99%, respectively.

M. tuberculosis H37Rv:pCHERRY3 in 7H9+OADC

The second technique used a different fluorescent reporter (mCHERRY) and media (7H9+OADC). Dose-response curve analysis was carried out on the same compounds as above. Dose response curves were performed by exposing *M. tuberculosis* H37Rv:pCHERRY3 to increasing concentrations of each compound in white flat bottom 96 well plates. *M. tuberculosis* H37Rv with and without mCHERRY was prepared as described in Section 3.2. In a white, flat bottom 96 well microtiter plate two-fold serial dilutions of the compounds were prepared with a 100 µL final volume and final bacterial OD₆₀₀ of 0.04. This method was adapted from a previously described method [59]. The controls included were a background control (*M. tuberculosis* H37Rv in 7H9+OADC), a negative control (*M. tuberculosis* H37Rv:pCHERRY3 in 7H9+OADC) and a positive control (*M. tuberculosis* H37Rv:pCHERRY3 in 7H9+OADC containing 2 µM RIF). The microtiter plate was sealed with a breathable film, placed in a secondary container and incubated at 37 °C for 5 days, after which a relative fluorescence measurement (Excitation: 587 nm; Emission: 610 nm) was taken using a BMG Labtech POLARstar Omega plate reader. To analyse the relative fluorescence data the average of the background control was subtracted from each well, and the subsequent data set was analysed in GraphPad Prism v.7.01. Data were first normalised using built in non-linear dose-response curve analysis. This gave an output of IC₅₀ as well as a Hill Slope which was used to determine the IC₉₀ and IC₉₉ of each compound. IC₉₀ and IC₉₉ was defined as the concentration where 90% and 99% of growth was inhibited, respectively.

3.5. Bovine Serum Albumin Binding Assay

The interaction between coumarin derivatives (**CM14** and **CM15**) and BSA were measured by fluorescence spectroscopy. BSA ($\geq 98\%$) was obtained from Sigma Aldrich (Kempton Park, South Africa) and dissolved in a Tris-HCl (0.10 mol L^{-1} , pH = 7.4) buffer to form the BSA solution with a concentration of $1.00 \times 10^{-5} \text{ mol L}^{-1}$. A Tris-HCl buffer (0.10 mol L^{-1} , pH = 7.4) containing 0.10 mol L^{-1} NaCl was selected to keep the pH value constant and to maintain the ionic strength of the solution. **CM14** and **CM15** stock solution ($1.00 \times 10^{-3} \text{ mol L}^{-1}$) was prepared in MeOH. All other reagents were of analytical grade and double-distilled water was used in the experiments. Fluorescence spectra were recorded on a Synergy Mx fluorescence plate reader (BioTek, Winooski, VT, USA). Black 96 well plates were used in all experiments. The excitation and emission slits were 9 nm. Fluorescence spectra were measured in the range of 315–500 nm at the excitation wavelength of 295 nm. All experiments were done at $22 \text{ }^\circ\text{C}$. The assay was conducted using a $200 \text{ }\mu\text{L}$ solution containing $1.00 \times 10^{-5} \text{ mol L}^{-1}$ BSA that was titrated by successive additions of $1.00 \times 10^{-3} \text{ mol L}^{-1}$ coumarin **CM14** or **CM15** solution. The final concentration of the compounds varied from 0 to $1.75 \times 10^{-5} \text{ mol L}^{-1}$. Titrations were done manually using a micro-pipette in 2 min intervals. Quenching values remained unchanged for more than 10 min after individual titrations.

3.6. Chinese Hamster Ovary Cell Cytotoxicity Assays

Cytotoxicity was evaluated on CHO cells utilizing a standard 3-[4,5-dimethylthiazol-2-yl]-2,5-diphenyl tetrazolium bromide (MTT) assay [49]. The MTT is a yellow tetrazolium salt that is reduced to purple formazan in the presence of living cells. This reduction reaction was used to measure growth and chemosensitivity. The test samples were tested in triplicate on one occasion. Cells were seeded in microtiter plates at a density of 10^5 cells/mL and incubated for 24 h prior to exposure. The test samples were prepared to a 20 mg/mL stock solution in 10% methanol or 10% DMSO and were tested as a suspension if not properly dissolved. Test compounds were stored at $-20 \text{ }^\circ\text{C}$ until use, and administered in volumes of $100 \text{ }\mu\text{L}$ to the plated cells. Emetine was used as the reference drug in all experiments. The highest concentration of each compound was $100 \text{ }\mu\text{g/mL}$, which was serially diluted in complete medium with 10-fold dilutions to give 6 concentrations, the lowest being $0.001 \text{ }\mu\text{g/L}$. The same dilution technique was applied to the all test samples. The highest concentration of solvent had no measurable effect on the cell viability (data not shown). Plates were developed after 44 h of exposure to the drug by the addition of a solution of MTT. After four hours, further incubation at $37 \text{ }^\circ\text{C}$ the supernatant was removed from the cells via suction and DMSO was added to each well to dissolve the reduced dye crystals. Plates were analysed at 540 nm wavelength using a spectrophotometer to determine the relative amount of formazan salt in each well. The amount of formazan produced in wells containing untreated cells only and growth medium only represent 100% survival and 0% survival respectively, and the amount in each treatment well was converted to a survival percentage relative to these two extremes. The IC_{50} values were obtained from full dose-response curves, using a non-linear dose-response curve fitting analysis via GraphPad Prism v.4 software.

3.7. Human Neuroblastoma SH-SY5Y Cell Viability Assays

Cell Line and Culture Conditions

The human neuroblastoma cell line SH-SY5Y was generously donated by our collaborator at the Division of Molecular Biology and Human Biology, Stellenbosch University, Tygerberg, Cape Town. Cells were cultured in monolayer using Dulbecco Modified Eagles Medium (DMEM, Gibco, Life Technologies Ltd. Carlsbad, CA, USA) supplemented with 10% foetal bovine serum (FBS, Gibco, Life Technologies Ltd.) and 1% 100 U/mL penicillin and 100 µg/mL streptomycin (Lonza Group Ltd., Basel, Switzerland). Cells were grown at 37 °C, in a humidified atmosphere at 5% CO₂. Media were replaced every two to three days and cells were sub-cultured by splitting with trypsin (Lonza Group Ltd.).

SH-SY5Y Cytotoxicity Assays

The standard MTT assay which measures cell metabolic activity was used to determine cytotoxicity of CM14, CM15 and CM9 as described by Mosmann [49]. Briefly, SH-SY5Y cells were plated in flat bottom 96 well plates in growth medium as stated in Section 3.7.1 at a density of 7500 cells/well. Cells were allowed to adhere to the plate surface for 24 h and used media were replaced with fresh media containing test compounds at 10 µM, 50 µM and 100 µM. Vehicle control cells were treated with DMSO (solvent for dissolving test compounds) at a concentration similar to the amount contained in the highest concentration of test compounds. After 48 h, 10 µL of MTT solution (5 mg/mL) was added to each well and incubated for 4 h and the purple formazan formed was solubilized with 100 µL DMSO and plates were read spectrophotometrically to determine absorbance at 570 nm using a BMG Labtech POLARStar Omega multimodal plate reader.

MPP⁺-Induced Cytotoxicity in SH-SY5Y Cells

SH-SY5Y cells were seeded onto a 96-well plate and treated with 1000 µM MPP⁺ for approximately 48 h. Different concentrations (1 µM, 5 µM, and 10 µM) of test compounds were administered two hours prior to MPP⁺ treatment. Afterwards, cell viability was measured by MTT colorimetric assay and performed as stated in Section 3.7.2.

4. Conclusions

As part of a collaborative project, compounds from the University of the Western Cape, School of Pharmacy drug-design group compound library were screened for antimycobacterial activity. Various coumarin derivatives, originally designed and synthesized as multifunctional neuronal enzyme inhibitors, demonstrated noteworthy antimycobacterial activity.

The coumarin **CM9** substituted with an *N*-benzylpiperidine-containing moiety on the 7-position and a 3-nitrile substitution on the coumarin nucleus showed the best MAO-B and AChE inhibitory activities. This study identified that structural modification on position 4 and/or 7 of the coumarin scaffold can be utilized to improve selectivity towards either inhibition of neuronal enzymes or antimycobacterial effect. Large substitutions on position 4 (4-trifluoromethyl moiety) and *p*-bromo-*N*-benzylpiperazine compared to *N*-benzylpiperidine substitutions on position 7 increase activity against *M. tuberculosis* but inversely affect monoamine oxidase and cholinesterase inhibition.

After validation of the antimycobacterial activity observed in the MTS; **CM8**, **CM12**, **CM14** (4-methyl substituted) and **CM15** (4-trifluoromethyl-substituted) were identified as the most active compounds in the series. In addition to activity in standard *M. tuberculosis* H37Rv, we also described activity of selected coumarin derivatives in fluoroquinolone resistant bacteria. Evaluations on three moxifloxacin resistant strains harbouring mutations in the QRDR of DNA gyrase indicate that the compound in series 1 will likely maintain potency in fluoroquinolone resistant mycobacteria.

The MICs of the four most active compounds were evaluated using two methods i.e., *M. tuberculosis* H37RvMA pMSP12:GFP in GAST-Fe media [32], and *M. tuberculosis* H37Rv:pCHERRY3 [31] in 7H9+OADC. The MIC values in the GAST-Fe assay were consistently lower (2–3 fold lower for **CM8**, **CM12**, and **CM14** and 14 fold lower for **CM15**). Difference in inoculum size and the lack and presence of albumin in GAST-Fe and 7H9+OADC media respectively were suggested as primary contributing factors to the MIC variations.

As coumarin derivatives are known to bind extensively to blood-soluble proteins, albumin binding properties of **CM15** and **CM14** (with the highest and lowest MIC fold difference between assays respectively) were evaluated. Fluorescence quenching of BSA in response to compound binding was evaluated in the presence of various concentrations of the compounds. Analysis of fluorescence quenching of tryptophan in BSA indicate that both **CM14** and **CM15** form concentration dependant complexes with BSA. These results suggest that albumin binding plays a large role in the observed differences in activity between the GAST-Fe and 7H9+OADC assays used in this study. The more extensive decrease in fluorescence observed with **CM15** likely indicates a higher binding affinity between **CM15** and thus explains the large MIC differences observed for this compound. This report therefore highlights the importance of early consideration of plasma binding properties of coumarin derivatives as it was shown here to influence in vitro evaluations in addition to its more commonly considered effect on in vivo, and future pharmacokinetic behaviour of the compounds.

CM8, **CM12**, **CM14**, and **CM15** showed moderate (CC_{50} : 15.5–41.2 μ M) cytotoxicity compared to the cytotoxic agent emetine (CC_{50} = 0.06 μ M). These compounds however showed low selectivity indices when both the GFP and mCHERRY MIC₉₉ assay results are compared to the CC_{50} results (Table 4). The compounds, in general, were slightly more selective towards the mycobacterial strain when using the GFP assay results, with **CM15** showing the best selectivity (SI = 3.16). The slight selectivity was however not retained when the results from the mCHERRY assay were used in the SI calculations. These poor selectivity indices may limit the further development of these coumarin derivatives. However, the structure-activity relationships identified in this paper may enable the design of coumarin structures with improved antimycobacterial activities and subsequently more favourable selectivity indices.

The viability of SHSY-5Y human neuroblastoma cells was also assessed at different concentrations of compounds **CM9**, **CM14**, or **CM15**. Treatment with the compounds at 10 μ M did not significantly affect the viability of the SH-SY5Y cells ($p > 0.05$). However, at higher concentrations (50 μ M and 100 μ M) the viability of the cells was significantly ($p < 0.001$) affected. Neuroprotective ability of the three compounds were therefore evaluated at concentrations between 1 μ M and 10 μ M. **CM9**, **CM14**, and **CM15** all demonstrated significant and comparable cytoprotection towards MPP⁺ insults to the SH-SY5Y neural cells. As these compounds differ significantly in their neuronal enzyme inhibitory activity it can be concluded that enzyme inhibition is not the only factor that plays a role in cytoprotection and

that other mechanisms of action are involved in the observed neuroprotection.

This article therefore describes the versatile neuronal enzyme inhibitory, neuroprotective and antimycobacterial nature of a range of coumarin derivatives. Importantly, comparison of corresponding structure-activity relationship, demonstrates that it is possible to reduce the promiscuous activity of the derivatives through careful modification on the coumarin scaffold. Furthermore the article highlights the importance of broader evaluation of pharmacological effects of coumarin derivatives over and above cytotoxicity assays to identify and afford early limitation of unwanted pharmacological effects. This report also shows that albumin binding properties of coumarin derivatives may impact on in vitro assay results and should therefore be taken into consideration even during early evaluations of coumarin-type compounds.

Acknowledgments: We are grateful to the National Research Foundation of South Africa, the South African Medical Research Council and the University of the Western Cape for financial support. Samantha L. Sampson is funded by the South African Research Chairs Initiative of the Department of Science and Technology and National Research Foundation (NRF) of South Africa, award number UID 86539. The content is solely the responsibility of the authors and does not necessarily represent the official views of the NRF. Research reported in this publication was supported by the South African Medical Research Council.

Author Contributions: E.K., S.L.S., E.M.S., H.V., D.F.W., S.I.O., A.B.E., S.F.M., F.T.Z., O.E.E. and J.J. conceived and designed the experiments; G.B.F. and J.J. synthesized the compounds; H.V., J.J., F.T.Z., D.F.W., G.B.F., S.I.O. and A.B.E. performed the experiments and analysis; E.K. and J.J. wrote the paper.

Conflicts of Interest: The authors declare no conflict of interest.

References

1. Brown, D.G.; Lister, T.; May-Dracka, T.L. New natural products as new leads for antibacterial drug discovery. *Bioorg. Med. Chem. Lett.* **2014**, *24*, 413–418. [[CrossRef](#)] [[PubMed](#)]
2. Hu, Y.Q.; Xu, Z.; Zhang, S.; Wu, X.; Ding, J.W.; Lv, Z.S.; Feng, L.S. Recent developments of coumarin-containing derivatives and their anti-tubercular activity. *Eur. J. Med. Chem.* **2017**, *136*, 122–130. [[CrossRef](#)] [[PubMed](#)]
3. Keri, R.S.; Sasidhar, B.S.; Nagaraja, B.M.; Santos, M.A. Recent progress in the drug development of coumarin derivatives as potent antituberculosis agents. *Eur. J. Med. Chem.* **2015**, *100*, 257–269. [[CrossRef](#)] [[PubMed](#)]
4. Stanley, S.A.; Kawate, T.; Iwase, N.; Shimizu, M.; Clatworthy, A.E.; Kazyanskaya, E.; Sacchettini, J.C.; Ioerger, T.R.; Siddiqi, N.A.; Minami, S.; et al. Diarylcoumarins inhibit mycolic acid biosynthesis and kill *Mycobacterium tuberculosis* by targeting FadD32. *Proc. Natl. Acad. Sci. USA* **2013**, *110*, 11565–11570. [[CrossRef](#)] [[PubMed](#)]
5. Heide, L. New aminocoumarin antibiotics as gyrase inhibitors. *Int. J. Med. Microbiol.* **2014**, *304*, 31–36. [[CrossRef](#)] [[PubMed](#)]
6. Schroder, W.; Goerke, C.; Wolz, C. Opposing effects of aminocoumarins and fluoroquinolones on the SOS response and adaptability in *Staphylococcus aureus*. *J. Antimicrob. Chemother.* **2013**, *68*, 529–538. [[CrossRef](#)] [[PubMed](#)]
7. Collin, F.; Karkare, S.; Maxwell, A. Exploiting bacterial DNA gyrase as a drug target: Current state and perspectives. *Appl. Microbiol. Biotechnol.* **2011**, *92*, 479–497. [[CrossRef](#)] [[PubMed](#)]

8. Flatman, R.H.; Howells, A.J.; Heide, L.; Fiedler, H.; Maxwell, A. Simocyclinone D8, an inhibitor of DNA gyrase with a novel mode of action. *Antimicrob. Agents Chemother.* **2005**, *49*, 1093–1100. [[CrossRef](#)] [[PubMed](#)]
9. Edwards, M.J.; Williams, M.A.; Maxwell, A.; McKay, A.R. Mass spectrometry reveals that the antibiotic simocyclinone D8 binds to DNA gyrase in a “bent-over” conformation: Evidence of positive cooperativity in binding. *Biochemistry* **2011**, *50*, 3432–3440. [[CrossRef](#)] [[PubMed](#)]
10. Hearnshaw, S.J.; Edwards, M.J.; Stevenson, C.E.; Lawson, D.M.; Maxwell, A. A New crystal structure of the bifunctional antibiotic simocyclinone D8 bound to DNA gyrase gives fresh insight into the mechanism of inhibition. *J. Mol. Biol.* **2014**, *426*, 2023–2033. [[CrossRef](#)] [[PubMed](#)]
11. Cheng, G.; Hao, H.; Dai, M.; Liu, Z.; Yuan, Z. Antibacterial action of quinolones: From target to network. *Eur. J. Med. Chem.* **2013**, *66*, 555–562. [[CrossRef](#)] [[PubMed](#)]
12. Aldred, K.J.; Blower, T.R.; Kerns, R.J.; Berger, J.M.; Osheroff, N. Fluoroquinolone interactions with *Mycobacterium tuberculosis* gyrase: Enhancing drug activity against wild-type and resistant gyrase. *Proc. Natl. Acad. Sci. USA* **2016**, *113*, E839–E846. [[CrossRef](#)] [[PubMed](#)]
13. Shadrack, W.R.; Ndjomou, J.; Kolli, R.; Mukherjee, S.; Hanson, A.M.; Frick, D.N. Discovering new medicines targeting helicases: Challenges and recent progress. *J. Biomol. Screen.* **2013**, *18*, 761–781. [[CrossRef](#)] [[PubMed](#)]
14. Li, B.; Pai, R.; Di, M.; Aiello, D.; Barnes, M.H.; Butler, M.M.; Tashjian, T.F.; Peet, N.P.; Bowlin, T.L.; Moir, D.T. Coumarin-based inhibitors of *Bacillus anthracis* and *Staphylococcus aureus* replicative DNA helicase: Chemical optimization, biological evaluation, and antibacterial activities. *J. Med. Chem.* **2012**, *55*, 10896–10908. [[CrossRef](#)] [[PubMed](#)]
15. Aiello, D.; Barnes, M.H.; Biswas, E.E.; Biswas, S.B.; Gu, S.; Williams, J.D.; Bowlin, T.L.; Moir, D.T. Discovery, characterization and comparison of inhibitors of *Bacillus anthracis* and *Staphylococcus aureus* replicative DNA helicases. *Bioorg. Med. Chem.* **2009**, *17*, 4466–4476. [[CrossRef](#)] [[PubMed](#)]
16. Chopra, S.; Matsuyama, K.; Tran, T.; Malerich, J.P.; Wan, B.; Franzblau, S.G.; Lun, S.; Guo, H.; Maiga, M.C.; Bishai, W.R.; et al. Evaluation of gyrase B as a drug target in *Mycobacterium tuberculosis*. *J. Antimicrob. Chemother.* **2011**, *67*, 415–421. [[CrossRef](#)] [[PubMed](#)]
17. Jeankumar, V.U.; Reshma, R.S.; Janupally, R.; Saxena, S.; Sridevi, J.P.; Medapi, B.; Kulkarni, P.; Yogeewari, P.; Sriram, D. Enabling the (3 + 2) cycloaddition reaction in assembling newer anti-tubercular lead acting through the inhibition of the gyrase ATPase domain: Lead optimization and structure activity profiling. *Org. Biomol. Chem.* **2015**, *13*, 2423–2431. [[CrossRef](#)] [[PubMed](#)]
18. Jeyachandran, M.; Ramesh, P.; Sriram, D.; Senthilkumar, P.; Yogeewari, P. Synthesis and in vitro antitubercular activity of 4-aryl/alkylsulfonylmethylcoumarins as inhibitors of *Mycobacterium tuberculosis*. *Bioorg. Med. Chem. Lett.* **2012**, *22*, 4807–4809. [[CrossRef](#)] [[PubMed](#)]
19. Anand, A.; Kulkarni, M.V.; Joshi, S.D.; Dixit, S.R. One pot Click chemistry: A three component reaction for the synthesis of 2-mercaptobenzimidazole linked coumarinyl triazoles as anti-tubercular agents. *Bioorg. Med. Chem. Lett.* **2016**, *26*, 4709–4713. [[CrossRef](#)] [[PubMed](#)]
20. Reddy, D.S.; Hosamani, K.M.; Devarajegowda, H.C. Design, synthesis of benzocoumarin-pyrimidine hybrids as novel class of antitubercular agents, their DNA cleavage and X-ray studies. *Eur. J. Med. Chem.* **2015**, *101*, 705–715. [[CrossRef](#)] [[PubMed](#)]
21. Zheng, P.; Somersan-Karakaya, S.; Lu, S.; Roberts, J.; Pingle, M.; Warriar, T.; Little, D.; Guo, X.; Brickner, S.J.; Nathan, C.F.; et al. Synthetic calanolides with bactericidal activity against replicating and nonreplicating *Mycobacterium tuberculosis*. *J. Med. Chem.* **2014**, *57*, 3755–3772. [[CrossRef](#)] [[PubMed](#)]

22. Basanagouda, M.; Jambagi, V.B.; Barigheid, N.N.; Laxmeshwar, S.S.; Devaru, V.; Narayanachar. Synthesis, structure-activity relationship of iodinated-4-aryloxymethyl-coumarins as potential anti-cancer and anti-mycobacterial agents. *Eur. J. Med. Chem.* **2014**, *74*, 225–233. [[CrossRef](#)] [[PubMed](#)]
23. Skalicka-Wozniak, K.; Orhan, I.E.; Cordell, G.A.; Nabavi, S.M.; Budzynska, B. Implication of coumarins towards central nervous system disorders. *Pharmacol. Res.* **2016**, *103*, 188–203. [[CrossRef](#)] [[PubMed](#)]
24. Carradori, S.; D'Ascenzio, P.; Chimenti, D.; Secci, A.; Bolasco, A. Selective MAO-B inhibitors. *Mol. Div.* **2016**, *254*, 219–243.
25. De Souza, L.G.; Rennó, M.N.; Figueroa-Villar, J. Coumarins as cholinesterase inhibitors: A review. *Chem. Biol. Interact.* **2016**, *254*, 11–23. [[CrossRef](#)] [[PubMed](#)]
26. Joubert, J.; Foka, G.B.; Repsold, B.P.; Oliver, D.W.; Kapp, E.; Malan, S.F. Synthesis and evaluation of 7-substituted coumarin derivatives as multimodal monoamine oxidase-B and cholinesterase inhibitors for the treatment of Alzheimer's disease. *Eur. J. Med. Chem.* **2017**, *125*, 853–864. [[CrossRef](#)] [[PubMed](#)]
27. Patil, P.O.; Bari, S.B.; Firke, S.D.; Deshmukh, P.K.; Donda, S.T.; Patil, D.A. A comprehensive review on synthesis and designing aspects of coumarin derivatives as monoamine oxidase inhibitors for depression and Alzheimer's disease. *Bioorg. Med. Chem.* **2013**, *21*, 2434–2450. [[CrossRef](#)] [[PubMed](#)]
28. Birks, J.; Harvey, R.J. Donepezil for dementia due to Alzheimer's disease. *Cochrane Database Syst. Rev.* **2006**, *1*, CD001190.
29. Kuhn, M.L.; Alexander, E.; Minasov, G.; Page, H.J.; Warwzrak, Z.; Shuvalova, L.; Flores, K.J.; Wilson, D.J.; Shi, C.; Aldrich, C.C.; et al. Structure of the essential Mtb FadD32 Enzyme: A promising drug target for treating tuberculosis. *ACS Infect. Dis.* **2016**, *2*, 579–591. [[CrossRef](#)] [[PubMed](#)]
30. Maruri, F.; Sterling, T.R.; Kaiga, A.W.; Blackman, A.; van der Heijden, Y.F.; Mayer, C.; Cambau, E.; Aubry, A. A systematic review of gyrase mutations associated with fluoroquinolone-resistant *Mycobacterium tuberculosis* and a proposed gyrase numbering system. *J. Antimicrob. Chemother.* **2012**, *67*, 819–831. [[CrossRef](#)] [[PubMed](#)]
31. Carroll, P.; Schreuder, L.J.; Muwanguzi-Karugaba, J.; Wiles, S.; Robertson, B.D.; Ripoll, J.; Ward, T.H.; Bancroft, G.J.; Schaible, U.E.; Parish, T. Sensitive detection of gene expression in mycobacteria under replicating and non-replicating conditions using optimized far-red reporters. *PLoS ONE* **2010**, *5*, e9823. [[CrossRef](#)] [[PubMed](#)]
32. Abrahams, G.L.; Kumar, A.; Savvi, S.; Hung, A.W.; Wen, S.; Abell, C.; Barry, C.E.; Sherman, D.R.; Boshoff, H.I.; Mizrahi, V. Pathway-selective sensitization of *Mycobacterium tuberculosis* for target-based whole-cell screening. *Chem. Biol.* **2012**, *19*, 844–854. [[CrossRef](#)] [[PubMed](#)]
33. Lounis, N.; Vranckx, L.; Gevers, T.; Kaniga, K.; Andries, K. In vitro culture conditions affecting minimal inhibitory concentration of bedaquiline against *M. tuberculosis*. *Med. Mal. Infect.* **2016**, *46*, 220–225. [[CrossRef](#)] [[PubMed](#)]
34. Dockal, M.; Carter, D.C.; Ruker, F. Conformational transitions of the three recombinant domains of human serum albumin depending on pH. *J. Biol. Chem.* **2000**, *275*, 3042–3050. [[CrossRef](#)] [[PubMed](#)]
35. Ran, D.; Wu, X.; Zheng, J.; Yang, J.; Zhou, H.; Zhang, M.; Tang, Y. Study on the interaction between Florasulam and bovine serum albumin. *J. Fluoresc.* **2007**, *17*, 721–726. [[CrossRef](#)] [[PubMed](#)]

36. Tian, J.; Liu, J.; Zhang, J.; Hu, Z.; Chen, X. Fluorescence studies on the interactions of barbaloin with bovine serum albumin. *Chem. Pharm. Bull.* **2003**, *51*, 579–582. [[CrossRef](#)] [[PubMed](#)]
37. Seetharamappa, J.; Kamat, B.P. Spectroscopic studies on the mode of interaction of an anticancer drug with bovine serum albumin. *Chem. Pharm. Bull. (Tokyo)* **2004**, *52*, 1053–1057. [[CrossRef](#)] [[PubMed](#)]
38. Sulkowska, A.; Rownicka, J.; Bojko, B.; Sulkowski, W. Interaction of anticancer drugs with human and bovine serum albumin. *J. Mol. Struct.* **2003**, *651*, 133–140. [[CrossRef](#)]
39. Kun, R.; Kis, L.; Dekany, I. Hydrophobization of bovine serum albumin with cationic surfactants with different hydrophobic chain length. *Colloids Surf. B Biointerfaces* **2010**, *79*, 61–68. [[CrossRef](#)] [[PubMed](#)]
40. Liu, B.; Guo, Y.; Wang, J.; Xu, R.; Wang, X.; Wang, D.; Zhang, L.; Xu, Y. Spectroscopic studies on the interaction and sonodynamic damage of neutral red (NR) to bovine serum albumin (BSA). *J. Lumin.* **2010**, *130*, 1036–1043. [[CrossRef](#)]
41. Xiang, G.; Tong, C.; Lin, H. Nitroaniline isomers interaction with bovine serum albumin and toxicological implications. *J. Fluoresc.* **2007**, *17*, 512–521. [[CrossRef](#)] [[PubMed](#)]
42. Hu, Y.; Liu, Y.; Zhang, L.; Zhao, R.; Qu, S. Studies of interaction between colchicine and bovine serum albumin by fluorescence quenching method. *J. Mol. Struct.* **2005**, *750*, 174–178. [[CrossRef](#)]
43. Gök, E.; Öztürk, C.; Akbay, N. Interaction of Thyroxine with 7 Hydroxycoumarin: A fluorescence quenching study. *J. Fluoresc.* **2008**, *18*, 781–785. [[CrossRef](#)] [[PubMed](#)]
44. Xu, H.; Gao, S.; Lv, J.; Liu, Q.; Zuo, Y.; Wang, X. Spectroscopic investigations on the mechanism of interaction of crystal violet with bovine serum albumin. *J. Mol. Struct.* **2009**, *919*, 334–338. [[CrossRef](#)]
45. Shaikh, S.M.T.; Seetharamappa, J.; Kandagal, P.B.; Manjunatha, D.H.; Ashoka, S. Spectroscopic investigations on the mechanism of interaction of bioactive dye with bovine serum albumin. *Dyes Pigment.* **2007**, *74*, 665–671. [[CrossRef](#)]
46. Papadopoulou, A.; Green, R.J.; Frazier, R.A. Interaction of flavonoids with bovine serum albumin: A fluorescence quenching study. *J. Agric. Food Chem.* **2005**, *53*, 158–163. [[CrossRef](#)] [[PubMed](#)]
47. Shi, X.; Li, X.; Gui, M.; Zhou, H.; Yang, R.; Zhang, H.; Jin, Y. Studies on interaction between flavonoids and bovine serum albumin by spectral methods. *J. Lumin.* **2010**, *130*, 637–644. [[CrossRef](#)]
48. Ware, W.R. Oxygen quenching of fluorescence in solution: An experimental study of the diffusion process. *J. Phys. Chem.* **1962**, *66*, 455–458. [[CrossRef](#)]
49. Mosmann, T. Rapid colorimetric assay for cellular growth and survival: Application to proliferation and cytotoxicity assays. *J. Immunol. Methods* **1983**, *65*, 55–63. [[CrossRef](#)]
50. Cui, W.; Zhang, Z.; Li, W.; Hu, S.; Mak, S.; Zhang, H.; Han, R.; Yuan, S.; Li, S.; Sa, F.; et al. The anti-cancer agent SU4312 unexpectedly protects against MPP(+)-induced neurotoxicity via selective and direct inhibition of neuronal NOS. *Br. J. Pharmacol.* **2013**, *168*, 1201–1214. [[CrossRef](#)] [[PubMed](#)]
51. Jantas, D.; Greda, A.; Golda, S.; Korostynski, M.; Grygier, B.; Roman, A.; Pilc, A.; Lason, W. Neuroprotective effects of metabotropic glutamate receptor group II and III activators against MPP(+)-induced cell death in human neuroblastoma SH-SY5Y cells: The impact of cell differentiation state. *Neuropharmacology* **2014**, *83*, 36–53. [[CrossRef](#)] [[PubMed](#)]
52. Pyszko, J.; Strosznajder, J.B. Sphingosine kinase 1 and sphingosine-1-phosphate in oxidative stress evoked by 1-methyl-4-phenylpyridinium (MPP+) in human dopaminergic neuronal cells.

- Mol. Neurobiol.* **2014**, *50*, 38–48. [[CrossRef](#)] [[PubMed](#)]
53. Wang, Y.; Gao, J.; Miao, Y.; Cui, Q.; Zhao, W.; Zhang, J.; Wang, H. Pinocembrin protects SH-SY5Y cells against MPP⁺-induced neurotoxicity through the mitochondrial apoptotic pathway. *J. Mol. Neurosci.* **2014**, *53*, 537–545. [[CrossRef](#)] [[PubMed](#)]
54. Nakaso, K.; Tajima, N.; Horikoshi, Y.; Nakasone, M.; Hanaki, T.; Kamizaki, K.; Matura, T. The estrogen receptor beta-PI3K/Akt pathway mediates the cytoprotective effects of tocotrienol in a cellular Parkinson's disease model. *Biochim. Biophys. Acta* **2014**, *1842*, 1303–1312. [[CrossRef](#)] [[PubMed](#)]
55. Tasaki, Y.; Omura, T.; Yamada, T.; Ohkubo, T.; Suno, M.; Iida, S.; Sakaguchi, T.; Asari, M.; Shimizu, K.; Matsubara, K. Meloxicam protects cell damage from 1-methyl-4-phenyl pyridinium toxicity via the phosphatidylinositol 3-kinase/Akt pathway in human dopaminergic neuroblastoma SH-SY5Y cells. *Brain Res.* **2010**, *1344*, 25–33. [[CrossRef](#)] [[PubMed](#)]
56. Zhu, G.; Wang, X.; Wu, S.; Li, Q. Involvement of activation of PI3K/Akt pathway in the protective effects of puerarin against MPP⁺-induced human neuroblastoma SH-SY5Y cell death. *Neurochem. Int.* **2012**, *60*, 400–408. [[CrossRef](#)] [[PubMed](#)]
57. Iøerger, T.R.; Feng, Y.; Ganesula, K.; Chen, X.; Dobos, K.M.; Fortune, S.; Jacobs, W.R., Jr.; Mizrahi, V.; Parish, T.; Rubin, E.; et al. Variation among genome sequences of H37Rv strains of *Mycobacterium tuberculosis* from multiple laboratories. *J. Bacteriol.* **2010**, *192*, 3645–3653. [[CrossRef](#)] [[PubMed](#)]
58. Goldstone, R.M.; Goonesekera, S.D.; Bloom, B.R.; Sampson, S.L. The transcriptional regulator Rv0485 modulates the expression of a *pe* and *ppe* gene pair and is required for *Mycobacterium tuberculosis* virulence. *Infect. Immun.* **2009**, *77*, 4654–4667. [[CrossRef](#)] [[PubMed](#)]
59. Ollinger, J.; Bailey, M.A.; Moraski, G.C.; Casey, A.; Florio, S.; Alling, T.; Miller, M.J.; Parish, T. A dual read-out assay to evaluate the potency of compounds active against *Mycobacterium tuberculosis*. *PLoS ONE* **2013**, *8*, e60531. [[CrossRef](#)] [[PubMed](#)]

Sample Availability: Samples of the compounds **CM1–CM19** are available from the authors.

Chapter 6: Antimycobacterial activity, Synergism and Mechanism of Action Evaluation of Novel Polycyclic Amines against *Mycobacterium tuberculosis*.

Kapp E, Joubert J, Sampson SL, et al. Antimycobacterial Activity, Synergism, and Mechanism of Action Evaluation of Novel Polycyclic Amines against *Mycobacterium tuberculosis*. *Adv Pharmacol Pharm Sci*. 2021. doi: [10.1155/2021/5583342](https://doi.org/10.1155/2021/5583342)

Copyright statement: This is an open access article distributed under the Creative Commons Attribution License, which permits unrestricted use, distribution, and reproduction in any medium, provided the original work is properly cited.



Antimycobacterial Activity, Synergism, and Mechanism of Action Evaluation of Novel Polycyclic Amines against *Mycobacterium tuberculosis*

Erika Kapp,¹ Jacques Joubert,¹ Samantha L. Sampson,² Digby F. Warner,³ Ronnett Seldon,⁴ Audrey Jordaan,³ Margaretha de Vos,² Rajan Sharma,¹ and Sarel F. Malan¹

¹School of Pharmacy, Faculty of Natural Sciences, University of the Western Cape, Cape Town, South Africa

²DSI/NRF Centre of Excellence for Biomedical Tuberculosis Research, SAMRC Centre for Tuberculosis Research,

Division of Molecular Biology and Human Genetics, Faculty of Medicine and Health Sciences, University of Stellenbosch, Cape Town, South Africa

³SAMRC/NHLS/UCT Molecular Mycobacteriology Research Unit, DSI/NRF Centre of Excellence for Biomedical Tuberculosis Research,

Department of Pathology and Institute of Infectious Disease and Molecular Medicine, Faculty of Health Sciences, University of Cape Town, Cape Town, South Africa

⁴H3D Drug Discovery and Development Centre, Department of Chemistry, University of Cape Town, Cape Town, South Africa

Correspondence should be addressed to Erika Kapp; ekapp@uwc.ac.za Received 11 January 2021; Accepted 24 May 2021; Published 21 June 2021 Academic Editor: Heng Yen Khong

Copyright © 2021 Erika Kapp et al. This is an open access article distributed under the [Creative Commons Attribution License](https://creativecommons.org/licenses/by/4.0/), which permits unrestricted use, distribution, and reproduction in any medium, provided the original work is properly cited.

ABSTRACT

Mycobacterium tuberculosis has developed extensive resistance to numerous antimycobacterial agents used in the treatment of tuberculosis. Insufficient intracellular accumulation of active moieties allows for selective survival of mycobacteria with drug resistance mutations and accordingly promotes the development of microbial drug resistance. Discovery of compounds with new mechanisms of action and physicochemical properties that promote intracellular accumulation, or compounds that act synergistically with other antimycobacterial drugs, has the potential to reduce and prevent further drug resistance. To this end, antimycobacterial activity, mechanism of action, and synergism in combination therapy were investigated for a series of polycyclic amine derivatives. Compound selection was based on the presence of moieties with possible antimycobacterial activity, the inclusion of bulky lipophilic carriers to promote intracellular accumulation, and previously demonstrated bioactivity that potentially support inhibition of efflux pump activity. The most potent antimycobacterial demonstrated a minimum inhibitory concentration (MIC₉₉) of 9.6 μM against *Mycobacterium tuberculosis* H37Rv. Genotoxicity and inhibition of the cytochrome *bc*₁ respiratory complex were excluded as mechanisms of action for all compounds. Inhibition of cell wall synthesis was identified as a likely mechanism of action for the two most active compounds (**14** and **15**). Compounds **5** and **6** demonstrated synergistic activity with the known Rv1258c efflux pump substrate, spectinomycin, pointing to possible efflux pump inhibition. For this series, the nature of the side chain, rather than the type of polycyclic carrier, seems to play a determining role in the antimycobacterial activity and cytotoxicity of the compounds. Contrariwise, the nature of the polycyclic carrier, particularly the azapentacycloundecane cage, appears to promote synergistic activity. Results point to the possibility of combining an azapentacycloundecane carrier with a side chain that promotes antimycobacterial activity to develop dual acting molecules for the treatment of *Mycobacterium tuberculosis*.

1. Introduction

The progressive development of resistance to various chemotherapeutic agents used in the management of infectious diseases presents a serious problem in global public health. Tuberculosis (TB) has re-emerged as one of the most concerning communicable diseases of our time. The notoriously complex structure of the mycobacterial cell wall and the abundance of efflux pumps (EPs) in *Mycobacterium tuberculosis* limit the intracellular accumulation and antimycobacterial efficacy of numerous antimicrobial classes successfully utilized against standard bacteria [1–4]. Treatment and control of the TB epidemic is further complicated by the development of multidrug-resistant (MDR) and extensively drug-resistant (XDR) strains. Current TB treatment regimens thus comprise a combination of antimycobacterial agents which, as drug resistance develops to the various first-line agents, not only decrease in efficacy and patient acceptability, but also increase in required treatment duration and toxicity. Based on their mechanisms of action (MOAs), available antimycobacterial drugs can be broadly categorized into three classes: those which disrupt cell wall integrity (e.g., isoniazid, ethambutol, ethionamide, and cycloserine, as well as the experimental 1,2-ethylenediamine, SQ109 [5]); those that limit the energy available for cellular processes (e.g., pyrazinamide and bedaquiline [6]); and compounds that inhibit normal cellular functionality by inhibiting or corrupting biosynthesis of essential macromolecules, cofactors, and metabolites (e.g., the rifamycin, fluoroquinolone, aminoglycoside and oxazolidinone class antibiotics, and para-aminosalicylic acid [7–9]). Reduced susceptibility to these antimycobacterial agents commonly results from spontaneous mutations in the

genome of mycobacteria with selective survival fuelled by suboptimal exposure to, or reduced intracellular accumulation of, active moieties [10, 11]. EPs, in particular, have been shown to play a role in inadequate accumulation of drugs within the mycobacterial cell [12]. Depending on the particular mechanism by which a drug's action is overcome, resistance may be specific to a particular molecule or, more alarmingly, result in reduced sensitivity to various drugs that target a particular cellular process (e.g., cell wall synthesis) or act as substrates for an overexpressed efflux pump.

Strategies that improve the accumulation of antimycobacterial compounds within the mycobacterial cell would likely increase the efficacy of the particular compound, but would also minimize genetically encoded resistance aided by sub inhibitory chemotherapeutic exposure [13]. Approaches that may promote intracellular accumulation of chemotherapeutic agents could include increasing cell wall permeability [14], facilitation of passive transport of drugs into the cell, alteration of the chemical structure of molecules to reduce their predisposition to efflux [15], as well as direct efflux pump inhibition through the utilization of EP inhibitors [16].

As part of a research project designed to evaluate the possibility of modulating drug resistance and increase accumulation of active moieties in *M. tuberculosis*, a series of polycyclic cage compounds were selected from the University of the Western Cape School of Pharmacy compound library to be evaluated for antimycobacterial and efflux pump inhibitory activity in *M. tuberculosis*. The polycyclic cage derivatives included in this study demonstrate, amongst others, L-type calcium channel and NMDA inhibitory properties [17] and feature a lipophilic scaffold likely to improve the barrier permeability of selected structures. Subsequent research demonstrated the ability of polycyclic amine derivatives (particularly compounds **3**, **5**, and **11**, Figure 1) to modulate antimalarial drug resistance [18–20]. Criteria for the selection of compounds to include in this study were therefore the presence of moieties with possible antimycobacterial activity, and the inclusion of bulky lipophilic carriers to promote compound accumulation within the mycobacterial cell, as well as biological effects which may promote resistance reversal activity. The possession of potential ion channel inhibitory properties, which may directly or indirectly inhibit efflux pump efficacy [21, 22], was an important consideration in compound selection.

Here, we report the antimycobacterial activities of the series of selected compounds and a preliminary investigation into possible MOAs of the active molecules. We also describe a possible modulation of Rv1258c efflux pump activity as indicated by synergistic activity with spectinomycin, a known substrate for the mycobacterial Rv1258c efflux pump [15].

2. Results and Discussion

The compounds selected for the study were classified into three categories based on the nature of the polycyclic cage scaffold. Figure 1 shows the oxapentacycloundecane class (compounds **1**, **2**, **4**, and **8**), the azapentacycloundecane class (compounds **3**, **5**, **6**, and **7**), and adamantane class (compounds **9–16**). Synthesis of compounds **1–15** (Figure 1) is described in detail in previous publications by our group, as indicated in Table 1. Compound **16** was purchased from Sigma-Aldrich®.

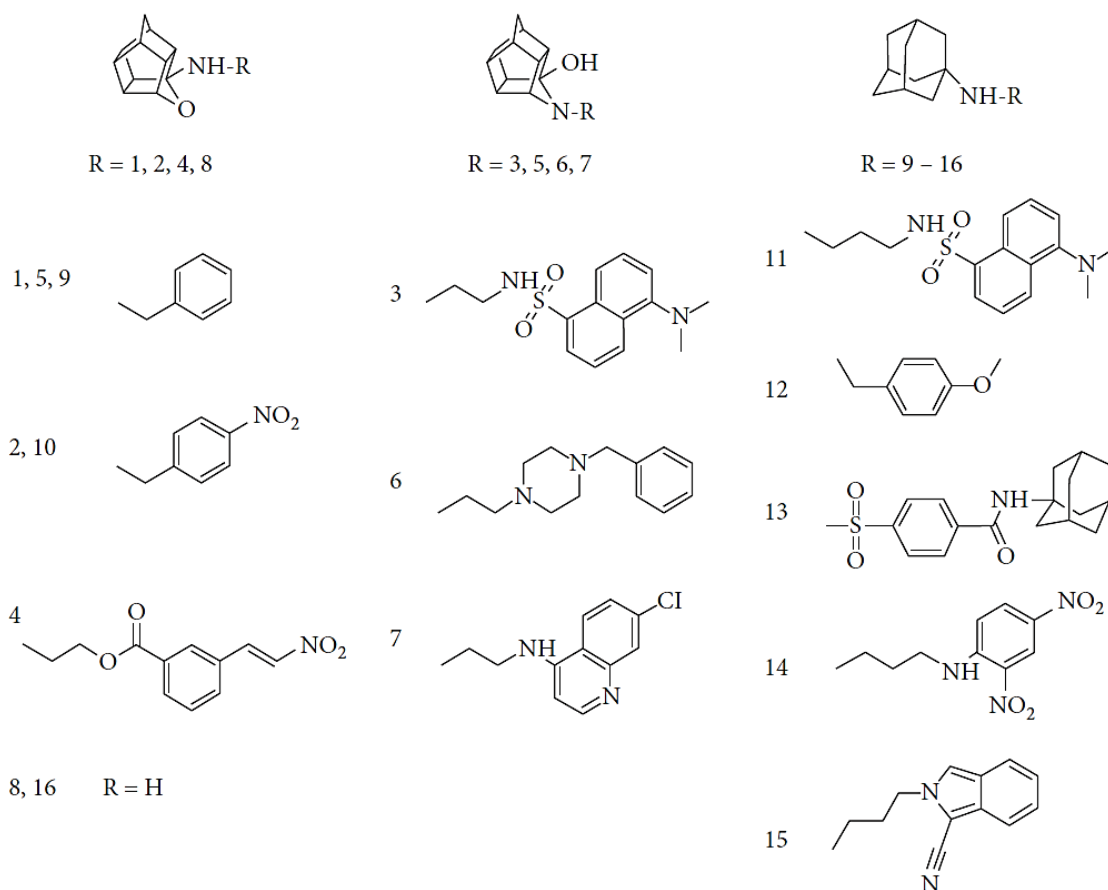


Figure 1: Structures of the evaluated compounds grouped based on the lipophilic scaffold.

2.1 Antimycobacterial Activity.

Minimum inhibitory concentrations (MIC₉₉) of the compounds (Table 1) were determined in nutrient-rich and nutrient-poor media types by the broth microdilution method utilizing an *M. tuberculosis* H37Rv reporter strain expressing GFP [29–31]. Compounds **3**, **5**, **7**, **11**, **14**, and **15** showed antimycobacterial activity with MIC₉₉ values ranging from 9.6 μM to 82.2 μM (Table 1); these were selected for further analysis to determine the possible MOA. Interestingly, during MIC determination, compound **5** showed activity in the GAST-Fe minimal medium, comprising glycerol, alanine, salts, iron, and Tween80, but not in the standard Middlebrook 7H9 albumin-dextrose-catalase (ADC) medium. This difference may point to the binding of the compound by albumin [22], interference of catalase in the MOA, or an MOA that has an impact on the ability of the bacillus to use glycerol as the primary carbon source [32]. In contrast, the activities of compounds **7** and **14** were much more pronounced in standard 7H9-ADC, while compounds **3**, **11**, and **15** showed comparable potencies in both media types.

An interesting observation pertaining to the structures of the compounds versus the observed antimycobacterial activity was the differences in MIC for the structurally similar compound **1**, an oxapentacycloundecane benzyl amine derivative, and the azapentacycloundecane benzyl amine derivative, compound **5**.

TABLE 1: Antimycobacterial activity and cytotoxicity data.

Compound	MIC ₉₉ 7H9-ADC	IC ₅₀ CHO	GAST-Fe
1 [23]	>125	>125	>10 [#]
2 [24]	>125	>125	>322
3 [19]	82.20	82.8	119.00
4 [23]	>125	>125	>254
5 [23]	125	80.9	84.80
6 [23]	125	>125	>254
7 [18]	68.70	>125	9.54
8 [25]	>125	>125	Nd
9 [26]	>125	>125	>414
10 [26]	>125	>125	>349
11 [27]	50.00	42.8	7.40
12 [26]	>125	>125	>386
13 [28]	>125	>125	>100 ⁺
14 [25]	9.60	18.8	8.01
15 [25]	13.90	15.2	8.20
16	>125	>125	>100 ⁺
Rifampicin	0.0149	0.0274	Nd
Emetine	Nd	nd	0.061

TB : MIC₉₉ 7H9 (μM) in *M. tuberculosis* H37Rv: *gfp*.

TB : MIC₉₉ GAST-Fe (μM) in *M. tuberculosis* H37Rv: *gfp*.

CHO: Chinese hamster ovarian cell

IC₅₀ (μM) as indication of cytotoxicity [18, 19].

nd: not determined.

#highest concentration measured.

⁺CellTiter-Glo[®] luminescent cell viability assay [28].

Results point towards antimycobacterial activity being linked to the presence of the tertiary amine and/or free hydroxyl group within the polycyclic aza-cage. Compounds **11**, **14**, and **15** containing an adamantane moiety showed better activity compared to oxa- and aza-PCU-based compounds in general. These are also the only 3 compounds containing the 1,3-diamine linker *versus* the 1,2-diamine present in compounds **3**, **6**, and **7**. This increased activity could, therefore, be due to the presence of the adamantane or the 1,3-diamine linker. Comparable activity (Figure 2) seen in compounds **2** (oxa- PCU) and **10** (adamantane derivative), however, suggest that the increased activity may be linked to the 1,3-diamine linker rather than the presence of the adamantane moiety.

2.2 Cytotoxicity Analysis.

Cytotoxicity of the compounds was evaluated using a Chinese hamster ovarian (CHO) cell line (Table 1). The marked cytotoxicity differences observed between compounds **3** and **11** were noteworthy. The adamantane moiety may contribute to increased cytotoxicity, but, as can be deduced from the similar IC₅₀ values of compounds **2** and **10**, it appears that this molecular feature cannot be solely responsible for the increased cytotoxicity observed for compound **11**. The propane-1,3-diamine

linker, however, seems to contribute to cytotoxicity as compounds **11**, **14**, and **15** all demonstrate significantly higher cytotoxicity, even when compared to most compounds containing the similar ethane-1,2-diamine moiety. The 1,3-diamine linker unfortunately also seems to play a role in antimycobacterial activity as these compounds demonstrate the lowest overall MIC values.

2.3 Preliminary Mechanism of Action Determination.

To explore the potential MOA of the compounds, a number of bioactivity reporter assays were utilized. To evaluate the possible impact of the compounds on respiration, comparative MIC values were determined for the respective compounds in wild-type *M. tuberculosis* H37Rv vs. (i) a cytochrome *bd* oxidase deficient mutant (Δ *cydKO*) and (ii) a Δ *cydKO/qcrBA317T* strain to determine possible QcrB inhibition [33, 34]. QcrB inhibitors are expected to exhibit increased potency (lower MIC) in the Δ *cydKO* but minimal activity in the Δ *cydKO/qcrBA317T* strain which carries an additional Ala317Thr point mutation in QcrB [35]. No significant shift in MIC was observed for any of the compounds against either of the mutant strains, strongly suggesting that none was likely to target QcrB [34, 36].

Next, a real-time bioluminescence assay [37] was used to investigate cell wall damage as a potential mechanism of action. Compounds with inhibitory effects on mycobacterial arabinogalactan, mycolic acid, and fatty acid synthesis have been shown to result in the upregulation of the *iniBAC* operon [38]. This operon is, however, not upregulated by other cell wall stressors, for example, exposure to hydrogen peroxide, heat, acidic conditions, or antibiotics that do not directly inhibit cell wall synthesis (e.g., aminoglycosides, fluoroquinolones, or rifampins) [38]. Compounds **14** and **15** were *PiniB*-LUX positive and showed early (day 1) and sustained luminescence signals, similar to the luminescence profile which was observed previously for ethambutol [37]. Figure 2 provides an example of bioluminescence observed for late and indirect cell wall damage (compound **11**), early cell wall damage (compound **15**), and the positive control SQ109 (also demonstrating early cell wall damage). Comparative background-corrected RLU data are presented as heat maps, ranging from white (minimum) to orange (maximum) as a function of the maximum RLU recorded for luminescence control. Given the presence of the adamantane and amine linker functional groups in SQ109 [39], it was decided to use SQ109 as a control compound in the *PiniB*-LUX assay. SQ109 also demonstrated early luminescence, but the signal was only sustained for approximately 5 days [37], whereas in the current study, a continued signal was observed for compounds **14** and **15** over the course of the 14-day assay. Compounds **3**, **7**, and **11** were associated with delayed production of bioluminescence. This suggests that the impact on cell wall homeostasis might be delayed or a secondary effect of a compound with polypharmacologic activity. These data suggest that compounds **14** and **15** directly target cell wall biosynthesis, although the precise target is still unknown.

Finally, we investigated whether any of the compounds were genotoxic using the *PrecA*-LUX bioluminescence reporter [37]. RecA is a key regulator of mycobacterial DNA damage response and is induced after the exposure to compounds which are directly genotoxic (i.e., altering or damaging to the nucleic acid) or which inhibit DNA metabolism (replication and/or repair). Placing the bacterial luciferase *luxCABE* cassette under the transcriptional control of the *recA* promoter results in increased bioluminescence following promoter induction in response to DNA damage [37]. None of the compounds evaluated in this study produced a positive luminescence signal over the full duration of the assay, eliminating DNA damage as potential MOA.

Compound 11 (μM)					Compound 15 (μM)				SQ109 (μM)					
15.62 31.25 62.5 125.0					7.8 15.62 31.25 62.5				0.08 0.156 0.312 0.625					
D1	0	0	0	0	D1	40	25	19	137	D1	2	0	45	76
D2	0	0	1	0	D2	207	746	339	21	D2	0	6	733	651
D3	0	0	0	0	D3	1010	2454	151	0	D3	56	247	1009	1106
D5	13	836	1034	0	D5	504	3470	0	0	D5	64	72	139	1041
D7	0	840	1214	0	D7	0	3705	0	0	D7	0	0	34	79

Figure 2: Observed luminescence data of compounds **11**, **15**, and SQ109 depicting cell wall damage over 7 days (D1–D7) at various concentration ranges (μM) spanning the MIC₉₀ (as indicated by the red dotted line).

2.4 Synergism Evaluations.

It was originally postulated that compounds from this series might act as mycobacterial efflux pump inhibitors (EPIs). As an initial screen to determine possible EPI activity, synergism assays were performed using the known Rv1258c efflux pump substrate, spectinomycin, as an anchor compound. Spectinomycin is an aminocyclitol antibiotic with a unique binding site on the bacterial 30S ribosomal subunit which affords it selective toxicity and a good side effect profile. Unfortunately, mainly due to extensive efflux by bacterial efflux pumps (specifically Rv1258c in *M. tuberculosis*), spectinomycin lacks significant antibacterial activity [15, 40, 41]. The activity of spectinomycin is increased substantially under conditions where efflux pump activity is inhibited [42] making it a useful agent to screen for possible efflux pump inhibitory activity using synergism assays. All compounds apart from compounds **14** and **15**, which were excluded due to inherent antimycobacterial activity, were screened for synergism with spectinomycin using a checkerboard assay. To this end, serial dilutions of the test compound and spectinomycin were added to an *M. tuberculosis* culture in 7H9 media on the y- and x-axis of a 96-well plate. Bacterial growth was measured, and data were analysed as described [43]. Compounds **5** and **6** showed evidence of synergism with spectinomycin, but no significant changes in MIC were observed with any of the other compounds. Inhibition of bacterial growth for compounds **1**, **5**, and **6** in combination with spectinomycin is shown in Figure 3.

The concentration of spectinomycin as a fraction of its MIC (i.e., 2 = 2 MIC, 1 = MIC, 0.5 = half MIC etc.) is given on the x-axis, combined with various fractions of the MIC of the test compound as indicated by the colours in the graph legend. The bacterial inhibition as measured in the spectinomycin-only wells at various multiples of spectinomycin MIC is depicted as the dark red (top) legend on the graph. If spectinomycin is combined with a test compound with which it synergizes, the percentage bacterial inhibition remains high despite decreases in spectinomycin concentration. Thus, compound **1** (A) which is provided for purposes of comparison with structurally similar compound **5** shows no evidence of synergism, but bacterial inhibition at lower concentrations of spectinomycin when combined with compounds **5** (B) and **6** (C) point to synergistic activity.

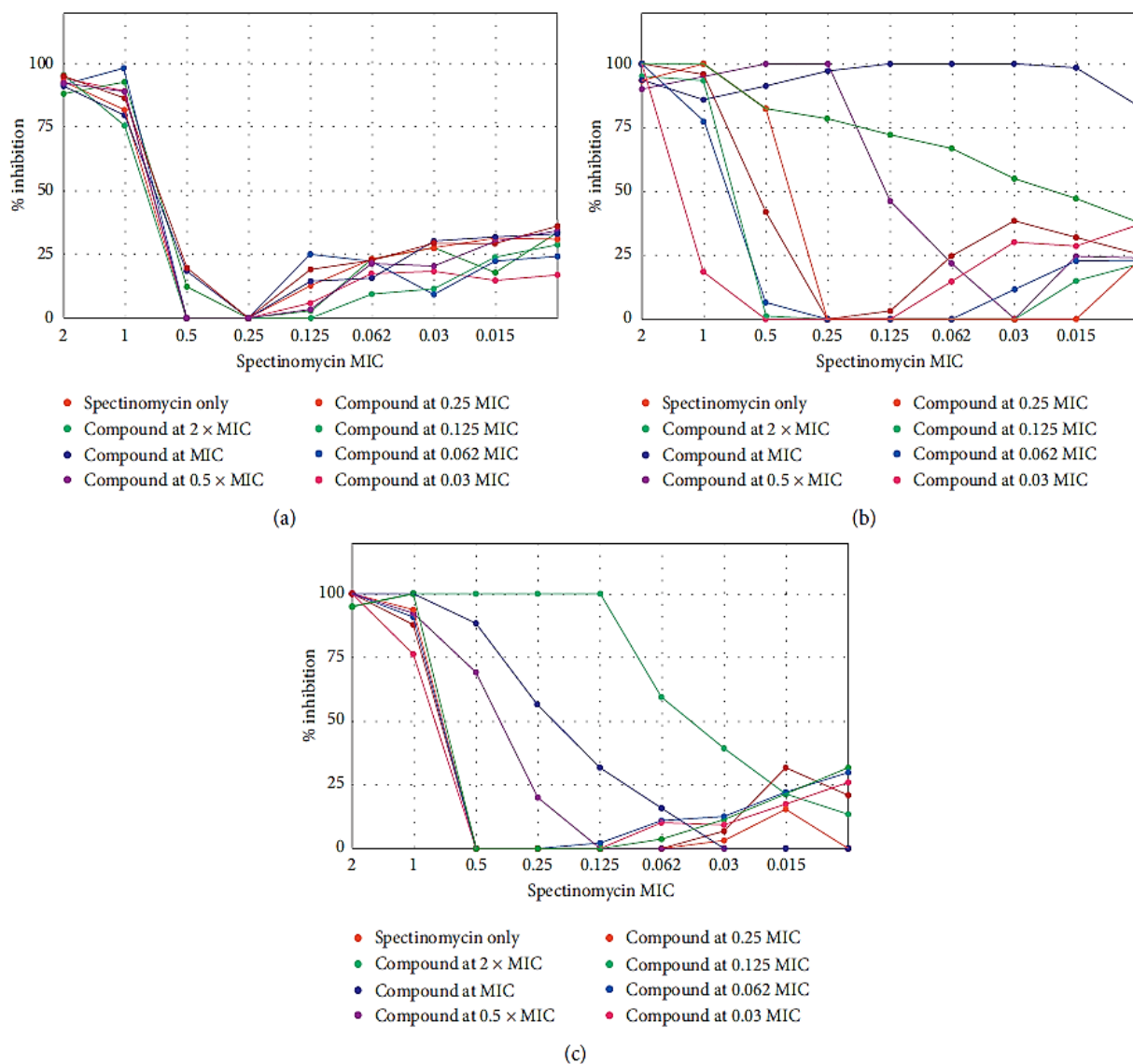


Figure 3: Percentage inhibition of compound **1** (a), **5** (b), and **6** (c) at various concentration combination points where the concentration of spectinomycin (as a function of MIC) is indicated on the x-axis combined with multiples of the MIC of the test compound as indicated by the colours in the legend.

Both compound **5** and **6** are aza-cage derivatives. Again, the differences between the activity of the structurally similar compounds **1** and **5** (Figure 1) are notable. Similar to what was seen with the antimycobacterial activity of these two compounds, the tertiary nitrogen and free hydroxyl group on the aza-cage are likely involved in the observed synergistic activity. Compounds **3** and **7**, contrariwise, appeared to increase the MIC of spectinomycin at higher concentrations (data not shown). This observation might point to reduced absorption of spectinomycin but would require further investigation to determine the mechanism of this possible antagonism.

3. Conclusions

In this study, we explored possible antimycobacterial activity, mechanism of action, and synergistic activity of a series of polycyclic amine derivatives. The compounds were selected based on the presence of pharmacophoric moieties with possible antimycobacterial activity, previously described resistance reversal activity, as well as for the presence of structural features and bioactivity that may increase the accumulation of active moieties and coadministered anti-mycobacterial drugs within *M. tuberculosis*. The most active compound (**15**) demonstrated an MIC₉₉ of 9.6 μ M against *M. tuberculosis* H37Rv and will serve as a lead compound to improve selective antimycobacterial activity.

Inhibition of the *b_{C1}* respiratory complex and DNA functionality as MOA as well as genotoxicity were excluded for the series. Cell wall damage, however, was identified as the likely mechanism of action of a number of compounds. Particularly, compounds **14** and **15** were shown to cause early and sustained cell wall damage in a fashion similar to ethambutol. Compounds **3**, **7**, and **11** showed delayed cell wall damage which may indicate cell wall stress as a secondary effect to interference with other cell systems or a delayed effect on cell wall integrity.

Compounds **5** and **6** showed evidence of synergistic activity with spectinomycin and thus possible efflux pump (specifically Rv1258c) inhibition. The azapentacycloundecane cage seems to play a role in the antimycobacterial activity in nutrient poor media as well as the ability to synergize with spectinomycin as is evident from the large variances between the structurally similar compounds **1** and **5** in the respective assays. The role of the aza-cage in antimycobacterial and synergistic activity thus warrants further exploration.

Although compounds from this series do not display sufficiently selective toxicity in single-drug *in vitro* assays, the ability of selected compounds from this series to act as chemosensitizers, may reduce the required MIC in combination therapy. Results from this preliminary study have contributed to our understanding of the structure activity relationships, possible synergistic activity, and toxicity for this series of compounds and will be used in conjunction with ongoing synergism assays to inform lead modification. Additional work exploring structure activity relationships for antimycobacterial activity (versus cytotoxicity) and, importantly, investigations pertaining to possible resistance reversal activity are underway in our laboratories.

4. Materials and Methodology

4.1 Minimum Inhibitory Concentration Determination. All assays were performed in a Biosafety Level III certified facility. *Mycobacterium tuberculosis* pMSp12:GFP [29, 44] was grown to an optical density (OD) of 0.6–0.7, and assays were performed using either GAST-Fe media [45, 46] or 7H9 media supplemented with 10% Albumin Dextrose Catalase (ADC) [45, 46]. 10 mM stock solutions of the test compounds in DMSO were serially diluted 2-fold, and plates were set up as previously described [47]. Rifampicin at 2xMIC was used as a minimum growth control. Relative fluorescence was measured and used to calculate the MIC as previously reported [22, 48].

4.2 Cytotoxicity Analysis.

The reduction of 3-[4,5-dimethylthiazol-2-yl]-2,5-diphenyl tetrazolium bromide (MTT) in the presence of living cells was used to evaluate cell viability [49]. 20 mg/mL stock solutions of the test compounds in 10% DMSO were serially diluted in a complete medium with 10-fold dilutions to obtain 6 concentrations. Cells were exposed to the respective test compounds for 44 hours after which MTT was added and cells were incubated at 37°C for a further 4 hours. Plates were analysed at 540 nm using a spectrophotometer with wells containing untreated cells and growth medium only used to determine 100% survival and 0% survival, respectively. Emetine was used as a positive control, and assays were performed in triplicate. Cell viability was not compromised at the highest concentration of DMSO to which the cells were exposed (data not shown). IC₅₀ values were obtained from full dose-response curves, using a nonlinear dose-response curve fitting analysis via GraphPad Prism v.4 software.

4.3 Respiratory Reporter Assay.

Mycobacterium tuberculosis H37Rv Δ cydKO and *Mycobacterium tuberculosis* H37Rv Δ cydKO/QcrBA317T [34, 35] were utilized as described above for the determination of the minimum inhibitory concentration (Section 4.1).

4.4 LUX Assays.

A modified bioluminescence (LUX) reporter assay was used to investigate cell wall damage and genotoxicity as possible mechanisms of action [37]. A 10 ml culture of the relevant *Mycobacterium tuberculosis* H37Rv strain (PiniB-LUX determining cell wall damage or PrecA- LUX determining DNA damage) was grown to an optical density (OD₆₀₀) of ± 0.4 . The strain culture was diluted 1 : 10 prior to inoculation of the assay. Two-fold serial dilutions of the test compounds and the assay control drugs were prepared in flat-bottomed 96-well microtiter plates. The relevant diluted *M. tuberculosis* reporter culture was added to each well to a final volume of 100 μ l per well. SQ109 and levofloxacin were used as a positive and negative control, respectively, in the PiniB-LUX assay, whereas levofloxacin and ethambutol were utilized as positive and negative control, respectively, in the PrecA-LUX assay.

Raw luminescent data (Relative Luminescence Units) were acquired using a SpectraMax i3x Plate reader (Molecular Devices Corporation, 1311 Orleans Drive, Sunnyvale, California 94089). Data were corrected for background luminescence using Softmax Pro 6 software (Version 6.5.1, Serial no. 1278552768867612530), Molecular Devices Corporation, 1311 Orleans Drive, Sunnyvale, California 94089. Data were converted to 2-colour 2-dimensional heat maps using Microsoft® Excel® for Mac2011, Version 14.6.5 (160527), latest installed update 14.6.5.

4.5 Synergism Assays.

Possible drug interactions of the various test compounds and spectinomycin were investigated utilizing a slightly modified standard two-dimensional (2D) checkerboard assay [42]. Serially diluted drugs were dispensed along the x-axis and y-axis of 96-well microtiter plates, respectively, at a starting concentration 100 times the final concentration. The assays were performed as previously described

[42], and results were reported as a percentage growth inhibition at various drug concentration combinations.

Data Availability

Data are available on request from the corresponding author through e-mail (ekapp@uwc.ac.za).

Conflicts of Interest

The authors declare no conflicts of interest.

Acknowledgments

The authors thank the National Research Foundation of South Africa for providing financial support for this project (grant no. 117887). SLS received funding from the South African Research Chairs Initiative of the Department of Science and Technology and National Research Foundation (NRF) of South Africa, (award no. UID 86539). This project was also supported through the Strategic Health Innovation Partnerships (SHIP) Unit of the South African Medical Research Council with funds received from the South African Department of Science Innovation. The content is solely the responsibility of the authors and does not necessarily represent the official views of the NRF.

References

1. M. Viveiros, M. Martins, L. Rodrigues et al., "Inhibitors of Mycobacterial efflux pumps as potential boosters for anti-tubercular drugs," *Expert Review of Anti-Infective Therapy*, vol. 10, pp. 983–998, 2012.
2. J. P. Sarathy, V. Dartois, and E. J. D. Lee, "The role of transport mechanisms in Mycobacterium tuberculosis drug resistance and tolerance," *Pharmaceuticals*, vol. 5, no. 11, pp. 1210–1235, 2012.
3. P. E. da Silva, A. V. Groll, A. Martin, and J. C. Palomino, "Efflux as a mechanism for drug resistance in Mycobacterium tuberculosis," *FEMS Immunology and Medical Microbiology*, vol. 63, no. 1, pp. 1–9, 2011.
4. S. M. Batt, C. E. Burke, A. R. Moorey, and G. S. Besra, "Antibiotics and resistance: the two-sided coin of the mycobacterial cell wall," *Cell Surface*, vol. 6, Article ID 100044, 2020.
5. K. Tahlan, R. Wilson, D. B. Kastinsky et al., "SQ109 targets MmpL3, a membrane transporter of trehalose monomycolate involved in mycolic acid donation to the cell wall core of Mycobacterium tuberculosis," *Antimicrobial Agents and Chemotherapy*, vol. 56, no. 4, pp. 1797–1809, 2012.
6. K. Hards, J. R. Robson, M. Berney et al., "Bactericidal mode of action of Bedaquiline," *Journal of Antimicrobial Chemotherapy*, vol. 70, no. 7, pp. 2028–2037, 2015.
7. J. Zheng, E. J. Rubin, P. Bifani et al., "Para-aminosalicylic acid is a prodrug targeting dihydrofolate reductase in Mycobacterium tuberculosis," *Journal of Biological Chemistry*, vol. 288, no. 32, pp. 23447–23456, 2013.
8. S. Chakraborty, T. Gruber, C. E. B. 3rd, H. I. Boshoff, and K. Y. Rhee, "Para-aminosalicylic acid acts as an alternative substrate of folate metabolism in Mycobacterium tuberculosis," *Science*, vol. 339, no. 6115, pp. 88–91, 2013.

9. S. Chetty, M. Ramesh, A. Singh-Pillay, and M. E. S. Soliman, "Recent advancements in the development of anti-tuberculosis drugs," *Bioorganic and Medicinal Chemistry Letters*, vol. 27, no. 3, pp. 370–386, 2017.
10. V. Dartois, "The path of anti-tuberculosis drugs: from blood to lesions to mycobacterial cells," *Nature Reviews Microbiology*, vol. 12, no. 3, pp. 159–167, 2014.
11. S. M. Gygli, S. Borrell, A. Trauner, and S. Gagneux, "Anti-microbial resistance in Mycobacterium tuberculosis: mechanistic and evolutionary perspectives," *FEMS Microbiology Reviews*, Oxford University Press, vol. 41, , pp. 354–373, 2017.
12. L. H. M. Te Brake, G. J. De Knecht, J. E. De Steenwinkel et al., "The role of efflux pumps in tuberculosis treatment and their promise as a target in drug development: unraveling the black box," *Annual Review of Pharmacology and toxicology*, vol. 58, pp. 271–291, 2018.
13. D. Fange, K. Nilsson, T. Tenson, and M. Ehrenberg, "Drug efflux pump deficiency and drug target resistance masking in growing bacteria," *Proceedings of the National Academy of Sciences of the United States of America*, vol. 106, no. 20, pp. 8215–8220, 2009.
14. F. P. Rodriguez-Rivera, X. Zhou, J. A. Theriot, and C. R. Bertozzi, "Visualization of Mycobacterial membrane dynamics in live cells," *Journal of the American Chemical Society*, vol. 139, no. 9, pp. 3488–3495, 2017.
15. R. E. Lee, J. G. Hurdle, J. Liu et al., "Spectinamides: a new class of semisynthetic antituberculosis agents that overcome native drug efflux," *Nature Medicine*, vol. 20, no. 2, pp. 152–158, 2014.
16. J. Jang, R. Kim, M. Woo et al., "Efflux attenuates the anti- bacterial activity of Q203 in Mycobacterium tuberculosis," *Antimicrobial Agents and Chemotherapy*, vol. 61, no. 7, 2017.
17. J. Joubert, W. J. Geldenhuys, C. J. der Schyf et al., "Polycyclic cage structures as lipophilic scaffolds for neuroactive drugs," *ChemMedChem*, vol. 7, no. 3, pp. 375–384, 2012.
18. J. Joubert, E. E. Fortuin, D. Taylor, P. J. Smith, and S. F. Malan, "Pentacycloundecylamines and conjugates thereof as chemosensitizers and reversed chloroquine agents," *Bioorganic and Medicinal Chemistry Letters*, vol. 24, no. 23, pp. 5516– 5519, 2014.
19. J. Joubert, E. Kapp, D. Taylor, P. J. J. Smith, and S. F. F. Malan, "Polycyclic amines as chloroquine resistance modulating agents in plasmodium falciparum," *Bioorganic and Medicinal Chemistry Letters*, vol. 26, no. 4, pp. 1151–1155, 2016.
20. E. Grobler, A. Grobler, C. J. der Schyf, and S. F. Malan, "Effect of polycyclic cage amines on the transmembrane potential of neuronal cells," *Bioorganic and Medicinal Chemistry*, vol. 14, no. 4, pp. 1176–1181, 2006.
21. E. Kapp, S. F. Malan, J. Joubert, and S. L. Sampson, "Small molecule efflux pump inhibitors in Mycobacterium tuberculosis: a rational drug design perspective," *Mini Reviews in Medicinal Chemistry*, vol. 18, no. 1, pp. 72–86, 2018.
22. E. Kapp, H. Visser, S. L. Sampson et al., "Versatility of 7- substituted coumarin molecules as antimycobacterial agents, neuronal enzyme inhibitors and neuroprotective agents," *Molecules*, vol. 22, no. 10, 2017.
23. J. Joubert, R. Sharma, M. Onani, and S. F. Malan, "Microwave- assisted methods for the synthesis of pentacyclo [5.4.0.02,6.03,10.05,9]Undecylamines," *Tetrahedron Letters*, vol. 54, no. 50, pp. 6923–6927, 2013.
24. S. F. Malan, J. V. der Walt, and C. V. der Schyf, "Structure- activity relationships of polycyclic amines with calcium channel blocking activity," *Archiv der Pharmazie*, vol. 333, pp. 10–16, 2000.

25. H.J. Lemmer, J. Joubert, S. van Dyk, F.H. van der Westhuizen, and S. F. Malan, "S-nitrosylation and attenuation of excessive calcium flux by pentacycloundecane derivatives," *Medicinal Chemistry*, vol. 8, no. 3, pp. 361–371, 2012.
26. Y. E. Kadernani, F. T. Zindo, E. Kapp, S. F. Malan, and J. Joubert, "Adamantane amine derivatives as dual acting NMDA receptor and voltage-gated calcium channel inhibitors for neuroprotection," *Medchemcomm*, vol. 5, no. 11, pp. 1678–1684, 2014.
27. J. Joubert, S. van Dyk, I. R. Green, and S. F. Malan, "Synthesis and evaluation of fluorescent heterocyclic aminoadamantanes as multifunctional neuroprotective agents," *Bioorganic and Medicinal Chemistry*, vol. 19, no. 13, pp. 3935–3944, 2011.
28. E. B. Foxen, *Novel Cinnamic-Adamantane Conjugates as Potential Anti-denque and Anti-malaria Agents*, 2012.
29. G. L. Abrahams, A. Kumar, S. Savvi et al., "Pathway-selective sensitization of Mycobacterium tuberculosis for target-based whole-cell screening," *Chemistry and Biology*, vol. 19, no. 7, pp. 844–854, 2012.
30. C. Changsen, S. G. Franzblau, and P. Palittapongarnpim, "Improved green fluorescent protein reporter gene-based microplate screening for antituberculosis compounds by utilizing an acetamidase promoter," *Antimicrobial Agents and Chemotherapy*, vol. 47, no. 12, pp. 3682–3687, 2003.
31. S. G. Franzblau, R. S. Witzig, J. C. McLaughlin et al., "Rapid, low-technology MIC determination with clinical Mycobacterium tuberculosis isolates by using the microplate Alamar blue assay," *Journal of Clinical Microbiology*, vol. 36, no. 2, pp. 362–366, 1998.
32. K. Pethe, P. C. Sequeira, S. Agarwalla et al., "A chemical genetic screen in Mycobacterium tuberculosis identifies carbon-source-dependent growth inhibitors devoid of in vivo efficacy," *Nature Communications*, vol. 1, p. 57, 2010.
33. Moosa, D. A. Lamprecht, K. Arora et al., "Susceptibility of Mycobacterium tuberculosis cytochrome bd oxidase mutants to compounds targeting the terminal respiratory oxidase, cytochrome c," *Antimicrobial Agents and Chemotherapy*, vol. 61, no. 10, 2017.
34. K. Arora, B. Ochoa-Montaña, P. S. Tsang et al., "Respiratory flexibility in response to inhibition of cytochrome c oxidase in Mycobacterium tuberculosis," *Antimicrobial Agents and Chemotherapy*, vol. 58, no. 11, pp. 6962–6965, 2014.
35. R. Van Der Westhuyzen, S. Winks, C. R. Wilson et al., "Pyrrolo[3,4-c]Pyridine-1,3(2H)-Diones: a novel anti-mycobacterial class targeting mycobacterial respiration," *Journal of Medicinal Chemistry*, vol. 58, no. 23, pp. 9371–9381, 2015.
36. N. P. Kalia, E. J. Hasenoehrl, N. B. A. Rahman et al., "Exploiting the synthetic lethality between terminal respiratory oxidases to kill Mycobacterium tuberculosis and clear host infection," *Proceedings of the National Academy of Sciences of the United States of America*, vol. 114, no. 28, pp. 7426–7431, 2017.
37. K. Naran, A. Moosa, C. E. Barry, H. I. M. Boshoff, V. Mizrahi, and D. F. Warner, "Bioluminescent reporters for rapid mechanism of action assessment in tuberculosis drug discovery," *Antimicrobial Agents and Chemotherapy*, vol. 60, no. 11, pp. 6748–6757, 2016.
38. D. Alland, A. J. Steyn, T. Weisbrod, K. Aldrich, and W. R. Jacobs, "Characterization of the Mycobacterium tuberculosis IniBAC promoter, a promoter that responds to cell wall biosynthesis inhibition," *Journal of Bacteriology*, vol. 182, no. 7, pp. 1802–1811, 2000.
39. M. Protopopova, C. Hanrahan, B. Nikonenko et al., "Identification of a new antitubercular drug candidate, SQ109, from a combinatorial library of 1,2-ethylenediamines," *Journal of*

- Antimicrobial Chemotherapy*, vol. 56, no. 5, pp. 968–974, 2005, [pii].
40. M. Balganes, N. Dinesh, S. Sharma, S. Kurupath, A. V. Nair, and U. Sharma, "Efflux pumps of Mycobacterium tuberculosis play a significant role in antituberculosis activity of potential drug candidates," *Antimicrobial Agents and Chemotherapy*, vol. 56, no. 5, pp. 2643–2651, 2012, [pii].
 41. J. Liu, D. F. Bruhn, R. B. Lee et al., "Structure-activity relationships of spectinamide antituberculosis agents: a dissection of ribosomal inhibition and native efflux avoidance contributions," *ACS Infectious Diseases*, vol. 3, no. 1, pp. 72–88, 2017.
 42. Omollo, V. Singh, E. Kigundu et al., "Developing synergistic drug combinations to restore antibiotic sensitivity in drug-resistant Mycobacterium Tuberculosis," *Antimicrobial Agents and Chemotherapy*, vol. 65, no. 5, Article ID 860288, 2021.
 43. K. Singh, M. Kumar, E. Pavadai et al., "Synthesis of new verapamil analogues and their evaluation in combination with rifampicin against Mycobacterium tuberculosis and molecular docking studies in the binding site of efflux protein Rv1258c," *Bioorganic and Medicinal Chemistry Letters*, vol. 24, no. 14, pp. 2985–2990, 2014.
 44. L. A. Collins, M. N. Torrero, and S. G. Franzblau, "Green fluorescent protein reporter microplate Assay for high- throughput screening of compounds against Mycobacterium tuberculosis," *Antimicrobial Agents and Chemotherapy*, vol. 42, no. 2, pp. 344–347, 1998.
 45. J. J. De Voss, K. Rutter, B. G. Schroeder, H. Su, Y. Zhu, and E. Barry, "The salicylate-derived mycobactin siderophores of Mycobacterium tuberculosis are essential for growth in macrophages," *Proceedings of the National Academy of Sciences of the United States of America*, vol. 97, no. 3, pp. 1252–1257, 2000.
 46. S. G. Franzblau, M. A. Degroote, S. H. Cho et al., "Comprehensive analysis of methods used for the evaluation of compounds against Mycobacterium Tuberculosis," *Tuberculosis*, vol. 92, no. 6, pp. 453–488, 2012.
 47. J. Ollinger, M. A. Bailey, G. C. Moraski et al., "A dual read-out assay to evaluate the potency of compounds active against Mycobacterium tuberculosis," *PLoS One*, vol. 8, no. 4, 2013.
 48. Collaborative Drug Discovery Inc. (CDD), "Collaborative drug discovery," Home—Collaborative Drug Discovery Inc. (CDD), 2020, <https://www.collaborativedrug.com/de/>.
 49. T. Mosmann, "Rapid colorimetric assay for cellular growth and survival: application to proliferation and cytotoxicity assays," *Journal of Immunological Methods*, vol. 65, no. 1–2, pp. 55–63, 1983.

Chapter 7: Conclusion and Future Outlook

The goal of this research study was to investigate the use of the polycyclic derivatives, available in the Drug Design compound library, as resistance modulators in *Mycobacterium tuberculosis* (Mtb). In parallel to this, the possibility of rational drug design of small molecule efflux pump inhibitors was also explored. The first phase included screening of the complete compound library for antimycobacterial activity. In conjunction to this, selected compounds were screened for synergistic activity with antimycobacterial substances which are known efflux pump substrates. A number of compounds from the screened library demonstrated promising antimycobacterial activity and/or synergistic activity that warranted further investigation. The compounds of interest were further explored through mechanism of action studies supplemented with *in silico* modelling to gain insight on the binding site interactions.

Adamantane-amide derivatives as MmpL3 inhibitors: The most promising compound identified in the initial screen, an adamantyl-amide derivative (**C1**) with a 0.244 μM MIC₉₀, was found to be a likely MmpL3 inhibitor. MmpL3 is a protein essential for mycobacterial survival and a very promising drug target. MmpL3 activity has been confirmed for a number of adamantyl derivatives including SQ109 which is currently in phase 2 clinical trials. Unfortunately, SQ109 has low oral bioavailability. This is likely linked to metabolism by the prominent CYP450 enzymes, CYP2D6 and CYP219 which both target the 2'-amine of the 1,2-diamine linker. **C1** however contains a unique amide linker rather than an ethylene diamine in its side chain which could be explored to develop metabolically stable drug ligands. *In silico* mutagenesis studies were used to gain insight into why the prominent mutation, Phe644Leu, observed in the *in vitro* assays reduce Mtb susceptibility to **C1**. It was observed that the mutation changes the orientation of **C1** within the binding pocket and decreases the binding affinity of the adamantyl moiety in the mutated MmpL3 protein. The mutation also decreases the solvation energy of the protein which would likely reduce its ability to interact with ligand molecules. The Phe644Leu mutation in MmpL3 affects the efficacy of a number of MmpL3 inhibitors including SQ109.

The knowledge gained on the influence of the mutation on the protein and its binding interaction with putative inhibitors can be used to design compounds which are not influenced by the Phe644Leu mutation. From the molecular interactions observed for **C1** in both the wild type and mutant proteins, it seems that the amide functional group is able to interact with an aspartic acid amino acid in the binding pocket of MmpL3. The **C1** amide oxygen also shows an additional interaction with Tyr646 in the mutant protein resulting in the observed change in orientation of the compound. This may stabilize the ligand in the binding pocket, but may also prevent the adamantane function from penetrating deep enough into the channel to efficiently interact with the 644 phenylalanine or lysine in the mutant protein. This could be addressed by the addition of lipophilic groups on the adamantane structure (S1 Figure 1) or by introducing additional carbons between the adamantane and amide functional groups (S2 Figure 1). It would also be of value to evaluate compounds where the amide linked side chain length is increased (S3 Figure 1), which could be supplemented by a series of substitutions on the benzyl ring. An alternative approach could be to replace one or both of the amine groups in SQ109 with amide groups and the addition of a second amide structure in **C1** to mimic the 1,2-diamine linker of SQ109 (S4 and S5 Figure 1). The next step in this research would be to use the wild type and mutant proteins to perform molecular docking studies to evaluate the likely interactions of a series of designed

adamantane derivatives. Adamantane derivatives can also be extracted from electronic compound databases and included as part of the screen.

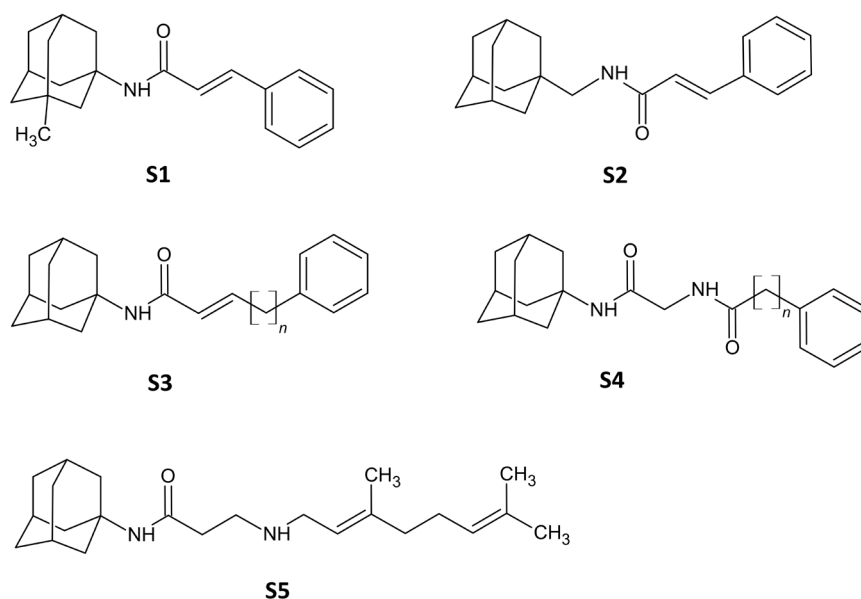


Figure 1: Suggested adamantane-amide derivatives for evaluation as metabolically stable MmpL3 inhibitors.

Identification of coumarin derivatives with selective antimycobacterial activity: The coumarin moiety, which is the common scaffold in the second series of compounds identified in the initial assay, is a well-known privileged scaffold. The challenge with coumarin containing molecules is to limit the off-target activity of the compounds. The first interesting observation from the MIC results of the coumarin based compounds, were the consistently lower MIC values obtained in GAST-Fe nutrient poor media compared to the values observed in standard albumin-dextrose-catalase containing 7H9 OADC nutrient rich media. There are a number of reasons why compounds could have different activity in the 2 media types. GAST-Fe contains, amongst others, glycerol rather than dextrose which forms part of the 7H9 OADC media. This could point to a mechanism of action that targets a function of mycobacteria which is particularly necessary in nutrient poor conditions. We however postulated that the difference in activity may rather be linked to the presence of albumin in the 7H9-OADC media. Coumarins are known to bind strongly to albumin. We therefore evaluated the protein binding of the coumarin compounds and found that they do indeed bind extensively to serum proteins. The protein binding property of coumarin based compounds may have overarching implications for research done on coumarin derivatives. Assays that compare the activity of coumarin derivatives on different cell lines or bacterial strains, may in actual fact only be comparable if the different assay methods contained the same percentage of serum proteins. This would be particularly problematic where results from cytotoxicity assays and activity assays, performed in different media types are used to determine selectivity indexes. It is therefore important to ensure that assay methods are specifically designed to allow for comparability of results across different cell types.

We also identified a number of preliminary structure activity relationships for antimycobacterial activity which point to the possibility of limiting off target effects through selective substitution.

Through utilization of larger substitutions on positions 4 and 7 of the coumarin scaffold, it may be possible to increase antimycobacterial activity and reduce monoamine oxidase (MOA) and choline esterase (AChE) inhibition. Although the exact target of the coumarin derivatives in Mtb is still unknown, follow-up research in our group has identified FadD32 as a possible target. This project can be taken forward through exploring the influence of various larger substitutions on positions 4 and 7, on the FadD32 activity of the coumarin derivatives. As higher lipophilicity seems to promote antimycobacterial activity, increasing the LogP of the designed compounds through the addition of larger lipophilic substitutions should not be a significant limitation. It was further noted that a nitrile substitution on position 3 increased MAO and AChE activity, but had no effect on antimycobacterial activity. The proposed molecules should therefore not be substituted in position 3. Larger substitutions on position 4 decreased neuronal enzyme activity, but increased antimycobacterial activity. Various bulky substitutions on position 4 can thus be explored. Methyl substitutions in positions 5 and 7 or 5 and 6 (A and B Figure 2 respectively) was noted to increase antimycobacterial activity.⁵⁹ Smaller substitutions in these positions should thus be assessed. Larger substitutions on either position 6 or 7, particularly with functional groups capable of forming a hydrogen bond interactions, promoted antimycobacterial activity. A piperazine ring is proposed, as a piperidine ring increased neuronal enzyme activity. A larger lipophilic substitution on the piperazine ring improved antimycobacterial activity. Molecular modelling could be utilized to evaluate the binding of the designed coumarin based compounds in the FadD32 enzyme for which crystal structure of the target protein is available.

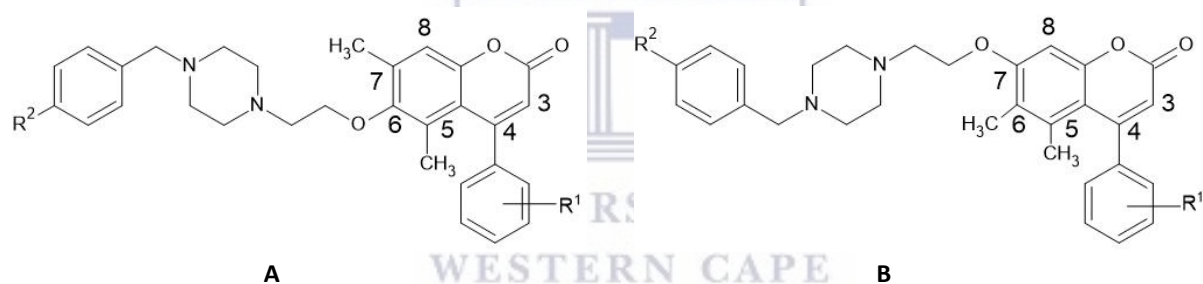


Figure 2: Proposed design for (A) 6- and (B) 7-substituted coumarin derivatives with selective antimycobacterial activity

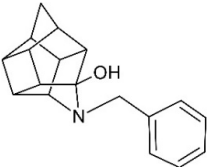
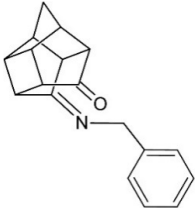
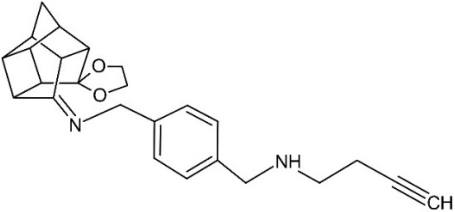
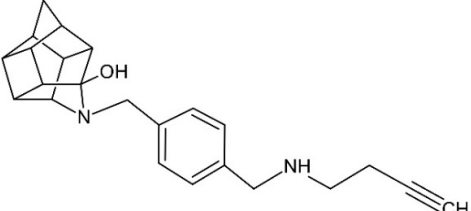
The synergistic activity of aza-cage compounds: In parallel to screening the compound library for antimycobacterial activity, a carefully selected series of compounds was evaluated for synergism with the known efflux pump substrate, spectinomycin. The compounds were selected based on their previously demonstrated biological activity. Verapamil and chlorpromazine, which are often used as reference efflux pump inhibitors in cell-based assays, are known to target L-type calcium channels and NMDA receptors respectively. Compounds within our library with known calcium channel- and NMDA receptor inhibition were thus selected for inclusion in the study. In addition to this, compounds which demonstrated drug resistance reversal activity in malaria parasites were also selected. A series of adamantane derivatives were included to evaluate the possible role of the specific lipophilic scaffold in efflux pump inhibition. An added motivation for inclusion of the adamantane derivatives was the likely role the adamantane moiety may play in MmpL3 inhibition.

During the MIC evaluation of the compounds done in preparation for the synergism assays, a number of the compounds demonstrated interesting antimycobacterial activity. It was decided to explore the

mechanism of action for antimycobacterial activity for the most active compounds in conjunction to the synergism evaluation. The compounds were found to inhibit cell wall synthesis with no genotoxicity or inhibition of the cytochrome *bc₁* respiratory complex was observed. The cell wall synthesis activity for the amantadine based compounds may be linked to the adamantane moiety which has been shown to play a role in MmpL3 activity. The compounds evaluated in this study however maintained their cell wall inhibitory signal over the full period of the assay, similar to what was previously observed for ethambutol, whereas SQ109, the adamantane containing control, only sustained the signal for the first few days of the assay. This may point to a mechanism of action other than MmpL3 inhibition or a polypharmacologic activity.

Synergistic activity was observed specifically for two aza-cage compounds and not for their structurally similar oxa-cage or adamantane-linked derivatives. This scaffold could thus be utilised to design active antimycobacterial compounds which may also synergise with co-administered antimycobacterial agents. A second series of aza-derivatives and other unique polycyclic structures, selected based on the activity found in the initial series, were thus screened for synergistic activity with spectinomycin. Additional aza-cage compounds with synergistic activity were identified and are depicted in table 1.

Table 1: Structures of aza-based compounds with synergistic activity identified in preliminary screening.

	Antimycobacterial activity	Synergism
	Yes (Nutrient poor media only) as reported for C5 in chapter 6	Yes, as reported in chapter 6
	No	Yes (preliminary results)
	No	Yes (preliminary results)
	Yes, 30 μ M MIC (Low level activity in standard and nutrient poor media)	Inconclusive (preliminary results)

As the main objective was to evaluate the synergistic activity of the aza-based compounds, the antimycobacterial mechanism of action was not evaluated. It may however be useful to investigate the mechanism of inhibition for compound 5 to determine the reason for the improved activity in poor media *versus* supplemented media.

Computer aided identification and design of Rv1258c efflux pump inhibitors: While investigations on the activity of the compound library was ongoing, a homology model of the Rv1258c efflux protein was developed. Rational drug design of efflux pump inhibitors is complicated by the absence of crystal structures of the transmembrane mycobacterial efflux pumps. Most studies investigating efflux pump inhibitors use a combination of assay methods to demonstrate likely efflux pump inhibition. These assays include, amongst others, comparison of MIC values, synergism assays with known antimycobacterial agents and knock out mutants of a particular efflux pump. Although the combination of results may point to probable efflux pump inhibition, it is difficult to exclude the involvement of alternate efflux pumps, indirect inhibition of efflux or other mechanisms by which synergistic activity is achieved. Direct inhibition of a particular efflux pump is seldom demonstrated. The complexity of proving conclusive efflux inhibition and the lack of mycobacterial efflux pump crystal structures, prompted the development and utilization of the Rv1258c homology model to identify small molecule inhibitors *in silico*. As part of the homology model validation, a probable binding site was identified through blind docking of a series of putative inhibitors identified in literature. Spectinamide, a derivative of spectinomycin, specifically designed to avoid efflux, was also included in the compound series. Interestingly, all the compounds included in the putative inhibitor series bound to a common area within the efflux pump channel while spectinamide bound to the outside surface of the protein. This may explain its ability to avoid efflux through the Rv1258c efflux pump. A number of amino acid interactions, common to compounds demonstrating high binding affinity within the identified binding site were also identified. This in turn was utilized in a molecular modelling study to identify a series of compounds demonstrating good binding affinity within the efflux pump channel. The methodology and detailed results of the *in silico* screen is described in Annexure 1.

A visual inspection of the predicted binding pose of the compounds within the efflux pump (Figure 3) was done for the top 100 dock scored compounds. A vast majority of the top compounds showed a hydrogen bond interaction between one of its secondary amines and GLU243A as well as general contacts with TRP32A, GLY360A and/or LEU260A, PRO248A and LEU364A.

Structural diversity and druggability of the ranked compounds were reviewed and fifteen compounds that satisfied our selection criteria were purchased for evaluation as putative efflux pump modulators (EPMs). Six compounds were selected for preliminary screenings (Figure 4). Although not generally included in the druggability parameters, compounds with a LogP of higher than 5 but below 7 were included as higher Log P values are common in antimycobacterial compounds currently in clinical use.

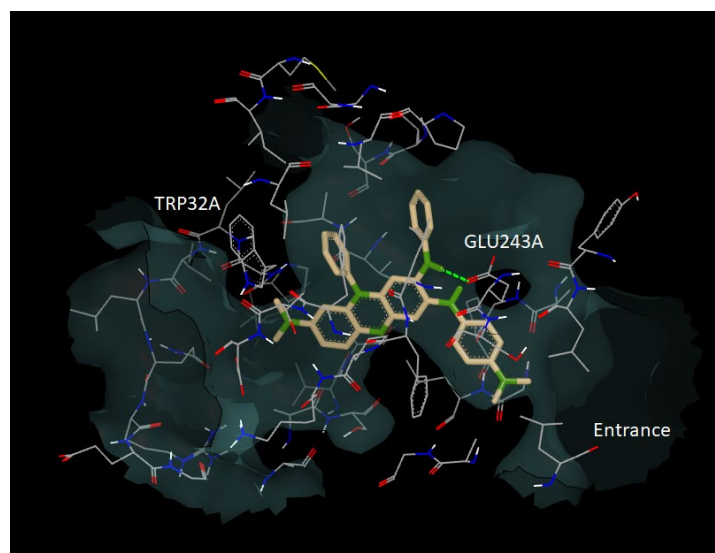


Figure 3: Predicted pose of EPM1 in the Rv1258c binding pocket.

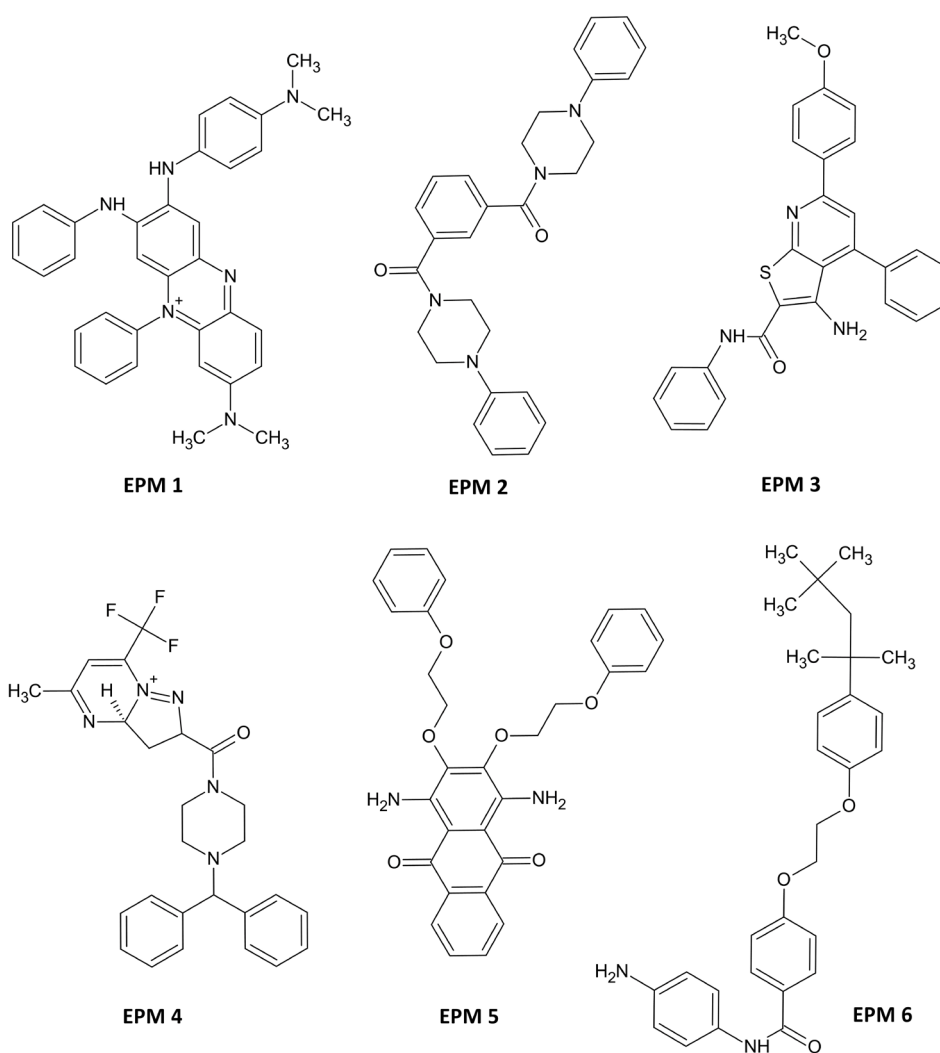


Figure 4: Structures of EPM1 – EPM6

Minimum inhibitory concentrations of the selected compounds were evaluated using standard H37Rv *Mycobacterium tuberculosis* as well as an Rv1258c efflux deficient knock out strain (Δ Rv1258c). The comparable MIC values in the H37Rv and Δ Rv1258c strains (Table 2) are an indication that the compounds do not act as Rv1258c substrates. This is a positive result and it is expected that good binding affinity within the channel, would result in competitive inhibition of efflux, rather than allowing the compound to be extruded by the efflux pump. Cytotoxicity was also evaluated to determine the suitability of the compounds and inform concentrations which can safely be used for the purposes of synergism assays. The next step in this research is to perform synergism assays with the known efflux pump substrate, spectinomycin. The assays will be performed using standard *Mycobacterium tuberculosis* H37Rv as well as the Δ Rv1258c strain. If the mechanism of synergistic activity is indeed inhibition of the Rv1258c efflux pump, compounds that act synergistically with spectinomycin in H37Rv should not show any synergistic activity in Rv1258c efflux deficient strains.

Table 2: MIC₉₀ of potential efflux pump inhibitors in *Mycobacterium tuberculosis*

	MIC ₉₀ (μM): 7D 7H9 GLU CAS Tx			MIC ₉₀ (μM): H37RvMA: 7D 7H9 GLU ADC TW			MIC ₉₀ (μM): Δ Rv1258c 7D 7H9 GLU ADC TW			Cytotoxicity IC ₅₀ (μM) CHO
	7D	7H9	CAS Tx	7D	7H9	GLU ADC TW	7D	7H9	GLU ADC TW	
EPM1	0.448			<0.244			< 0.244			4.24
EPM2	62.5			62.5			62.5			37.4
EPM3	>125			>125			> 125			>50
EPM4	15.625			>125			> 62.5			>50
EPM5	>125			>125			> 125			>50
EPM6	62.5			>125			> 125			21.2
Emetine										0.0735

7D 7H9 GLU CAS Tx: Gaste-Fe minimal medium supplemented with glycerol, alanine, salts, iron, and Tween80.

H37RvMA: 7D 7H9 GLU ADC TW: *Mycobacterium tuberculosis* H37Rv in Middlebrook 7H9 supplemented with albumin, dextrose, and catalase.

Δ Rv1258c 7D 7H9 GLU ADC TW: Efflux deficient *Mycobacterium tuberculosis* in Middlebrook 7H9 supplemented with albumin, dextrose, and catalase.

CHO: Chinese Hamster Ovary cells

In conclusion, steadily rising antimicrobial resistance is a serious public health concern. South Africa and other lower income countries are reporting consistently increasing levels of MDR and XDR TB. Mtb has the ability to limit intracellular accumulation of antimycobacterial compounds by means of an impenetrable cell wall and effective active efflux. In this project, a number of research studies were performed to determine the antimycobacterial and resistance modulating activity of a series of polycyclic compounds with a specific focus on cell wall and efflux pump inhibition. This was supplemented by computer aided design and identification of putative efflux pump inhibitors. Several opportunities for further research pertaining to structural modification of hit compounds were identified. Ongoing studies on the synergism activity of the aza-cage based compounds and novel efflux pump modulators will be used to further explore the use of polycyclic compounds in combination with other antimycobacterial agents. The polycyclic compounds evaluated in this study thus has the potential to address antimycobacterial drug resistance through various mechanisms and the resistance modulating activity of these compounds should be actively explored going forward.

Annexure 1: Identification of putative inhibitors of the *Mycobacterium tuberculosis* Rv1258c efflux pump utilizing *in silico* methods.

This annexure describes the method and preliminary results of identification of putative inhibitors of the Mycobacterium tuberculosis Rv1258c efflux pump utilizing in silico methods.

1. INTRODUCTION

Continuous and rapid development of antimicrobial resistance is a serious global health concern. Drug resistance in *Mycobacterium tuberculosis* (Mtb) is of particular concern in low- and middle-income countries who are reporting steadily increasing levels of multidrug resistant (MDR) tuberculosis.^{1,2} Mtb has the ability to limit intracellular accumulation of antimycobacterial compounds through decreased entry or active efflux. The resulting sub-therapeutic intracellular levels of chemotherapeutic agents complicate the management of TB and contribute to the development of drug resistance.³⁻⁶ Studies have shown that the Mtb expresses a range of efflux pumps that have been implicated in clinically significant drug resistance to various antimycobacterial agents.^{5,7-10}

Rv1258c, a major facilitator superfamily (MFS) type mycobacterial active efflux transporter, has been linked to drug resistance to a number of classes of antimycobacterial and antibiotic agents including rifampicin, isoniazid, pyrazinamide, aminoglycoside antibiotics, fluoroquinolone antibiotics and spectinomides.¹⁰⁻¹² Overexpression of this pump has also been observed in multidrug resistant (MDR) Mtb clinical isolates.¹³

Although studies have identified a number of putative efflux pump inhibitors (EPI), therapeutic use of these compounds is limited by their side effects, toxicity and drug-drug interaction profiles. Various research groups are actively exploring this promising field, but the complexity of demonstrating conclusive inhibition of a particular efflux pump remains a challenge. Most studies investigating efflux pump inhibitors use a combination of assay methods to demonstrate likely efflux pump inhibition. These assays include, amongst others, comparison of minimum inhibitory concentrations, synergism assays with known antimycobacterial agents and knock out mutants of a particular efflux pump. Although the combination of results may point to probable efflux pump inhibition, it is difficult to exclude the involvement of alternate efflux pumps, indirect inhibition of efflux or other mechanisms by which synergistic activity is achieved. Direct inhibition of a particular efflux pump is seldom demonstrated.¹⁴ The complexity of demonstrating conclusive interaction of a putative inhibitor with a particular efflux pump and the lack of crystal structures of efflux proteins in Mtb, makes rational drug design of safe and selective efflux pump inhibitors particularly difficult.

In an effort to further investigate the mechanism of efflux inhibition and promote rational drug design of efflux pump inhibitors, we utilized an accurate three-dimensional (3D) model of Rv1258c previously developed by our group¹⁵ and performed molecular docking studies to identify putative inhibitors of the efflux pump.

2. RESULTS AND DISCUSSION

2.1 Molecular modelling

The Rv1258c model protein was initially prepared in Molecular Operating Environment (MOE, 2020.09 Chemical Computing Group ULC, 1010 Sherbooke St. West, Suite #910, Montreal, QC, Canada, H3A 2R7, 2022) through overlay of clusters modelled with various putative efflux pump inhibitors as described previously.¹⁵ The overlay of the different clusters allowed for the identification of a comprehensive possible binding site within the channel of the efflux protein. The protein was prepared using MOE after which the complex was exported to the OpenEye (OpenEye Scientific Software Inc. Santa Fe, NM. <https://docs.eyesopen.com/applications/oedocking/citation.html> scientific OEDocking application), Make Receptor 4.1.0.1,¹⁶ for further processing.

Make Receptor is a graphical user interface program that allows for the preparation of a protein for use in other OpenEye software applications. After the protein and ligand molecules were selected, the active site box was created around the clustered ligands. The box was visually inspected to ensure that it included all important amino acid residues that were identified during blind docking of the putative efflux pump inhibitors (piperine, verapamil, chlorpromazine) when the homology model was originally created¹⁵. All the previously identified amino acids apart from Glu243 were already included in the automatically created box and the box was therefore manually expanded to include Glu243. The site shape potential was calculated and the shape created with an outer contour of 1692 Å³ which falls well within the suggested volume of 500 to 2000 Å³. Little is known about important protein-ligand interactions within the efflux pump and, as such, no custom constraints were selected to allow for the maximum number of successful docked poses.

Compounds for screening were downloaded from the HitDiscover compound collection from the ThermoFisher scientific platform. Structural comparison of compounds that have been identified as putative efflux pump inhibitors show that these compounds are commonly amphiphilic and contain various amines of which at least one will likely protonate at physiological pH.¹⁴ Only amine containing compounds were therefore selected for screening in this study. The compounds were prepared for docking using Omega 4.1.1.1 software¹⁷ to create 3D conformers of the compounds in preparation for docking using the OE application FRED.¹⁶

Virtual screening of the multiconformer database was performed using FRED 4.0.0.2 docking software and the top 500 compounds, ranked using the Chemgause4 score, were identified. The top 100 dock scored compounds were selected for further binding and interaction analysis using VIDA 4.4.0.4.¹⁶ Compounds were then ranked based on binding affinity score and through visual inspection of the predicted binding pose in the pump. A vast majority of the top compounds showed a hydrogen bond interaction between one of its secondary amines and GLU243A as well as general contacts with TRP32A, GLY360A and/or LEU260A, PRO248A and LEU364A.

Further prioritization considered structural diversity and druggability of the ranked compounds. Fifteen compounds that satisfied our selection criteria were purchased for evaluation as putative efflux pump modulators (EPMs). The selection criteria included compliance with the majority of Lipinski's rules of 5, no long terminal saturated aliphatic chains and no ester linkages to reduce the risk of fast metabolism. Although not generally included in the druggability parameters, compounds with a Log P of higher than 500 but below 600 were included as higher Log P values are common in antimicrobial compounds currently in clinical use.^{18,19}

2.2 Minimum inhibitory concentration

Minimum inhibitory concentrations of the selected compounds in standard H37Rv *Mycobacterium tuberculosis* as well as efflux deficient (Δ Rv1258c) were calculated and data of the first 6 compounds are provided in Table 1. EPM1 showed a low micro molar MIC₉₀ and, as these compounds were not identified as antimycobacterial agents *per se*, it was an interesting observation that may warrant additional investigation into the mechanism of antimycobacterial action. EPM4 showed antimycobacterial activity in Gaste-Fe minimal medium - comprising glycerol, alanine, salts, iron, and Tween80 – but not in standard Middlebrook 7H9 albumin-dextrose-catalase (ADC) medium. This difference may point to the binding of the compound by albumin,²⁰ interference of catalase in the mechanism of action, or a mechanism of action that impacts on the ability of the bacillus to use glycerol as a carbon source.²¹ The other EPMs, as anticipated, did not show any significant antimycobacterial activity as single agents. The similar MIC values in standard H37Rv, and Rv1258c efflux deficient mycobacterial strains likely indicate that these compounds do not act as substrates for this particular efflux pump. This is not unexpected as good binding stability within the pump would keep the compound bound in the channel, possibly resulting in competitive inhibition of efflux, rather than allowing the compound to be extruded by the efflux pump.

Table 1: MIC₉₀ of potential efflux pump inhibitors in *Mycobacterium Tuberculosis*

	MIC ₉₀ (μM): 7D 7H9 GLU CAS Tx ^a	MIC ₉₀ (μM): H37RvMA: 7D 7H9 GLU ADC TW ^b	MIC ₉₀ (μM): Δ Rv1258c 7D 7H9 GLU ADC TW ^c	Cytotoxicity IC ₅₀ (μM) CHO ^d
EPM1	0,448	<0.244	< 0.244	4.24
EPM2	62,5	62,5	62,5	37.4
EPM3	>125	>125	> 125	>50
EPM4	15,625	>125	> 62.5	>50
EPM5	>125	>125	> 125	>50
EPM6	62,5	>125	> 125	21.2
Emetine				0.0735

a) 7D 7H9 GLU CAS Tx: Gaste-Fe minimal medium supplemented with glycerol, alanine, salts, iron, and Tween80.

b) H37RvMA: 7D 7H9 GLU ADC TW: *Mycobacterium tuberculosis* H37Rv in Middlebrook 7H9 supplemented with albumin, dextrose, and catalase.

c) Δ Rv1258c 7D 7H9 GLU ADC TW: Efflux deficient *Mycobacterium tuberculosis* in Middlebrook 7H9 supplemented with albumin, dextrose, and catalase.

d) CHO: Chinese Hamster Ovary cells

2.3 Cytotoxicity analysis

EPM 3, 4 and 5 did not show cytotoxicity up 50 μM which was the highest concentration measured. EPM2 and 6 were moderately cytotoxic with EPM1 showing the highest cytotoxicity of the evaluated compounds. The antimycobacterial selectivity index for EPM1 is 17 which indicates, that despite its higher cytotoxicity, it still shows sufficient selective toxicity.

3. CONCLUSION

An accurate 3D model of the mycobacterial efflux pump Rv1258c previously developed by our group was used to identify novel compounds that show high binding affinity within the cavity of the efflux pump. Six compounds were selected and MIC₉₀ values were determined in Mtb as well as an Rv1258c efflux deficient strain thereof. Apart from EPM1 and EPM4 the compounds did not show any significant antimycobacterial activity in either of the strains indicating that these compounds, as expected, do not demonstrate antimycobacterial activity as single agents. Similar MIC values in the standard H37Rv *Mycobacterium tuberculosis* strain and the R1258c efflux deficient strain show that these compounds likely do not act as substrates for the Rv1258 efflux pump. These encouraging preliminary results will be followed up with synergism assays with the known efflux pump substrate, spectinomycin, to confirm efflux pump inhibition.

4. METHODOLOGY

4.1 Virtual screening

The homology model protein¹⁵ was prepared using MOE. The protein was prepared at pH 7.4 using the QuickPrep function to perform 3D protonation and minimize the structure (forcefield: AMBER10:EHT). The prepared protein was loaded in Make Receptor (4.0.0.2) and the protein and ligand molecule selected in the Molecules tab in the work stage flow sector. After the molecules were selected the active site box was automatically created around the ligand in the Box tab of the work stage flow sector. The box was displayed as a wire frame and the important amino acids as identified previously,¹⁵ labelled through selection in the Sequence viewer section of the workflow stage controls. Val28, Trp32, Gly161, Ile165, Phe247, Pro248, Phe251, Leu264 and Gly363 were already included within the box outline and the box was further expanded to include Glu243. The Shape controls were used to calculate the inner and outer contours of the binding site. Balanced was selected as the type of shape potential to be used when the binding site contours are created. The outer contour was automatically created with a value of 1692 Å³ and the inner contour was left as disabled.

The HitDiscover compound collection was downloaded from the ThermoFisher scientific platform and all compounds that do not contain amines were filtered out with OpenBabel using the OGREP command line tool of OpenBabel 2.2.3.²² The database was narrowed down to 64 124 amine containing compounds. Conformers were then generated in Omega 4.1.1.1¹⁷ using the 'omegapose' command to prepare a multiconformer database in oeb.gz format. The prepared Rv1258c protein and conformer database was evaluated for possible ligand poses, shape complementarity and chemical feature alignment using FRED 4.0.0.2.¹⁶ The compounds were scored using Chemgauss4 scoring and the top 500 compounds were identified. The top 100 dock scored compounds were selected for further binding and interaction analysis using VIDA 4.4.0.4 (OpenEye Scientific Software) and 15 compounds were identified for purchase.

4.2 Minimum inhibitory concentration evaluation

All assays were performed in a Biosafety Level III certified facility. *Mycobacterium tuberculosis*

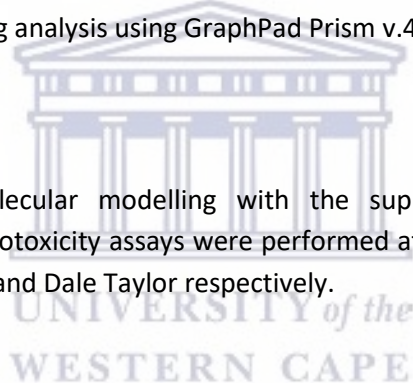
pM_{Sp}12:GFP^{23,24} was grown to an optical density (OD) of 0.6–0.7, in either GAST-Fe media or 7H9 media supplemented with 10% Albumin Dextrose Catalase (ADC).^{24,25} The plates were set using a 2-fold serial dilution of test compounds as previously described.²⁶ Rifampicin was used as the minimum growth control. Relative fluorescence was measured and MIC calculated as previously reported.^{20,27}

4.3 Cytotoxicity analysis

A colorimetric evaluation of the reduction of 3-(4,5-dimethylthiazol-2-yl)-2,5-diphenyl-2H-tetrazolium bromide (MTT)²⁸ in Chinese Hamster ovary cells (CHO-K1, ATCC, Manassas VA, USA) was used to determine cell survival in the presence of test compounds. Cells were cultured in Hams/F12 media supplemented with 10% foetal bovine serum (Thermo Fisher Scientific; origin South America). Emetine was used as the reference drug in all experiments. Test compounds were serially diluted in complete medium to yield a range of test concentrations for all compounds. 50 µM was the highest concentration measured. The uppermost concentration of DMSO to which the cells were exposed did not affect the cell viability. Cells were incubated at 37 °C with the test compounds for 44 hours after which MTT was added and the cells incubated for a further four hours. After final incubation, DMSO was added to each well to dissolve the reduced dye crystals. Plates were analysed at 540 nm wavelength to determine the relative amount of formazan in each well. All test samples were tested in triplicate on one occasion. IC₅₀ values were obtained from full dose-response curves through a non-linear dose-response curve fitting analysis using GraphPad Prism v.4.

Contributions to research

Erika Kapp performed the molecular modelling with the support of Jacques Joubert. The antimycobacterial activity-and cytotoxicity assays were performed at the University of Cape Town in the laboratories of Digby Warner and Dale Taylor respectively.



REFERENCES

1. World Health Organization. Progress towards global TB targets – an overview. *Glob Tuberc Rep 2020*. 2020:Chapter 2.2, 7. <http://apps.who.int/bookorders>. Accessed October 25, 2022.
2. World Health Organisation. Global tuberculosis report 2021. <https://www.who.int/publications/i/item/9789240037021>. Published 2021. Accessed September 9, 2022.
3. Te Brake LHM, De Knecht GJ, De Steenwinkel JE, et al. The Role of Efflux Pumps in Tuberculosis Treatment and Their Promise as a Target in Drug Development: Unraveling the Black Box. *Annu Rev Pharmacol Toxicol*. 2018;58:271-291. doi:10.1146/annurev-pharmtox-010617-052438
4. Peterson E, Kaur P. Antibiotic resistance mechanisms in bacteria: Relationships between resistance determinants of antibiotic producers, environmental bacteria, and clinical pathogens. *Front Microbiol*. 2018;9(NOV):2928. doi:10.3389/fmicb.2018.02928
5. Viveiros M, Martins M, Rodrigues L, et al. Inhibitors of mycobacterial efflux pumps as potential boosters for anti-tubercular drugs. *Expert Rev Anti Infect Ther*. 2012;10(9):983-998. doi:10.1586/eri.12.89
6. Sarathy JP, Dartois V, Lee EJD. The Role of Transport Mechanisms in Mycobacterium Tuberculosis Drug Resistance and Tolerance. *Pharmaceuticals*. 2012;5(11):1210-1235. doi:10.3390/ph5111210
7. Rodrigues L, Cravo P, Viveiros M. Efflux pump inhibitors as a promising adjunct therapy against drug resistant tuberculosis: a new strategy to revisit mycobacterial targets and repurpose old drugs. *Expert Rev Anti Infect Ther*. 2020;18(8):741-757. doi:10.1080/14787210.2020.1760845
8. Machado D, Coelho TS, Perdigão J, et al. Interplay between Mutations and Efflux in Drug Resistant Clinical Isolates of Mycobacterium tuberculosis. *Front Microbiol*. 2017;0(APR):711. doi:10.3389/FMICB.2017.00711
9. Louw GE, Warren RM, van Pittius NC, McEvoy CR, Helden PD Van, Victor TC. A balancing act: efflux/influx in mycobacterial drug resistance. *Antimicrob Agents Chemother*. 2009;53(8):3181-3189. doi:10.1128/AAC.01577-08
10. Rodrigues L, Parish T, Balganesch M, Ainsa JA. Antituberculosis drugs: reducing efflux = increasing activity. *Drug Discov Today*. 2017;22(3). doi:10.1016/j.drudis.2017.01.002
11. Liu J, Shi W, Zhang S, et al. Mutations in Efflux Pump Rv1258c (Tap) Cause Resistance to Pyrazinamide, Isoniazid, and Streptomycin in M. tuberculosis. *Front Microbiol*. 2019;0(FEB):216. doi:10.3389/FMICB.2019.00216
12. Lee RE, Hurdle JG, Liu J, et al. Spectinamides: a new class of semisynthetic antituberculosis agents that overcome native drug efflux. *Nat Med*. 2014;20(2):152-158. doi:10.1038/nm.3458
13. Shahi F, Khosravi AD, Tabandeh MR, Salmanzadeh S. Investigation of the Rv3065, Rv2942, Rv1258c, Rv1410c, and Rv2459 efflux pump genes expression among multidrug-resistant Mycobacterium tuberculosis clinical isolates. *Heliyon*. 2021;7(7). doi:10.1016/J.HELIYON.2021.E07566
14. Kapp E, Malan SFF, Joubert J, Sampson SLL. Small Molecule Efflux Pump Inhibitors in Mycobacterium tuberculosis: A Rational Drug Design Perspective. *Mini Rev Med Chem*. 2018;18(1):72-86.
15. Cloete R, Kapp E, Joubert J, Christoffels A, Malan SF. Molecular modelling and simulation

- studies of the Mycobacterium tuberculosis multidrug efflux pump protein Rv1258c. *PLoS One*. 2018;13(11). doi:10.1371/journal.pone.0207605
16. OEDOCKING 4.1.1.0: OpenEye Scientific Software, Inc., Santa Fe, NM. <https://docs.eyesopen.com/applications/oedocking/citation.html>. Accessed December 29, 2021.
 17. OMEGA 4.1.2.0: OpenEye Scientific Software, Santa Fe, NM. <https://docs.eyesopen.com/applications/omega/citation.html>. Accessed December 29, 2021.
 18. Dashti Y, Grkovic T, Quinn RJ. Predicting natural product value, an exploration of anti-TB drug space. *Nat Prod Rep*. 2014;31(8):990-998. doi:10.1039/c4np00021h
 19. Piccaro G, Poce G, Biava M, Giannoni F, Fattorini L. Activity of lipophilic and hydrophilic drugs against dormant and replicating Mycobacterium tuberculosis. *J Antibiot* 2015 6811. 2015;68(11):711-714. doi:10.1038/ja.2015.52
 20. Kapp E, Visser H, Sampson SL, et al. Versatility of 7-Substituted Coumarin Molecules as Antimycobacterial Agents, Neuronal Enzyme Inhibitors and Neuroprotective Agents. *Molecules*. 2017;22(10):10.3390/molecules22101644. doi:E1644 [pii]
 21. Pethe K, Sequeira PC, Agarwalla S, et al. A chemical genetic screen in Mycobacterium tuberculosis identifies carbon-source-dependent growth inhibitors devoid of in vivo efficacy. *Nat Commun*. 2010;1:57. doi:10.1038/ncomms1060
 22. O'Boyle NM, Banck M, James CA, Morley C, Vandermeersch T, Hutchison GR. Open Babel: An Open chemical toolbox. *J Cheminform*. 2011;3(10). doi:10.1186/1758-2946-3-33
 23. Abrahams GL, Kumar A, Savvi S, et al. Pathway-selective sensitization of Mycobacterium tuberculosis for target-based whole-cell screening. *Chem Biol*. 2012;19(7):844-854. doi:10.1016/j.chembiol.2012.05.020 [doi]
 24. Collins LA, Torrero MN, Franzblau SG. Green fluorescent protein reporter microplate assay for high-throughput screening of compounds against Mycobacterium tuberculosis. *Antimicrob Agents Chemother*. 1998;42(2):344-347. doi:10.1128/aac.42.2.344
 25. De Voss JJ, Rutter K, Schroeder BG, Su H, Zhu Y, Barry CE. The salicylate-derived mycobactin siderophores of Mycobacterium tuberculosis are essential for growth in macrophages. *Proc Natl Acad Sci U S A*. 2000;97(3):1252-1257. doi:10.1073/pnas.97.3.1252
 26. Ollinger J, Bailey MA, Moraski GC, et al. A Dual Read-Out Assay to Evaluate the Potency of Compounds Active against Mycobacterium tuberculosis. *PLoS One*. 2013;8(4). doi:10.1371/journal.pone.0060531
 27. Collaborative drug discovery. Home - Collaborative Drug Discovery Inc. (CDD). <https://www.collaborativedrug.com/de/>. Accessed October 13, 2020.
 28. Mosmann T. Rapid colorimetric assay for cellular growth and survival: application to proliferation and cytotoxicity assays. *J Immunol Methods*. 1983;65(1-2):55-63. doi:0022-1759(83)90303-4

Annexure 2: Copyright Policy Bentham Science Publishers: Small Molecule Efflux Pump Inhibitors in *Mycobacterium tuberculosis*: a Rational Drug Design Perspective.

BENTHAM SCIENCE PUBLISHERS COPYRIGHT / ARCHIVING POLICY

COPYRIGHT

Authors who publish in Bentham Science print & online journals will transfer copyright to their work to **Bentham Science Publishers**. Submission of a manuscript to the respective journals implies that all authors have read and agreed to the content of the Copyright Letter or the Terms and Conditions. It is a condition of publication that manuscripts submitted to this journal have not been published and will not be simultaneously submitted or published elsewhere. Plagiarism is strictly forbidden, and by submitting the article for publication the authors agree that the publishers have the legal right to take appropriate action against the authors, if plagiarism or fabricated information is discovered. By submitting a manuscript the authors agree that the copyright of their article is transferred to the publishers if and when the article is accepted for publication. Once submitted to the journal, the author will not withdraw their manuscript at any stage prior to publication.

Copyright Letter

It is mandatory that a signed copyright letter also be submitted along with the manuscript by the author to whom correspondence is to be addressed, delineating the scope of the submitted article declaring the potential competing interests, acknowledging contributions from authors and funding agencies, and certifying that the paper is prepared according to the '**Instructions for Authors**'. All inconsistencies in the text and in the reference section, and any typographical errors must be carefully checked and corrected before the submission of the manuscript. The article should not contain any such material or information that may be unlawful, defamatory, fabricated, plagiarized, or which would, if published, in any way whatsoever, violate the terms and conditions as laid down in the copyright agreement. The authors acknowledge that the publishers have the legal right to take appropriate action against the authors for any such violation of the terms and conditions as laid down in the copyright agreement. **Download the Copyright letter**

PERMISSION FOR REPRODUCTION

Permission to Reuse Bentham Content

Bentham Science has collaborated with the Copyright Clearance Centre to meet our customer's licensing, besides rights & permission needs.

The Copyright Clearance Centre's RightsLink® service makes it faster and easier to secure permission from Bentham Science's journal titles. Visit Journals by Title and locate the desired content. Then go to the article's abstract and click on "Rights and Permissions" to open the RightsLink's page. If authors can't find the content they are looking for or can't get the rights they need, please contact us at **permissions@benthamscience.net**

Third-Party Permissions

Authors are responsible for managing the inclusion of third-party content as an author/editor of a work. We refer to 'third party content' as any work that authors haven't developed themselves and have copied

or adapted from other sources. Text, figures, photographs, tables, screenshots, and other items may be included.

Unless the figure is in the public domain (copyright-free) or permitted for use under a Creative Commons or other open licences, the author must get permission from the copyright holder(s).

Published/reproduced material should not be included unless written permission has been obtained from the copyright holder, which should be forwarded to the Editorial Office in case of acceptance of the article for publication.

SELF-ARCHIVING

By signing the Copyright Letter, the authors retain the rights of self-archiving (subject to certain restrictions).

Following are the important features of the self-archiving policy of Bentham Science journals:

Authors can deposit the first draft of a submitted article on their personal websites or their institution's repositories for personal use, internal institutional use, or for permitted scholarly posting only.

Authors may deposit the **ACCEPTED VERSION** of the peer-reviewed article on their personal websites, their institution's repository or the non-commercial repositories, PMC and arXiv, after **12 MONTHS** of publication on the journal website. For personal use, internal institutional use, or for permitted scholarly posting only.

In case of (b) above, an acknowledgement must be given to the original source of publication and a link must be inserted to the published article on the journal's/publisher's website. The link to the original source of publication should be provided by inserting the DOI number of the article in the following sentence: "The published manuscript is available at EurekaSelect via <http://www.eurekaselect.com/>[insert DOI]."

If the research is funded by NIH, Wellcome Trust or any other Open Access Mandate, authors are allowed the archiving of published versions of manuscripts in the nominated institutional repositories, after the mandatory embargo period. Authors should first contact the Editorial Office of the journal for information about depositing a copy of the manuscript to a repository. Consistent with the copyright agreement, Bentham Science does not allow archiving of FINAL PUBLISHED VERSION of manuscripts unless under an Open Access mandate as above. Archiving, under any of the above mentioned Open Access mandates, is done under the terms of the Creative Commons License CC BY-NC-ND 4.0 - Attribution-NonCommercial-NoDerivatives 4.0 International.

There is no embargo on the archiving of articles published under the **OPEN ACCESS PLUS** category. Authors are allowed deposition of such articles on institutional, non-commercial repositories and personal websites immediately after publication on the journal website. This is done under the terms of the Creative Commons Attribution 4.0 International Public License CC-BY 4.0.

In case of any form of archiving, an acknowledgement must be given to the original source of publication and a link must be inserted to the published article on the journal's/publisher's website. The link to the original source of publication should be provided by inserting the DOI number of the article in the following sentence: "The published manuscript is available at EurekaSelect via <http://www.eurekaselect.com/>[insert DOI]."

LONG-TERM ARCHIVING OF BENTHAM SCIENCE CONTENT

To ensure permanent access to our publications, Bentham Science has an agreement with Portico to have a long-term preservation of the content published in its journals.

...

